AN ABSTRACT OF THE DISSERTATION OF

Christopher Liam Cosgrove for the degree of Doctor of Philosophy in Geography presented on December 3, 2020

Title: Mapping Wildlife-Relevant Snow Properties in Arctic-Boreal North America; Novel Modelling, Remote-Sensing, and Ground Observation Approaches.

Abstract approved:

Anne W. Nolin

Arctic-boreal regions are exhibiting the symptoms of profound ecological shifts as they experience pronounced warming. Wildlife in high-latitudes are one such harbinger of change, and their populations are undergoing range-shifts, declines, and extinctions in response to their rapidly altering habitats. As the circumpolar and boreal north is snow-covered for up to 10 months of the year, changes to the quality, quantity and duration of snow are major factors driving disturbances in the region's ecology. Yet the area's vast expanse and inaccessibility presents great difficulty in obtaining data to better understand snow-wildlife interactions and their consequences for population dynamics. This dissertation hence presents novel approaches to produce maps of wildlife-relevant snow properties in Arctic-boreal North America, answering a call for improved data to compare to modern GPS-tracking sensors and long-term datasets of wildlife demography.

To do so, it stands on the three fundamental supports of modern snow-science; modelling, remote-sensing, and ground observations. Chapter 1 presents the motivations for this research and provides a general literature review of; the observed changes to Arctic-boreal North American snow in recent decades, the effects of different snow properties on the endemic wildlife of the region and

how these properties relate to observations of changing wildlife behaviour and populations, and lastly the state-of-the-science of snow modelling, remote-sensing, and ground-observations in relation to wildlife studies.

Chapter 2 presents a snow modelling study in the Wrangell St Elias National Park, Alaska that demonstrates the incorporation of ground-observations to improve the simulation of snow conditions in the study region. Using the improved model, it compares a 1980 to 2017 dataset of snow properties with observations of Dall's sheep (*Ovis dalli dalli*) productivity. It reveals the importance of the seasonality of snow depth to Dall's sheep, with fall snow depths better predicting productivity than spring snow depths, which previous work had suggested.

Chapter 3 assesses the application of a high-density snow and ice layer detection algorithm across Alaska and uses a recently released, enhanced-resolution remote-sensing dataset to do so. It finds that high-density layers are mostly detected in coastal regions of low topographic complexity and of tundra-type vegetation. The occurrence, persistence, and disappearance of high-density layers were also linked to ground-observations of meteorological variables, and weather conditions corresponding to known controls on high-density layer establishment, maintenance and destruction, were established – suggesting the algorithm has promise.

Chapter 4 details the development of an open-source, low-cost wireless sensor network for snow-based applications and compares its performance to research-grade traditional equipment. The network is shown to take comparably accurate measurements of snow depth, air temperature and relative humidity at a significantly lower cost. The addition of a satellite modem for data-transmission establishes its credentials for use in remote regions where the difficulty of access for data-retrieval exasperates data-scarcity.

Finally, Chapter 5 discusses the broader significance of the preceding chapter's findings and proposes future research combining the three methodologies in a 'data-model fusion'. Such an approach would overcome each method's limitations and leverage their advantages, ultimately providing better data for use in wildlife ecology.

Mapping Wildlife-Relevant Snow Properties in Arctic-Boreal North America; Novel Modelling, Remote-Sensing, and Ground Observation Approaches.

by

Christopher Liam Cosgrove

A DISSERTATION

submitted to

Oregon State University

in partial fulfillment of
the requirements for the
degree of

Doctor of Philosophy

Presented December 3, 2020
Commencement June 2021

Doctor of Philosophy dissertation of Christopher Liam Cosgrove presented on December 3, 2020

APPROVED:

Major Professor, representing Geography

Dean of the College of Earth, Ocean, and Atmospheric Sciences

Dean of the Graduate School

I understand that my dissertation will become part of the permanent collection of Oregon State University libraries. My signature below authorizes release of my dissertation to any reader upon request.

Christopher L. Cosgrove, Author

ACKNOWLEDGEMENTS

First and foremost, I thank Dr. Anne Nolin for the opportunity to work on this research and for her unequivocal support, both academically and personally, throughout its development. I could never have anticipated how much my life has been enriched after we spoke about the position on New Year's Eve 2015. You mostly talked about skiing down volcanoes so I figured it would be a relatively safe bet to move myself to Oregon to work with you. Your generous welcome when you picked me up from the Amtrak in Albany and took me directly to the North co-op only confirmed my belief that you would look after me. Thank you for four-and-a-bit years of wonder and for opening the doors of research and your home to me.

I am in great debt to my committee members, Dr. Julia Jones, Dr Robert Kennedy, and Dr Bo Zhao. Julia – I always left your office feeling brighter and lighter than when I went in, and I didn't often enter with heavy-heart or mind. Thank you for radically changing my perception of the world through your teaching on GEOG 596 and introduction to Landscape Ecology. Your invitation to me to join faculty meetings as a student-representative was much appreciated, likewise your care and steering of the Geography program at OSU – a group that I'm very proud to be a part of. Robert – I think you might have been the first professor to teach me at OSU and I remember being very struck both by your natty dress-sense – a white button down under a plaid button-down – and skilled, fresh pedagogy. Thank you for any number of interesting chats, being the quintessential nice guy, and for teaching me programming – without which none of the following work would be possible. Bo – thank you for inspiring me to develop the micro-weather stations described in Chapter 4. They've evolved into a product I could never have imagined myself being capable of building and I'm not finished with them yet. You're also a proper Geographer whose suggestions to read Tuan, Heidegger, and Ihde for my prelims granted me many happy and interesting hours in a hammock, maturing philosophical thoughts I've been carrying for years – I'm looking forward to delving deeper into the work of each.

Considerable thanks go to Dr. Laura Prugh of the University of Washington who was the PI on the NASA project that funded the majority of this research. Your collaboration and comments on my 2nd chapter greatly improved it and me as an academic. Cheers too for sharing three field campaigns in the Wrangells and sharing your deep ecological knowledge and backcountry stories of the area. I will never look at a tuna can in the same way again.

Jeff Wells of the Alaska Department of Fish and Game also greatly assisted with getting Chapter 2 into submittable shape. Though we've never met in person, or even on Zoom, I am hugely grateful for your positive emails when it felt like everything to do with the paper was going wrong.

Without Dr. Glen Liston's instruction and help Chapter 2 would also have been impossible – thank you for hosting me in Fort Collins and for teaching me the fundamentals of SnowModel. Your research, alongside that of Dr. Matthew Sturm's, is a constant source of inspiration.

The American Alpine Club gave me a small grant that both confirmed my belief that the open-source weather station described in Chapter 4 was a good idea and incubated its tentative beginnings. The OPEnS lab at OSU, and Dr. Chet Udell in particular, greatly aided my understanding of its eventual technology.

The opportunity to be involved with the ABoVE 'Snowscapes' group and be a co-author on its paper 'Integrating snow science and wildlife ecology in Arctic-boreal North America' published in ERL has been greatly beneficial. This paper best narrates the motivation of this dissertation and is hence relied heavily upon throughout – I hope I have offered a few small answers to its call.

The Mountain Hydroclimatology Group of OSU through 2016 to 2018 will forever be my academic family; Dr. Travis Roth, Dr. Ryan Crumley, Andy Wilson, Sydney Weiss and Michelle Hu, thank you all for making work feel like hanging out with your mates. Travis – you rock a fine hat and ride a wild snowmobile, thank you for being just a little bit more anarchic than your average academic and much gracious hospitality. Ryan – thank you for the many hours chewing over SnowModel and life, and the great and many kindnesses you extended to Kajsa and me. Corvallis is drifting down the Willamette on an evening in your canoe. Andy – thank you for the many trips up Highway 20 and other roads to beautiful places. Playing in the mountains with you is a pleasure, always with good tunes and conversation on the way. Sydney – thank you for being a force of great energy and laughter, I am ever impressed by your dedication to whatever it is that you're doing and ability to transcend its seriousness. Michelle – I learnt so much Matlab looking over your shoulder and am ever awed at your scientific sharpness and ability.

Thank you to my Alaskan fieldwork friends Kelly Sivy, Dr. Molly Tedesche, Anika Pinzner, Dr. Qobiljon 'Kobil' Shokirov, and Andrew Johnson. All of you added to the enjoyment of my favourite aspect of research. Special thanks to Kelly and Molly who opened their Fairbank's lives and dry-cabins to me - lifestyles and homes I envy hugely. Thanks too, to Sarah Sackett at the ABoVE logistics office for her help and humour in fieldwork logistics.

Thank you to the CEOAS Professional Learning Community who opened my eyes wider to the injustices of the world. Being involved in the group was a great privilege – the academy will be a better place because of your work.

Thank you to Dr. Cara Steger, Dr. Eric Nost, Dr. Shana Hirsch, Dr. Sarah Inman, Dr Xoco Shinbrot, and Dr. Jessica Thorn for letting me be involved in the failed SeSYNC Graduate Pursuit that blossomed into a hugely interesting and fun collaboration on SES modelling in mountain regions. Working with you all has set a very high bar for future collaborative projects.

Thank you to Kuuipo Walsh and Dr Jenna Tilt for giving me free-rein to be the TA I wanted to be this past year – your easiness to work with has massively reduced the burden of finishing this dissertation.

Thank you to my cohort and that following us in the Geography program, whether it's been trying to run around Mount Hood or meeting to discuss Critical Physical Geography I've hugely enjoyed your company and been much inspired by your care for the world and each other.

Thank you to Dr. Laura Peters and Dr. Jamon Van Den Hoek for our first Thanksgiving dinner and many other enjoyable evenings besides. Hurry up and move to London.

Thank you to the Ashtanga and Ecstatic Dance communities of Corvallis, and especially Tiffany Bailey, Tony Wilcox, and Peter Weinstein - without whom I would have been an even more stressed grad student.

Finally, but far from least, thank you to my nearest and dearest - Kate and Tom Cosgrove, who have been ever encouraging of their son's pursuits, whichever corner of the world he manages to find himself in and however difficult he's making it for himself, and to Kajsa Skarsgård, who's companionship throughout the past 5 years has been an ever-deepening experience of love and light.

CONTRIBUTION OF AUTHORS

In chapter 2, Christopher Liam Cosgrove, Dr. Anne W. Nolin, and Dr. Laura R. Prugh designed the overall research and conducted fieldwork. CLC, AWN, LRP, and Dr. Jeff Wells developed the analytical methods. JW and Judy Putera contributed Dall's sheep data and guided its correct use. CLC led the writing, with editorial assistance from LRP and JW.

In chapter 3, Christopher Liam Cosgrove and Dr. Anne W. Nolin designed the overall research and analytical methods. CLC is solely responsible for the writing.

In chapter 4, Christopher Liam Cosgrove designed the overall research and analytical methods. Dr. Anne W. Nolin assisted with field installation. CLC led the writing, with editorial assistance from AWN.

TABLE OF CONTENTS

TABLE OF CONTENTS (Continued)

TABLE OF CONTENTS (Continued)

TABLE OF CONTENTS (Continued)

TABLE OF CONTENTS (Continued)

LIST OF FIGURES

LIST OF FIGURES (Continued)

LIST OF TABLES

LIST OF APPENDICES

LIST OF APPENDICES (Continued)

DEDICATION

This dissertation is dedicated to Kajsa Skarsgård, whose life, apart from my own, has been most transformed by its undertaking – hopefully for the better too! Without her courage, love and patience, it would have been a lesser and far tougher adventure.

Du är bäst och jag älskar dig!

😬🇸🇪🛫🌎🇺🇸🗻🐑🐏❄️

🏠🍁☔🌧️🌧️🌧️🌧️😱

♀️✊🌈

🚗🏔️🧗‍♀️🏕️🛶🏄‍♀️⛷️🌳🌲🌵

🥕🥦🥒🥑🥬🌽🍆🍇🍉🍎🍑🌮🌯

🦺

🥤🍔🍟

🍿🎫👂💃🥁💆‍♀️

⛴️🇨🇦⛈️🕯️🎄

🇲🇽⛩️🧳💌

😢🛤️🌁🛬🇸🇪

🤯❤️👨‍🎓👶

🥰

💋

Chapter 1 General Introduction

1.1 Research Motivation

The Arctic-boreal region is changing profoundly. Warming at a rate greater than any place on Earth, its physical, chemical and biological systems are shifting as its most distinctive yet sensitive features – the perennial and seasonal expanses of frozen water held in ice and snow – are diminished in space and time (AMAP, 2017). The National Aeronautics and Space Administration's (NASA) Arctic-Boreal Vulnerability Experiment (ABoVE), which funded the majority of the following research and is ongoing, seeks to better understand the vulnerability and resilience of Arctic-boreal North America in the face of such changes (Goetz et al., 2011). Of ABoVE's six Science Questions[1], this dissertation primarily responds to the 5th; 'How are flora and fauna responding to changes in biotic and abiotic conditions, and what are the impacts on ecosystem structure and function?'. Likewise, the Science Objective to 'Quantify how changes in the spatial and temporal distribution of snow impacts ecosystem form and structure' directs its enquiry. As with ABoVE, the research herein seeks to reach across disciplines to advance a holistic comprehension of the impacts of climate change in the Arctic-boreal region. Hence, the three central chapters present novel approaches in the three fundamental technical areas of modern snow science - modelling, remote-sensing, and ground observations - to answer a recognised need in Arctic-boreal wildlife ecology; high-resolution maps of wildlife relevant snow properties (Boelman et al., 2019).

Arctic-boreal wildlife are crucial components of ecosystem function and provide vital economic and cultural ecosystem services to remote human populations (Callaghan et al., 2011a). As the Arctic-boreal region is snow-covered for up 10 months of the year, mapping the presence and absence of snow properties that affect wildlife, and understanding how these properties vary in space and time, is critical to knowledge-based management of their populations. To date, studies have investigated the mechanics of different species' movement, forage and migration, winter habitat selection preferences, behavioural and productivity responses to disappearance dates, as well as survival during and after extreme weather events, in relation to snow. However, research is

---

[1] https://above.nasa.gov/about.html?#questions

severely limited by the availability, type, quality, and scale of snow observations in the ABR region (Boelman et al., 2019). Remotely sensed snow data, such as snow-covered area (SCA), is available over large extents and at daily resolutions but does not capture wildlife-relevant snow properties such as snow depth, density, and the presence of ice-layers. Their relatively coarse spatial resolution, 500 m at best for daily Moderate Resolution Spectroradiometer (MODIS) products (Hall et al., 2002), is additionally problematic in mountain regions where the fine-scale spatial variability of snow is high as a result of heterogeneous terrain. Where snow observations are available at fine resolutions, i.e., ≤30 m and sub-daily, they are limited to sparse networks of single-point observations made by meteorological stations or are the result of expensive field campaigns increasingly restricted to a small spatial and temporal extent or single, long transects (Sturm, 2015).

In an era described as the 'golden age' of animal-born sensors (Wilmers et al., 2015), when animal locations, movement patterns, and physiology can be monitored with ever-increasing accuracy and frequency, there hence exists a pressing need for snow products that complement the spatial and temporal granularity of this new frontier in wildlife-ecology. Longer-term datasets of wildlife observations, e.g. population per unit area and adult-to-juvenile ratios, are also under-served by snow data that does not capture interannual variability in properties that influence wildlife survival. There is hence limited opportunity to understand wildlife behavioural responses to snow properties at fine spatio-temporal scales, and in-turn linkages between these responses to population dynamics via comparison to long-term and spatially extensive observations of snow variability. Assessing the vulnerability of Arctic-boreal wildlife, and the communities that derive cultural and economic value from them, to projected changes in Arctic-boreal snow regimes is therefore subject to uncertainty.

The research in this dissertation is consequently motivated by addressing the issue of data gaps in wildlife-relevant snow properties. It does so by; (1) demonstrating how a spatially-explicit, physically based snow evolution model can be combined with ground-based measurements to provide a multi-decadal dataset of detailed snow properties in an alpine region, and how this dataset can be used to examine the response in productivity of an iconic North American animal, the Dall's sheep (*Ovis dalli dalli*), to annually and seasonally variable snow conditions; (2) assessing the potential of a long-term, daily, enhanced-resolution space-borne passive microwave observation dataset to map layers of high-density snow and ice across the state of Alaska; (3) development of a low-cost, open-source, wireless sensor network for snow-based applications in remote regions; (4) reflecting how using these methodologies in combination can further improve the accuracy of wildlife-relevant snow data, and how this research impacts other Arctic-boreal concerns.

1.1 General Literature Review

1.1.1 Changing snow conditions in Arctic-boreal North America

Across the Arctic there is multi-dataset evidence that seasonal snow cover is reducing in volume and duration (Brown et al., 2017). The amplified warming trend, resulting from stronger albedo feedbacks as the region loses sea-ice and snow cover, is driving a shortening of the snow season by 2 to 4 days per decade for the area north of 60ºN in North America, with the greatest losses occurring in high-latitude and high-altitude areas (Brown et al., 2017). Snow depth, for the same area and as measured by meteorological stations spanning a time-frame from 1950 to 2013, is decreasing by 0.6 cm a decade (Brown et al., 2017). Snow water equivalent (SWE), as reconstructed from climate reanalysis products and remote-sensing observations, has likewise declined by 3.9 to 4.2 mm per decade in Arctic land areas, with most of the interior of Alaska and Canada showing pronounced decreasing trends but with variability between datasets (Brown et al., 2017). Increased frequencies of mid-winter warming and rain-on-snow events (Liston and Hiemstra, 2011; Semmens et al., 2013) have been observed, resulting in higher bulk densities (Liston and Hiemstra, 2011) and ice-content of the snowpack (Chen et al., 2013).

1.1.2 Wildlife-relevant snow properties

The impact of seasonal snow cover upon wildlife, both mammalian and avian, is controlled by both the quantity and quality of snow properties and these properties' distribution in time and space (Formozov, 1946). Certain conditions can lead to opportunity for some species while threaten the survival of others, despite specific adaptations to snow (Pruitt, Jr., 1959; Telfer and Kelsall, 1984; Pomeroy and Brun, 2001).

From a mechanistic and behavioural point of view, the effects of snow depth, density and hardness, on locomotion and forage efficacy has been well-documented for grazing ungulates, where deep snow and high-density snow typically increases an animal's energy expenditure in both activities, leading to preferential selection of areas less deep and dense snow (e.g. Kelsall, 1969;

Hoefs, 1976; LaPerriere and Lent, 1977; Skogland, 1978; Fancy and White, 1985; Collins and Smith, 1991; Schaefer and Messier, 1995; Lundmark and Ball, 2008; Fancy and White, 2011; Robinson and Merrill, 2012). Conversely, high-density or hard snow conditions can also make locomotion more efficient relative to areas of low-density or soft snow, which has led to observations of preference for high-density snow when migrating or moving at larger scales typical of forage behaviour (e.g. Duquette, 1988; Mahoney et al., 2018). However, the ease of movement is dependent on the ratio of body-mass to footprint area, and snow-density thresholds for whether different species will sink into the snow have been found (Telfer and Kelsall, 1984; Sivy et al., 2018). This variable response has consequences for predator-prey dynamics, with some species of predator, e.g. wolves (*Canis lupus*) and coyotes (*Canis latrans*), able to move more efficiently on softer snow than the ungulates they prey upon (Fuller, 1991; Pozzanghera et al., 2016; Droghini and Boutin, 2017). Other species rely on the high thermo-insulative properties of snow to protect them from the harsh surface weather of Arctic-boreal winters (Pomeroy and Brun, 2001). Two mammals at either end of the body-mass spectrum, lemmings (*Lemmus lemmus*) and bears (e.g. *Ursus arctos*), take advantage of this insulation for their winter nests and dens respectively (Reid et al., 2012; Vroom et al., 1980). Lemmings, and other small rodents that burrow in the *sub-niveum,* also benefit from the concealment of snow cover against avian predators. Similarly, many Arctic-boreal dwelling mammals and birds gain from the camouflage of changing their pelage or plumage white during winter. Another property, the date of snow disappearance, has been shown to influence the timing of large-scale migrations of caribou (*Rangifer tarandus*) (Le Corre et al., 2017) and egg-laying by migratory shorebirds and passerines (Meltofte et al., 2006).

Cumulative behavioural responses to snow conditions across the seasonal snow period, or indeed multiple periods, ultimately influence an animal's fitness and hence ability to both survive and reproduce. While other factors are important, such as the clemency of the preceding or intervening summer(s) and nutrition abundance and quality, studies have begun to link population dynamics of both single animals but also trophic interactions to snow conditions (Penczykowski et al., 2017). Notable in the instance of this dissertation is a range of studies that connect mass-mortality events of caribou to the presence of ice-layers in the snowpack as a result of rain-on-snow events (e.g. Putkonen and Roe, 2003; Putkonen et al., 2009; Hansen et al., 2013, 2011; Langlois et al., 2017; Dolant et al., 2017). Further studies have linked such events to increase of scavengers in the area's affected (e.g. Sokolov et al., 2016). For Dall's sheep (*Ovis dalli dalli*), an ungulate species endemic to Arctic-boreal North America and the focus of Chapter 2, two studies found that later spring snow decreased the number of lambs that were observed relative to the number of ewes the following summer (Kerk et al., 2018; Rattenbury et al., 2018).

1.1.3 Modelling snow for wildlife ecology research

Using physically-based snow evolution models in wildlife research is underexplored (Boelman et al., 2019). This is despite their ability to simulate a wide-range of wildlife-relevant snow properties at great detail and in extents flexible to the requirements of a particular study. However, there do exist instances of their interface with wildlife ecology. An early study by Vikhamar-Schuler et al. (2013) used a 1-D physical multilayer snow model, SNOWPACK (Bartelt and Lehning, 2002) and compared its output to records of restricted grazing pastures for reindeer in northern Norway. Ouellet et al. (2017), attempted a spatialisation of this methodology using meteorological data from the Canadian Regional Climate Model reanalysis to force SNOWPACK across the range of the Peary caribou herd in the Canadian Arctic, albeit at a resolution of 45 km.

More recently, spatially distributed snow evolution models, such as SnowModel (Liston and Elder, 2006), iSNOBAL (Marks et al., 1999), Alpine-3D (Lehning et al., 2006), have shown greater promise for wildlife studies. These models are capable of simulating blowing snow processes and the fine-scale variability of snowpack properties both horizontally and vertically. For instance, Liston et al. (2016), demonstrated how SnowModel could simulate the requisite depth and distribution of snow-drifts for the winter dens of polar bears (*Ursus maritimus*) in a coastal area of the North Slope of Alaska. Another Alaska based study, but on the opposite coast in Lake Clark National Park, used SnowModel to test the scale-dependent response of Dall's sheep to snow depth and density (Mahoney et al., 2018).

Despite their potential, the adoption of the latest snow evolution models in wildlife ecology is hampered by several issues. The technical expertise needed to run such models is highly concentrated within the hydrological research fields where they were first developed, limiting their exposure to wildlife ecologists. In the Arctic-boreal region, there is also the problem of not having meteorological data sufficient in quantity and accuracy to force the models, nor *in-situ* snow data to calibrate and validate them to (Sturm, 2015; Boelman et al., 2019). This data-scarcity is a product of the region's remoteness and inaccessibility, but also its low-density of human settlements, which would otherwise require local meteorological and snow observations for the estimation of water resources available to agriculture and other activities.

1.1.4 Remote sensing of snow conditions for wildlife ecology research

Remotely-sensed snow products have been utilised by wildlife studies with greater frequency than data derived from snow modelling due to their relative ease of use and access. They have the capacity to map snow properties at hemispherical scales yet provide comparatively little insight into the vertical dimensions of snowpacks, e.g. depth, density and stratigraphy, at resolutions useful to animal-ecology. However, approaches exploiting the visible and near-infrared bands (NIR) of sensors upon numerous satellite platforms have advanced SCA mapping in recent decades, and their products have had relatively widespread use in wildlife ecology. An example of such data is a pre-processed product that classifies the fractional SCA in 500m MODIS pixels – the MODIS snow-covered area and grain size (MODSCAG) product (Painter et al., 2009). Verbyla et al., (2017) used MODSCAG to predict May 15th snowline elevations from 2000 to 2016 in 28 mountain areas where Dall's sheep are found, data that was later used to show that a low-elevation of spring snowline was detrimental to Dall's sheep productivity (Kerk et al., 2018). Mahoney et al., (2018) complemented this work by linking large scale movements of Dall's sheep to the selection of MODSCAG pixels where the fractional snow cover was less, indicating a selection for areas with improved access to forage. Other wildlife-related studies employing remotely-sensed snow cover products derived from visible light and NIR observations include Copeland et al.'s (2010) mapping of wolverine (*Gulo gulo)* distribution in relationship to MODIS SCA and LeCorre et al.'s (2017) investigation into the timing of spring and autumn caribou migration in Canada using the same product. In these studies, SCA serves only as a proxy for snow depth, with this and other variables pertaining to the amount and quality of snow inferred only by the persistence of the detected snow in the satellite product, and knowledge of the likely type of snow found in that region (Sturm et al., 1995). Uncertainty is inherent in this inference of snow depth as persistence may also be a result of cooler temperatures or additional fresh snowfall of unknown quantities. Additional issues with products utilising observations from MODIS and similar platforms is data-gaps caused by cloud-coverage, low-solar illumination, and polar night. Landsat derived SCA does improve on the spatial resolution of MODIS, 30 m versus 500 m, but at the cost of coarser temporal resolution, 16 days vs 1 day.

A remote sensing approach that is showing promise in detecting snow properties pertinent to wildlife is space-borne microwave radiometry. Dolant et al. (2016), building on work by Grenfell and Putkonen (2008), developed an empirical approach for detecting RoS events from ground-based passive microwave (PM) measurements. Their algorithm, ran with data from the Advanced Microwave Scanning Radiometer for Earth Observing System (AMSR-E), showed reasonable agreement to observations of RoS from citizen observers in the Canadian Arctic. Pan et al. (2018) extended this approach for a study domain across the entire state of Alaska, validating RoS detections with data from first-order meteorological stations. However, a RoS event does not always necessarily result in a snow property, such as an ice-layer, that could have a detrimental effect on wildlife. Hence, Langlois et al. (2017), used the RoS detection algorithm alongside a PM based ice-detection method developed by Montpetit (2015), in the context of the Peary caribou herd's decline, finding a negative relationship between the frequency of both RoS and icing events and caribou population. This ice-layer detection methodology has clear application to other ABR areas and species when mapped over a greater extent. However, the coarse resolution of traditional PM datasets (typically 25 km) complicates their use in areas with heterogeneous terrain nor provides the requisite detail for studies using fine-scale observations of animal location and movement. In this dissertation, the potential of an enhanced-resolution PM product is hence assessed.

1.1.5 Ground observations of snow in Arctic-boreal North America

A variety of networks of meteorological stations, such as the Snow Telemetry (SNOTEL) stations ran by the Natural Resource Conservation Service (NCRS), provide the majority of *in situ* snow observations across the conterminous United States, Canada, and Alaska. While these networks do measure some wildlife-relevant snow properties, such as depth and density, as latitude increases their coverage decreases, limiting their usefulness. Boelman et al. (2019) elegantly described this problem by contrasting the yearly snow coverage of the Western states of the conterminous US, <50% snow-covered for 6 months of the year, to that of Alaska, >95% snow-covered for >7 months of the year, and the density of the respective areas' *in situ* observation networks, finding that Alaska had <1/8 of the density of observations made by active meteorological stations. While other *in situ* data sources do exist in Arctic-boreal North America, such as that from snow courses or measured by field campaigns, they are uneven in time and space and often favour accessible sites near transport infrastructure that may not be representative of wildlife habitats (Boelman et al., 2019;

Brown et al., 2017). A confounding issue is the lack of a coordinated data archive of observations, but progress is being made with both the National Oceanic and Atmospheric Administration's (NOAA) Sustaining Arctic Observing network[2] and the National Science Foundation's (NSF) Arctic Data Center[3] increasing their archives. Extending networks is an expensive undertaking in remote Arctic-boreal areas as traditional meteorological stations require heavy equipment to install and must be robust enough to the severe climate in order to operate without maintenance for long periods. Similarly, field campaigns are costly and rely on observers trained in the measurement of snow properties.

An opportunity to overcome these barriers of cost and representativeness is the burgeoning development of low-cost, open-source solutions for environmental monitoring. These platforms, such as those based on the Raspberry Pi[4] and Arduino[5] microcontrollers, utilise cost-effective sensors and balance the shortcomings of traditional and proprietary technology (Mao et al., 2019). Easily customisable for near real-time data transfer and site-specific applications, they are also sufficiently cost-efficient to set-up in extensive wireless sensor networks (WSN) that can capture important variability in snow properties caused by gradients of elevation, aspect and land cover. A variety of studies have shown their applicability in snow research (e.g. Varhola et al., 2010; Kerkez et al., 2012; Pohl et al., 2014; Skalka and Frolik, 2014; Malek et al., 2017) but at lower latitudes where maintenance and remote data-transfer are easier due to accessibility and cellular networks respectively. Chapter 4 of this dissertation hence describes the development of an open-source, wireless sensor network for snow applications in both high-latitude and high-altitude regions, where the use of the Iridium satellite network[6] overcomes the lack of communications infrastructure.

1.2 Dissertation Organisation

This research seeks to exhibit how novel approaches in snow modelling, remote-sensing, and ground observations can be used both in isolation and in combination to provide improved, wildlife-relevant snow data. In Chapter 2, an example of how snow-modelling and ground observations,

---

[2] arcticobserving.org/
[3] arcticdata.io/
[4] raspberrypi.org/
[5] arduino.cc/
[6] iridium.com/

when used together, can better inform insights into the influence of snow on Dall's sheep productivity is presented. Chapter 3 assesses the ability of a PM algorithm to map high-density snow and ice layers at enhanced resolutions across Alaska. The development of a low-cost, open-source, wireless sensor network for snow-based research, and its performance relative to traditional, proprietary equipment, is described in Chapter 4. Finally, in Chapter 5, how the methods presented in the preceding chapters could be effectively integrated into a hybrid or 'data-fusion' approach to overcome the limitations of each, is discussed alongside the broader impacts of the work.

1.3 References

AMAP, 2017. Snow, Water, Ice and Permafrost in the Arctic (SWIPA) 2017 | AMAP. Arctic Monitoring and Assessment Programme (AMAP), Oslo, Norway.

Bartelt, P., Lehning, M., 2002. A physical SNOWPACK model for the Swiss avalanche warning Part I: numerical model. Cold Regions Science and Technology 23.

Boelman, N.T., Liston, G.E., Gurarie, E., Meddens, A.J.H., Mahoney, P.J., Kirchner, P.B., Bohrer, G., Brinkman, T.J., Cosgrove, C.L., Eitel, J.U.H., Hebblewhite, M., Kimball, J.S., LaPoint, S., Nolin, A.W., Pedersen, S.H., Prugh, L.R., Reinking, A.K., Vierling, L.A., 2019. Integrating snow science and wildlife ecology in Arctic-boreal North America. Environ. Res. Lett. 14, 010401. https://doi.org/10.1088/1748-9326/aaeec1

Brown, R., Vikhamar Schuler, D., Bulygina, O.N., Derksen, C., Luojus, K., Mudryk, L.R., Wang, L., Yang, D., 2017. Arctic Terrestrial Snow Cover, in: Snow, Water, Ice and Permafrost in the Arctic (SWIPA) 2017. Arctic Monitoring and Assessment Programme (AMAP), Oslo, Norway. (www.amap.no).

Callaghan, T.V., Johansson, M., Brown, R.D., Groisman, P.Y., Labba, N., Radionov, V., Barry, R.G., Bulygina, O.N., Essery, R.L.H., Frolov, D.M., Golubev, V.N., Grenfell, T.C., Petrushina, M.N., Razuvaev, V.N., Robinson, D.A., Romanov, P., Shindell, D., Shmakin, A.B., Sokratov, S.A., Warren, S., Yang, D., 2011. The changing face of arctic snow cover: A synthesis of observed and projected changes. Ambio 40, 17–31. https://doi.org/10.1007/s13280-011-0212-y

Chen, W., Russell, D.E., Gunn, A., Croft, B., Chen, W.R., Fernandes, R., Zhao, H., Li, J., Zhang, Y., Koehler, K., Olthof, I., Fraser, R.H., Leblanc, S.G., Henry, G.R., White, R.G., Finstad, G.L., 2013. Monitoring habitat condition changes during winter and pre-calving migration for Bathurst Caribou in northern Canada. Biodiversity 14, 36–44. https://doi.org/10.1080/14888386.2012.705110

Collins, W.B., Smith, T.S., 1991. Effects of Wind-Hardened Snow on Foraging by Reindeer (Rangifer tarandus). Arctic 44, 217–222.

Dolant, C., Langlois, A., Brucker, L., Royer, A., Roy, A., Montpetit, B., 2017. Meteorological inventory of rain-on-snow events and detection assessment in the Canadian arctic archipelago using passive microwave radiometry, in: 2017 IEEE International Geoscience and Remote Sensing Symposium (IGARSS). Presented at the 2017 IEEE International Geoscience and Remote Sensing Symposium (IGARSS), pp. 315–318. https://doi.org/10.1109/IGARSS.2017.8126959

Droghini, A., Boutin, S., 2017. Snow conditions influence grey wolf (Canis lupus) travel paths: the effect of human-created linear features. Can. J. Zool. 96, 39–47. https://doi.org/10.1139/cjz-2017-0041

Duquette, L.S., 1988. Snow Characteristics along Caribou Trails and within Feeding Areas during Spring Migration. ARCTIC 41, 143–144. https://doi.org/10.14430/arctic1706

Fancy, S.G., White, R.G., 2011. Energy expenditures for locomotion by barren-ground caribou. Canadian Journal of Zoology. https://doi.org/10.1139/z87-018

Fancy, S.G., White, R.G., 1985. Energy Expenditures by Caribou while Cratering in Snow. The Journal of Wildlife Management 49, 987–993. https://doi.org/10.2307/3801384

Formozov, A.N., 1946. Snow cover as an integral factor of the environment and its importance in the ecology of mammals and birds. Fauna and Flora of the USSR. New Ser. Zool. 5, 1–152.

Fuller, T.K., 1991. Effect of snow depth on wolf activity and prey selection in north central Minnesota. Can. J. Zool. 69, 283–287. https://doi.org/10.1139/z91-044

Goetz, S., Kimball, J., Mack, M., Kasischke, E., 2011. Scoping Completed for an Experiment to Assess Vulnerability of Arctic and Boreal Ecosystems. Eos, Transactions American Geophysical Union 92, 150–151. https://doi.org/10.1029/2011EO180002

Hall, D.K., Riggs, G.A., Salomonson, V.V., DiGirolamo, N.E., Bayr, K.J., 2002. MODIS snow-cover products. Remote Sensing of Environment 83, 181–194.

Hansen, B.B., Aanes, R., Herfindal, I., Kohler, J., S\a ether, B.-E.E., Oli, M.K., 2011. Climate, icing, and wild arctic reindeer: Past relationships and future prospects. Ecology 92, 1917–1923. https://doi.org/10.1890/11-0095.1

Hansen, B.B., Grotan, V., Aanes, R., Saether, B.-E., Stien, A., Fuglei, E., Ims, R.A., Yoccoz, N.G., Pedersen, A.O., 2013. Climate Events Synchronize the Dynamics of a Resident Vertebrate Community in the High Arctic. Science 339, 313–315. https://doi.org/10.1126/science.1226766

Hoefs, M., 1976. Ecological investigation of Dall sheep (Ovis dalli dalli, Nelson) and their habitat on Sheep Mountain, Kluane National Park, Yukon Territory, Canada (Text). The University of Bristish Columbia.

Kelsall, J.P., 1969. Structural Adaptations of Moose and Deer for Snow. Journal of Mammalogy 50, 302–310. https://doi.org/10.2307/1378347

Kerk, M. van de, Verbyla, D., Nolin, A.W., Sivy, K.J., Prugh, L.R., 2018. Range-wide variation in the effect of spring snow phenology on Dall sheep population dynamics. Environ. Res. Lett. 13, 075008. https://doi.org/10.1088/1748-9326/aace64

Kerkez, B., Glaser, S.D., Bales, R.C., Meadows, M.W., 2012. Design and performance of a wireless sensor network for catchment-scale snow and soil moisture measurements. Water Resources Research 48, 1–18. https://doi.org/10.1029/2011WR011214

Langlois, A., Johnson, C.-A.A., Montpetit, B., Royer, A., Blukacz-Richards, E.A.A., Neave, E., Dolant, C., Roy, A., Arhonditsis, G., Kim, D.-K.K., Kaluskar, S., Brucker, L., 2017. Detection of rain-on-snow (ROS) events and ice layer formation using passive microwave radiometry: A context for Peary caribou habitat in the Canadian Arctic. Remote Sensing of Environment 189, 84–95. https://doi.org/10.1016/j.rse.2016.11.006

LaPerriere, A.J., Lent, P.C., 1977. Caribou Feeding Sites in Relation to Snow Characteristics in Northeastern Alaska. ARCTIC 30, 101–108. https://doi.org/10.14430/arctic2690

Le Corre, M., Dussault, C., Côté, S.D., 2017. Weather conditions and variation in timing of spring and fall migrations of migratory caribou. J Mammal 98, 260–271. https://doi.org/10.1093/jmammal/gyw177

Liston, G.E., Hiemstra, C.A., 2011. The Changing Cryosphere: Pan-Arctic Snow Trends (1979–2009). J. Climate 24, 5691–5712. https://doi.org/10.1175/JCLI-D-11-00081.1

Liston, G.E., Perham, C.J., Shideler, R.T., Cheuvront, A.N., 2016. Modeling snowdrift habitat for polar bear dens. Ecological Modelling 320, 114–134. https://doi.org/10.1016/j.ecolmodel.2015.09.010

Lundmark, C., Ball, J.P., 2008. Living in Snowy Environments: Quantifying The Influence of Snow on Moose Behavior. Arctic, Antarctic, and Alpine Research 40, 111–118. https://doi.org/10.1657/1523-0430(06-103)[LUNDMARK]2.0.CO;2

Mahoney, P.J., Liston, G.E., LaPoint, S., Gurarie, E., Mangipane, B., Wells, A.G., Brinkman, T.J., Eitel, J.U.H., Hebblewhite, M., Nolin, A.W., Boelman, N., Prugh, L.R., 2018. Navigating snowscapes: scale-dependent responses of mountain sheep to snowpack properties. Ecological Applications 0. https://doi.org/10.1002/eap.1773

Malek, S., Avanzi, F., Brun-Laguna, K., Maurer, T., Oroza, C., Hartsough, P., Watteyne, T., Glaser, S., Malek, S.A., Avanzi, F., Brun-Laguna, K., Maurer, T., Oroza, C.A., Hartsough, P.C., Watteyne, T., Glaser, S.D., 2017. Real-Time Alpine Measurement System Using Wireless Sensor Networks. Sensors 17, 2583. https://doi.org/10.3390/s17112583

Mao, F., Khamis, K., Krause, S., Clark, J., Hannah, D.M., 2019. Low-Cost Environmental Sensor Networks: Recent Advances and Future Directions. Front. Earth Sci. 7. https://doi.org/10.3389/feart.2019.00221

Meltofte, H., Høye, T.T., Schmidt, N.M., Forchhammer, M.C., 2006. Differences in food abundance cause inter-annual variation in the breeding phenology of High Arctic waders. Polar Biol 30, 601. https://doi.org/10.1007/s00300-006-0219-1

Montpetit, B., 2015. Analyse de la modélisation de l'émission multi-fréquences micro-onde des sols et de la neige, incluant les croutes de glace à l'aide du modèle Microwave Emission Model of Layered Snowpacks (MEMLS). Université de Sherbrooke.

Ouellet, F., Langlois, A., Blukacz-Richards, E.A., Johnson, C.A., Royer, A., Neave, E., Larter, N.C., 2017. Spatialization of the SNOWPACK snow model for the Canadian Arctic to assess Peary caribou winter grazing conditions. Physical Geography 38, 143–158. https://doi.org/10.1080/02723646.2016.1274200

Painter, T.H., Rittger, K., McKenzie, C., Slaughter, P., Davis, R.E., Dozier, J., 2009. Retrieval of subpixel snow covered area, grain size, and albedo from MODIS. Remote Sensing of Environment 113, 868–879. https://doi.org/10.1016/j.rse.2009.01.001

Pan, C.G., Kirchner, P.B., Kimball, J.S., Kim, Y., Du, J., 2018. Rain-on-snow events in Alaska, their frequency and distribution from satellite observations. Environ. Res. Lett. 13, 075004. https://doi.org/10.1088/1748-9326/aac9d3

Penczykowski, R.M., Connolly, B.M., Barton, B.T., 2017. Winter is changing: Trophic interactions under altered snow regimes. Food Webs 13, 80–91. https://doi.org/10.1016/j.fooweb.2017.02.006

Pohl, S., Garvelmann, J., Wawerla, J., Weiler, M., 2014. Potential of a low-cost sensor network to understand the spatial and temporal dynamics of a mountain snow cover. Water Resources Research 50, 2533–2550. https://doi.org/10.1002/2013WR014594

Pomeroy, J.W., Brun, E., 2001. Physical Properties of Snow Introduction: Snow Physics and Ecology, in: Snow Ecology.

Pozzanghera, C. b., Sivy, K. j., Lindberg, M. s., Prugh, L. r., 2016. Variable effects of snow conditions across boreal mesocarnivore species. Can. J. Zool. 94, 697–705. https://doi.org/10.1139/cjz-2016-0050

Pruitt, Jr., W.O., 1959. Snow as a Factor in the Winter Ecology of the Barren Ground Caribou (*Rangifer arcticus*). ARCTIC 12. https://doi.org/10.14430/arctic3723

Putkonen, J., Grenfell, T.C., Rennert, K., Bitz, C., Jacobson, P., Russell, D., 2009. Rain on Snow: Little Understood Killer in the North. Eos, Transactions American Geophysical Union 90, 221–222. https://doi.org/10.1029/2009EO260002

Putkonen, J., Roe, G., 2003. Rain-on-snow events impact soil temperatures and affect ungulate survival. Geophysical Research Letters 30. https://doi.org/10.1029/2002GL016326

Rattenbury, K.L., Schmidt, J.H., Swanson, D.K., Borg, B.L., Mangipane, B.A., Sousanes, P.J., 2018. Delayed spring onset drives declines in abundance and recruitment in a mountain ungulate. Ecosphere 9, e02513. https://doi.org/10.1002/ecs2.2513

Reid, D.G., Bilodeau, F., Krebs, C.J., Gauthier, G., Kenney, A.J., Gilbert, B.S., Leung, M.C.-Y., Duchesne, D., Hofer, E., 2012. Lemming winter habitat choice: a snow-fencing experiment. Oecologia 168, 935–946. https://doi.org/10.1007/s00442-011-2167-x

Robinson, B.G., Merrill, E.H., 2012. The influence of snow on the functional response of grazing ungulates. Oikos 121, 28–34. https://doi.org/10.1111/j.1600-0706.2011.19408.x

Schaefer, J.A., Messier, F., 1995. Winter Foraging by Muskoxen: A Hierarchical Approach to Patch Residence Time and Cratering Behaviour. Oecologia 104, 39–44.

Semmens, K.A., Ramage, J., Bartsch, A., Liston, G.E., 2013. Early snowmelt events: detection, distribution, and significance in a major sub-arctic watershed. Environ. Res. Lett. 8, 014020. https://doi.org/10.1088/1748-9326/8/1/014020

Sivy, K.J., Nolin, A.W., Cosgrove, C., Prugh, L., 2018. Critical snow density threshold for Dall sheep (Ovis dalli dalli). Can. J. Zool. https://doi.org/10.1139/cjz-2017-0259

Skalka, C., Frolik, J., 2014. Snowcloud: A Complete Data Gathering System for Snow Hydrology Research. Springer International Publishing, pp. 3–14. https://doi.org/10.1007/978-3-319-03071-5_1

Skogland, T., 1978. Characteristics of the Snow Cover and Its Relationship to Wild Mountain Reindeer (Rangifer tarandus tarandus L.) Feeding Strategies. Arctic and Alpine Research 10, 569–579. https://doi.org/10.2307/1550680

Sokolov, A.A., Sokolova, N.A., Ims, R.A., Brucker, L., Ehrich, D., 2016. Emergent Rainy Winter Warm Spells May Promote Boreal Predator Expansion into the Arctic. Arctic 69, 121–129.

Sturm, M., 2015. White water: Fifty years of snow research in WRR and the outlook for the future. Water Resources Research 51, 4948–4965. https://doi.org/10.1002/2015WR017242

Telfer, E.S., Kelsall, J.P., 1984. Adaptation of Some Large North American Mammals for Survival In Snow. Ecology 65, 1828–1834. https://doi.org/10.2307/1937779

Varhola, A., Wawerla, J., Weiler, M., Coops, N.C., Bewley, D., Alila, Y., Varhola, A., Wawerla, J., Weiler, M., Coops, N.C., Bewley, D., Alila, Y., 2010. A New Low-Cost, Stand-Alone Sensor

System for Snow Monitoring. Journal of Atmospheric and Oceanic Technology 27, 1973–1978. https://doi.org/10.1175/2010JTECHA1508.1

Verbyla, D., Hegel, T., Nolin, A.W., van de Kerk, M., Kurkowski, T.A., Prugh, L.R., 2017. Remote Sensing of 2000–2016 Alpine Spring Snowline Elevation in Dall Sheep Mountain Ranges of Alaska and Western Canada. Remote Sensing 9, 1157. https://doi.org/10.3390/rs9111157

Vikhamar-Schuler, D., Hanssen-Bauer, I., Schuler, T.V., Mathiesen, S.D., Lehning, M., 2013. Use of a multilayer snow model to assess grazing conditions for reindeer. Annals of Glaciology 54, 214–226. https://doi.org/10.3189/2013AoG62A306

Vroom, G.W., Herrero, S., Ogilvie, R.T., 1980. The ecology of winter den sites of grizzly bears in Banff National Park, Alberta. Bears: their biology and management 321–330.

Chapter 2 Seasonal influence of snow conditions on Dall's sheep productivity in Wrangell-St Elias National Park and Preserve

Seasonal influence of snow conditions on Dall's sheep productivity in Wrangell-St Elias National Park and Preserve

Christopher L. Cosgrove[1*], Jeff Wells[2], Anne W. Nolin[1,3], Judy Putera[4], and Laura R. Prugh[5]

[1]Oregon State University, College of Earth Ocean and Atmospheric Sciences, Administration Building 104, 101 SW 26th St, Corvallis, OR 97331

[2]Alaska Department of Fish and Game, PO Box 355, Tok, AK 99780

[3]University of Nevada, Reno; Department of Geography, 1664 N. Virginia Street, Reno, NV 89557

[4]Wrangell-St. Elias National Park and Preserve and Central Alaska Inventory & Monitoring Network, PO Box 439, Copper Center, AK 99573

[5]University of Washington, School of Environmental and Forest Sciences, Box 352100, Seattle, WA 98195

PLOS One

Accepted December 2020

2.1 Abstract

Dall's sheep (*Ovis dalli dalli*) are endemic to alpine areas of sub-Arctic and Arctic northwest America and are an ungulate species of high economic and cultural importance. Populations have historically experienced large fluctuations in size, and studies have linked population declines to decreased productivity as a consequence of late-spring snow cover. However, it is not known how the seasonality of snow accumulation and characteristics such as depth and density may affect Dall's sheep productivity. We examined relationships between snow and climate conditions and summer lamb production in Wrangell-St Elias National Park and Preserve, Alaska over a 37-year study period. To produce covariates pertaining to the quality of the snowpack, a spatially-explicit snow evolution model was forced with meteorological data from a gridded climate re-analysis from 1980 to 2017 and calibrated with ground-based snow surveys and validated by snow depth data from remote cameras. The best calibrated model produced an RMSE of 0.08 m (bias 0.06 m) for snow depth compared to the remote camera data. Observed lamb-to-ewe ratios from 19 summers of survey data were regressed against seasonally aggregated modelled snow and climate properties from the preceding snow season. We found that a multiple regression model of fall snow depth and fall air temperature explained 41% of the variance in lamb-to-ewe ratios ($R^2 = .41$, $F(2,38) = 14.89$, $p<0.001$), with decreased lamb production following deep snow conditions and colder fall temperatures. Our results suggest the early establishment and persistence of challenging snow conditions is more important than snow conditions immediately prior to and during lambing. These findings may help wildlife managers to better anticipate Dall's sheep recruitment dynamics.

2.2 Introduction

The terrestrial ecology of the Arctic Boreal region (ABR) is changing rapidly as a result of amplified increases in temperatures (Chapin et al., 2005; Cooper, 2014; Hinzman et al., 2005; Serreze and Barry, 2011). Seasonal snow coverage exists in the ABR for up to 10 months annually and profoundly impacts ecosystem function. Studies point towards continued reduction in the annual duration of snow cover and overall accumulation in the ABR, with region and elevation dependent variations in trend and severity (Brown et al., 2017). Mid-winter warming events have been seen to cause substantial alteration to snow properties and the incidence and severity of these events are thought to be increasing (Bokhorst et al., 2016; Johansson et al., 2011; Liston and Hiemstra, 2011).

Snow processes have been linked to the population dynamics, movement, habitat selection, and life-cycles of a wide variety of mammals living in the ABR ranging in size from polar bears (*Ursus maritimus*, 13) and moose (*Alces alces*, 14), through to lemmings (*Lemus lemus,* 15) and snowshoe hares (*Lepus americanus*, 16). Due to their importance to Northern societies, ungulates native to the ABR, such as moose, caribou (*Rangifer tarandus*) and muskoxen (*Ovibos moschatus*) have been subject to broad scientific enquiry (e.g. Pruitt, Jr., 1959; Kelsall, 1969; LaPerriere and Lent, 1977; Duquette, 1988; Collins and Smith, 1991; Lundmark and Ball, 2008; Hansen et al., 2010; Gilbert et al., 2017; Schaefer and Messier, 1995). These studies indicate that ungulate populations in the ABR are negatively affected by extreme conditions that could increase in severity and frequency due to climate change (Tyler N. J. C., 2010; Vors and Boyce, 2009). For example, 'locked-pastures', where access to winter forage is restricted through either deep snow or ice-layers, have been linked to caribou and muskox mass mortality events (Hansen et al., 2011; Langlois et al., 2017; Tyler N. J. C., 2010; Vikhamar-Schuler et al., 2013).

Snow cover in mountain areas is highly variable in both space and time (Sturm et al., 1995) as the interplay of temperature, precipitation, solar radiation, vegetation cover and wind produces intricate patterns of depth, density and stratigraphy in complex terrain. While remote sensing products utilising optical and infrared wavelengths have some ability to detect this variability, their coarse spatial grain (~500 m) at daily time scales, impediment by cloud cover, and inability to quantify snow depth and density, limit their application in snow ecology questions (Boelman et al., 2018). Passive microwave derived remote-sensing products have shown promise in mapping snow properties such as water equivalent (Pulliainen and Hallikainen, 2001) and rain-on-snow events (Pan et al., 2018), but these products currently have a spatial resolution of >5 km, limiting their usefulness in mountain contexts.

Physically-based snow evolution models offer a promising means of obtaining a variety of snow properties that cannot be obtained from remote sensing alone. These models solve the surface mass-energy balance to map snow properties at a user-defined spatial and temporal resolution. However, there has been limited application of these models in wildlife research relative to those incorporating remotely sensed snow data, possibly due to the different technical skills required. Models have been used to simulate detailed snow data at single point locations for comparison to long-term wildlife data (Domine et al., 2018; Vikhamar-Schuler et al., 2013), or to quasi-spatialize a single grid cell model at a coarse, 45 km resolution (Ouellet et al., 2017). To our knowledge, no study has yet exploited the ability of modern snow models to produce longer time series of spatially-distributed data to compare to population dynamics of wildlife. Here, we use a leading snow evolution model, SnowModel (Liston and Elder, 2006), capable of operating with a 3D snow redistribution sub-model (Liston et al., 2007), to map daily snow and climate conditions at a high spatial resolution for a mountainous sub-Arctic domain inhabited by a population of Dall's sheep (*Ovis dalli dalli*) that has been surveyed periodically over the past 50 years. The advantage of this approach is that it allows identification of important seasonal snow properties, and allows the simulation of snow conditions across Dall's sheep alpine habitat as opposed to potentially non-representative point-locations, such as meteorological stations in valley-bottoms (Molotch and Bales, 2005).

We examined the importance of the preceding season's snow conditions on summer lamb production of Dall's sheep in Wrangell-St Elias National Park and Preserve, Alaska, USA (WRST) using model derived covariates of snowpack quality. Dall's sheep are a wild ungulate endemic to mountains of the ABR in north-western North America and are an important herbivore in high-latitude alpine ecosystems that may be acutely vulnerable to climate change (Dirnböck et al., 2011). They are also a highly prized Alaskan game species (Alaska Department of Fish and Game, 2014). Dall's sheep often use windward aspects during snow-covered months, where they rely on wind-scoured patches of snow-free or soft and shallow snow-covered forage to buffer caloric deficit (Bunnell, 1982). Populations of Dall's sheep have historically fluctuated widely in size (Alaska Department of Fish and Game, 2014; Lambert Koizumi et al., 2011; Mitchell et al., 2015; Murphy and Whitten, 1976). These fluctuations are thought to be largely governed by variations in the production and survival of lambs, as adult survival has been shown to be relatively stable except after extreme winter events (Gaillard et al., 1998; Rattenbury et al., 2018), and only a limited number of mature rams are harvested each year (Arthur and Prugh, 2010). Mature Dall's sheep ewes typically produce one lamb in mid-May to early-June (Rachlow and Bowyer, 1994), and decreased summer production and survival of lambs has been linked to adverse winter weather and persistent or deep snow conditions (Burles and Hoefs, 1984; van de Kerk et al., 2018; Murphy and Whitten, 1976; Rattenbury et al., 2018; Schults, 2004). However, previous studies have relied upon remotely-sensed snow cover phenology metrics, with vertical properties of snow, e.g. greater depth and density, inferred from the longer persistence of snow covered areas (van de Kerk et al., 2018; Rattenbury et al., 2018). Thus, the seasonal importance of different snow properties such as depth and density on Dall's sheep remains unknown.

Snow properties are thought to affect ungulates such as Dall's sheep in 3 main ways. First, access to forage may be restricted where snow is deeper or harder (Robinson and Merrill, 2012). Second, movement may be energetically expensive where deeper snow does not support an animal's weight (Parker et al., 1984). Third, susceptibility to predation may be enhanced in deep snow conditions where the snow density supports a predator's foot load but impedes movement of an ungulate (Telfer and Kelsall, 1984). Forage restriction from deep or hard snow cover established in fall has been shown to have stronger impacts on reindeer populations than restriction later in the winter or spring (Douhard et al., 2016), but whether these patterns occur in mountainous regions with more heterogeneous snow properties is not known.

Here, we examine the relationships between preceding snow conditions and Dall's sheep productivity, measured as the number of lambs per ewe-like sheep (hereafter, lamb-to-ewe ratios). Our methodology affords the novelty of examining *when* and *which* snow properties are most important. In other studies of alpine ungulates and Dall's sheep low winter temperatures and high snowfall have been shown to decrease summer productivity (Burles and Hoefs, 1984; Coulson et al., 2000), so we study these climate variables for influence relative to, and in combination with, model derived snow properties. Additionally, we present trends in modelled snow and climate covariates from 1980 to 2017 to shed light on potential linkages between climate change, snow properties, and Dall's sheep population dynamics.

To establish the relative importance of the seasonality of snow conditions we tested two contrasting hypotheses: (H1) the cumulative effects of persistent snow conditions that are unfavourable for Dall's sheep productivity will be most important, in which case snow conditions established in the fall months and persisting through the winter months should better explain summer lamb-to-ewe ratios; (H2) snow conditions in the lambing season will have the strongest effect, in which case snow conditions in the spring months should better explain lamb-to-ewe ratios. As adult survival is considered stable relative to that of Dall's sheep lambs, our first hypothesis proposes that the effect of snow conditions indirectly influences lamb production and survival via ewe body condition, which is affected by the winter-long accumulative effect of snow conditions aiding or abetting forage and movement. The second hypothesis instead emphasises that snow conditions may have a more direct influence on lamb survival, and hence productivity, both through their effect on foraging and movement immediate to and after birth.

2.3 Materials and Methods

2.3.1 Study Area

Our study area was a 8,678 km^2 region located in northern Wrangell-St Elias National Park and Preserve (WRST; 62°18'46"N, 143° 15' 31"W; Figure 2.1). A small portion of the study area was outside WRST and included portions of state, U.S. Fish and Wildlife Service, and private lands. Our study area falls within the Southeast Interior Alaska climate division, as mapped by Bieniek et al. (2012). Precipitation is relatively low, given the rain-shadowing of the Chugach mountain range to the south, and falls predominantly in May through to October. The annual range of mean monthly temperatures is ~15 ºC in July to ~-20 ºC in January (Bieniek et al., 2012). In the subalpine zone (1200 – 1400 m.a.s.l), patches of 1 to 2 m high dwarf birch (*Betula glandulosa*) and willow (*Salix* spp.) are separated by lichens and moss (Danby and Slocombe, 2005). Alpine areas (> 1400 m.a.s.l) are either dry communities of low, matted alpine vegetation, consisting mostly of *Dryas*, or moist areas of grasses (*Festuca* spp. and *Poa* spp.) and sedges (*Carex* spp.) with occasional patches of low willow and birch shrubs (Danby and Slocombe, 2005). Dall's sheep habitat extends from shrubline (~1400 m) into alpine areas where they favor areas close to rugged escape terrain (Geist, 1971). Using Moderate Resolution Imaging Spectroradiometer (MODIS) derived snow cover data from 2000 to 2015, Cherry et al. (2017) found a median start of the continuous snow season (CSS) of the 26th September (±32 days SD) for elevations between 1219 m and 1524 m, and 30th August (±34 days SD) for elevations above 1524 m, across Denali National Park, Yukon Charley National Preserve and WRST. The median date for the end of the CSS at these elevations were respectively 30th May (±37 days SD) and the 28th June (±34 days SD) (Cherry et al., 2017).

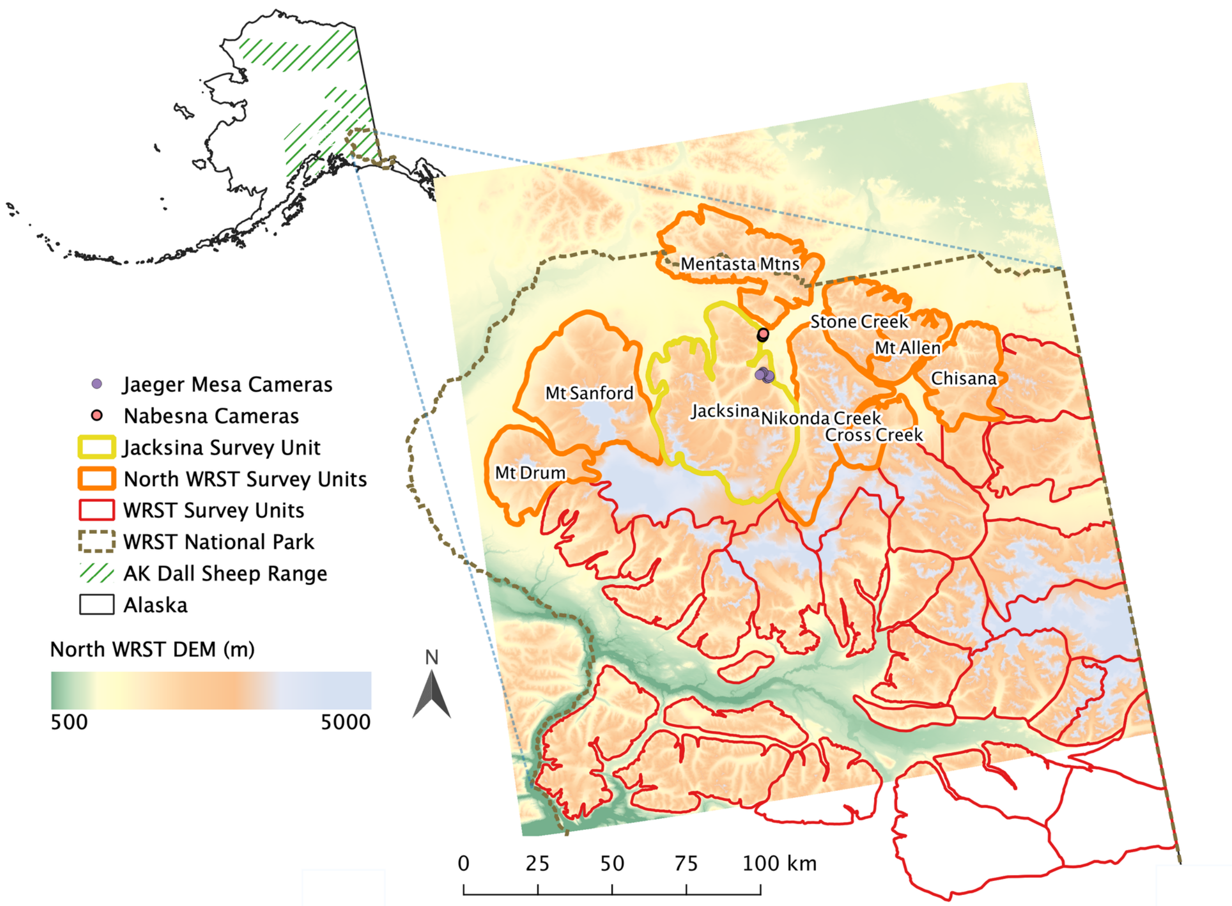

Figure 2.1. Map of study area located in the in the northern Wrangell-St. Elias National Park and Preserve (WRST; brown dashed outline) and Alaska (inset). Field-based snow surveys, including the installation of remote cameras upon Jaeger Mesa and near Nabesna, took place in the central Jacksina sheep survey unit (yellow outline) to calibrate a physically-based, spatially distributed snow evolution model. With the calibrated model we simulated daily snow conditions for high-elevation Dall's sheep terrain within the Jacksina survey unit domain from 1980 to 2017. A remote sensing analysis determined that the mean snow disappearance date (SDD) in 8 other survey units (outlined orange) was more similar to that of Jacksina compared to that of other units in the WRST (outlined red). We hence used observations of summer lamb-to-ewe ratios from Jacksina and these 8 nearby units to compare to model-derived metrics of seasonal snow conditions. GIS data for sheep survey units and WRST park boundary were sourced from (WRST Sheep and Goat Count Units - data.doi.gov; NPS - Land Resources Division, 2020) respectively, the background digital elevation model is built from 1 Arc-second Digital Elevation Models (DEMs) of the United States Geological Service National Map 3D Elevation Program (U.S. Geological Survey, 2017).

2.3.2 Survey Unit Selection

Within WRST there are 34 survey units in which summer Dall's sheep surveys are conducted by the Alaska Department of Fish and Game (ADF&G) and National Park Service (NPS) (Figure 2.1). These are delineated by high elevation terrain bounded by water courses or glaciated valleys and are kept to a manageable size for surveying. We used survey data from 9 northern units that were selected based on proximity and similarity to the Jacksina survey unit (JSU) where our ground-based snow surveys were conducted (Figure 2.1). In the absence of long-term in-situ snow cover data within each survey unit, we used a 500 m MODIS-based remote sensing product, snow disappearance date (SDD), to identify units with similar snow cover phenology as the JSU from 2000-2016 (Verbyla et al., 2017). We evaluated all units whose center point was within 100 km of the centre of the JSU (n = 17 units; Appendix 2.2). This search diameter of 200 km approximates to the maximum meso-β scale length forwarded by Orlanski (1975) as typical for mountain disturbances on meteorology, thus ensuring all units had similar climatic influences. SDDs were generally later for units south of the JSU, whereas units to the north, east, and west had similar values (Appendix 2.3), suggesting the high-elevation ice-fields that separated the northern and southern units influenced snow conditions. Thus, we used sheep survey data from units 1 (Mentasta Mountains), 2 (Mount Sandford), 4E (Cross Creek), 4W (Nikonda Creek), 5E (Mount Allen), 5W (Stone Creek), 7W (Chisana) and 10 (Mount Drum), alongside that of the JSU, unit 3 (Figure 2.1).

2.3.3 Sheep Surveys

Sheep survey data was obtained from a collated dataset of state and federal monitoring surveys conducted by ADF&G and NPS. A study period of 1980 to 2017 was determined by the availability of meteorological forcing data for SnowModel (see below), and within this period 19 years of sheep survey data were available from 41 surveys in our selected survey units (Appendix 2.1, Figure 2.1). The earliest survey date was 21st June and the latest the 4th of August. Mean lamb-to-ewe ratio was 0.30 (Max. = 0.55; Min. = 0.09, SD ±0.10) and the mean total sheep counted in each survey was 654 (Max. = 2549 Min. = 87, SD ±564). Surveys were conducted using either a small fixed-wing plane or by helicopter and all followed a minimum count method (Wells, 2018). We note that aerial minimum count methods are subject to potential biases in comparison to distance-based population estimates (Schmidt et al., 2012) but we only use full surveys, i.e. where the entire Survey Unit is reported as covered, in our dataset. The difficulty of distinguishing the sex of non-mature Dall's sheep via aerial survey can lead to yearlings of both sexes and small-horned rams often being counted as ewes. A 'ewe-like' category is often used due to this uncertainty, and we therefore used reported 'ewe-like' counts as the denominator in lamb-to-ewe ratios where they are available. While this ratio is not a perfect measure of productivity because it is affected by a combination of factors including parturition rates, lamb survival, and adult survival, the juvenile-to-female ratios have been shown to be a useful measure of productivity in other ungulate species because the majority (96%) of the variation in the ratio is caused by variation in juvenile survival (Gaillard et al., 1998). The inclusion of 'ewe-likes' leads to lower values than the true lamb-to-ewe ratio, but it is still a useful index of productivity and has been used as such in other Dall's sheep studies (van de Kerk et al., 2018; Rattenbury et al., 2018).

2.3.4 SnowModel

Snow and climate covariates were produced using SnowModel (Liston and Elder, 2006) at a daily timestep for the Jacksina study domain. SnowModel has been used successfully in wide variety of latitudinal settings and has previously been used for studies in continental Alaska and mountain regions (Liston et al., 2002; Mahoney et al., 2018; Sexstone et al., 2018) SnowModel's five sub-models, MicroMet (Liston et al., 2006), EnBal (Liston, 1995), SnowPack (Liston and Hall, 1995), SnowTran-3D (Liston et al., 2007), and SnowAssim (Liston and Hiemstra, 2008) in combination with topographic, land cover and meteorological data simulate a comprehensive set of snowpack evolution processes in a physically based manner (please refer to sub-model references for details on their physics and validation). MicroMet ingests meteorological data and distributes them throughout the model domain at each timestep on the basis of known relationships between landscape and meteorological variables. EnBal simulates the surface energy exchange according to the meteorological data distributed by MicroMet and snow evolution from the previous timestep. SnowPack evolves snow depth, density, and temperature according to precipitation input and surface conditions produced by EnBal. Last in the modelling process, SnowTran-3D redistributes snow in response to the interaction between the wind-fields at each timestep, surface topography, and vegetation snow holding capacity. SnowAssim allows the user to input in-situ or remotely sensed measurements of snow water equivalent and corrects the precipitation forcing retroactively before a second model simulation. A workflow diagram of the modelling procedure can be found in the Supplementary Materials (Appendix 2.5).

We obtained meteorological data from the NASA Modern Era Retrospective-Analysis for Research and Applications Version 2 (MERRA-2; Gelaro et al., 2017). This gridded climate data is available hourly from 1980 to present at a resolution of 0.5º latitude to 0.625º longitude (~55 km by ~32 km). We aggregated the hourly surface forcing variables from 16 grid points covering the study domain into daily values, using the meteorological inputs required by MicroMet; temperature, relative humidity, wind speed, wind direction and precipitation. The topographic and vegetation layers required by SnowModel were derived from the Advanced Spaceborne Thermal Emission and Reflection Radiometer Global Digital Elevation Model Version 2 (ASTER GDEM; NASA/METI/AIST/Japan Spacesystems, 2009) and the National Land Cover Database 2011 (NLCD; Homer et al., 2015) respectively. We conducted a simple analysis of the land cover change in each of the 9 survey units by cropping a further dataset, the NLCD 2011 Land Cover Alaska 2001 to 2011 From To Change Index (U.S. Geological Survey, 2015), and analysing the extent of landcover change from 2001 to 2011. Of the 8678 km^2 of all 9 units, only 27 km^2, or 0.32%, had been classified in this dataset has having changed in landcover over the 10 year period (Appendix 2.4). We do not believe that the rate and magnitude of this change was fast or great enough to impinge on Dall's sheep populations within the timeframe of this study, and we therefore kept land cover as a static layer in the modelling procedure. The ASTER GDEM was chosen for its complete coverage of the study domain and comparable 1-arc second resolution to the 30 m NLCD data. It was resampled (bilinear) to this resolution and reprojected into the Alaska Albers Equal Area Conic coordinate reference system to match that of NLCD. To cover the JSU, a domain of 1680 by 2244 30-m grid cells (~50 km by 67 km) was created. The 30 m resolution represents a balance between computational efficiency and the ability of the model to simulate important features of the snowscape, e.g., wind-blown areas and drifts, that occur in mountainous regions.

2.3.5 Snow surveys

We obtained ground-based snow observations from September 2016 to August 2017 to calibrate and validate SnowModel. We installed 22 Reconyx Hyperfire PC900 (Reconyx, 2017) time-lapse cameras in two areas of the domain, Jaeger Mesa (~1600 m to ~2100 m elevation) and a site near Rambler Mine, Nabesna (~900 m to ~1200 m elevation). Each camera was aimed at a 1.5 m tall snow stake with bands every 5 cm, and cameras were programmed to take hourly photos (Figure 2.2). Camera sites were selected to capture gradients in elevation, vegetation and aspect with consideration for field safety in steep and rugged terrain. We conducted snow surveys in and around the camera sites from 18th to 24th March 2017. A snow pit was excavated at a randomly selected location within 5 m of each camera and we recorded the stratigraphic profile, the temperature profile at 10 cm intervals using a digital thermometer, and the density profile double-sampled at 10 cm intervals using a Snowmetrics 1000c cutter and a digital scale. For ingestion into SnowAssim, the mean density of the double sample at each interval was calculated and converted into snow water equivalent (SWE). The product of each interval's SWE was then used to calculate the bulk SWE for each pit location. In total 18 pits were possible with the remaining 4 cameras being located in areas that were snow-free. Alongside the snow pit measurements, 7806 snow depth measurements were taken and recorded using both manual and automated methods (Sturm and Holmgren, 2018), with location recorded by GPS in both instances. These measurements were obtained at 2 m intervals using 4 sampling configurations: (1) 50 m transects in a cross-pattern from each camera site, (2) transects following the elevation gradient between cameras grouped by aspect on the east and west sides of Jaeger Mesa and at Rambler Mine, (3) 50 m 'spirals' randomly located on top of Jaeger Mesa, and (4) a sequence of traverses running north-to-south, east-to-west and along the edge of the northern tip of Jaeger Mesa. This sampling strategy was conducted to characterise different scales of snow-depth variability in different configurations of topography and vegetation.

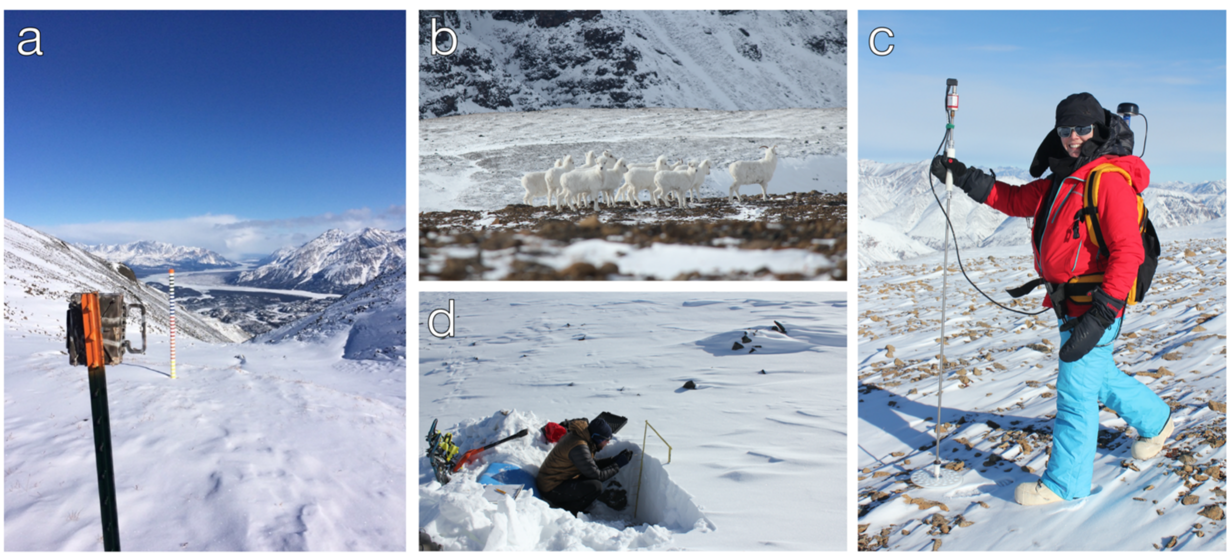

Figure 2.2. (a) Remote camera and snow stake installation looking northeast to the Nabesna river from Jaeger Mesa on 20th March 2017. Note the wind-blown, snow free areas on the slopes to the immediate sides of the snow stake. Photo C. Cosgrove. (b) Nursery band of Dall's sheep on Jaeger Mesa. (c) Laura Prugh operating the Magnaprobe to survey snow depth atop Jaeger Mesa. Photo Anne Nolin. (d) Chris Cosgrove surveying a snow pit for stratigraphy, temperature and density profile. Photo L. Prugh.

2.3.6 Calibration of SnowModel

A fundamental first step in improving the modelled description of snow evolution is to assess and correct the precipitation forcing ingested in the model. To do this, SnowAssim was utilised with our recorded SWE measurements in low-elevation, sparsely forested areas near Rambler Mine within a modelling run from 1st September 2016 to 1st April 2017. Using only the forested SWE data protected against error caused by assimilating SWE values from areas subject to greater wind redistribution. The synoptic scale of precipitation in the region is greater in size than that of the modelling domain, so the precipitation accumulating in low-elevation forest areas is proxy to that falling in high elevations but is less likely to be highly redistributed by wind. A precipitation correction factor of 0.37 was found using this procedure and hence applied to the precipitation forcing from 1980 to 2017.

To reproduce the field-observed patterns of snow distribution in our model simulations, we compared snow depth, density and water equivalent field measurements from a subset of the domain to their equivalent modelled outputs. Given the focus of this study on snow conditions in Dall's sheep habitat (see below), we calibrated the model for optimum performance at high-elevations and thus used only field observations from alpine areas in this part of the calibration procedure.

Initial examination of the wind forcing data derived from MERRA-2 revealed it to be insufficiently strong to redistribute snow, a potential bias in the original data but also likely due to the suppression caused by aggregating hourly data into daily values. As snow density and wind speed interact with one another, we adjusted a scalar increasing the windspeed in the meteorological forcing data and a SnowModel parameter controlling the snow density evolution together. After an initial sensitivity analysis, our calibration involved 72 SnowModel simulations from 1st September 2016 to 1st April 2017 with the density adjustment factor ranging from 2.0 to 10.0 in increments of 1.0, and the wind speed scalar ranging from 1.5 to 5.0 in increments of 0.5. To establish the best calibration, each snowpit-observed bulk snow density measurement was compared to the modelled bulk snow density in the equivalent model grid-cell and the Root Mean Squared Error (RMSE) was computed. Using the same procedure, observed snow depth was compared to modelled snow depth, with observed snow depths being aggregated into a mean value for each grid cell given the high resolution of our depth surveys. Additionally, for the grid cells where bulk density was available, we compared observed SWE to modelled SWE. RMSE values for density, depth, and SWE were ranked among the 72 simulations, and the mean ranking of each simulation was then calculated. The parameters from the top-ranked calibration were then used to model snow properties for the study domain from September 1st 1980 to August 31st 2017. To further test the calibration, a validation was conducted using the snow depths acquired from the remote camera installations.

2.3.7 Model derived covariates

To limit our modelled snow properties to Dall's sheep habitat, we selected only pixels that correspond to their preferred land cover above 1200 m. Roffler et al. (2017; see supplementary materials), found this elevation to be the lower limit of Dall's sheep core habitat in WRST using locations of sheep observed during surveys, albeit for summer months. To delineate the land cover that Dall's sheep select for, we included only pixels corresponding to the Dwarf Shrub and Barren Land classifications in the NLCD product (Homer et al., 2015). This follows numerous studies that have found that Dall's sheep select for open, sparsely vegetated areas at mid- to high-elevations (e.g. Geist, 1971), and recent habitat selection models driven by GPS-collar data have confirmed this (Mahoney et al., 2018). We recognise that Dall's sheep may use lower elevations in winter, but there are no currently published data describing their winter distribution in our study region.

Four snow covariates were derived for comparison to the following summer's lamb-to-ewe ratios: mean snow depth, mean snow density, total snowfall and percent 'forageable area'. Additionally, we included SnowModel-derived mean air temperature as a climate covariate. For mean snow depth, mean snow density, total snowfall, and mean air temperature, the daily mean was found for all grid cells matching the above criteria first. Seasonal means (fall = September, October and November; winter = December, January and February; spring = March, April and May) were then calculated from the daily data in the case of mean snow depth, mean snow density and mean air temperature, whereas the daily data was summed by season for total snowfall. Higher incidences of snow depth, snow density and snowfall were expected to be deleterious to Dall's sheep productivity, with increases in air temperature anticipated to lead to increases in lamb-to-ewe ratios. The final covariate, mean percent 'forageable area', was calculated as the seasonal mean of the daily percentage of Dall's sheep habitat with snow depth beneath half-chest height (0.25 m) and snow density beneath 330 kg m^{-3}. These snow conditions were found by Mahoney et al. (2018), and confirmed in the field by Sivy et al. (2018), to be selected by Dall's sheep at movement scales typical of foraging behaviour. We hence expected greater percentages of forageable area to correlate with increased

Dall' sheep productivity. To test whether there was a delayed effect from conditions in the previous snow season to parturition, i.e. >1 yr previous to the summer of sheep survey, we also calculated aggregate metrics for all of the above variables for both the previous summer (reported as 'Previous Summer') and all months where snow cover is a dominant feature in the study area (September through May, reported as 'Previous Year').

2.3.8 Statistical Analyses

To examine the relationships between the model derived snow and climate metrics and lamb-to-ewe ratios, we employed multiple regression models after a covariate selection process. All analyses were conducted in the R program (R Core Team, 2019). As a first step we tested whether the inclusion of Survey Unit as a random effect was significant in models using each of our seasonal snow and climate covariates as a single predictor. To do this we used ANOVA to test for significant difference between paired models of the same predictor but fitted with and without Survey Unit as a random effect using the R package nlme (Pinheiro et al., 2019). At this step, all models were fitted using restricted maximum likelihood (REML) to allow for valid comparison between the model with and the model without the random effect (Zuur et al., 2009) and we additionally tested a null model. We then ranked each single predictor model and the null model, when fitted without the addition of the random effect term and using Ordinary Least Squares (OLS), by their second-order Akaike Information Criterion (AICc). Covariates that were found to be ranked higher than the null model as single predictors were subsequently considered as additional additive terms in multiple regression models. To avoid over-parameterization on a small dataset we restricted the number of predictors per model to three and excluded any covariates that had a collinearity of greater than 0.7 in the same model. The final list of single- and multi-predictor models was finally ranked by their AICc to discern which snow and climate covariates had the greatest explanatory power in isolation or combination. Linear regression was used to test for trends in covariate values from 1980 to 2017 by season. Likewise, the coefficient of variation (CV) was calculated for a rolling 10-year window for each snow and climate metric, and linear regression was used to test whether the degree of interannual variability increased over time. An alpha of 0.05 was used for evaluating statistical significance throughout, with the exception of testing each productivity model's intercept and predictor estimates, where a Bonferroni-corrected alpha level, as calculated by alpha divided by the total number of models in the final list, is reported to reduce the chance of type 1 error.

2.4 Results

2.4.1 SnowModel Calibration

The parameter combination that best produced our observations of depth, density and SWE was a density adjustment factor of 6.0 and a wind speed increase of 2.5, producing RMSEs of 0.09 m snow depth, 31.71 kg m^{-3} snow density and 0.04 m SWE (Appendix 2.6 and Appendix 2.7). Taking the snow depth from images recorded daily at 12:00 Alaska Standard Time, there were 4996 available days of data from 17 cameras located outside of forested and shrub areas. Comparison of the camera snow depth to model snow depth yielded an RMSE of 0.08 m, which is comparable to that from the spatial calibration albeit with an average 0.06 m bias towards over estimation (Appendix 2.8).

2.4.2 Summary of sheep surveys and modelled snow and climate metrics

Of the 41 surveys across 19 years included in the analysis (Appendix 2.1), the mean lamb-to-ewe ratio was 0.30 (±0.10 SD), with a maximum of 0.55 sampled in the Mount Drum survey unit in 1981 and a minimum of 0.09 sampled in Jacksina in 1993. Snow depths in fall (mean = 0.28 m ±0.06 SD) were always lower than both winter (mean = 0.40 m ±0.06 SD) and spring (mean = 0.42 m ±0.07 SD), which generally had a similar mean snow depth and closely followed the interannual variability established in fall (Appendix 2.9; Figure 2.3).

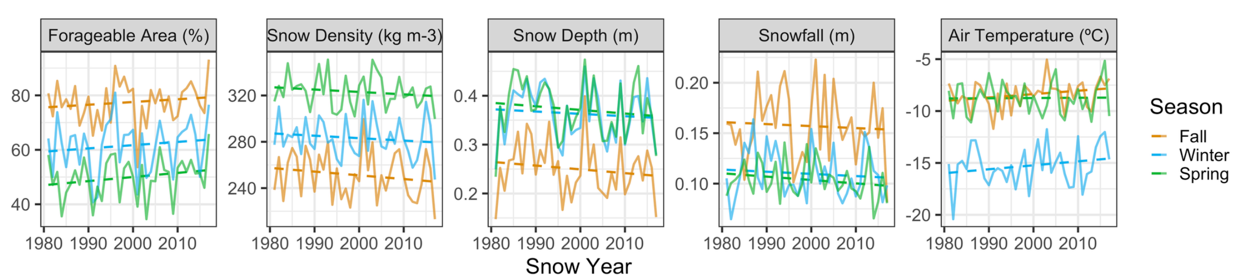

Figure 2.3. Time series and trends of each snow and climate covariate by season 1980 to 2017 within the Jacksina sheep survey unit within Wrangell-St. Elias National Park and Preserve, Alaska. Note the similar pattern of snow depth year-on-year across all three seasons and the close similarity of the mean snow depth in winter and spring.

2.4.3 Model derived covariates and lamb-to-ewe ratios

The addition of Survey Unit as a random effect was not shown to be significant for any of the initial single predictor models (see Appendix 2.10). Hence, we continued our model selection with models fitted by OLS. When comparing the single predictor models of each snow and climate covariate 11 models were ranked higher by AICc than the null model (Appendix 2.10), none of which contained a covariate pertaining to the previous year's Summer or snow season indicating that there wasn't a delayed-effect from the previous snow season. Of the covariates ranked higher than the model only snowfall (fall, winter, and spring in order of weighting) and air temperature (fall) were found to be under the cut-off for collinearity. Fall snowfall and fall air temperature were therefore used in two and three predictor linear models in combination with the other covariates leaving 40 models, inclusive of the null model, in our final list (see Appendix 2.11).

Of the top ranked models, 5 are shown to be well supported (ΔAICc < 2) and all include a seasonal covariate of snow depth and fall air temperature in their predictors (Table 2.1). The highest ranked model, fall snow depth and fall air temperature has an adjusted R-squared of 0.41 and is significant to the Bonferroni-corrected alpha level for the intercept and fall snow depth terms, and alpha for fall temperature (Table 2.1). Coefficients from this model indicate that increases in fall snow depth and decreases in fall air temperature lead to a decline in the following summer's lamb-to-ewe ratio (Figure 2.4). All models that contain snow depth as a term outperform models using other snow and climate metrics (see Appendix 2.11). Estimates of snow depth, snow density and snowfall in all models indicate that increases in these variables decreased lamb-to-ewe ratios, whereas estimates for air temperature and forageable area showed a positive relationship between these predictors and lamb-to-ewe ratios, following expected relationships (Table 2.1).

Table 2.1. Top 10 models as ranked by second order Akaike Information Criterion (AICc). Standard error (SE) shown in brackets for both the intercept and estimate of each predictor in each model. 1st Predictor indicates the 1st snow and climate covariable listed in the Model column. ** indicates significance at a Bonferroni corrected alpha level of 0.00125 (alpha / total models); * indicates significance at alpha = 0.05. P-values were computed in R by the Wald test method via use of the 'summary' core package (R Core Team, 2019).

Model	Intercept (SE)	1st Predictor Estimate (SE)	Fall Air Temperature (SE)	Fall Snowfall (SE)	K	Delta AICc	AICc weight	R-Sq.	Adjusted R-Sq.
Fall Snow Depth + Fall Air Temperature	0.690 (0.094)**	-0.738 (0.193)**	0.027 (0.012)*	–	3	0	0.188	0.439	0.41
Winter Snow Depth + Fall Air Temperature + Fall Snowfall	0.900 (0.112)**	-0.599 (0.214)*	0.032 (0.012)*	-0.818 (0.398)*	4	0.134	0.176	0.472	0.429
Spring Snow Depth + Fall Air Temperature + Fall Snowfall	0.851 (0.111)**	-0.522 (0.192)*	0.027 (0.013)*	-0.940 (0.388)*	4	0.523	0.145	0.467	0.424
Fall Snow Depth + Fall Air Temperature + Fall Snowfall	0.780 (0.114)**	-0.593 (0.219)*	0.030 (0.012)*	-0.593 (0.435)	4	0.592	0.14	0.466	0.423
Winter Snow Depth + Fall Air Temperature	0.792 (0.103)**	-0.738 (0.211)**	0.029 (0.012)*	–	3	1.963	0.071	0.412	0.381
Fall Snow Depth	0.511 (0.046)**	-0.895 (0.187)**	–	–	2	2.328	0.059	0.37	0.354
Spring Snow Depth + Fall Snowfall	0.689 (0.081)**	-0.720 (0.173)**	–	-0.848 (0.402)*	3	2.374	0.057	0.406	0.375
Spring Snow Depth + Fall Air Temperature	0.706 (0.099)**	-0.623 (0.199)*	0.023 (0.014)	–	3	3.949	0.026	0.383	0.35
Fall Snow Depth + Fall Snowfall	0.552 (0.068)**	-0.818 (0.211)**	–	-0.367 (0.452)	3	4.084	0.024	0.381	0.348
Spring Snow Depth	0.577 (0.064)**	-0.788 (0.177)**	–	–	2	4.45	0.02	0.336	0.319

2.4.4 Trends and variance in seasonal covariates 1980 to 2017

No statistically significant trends were found for modelled snow metrics from 1980 to 2017 (Appendix 2.12; Figure 2.3). However, model estimates indicated decreasing snowfall, snow depth and snow density, and increasing forageable area and air temperature for all seasons (Figure 2.3). The interannual variation in winter snow density significantly increased during the time series (Appendix 2.13; Figure 2.5). In contrast, winter snowfall was found to be significantly less variable over time (Appendix 2.13; Figure 2.5). The highest interannual CVs (non-rolling) occurred in fall for both snow depth (CV = 22.21 %) and snow density (CV = 8.06 %), winter for both snowfall (CV = 21.87 %) and forageable area (CV = 15.46 %), and spring for air temperature (CV = 17.36%; Appendix 2.9).

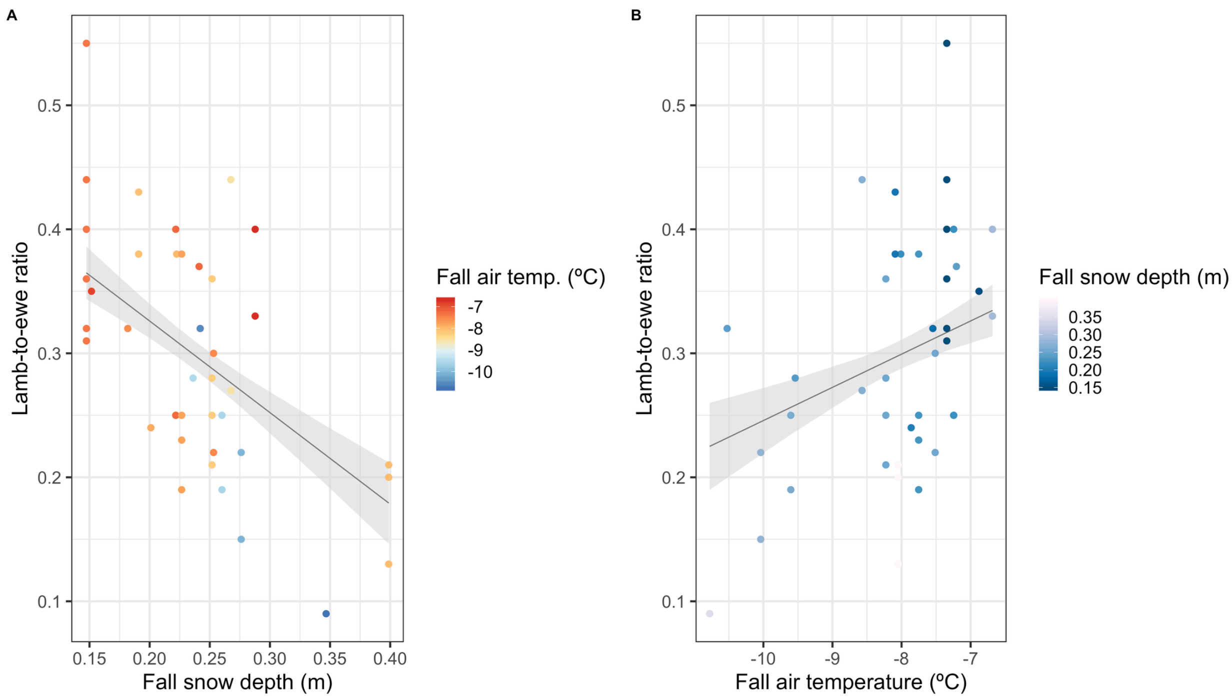

Figure 2.4. A) An increase in fall mean snow depth decreases Dall's sheep summer productivity, here defined as lamb-to-ewe ratio, whereas B) increased fall mean air temperature increases summer productivity. Estimates and the shaded grey 95 % confidence interval are derived from the top model as ranked by AICc in Table 3.

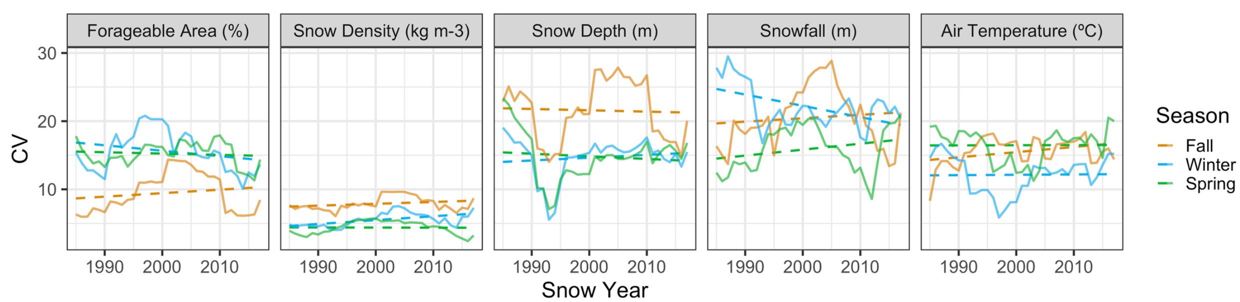

Figure 2.5. Time series of 10-year rolling coefficient of variability (CV) for each snow and climate covariate by season within the Jacksina sheep survey unit within Wrangell-St. Elias National Park and Preserve, Alaska.

2.5 Discussion

The impact of changing snow conditions on wildlife in northern ecosystems is of both ecological and societal concern as these remote regions are signalling major impacts of accelerated warming (Callaghan et al., 2011). However, studies are limited by data that are scarcely distributed in time and space in the region, especially in alpine areas (Boelman et al., 2018), and there remains uncertainty as to when and what snow conditions are most important to wildlife demography. Here we use a spatially distributed snow model to simulate snow and climate conditions over 37 years in the northern Wrangell-St Elias National Park and Preserve (WRST) to better understand the influence of snow properties on the dynamics of Dall's sheep. Snow conditions, most notably increased snow depth, were strongly associated with declines in Dall's sheep productivity, with decreased air temperature and increased snowfall also leading to decreased lambs being observed in summer, though with less predictive power in comparison to snow depth. Our top-ranked model(s) indicated that fall was the time period that these snow and climate conditions were most important. These findings suggest that challenging snow conditions that persist throughout the snow year, as per our first hypothesis, are more important to Dall's sheep productivity than conditions during the spring lambing season, as described by our second hypothesis.

Similar to other alpine and Arctic ungulates, Dall's sheep access forage by either 'cratering', wherein they dig through the snow, or by finding snow-free areas. Deeper snow has been shown to reduce foraging efficiency in studies of other ungulates, potentially leading to increased caloric deficit and decreased birth mass in offspring (Couturier et al., 2009; Robinson and Merrill, 2012). Thus, early establishment of deep snow conditions may lead to energetically challenging conditions over many months, protractedly decreasing the body condition of ewes and therefore decreasing their ability to successfully produce, protect and nurse healthy lambs in the weeks immediately after birth. The significance of Fall air temperature as an additional term in the top models further suggests that early-season calorific expenditure, through the increased cost of thermoregulation in this instance (Jensen et al., 1999), is more damaging to productivity than that occurring closer to lambing.

Two recent large-scale studies stand in contrast to our results. Van de Kerk et al. (2018) and Rattenbury et al. (2018) found that the date of snow disappearance best predicted Dall's sheep productivity, with later dates resulting in lower lamb-to-ewe ratios. Both studies noted that this relationship was weaker at lower latitudes, including that of WRST, and suggested the comparatively extended growing season in these ranges may buffer the effect of severe winters due to increased forage abundance and quality. However, van de Kerk et al. (2018) additionally found that snow cover duration, i.e. the number of days snow is present each winter, also had an effect on lamb-to-ewe ratios, albeit relatively weaker than snow disappearance date, and hence proposed that extended exposure to difficult conditions is less important than the snow cover immediately before or after to lambing. Snow disappearance dates depend on the energy balance of a snowpack, along with weather conditions and other variables. Thin, low density snow cover can extend later into the year if air temperatures are cool enough to preserve it, while deep, dense snows can rapidly disappear due to early spring conditions with high temperatures and rain (McCabe et al., 2007). Hence, inference of the vertical properties of snow from its extended presence in remote sensing data is not always reliable and cannot describe the evolution of snow depth and density throughout the entirety of a snow season. Our methods here highlight the importance of vertical snow properties on northern wildlife such as Dall's sheep and show that detailed, local analyses of snow properties can reveal new insights that range-wide remote sensing methodologies, such as van de Kerk et al. (2018) and Rattenbury et al. (2018), may not be able to detect. Our results also compare well statistically; while van de Kerk et al. (2018) do not report comparable metrics, for the Nabesna area within their analysis, which is within our study area, Rattenbury et al. (2018; see Figure 2.4) report an R-squared of 0.33, which is lower than our top model's adjusted R-squared of 0.41.

The effects of snow on the movement, habitat selection, and energetics of various wildlife has been relatively well studied (Boelman et al., 2018), but there is a lack of evidence linking the impact of snow conditions on fine-scale behavior to broad-scale demographic consequences (Mahoney et al., 2018). Mahoney et al. (2018) found that Dall's sheep in Lake Clark National Park strongly favoured areas of less dense, shallow snow at fine-scale movements associated with foraging, illustrating that habitat selection is affected by snow density as well as depth. Forageable area, a variable derived from the area available below a threshold density and snow depth found in Mahoney et al. (2018), showed relatively poor predictive power (Appendix 2.10). This was unexpected given the forageable area metric's increased detail and foundation in field observations (Sivy et al., 2018). However, we suggest that an explanation for this might be that the *actual* forageable area is quite different from the *modelled* forageable area. For example, low-snow or snow-free areas might be devoid of forage or, even if forage is present, these areas might be in terrain that is avoided by Dall's sheep due to predation risk. Mean snow depth, conversely, is highly ranked for all seasons and is possibly a more reliable metric for describing the relative efficiency of winter foraging behaviour.

Here we have focused on the impact of snow conditions on Dall's sheep productivity. However, it is important to note that productivity and survival are influenced by additional factors, including predation and interspecific population dynamics (e.g. Burles and Hoefs, 1984; Murie, 1944; Arthur and Prugh, 2010), forage quantity and quality (e.g. Burles and Hoefs, 1984; Rachlow and Bowyer, 1994), and in rare cases by disease (e.g. Murie, 1944). Other mountain ungulates have shown declines in productivity in response to high population densities and climactic forcing (e.g. Jacobson et al., 2004; Portier et al., 1998; Serrano et al., 2011; White et al., 2011). However, a preliminary study of a simple regression of density (as calculated by the total number of surveyed adult sheep, inclusive of yearlings, divided by the area of the Survey Unit) vs lamb-to-ewe ratios in our dataset did not show any relationship suggesting density dependence was not important in our study area. This follows the findings of van de Kerk et al. (2018; see Appendix 2) that found no effect of the survey date and population density on lamb-to-ewe ratios and used data from a much larger, range-wide dataset of 534 surveys. However, habitat-selection models of Dall's sheep, e.g. Roffler et al. (2017), suggest that Dall's sheep likely utilize only certain locations of the Survey Units they are reported within, e.g. areas predominantly near escape terrain and devoid of tall vegetation. Hence, the simple calculation of density described above, and used by van de Kerk et al. (2018), is likely to be prone to underestimation and vary in accuracy according to the relative abundance of preferred habitat in each Survey Unit. We therefore suggest that further work incorporates insights from habitat selection modelling to better test for any density dependence on productivity in Dall's sheep.

In response to other studies that show a lagged effect of snow and climate conditions on the body condition and parturition rate of other ungulates (e.g. Boertje et al., 2019; Serrano et al., 2011) we tested the importance of the previous summer's and the previous snow season's snow and climate conditions on productivity. No significant relationships were found (Appendix 2.10), suggesting that the snow and climate conditions for the season immediately before lambing are more important for productivity. Our dataset however does not include variables pertaining to the quality of vegetation available to ewes in the summer preceding or current to lambing. Both early (Hoefs, 1984) and more recent work (van de Kerk et al., 2020) has connected metrics of summer forage quality with both lamb survival rates (Hoefs, 1984; van de Kerk et al., 2020) and Dall's sheep productivity (Hoefs, 1984). Also beyond the scope of the current study are the effects of interspecific relationships. The primary predators of Dall's sheep, coyote (*Canis latrans*) and golden eagles (*Aquila chrysaetos*), have been shown to account for less lamb mortality in summers with a high Normalized Difference Vegetation Index (NDVI) (van de Kerk et al., 2020) and are likely to prey more on Dall's sheep during years with low snowshoe hare numbers (Arthur and Prugh, 2010;

Burles and Hoefs, 1984). To gain a more holistic understanding of Dall's sheep productivity and population dynamics, attention needs to be paid to a wide range of biotic and abiotic factors that are not considered here. The adjusted R-squared of our top ranked model with only snow properties included (fall snow depth, R-sq. = 0.35; Table 2.1), is likely indicative of our narrow focus. However, our findings do illustrate that snow properties, and in particular their early establishment, are important factors for Dall's sheep productivity and stand to inform further research into population dynamics of Dall's sheep and other wild ungulates.

Seasonal snow throughout the northern hemisphere is being altered in terms of its coverage, timing, duration and physical properties as a response to climate change (Liston and Hiemstra, 2011). The increase in extreme events, such as late snow disappearance in spring 2013 in Alaska, are considered a likely product of climate change that might impinge on Dall's sheep productivity (Coumou and Rahmstorf, 2012). However, we found no evidence that snow conditions important to Dall's sheep productivity have markedly changed in WRST from the long-term mean or have increased in terms of interannual variability during our study period. This may be due to the sub-Arctic location of northern WRST in Alaska's dry interior where changes to the form and volume of precipitation are less pronounced than in wetter and warmer maritime regions (Liston and Hiemstra, 2011).

Verbyla et al. (2017) noted substantial differences in climate and snowline elevation throughout Dall's sheep ranges and found that the mean snow line elevation on May 15th had pronounced interannual variability in the central and eastern Brooks Range. It is in these Arctic Alaskan ranges that are on the fringe of suitable Dall sheep habitat where the greatest population decreases in Dall's sheep have been observed, prompting emergency harvest closures in some areas (Alaska Department of Fish and Game, 2014). Dall's sheep sensitivity to spring snow conditions at these high latitudes has been established by van de Kerk et al. (2018) and Rattenbury et al. (2018), and it may be that higher interannual variability in the elevation of spring snow line, potentially indicating a greater frequency of extreme events, is responsible for the recent declines in Dall's sheep populations in these areas (van de Kerk et al., 2018; Rattenbury et al., 2018; Verbyla et al., 2017). Dall's sheep populations in *sub*-Arctic ranges in Alaska, including WRST, have population trends that are generally regarded as being stable, with the exception of the maritime Kenai peninsula (Alaska Department of Fish and Game, 2014). If the impact of climate change on snow conditions in these ranges has yet to be acute, such as in the case of our results, it is possible that low-latitude interior mountain ranges may represent refugia for Dall's sheep and other snow-influenced alpine species (Keppel et al., 2012). Wildlife populations, particularly those that have low reproductive rates like Dall's sheep, may be resilient to sporadic extreme conditions but become vulnerable if extreme conditions become more frequent (Boyce et al., 2006). Hence, further work examining regional, long-term trends in the interannual variability of snow conditions would prove valuable in determining where climate change poses the greatest threat to alpine wildlife populations.

Our modelling approach combined with several decades of survey data demonstrated seasonal variation in the impact of snow conditions on Dall's sheep productivity in Wrangell-St Elias National Park and Preserve. However, some caution should be exercised when extending our results to other regions given the specificity and assimilation of in-situ data from our study area. While our methodological approach yields novel insights regarding seasonal snow properties in comparison to alternative approaches using optical remote sensing datasets, it also comes with its own inherent disadvantages, including limited spatial coverage, high computational demand, necessity of technical expertise, and inherent uncertainties when modelling a physical environment. Although we conducted intensive field surveys to improve the calibration of our model, these surveys occupied a small spatial and temporal extent within the larger modelling domain. This is despite efforts made to sample a wide representation of elevation, aspect and landcover during snow surveys and the installation of remote cameras. With data lacking to test the model against in-situ measurements from previous years it is possible that the model is only representative to its calibration year. While this is an important source of uncertainty, the small RMSE and bias shown in our calibration and temporal validation results does suggest our approach has promise in long-term studies of other wildlife, especially so where there are in-situ, long-term snow and meteorological datasets for model-forcing and assimilation.

2.6 Conclusions

The establishment of a deep snowpack in fall alongside low fall temperatures was found to best explain decreased Dall's sheep productivity during the following summer. An incremental effect of season-long environmental conditions on ewe body condition hence appears to be of greater importance than spring snow conditions in our study area, a finding contrary to studies based on snow cover rather than depth (van de Kerk et al., 2018; Rattenbury et al., 2018). Our results potentially demonstrate an important link between known fine-scale effects of snow conditions, i.e. selection of shallow and/or less dense snow, with broad-scale patterns of demography. We hence propose that our utilization of a spatially distributed snow model has scope for application in studies of other snow-influenced wildlife. Though additional data that establishes direct links between snow properties, animal movements and body condition, forage opportunity, and infant survival rates are needed for a complete mechanistic understanding of snow impacts. We found no significant trends in the long-term mean, or in a rolling measure of interannual variation, of modelled snow properties that were shown to be important to Dall's sheep productivity. Climate change hence appears to not yet be having a strong effect on snow conditions in our study domain, a result that is of broader ecological interest. However, if climate change does lead to major changes in future snow depths, our findings indicate that Dall's sheep productivity may be strongly affected.

2.7 Acknowledgements

Major thanks go to Glen Liston for assisting in the calibration and running of SnowModel. NASA ABoVE grants to Anne Nolin (NNX15AV86A) and Laura Prugh (NNX15AU21A) funded this research. The Ellis family in Nabesna, AK and 40 Mile Air in Tok, AK greatly aided field logistics. Kelly Sivy and Anika Pinzner assisted with the field surveys. We thank the ADF&G, NPS and contracted (e.g. pilots) personnel who conducted the sheep surveys. Comments and insight from the academic editor and 3 reviewers appreciably improved the paper.

2.8 References

Alaska Department of Fish and Game, 2014. Trends in Alaska Sheep Populations, Hunting, and Harvests. Division of Wildlife Conservation, Wildlife Management Report ADF&G/DWC/WMR-2014-3, Juneau.

Arthur, S.M., Prugh, L.R., 2010. Predator-Mediated Indirect Effects of Snowshoe Hares on Dall's Sheep in Alaska. J. Wildl. Manag. 74, 1709–1721. https://doi.org/10.2193/2009-322

Bieniek, P.A., Bhatt, U.S., Thoman, R.L., Angeloff, H., Partain, J., Papineau, J., Fritsch, F., Holloway, E., Walsh, J.E., Daly, C., Shulski, M., Hufford, G., Hill, D.F., Calos, S., Gens, R.,

2012. Climate Divisions for Alaska Based on Objective Methods. J. Appl. Meteorol. Climatol. 51, 1276–1289. https://doi.org/10.1175/JAMC-D-11-0168.1

Boelman, N., Liston, G.E., Gurarie, E., Meddens, A.J.H., Mahoney, P.J., Kirchner, P.B., Bohrer, G., Brinkman, T.J., Cosgrove, C.L., Eitel, J., Hebblewhite, M., Kimball, J.S., LaPoint, S.D., Nolin, A.W., Pedersen, S.H., Prugh, L.R., Reinking, A.K., Vierling, L., 2018. Integrating snow science and wildlife ecology in Arctic-boreal North America. Environ. Res. Lett. https://doi.org/10.1088/1748-9326/aaeec1

Boertje, R.D., Frye, G.G., Young, D.D., 2019. Lifetime, known-age moose reproduction in a nutritionally stressed population. J. Wildl. Manag. 83, 610–626. https://doi.org/10.1002/jwmg.21613

Bokhorst, S., Pedersen, S.H., Brucker, L., Anisimov, O., Bjerke, J.W., Brown, R.D., Ehrich, D., Essery, R.L.H., Heilig, A., Ingvander, S., Johansson, C., Johansson, M., Jónsdóttir, I.S., Inga, N., Luojus, K., Macelloni, G., Mariash, H., McLennan, D., Rosqvist, G.N., Sato, A., Savela, H., Schneebeli, M., Sokolov, A., Sokratov, S.A., Terzago, S., Vikhamar-Schuler, D., Williamson, S., Qiu, Y., Callaghan, T.V., 2016. Changing Arctic snow cover: A review of recent developments and assessment of future needs for observations, modelling, and impacts. Ambio 45, 516–537. https://doi.org/10.1007/s13280-016-0770-0

Boyce, M.S., Haridas, C.V., Lee, C.T., the NCEAS Stochastic Demography Working Group, 2006. Demography in an increasingly variable world. Trends Ecol. Evol. 21, 141–148. https://doi.org/10.1016/j.tree.2005.11.018

Brown, R., Vikhamar Schuler, D., Bulygina, O.N., Derksen, C., Luojus, K., Mudryk, L.R., Wang, L., Yang, D., 2017. Arctic Terrestrial Snow Cover, in: Snow, Water, Ice and Permafrost in the Arctic (SWIPA) 2017. Arctic Monitoring and Assessment Programme (AMAP), Oslo, Norway. (www.amap.no).

Bunnell, F.L., 1982. The lambing period of mountain sheep: synthesis, hypotheses, and tests. Can. J. Zool. 60, 1–14. https://doi.org/10.1139/z82-001

Burles, D.W., Hoefs, M., 1984. Winter mortality of Dall sheep, Ovis dalli dalli , in Kluane National Park, Yukon. Can. Field-Nat. 98(4), 479–484.

Callaghan, T.V., Johansson, M., Brown, R.D., Groisman, P.Ya., Labba, N., Radionov, V., Bradley, R.S., Blangy, S., Bulygina, O.N., Christensen, T.R., Colman, J.E., Essery, R.L.H.H., Forbes, B.C., Forchhammer, M.C., Golubev, V.N., Honrath, R.E., Juday, G.P., Meshcherskaya, A.V., Phoenix, G.K., Pomeroy, J., Rautio, A., Robinson, D.A., Schmidt, N.M., Serreze, M.C., Shevchenko, V.P., Shiklomanov, A.I., Shmakin, A.B., Sköld, P., Sturm, M., Woo, M.K., Wood, E.F., Skoľd, P., Sturm, M., Woo, M.K., Wood, E.F., 2011. Multiple Effects of Changes in Arctic Snow Cover. AMBIO 40, 32–45. https://doi.org/10.1007/s13280-011-0213-x

Chapin, F.S., Sturm, M., Serreze, M.C., McFadden, J.P., Key, J.R., Lloyd, A.H., McGuire, A.D., Rupp, T.S., Lynch, A.H., Schimel, J.P., Beringer, J., Chapman, W.L., Epstein, H.E., Euskirchen, E.S., Hinzman, L.D., Jia, G., Ping, C.-L., Tape, K.D., Thompson, C.D.C., Walker, D.A., Welker, J.M., 2005. Role of Land-Surface Changes in Arctic Summer Warming. Science 310, 657–660. https://doi.org/10.1126/science.1117368

Cherry, J.E., Zhu, J., Kirchner, P.B., 2017. Snow Cover Monitoring with MODIS Satellite Data in Alaska's National Parks, 2000-2015. Natl. Park Serv. Fort Collins Colo., Natural Resource Report NPS/SWAN/NRR—2017/1566 96.

Collins, W.B., Smith, T.S., 1991. Effects of Wind-Hardened Snow on Foraging by Reindeer (Rangifer tarandus). Arctic 44, 217–222.

Cooper, E.J., 2014. Warmer Shorter Winters Disrupt Arctic Terrestrial Ecosystems. Annu. Rev. Ecol. Evol. Syst. 45, 271–295. https://doi.org/10.1146/annurev-ecolsys-120213-091620

Coulson, T., Milner–Gulland, E.J., Clutton–Brock, T., 2000. The relative roles of density and climatic variation on population dynamics and fecundity rates in three contrasting ungulate species. Proc. R. Soc. Lond. B Biol. Sci. 267, 1771–1779. https://doi.org/10.1098/rspb.2000.1209

Coumou, D., Rahmstorf, S., 2012. A decade of weather extremes. Nat. Clim. Change 2, 491–496. https://doi.org/10.1038/nclimate1452

Couturier, S., Côté, S.D., Otto, R.D., Weladji, R.B., Huot, J., 2009. Variation in Calf Body Mass in Migratory Caribou: The Role of Habitat, Climate, and Movements. J. Mammal. 90, 442–452. https://doi.org/10.1644/07-MAMM-A-279.1

Danby, R.K., Slocombe, D.S., 2005. Regional Ecology, Ecosystem Geography, and Transboundary Protected Areas in the St. Elias Mountains. Ecol. Appl. 15, 405–422. https://doi.org/10.1890/04-0043

Dirnböck, T., Essl, F., Rabitsch, W., 2011. Disproportional risk for habitat loss of high-altitude endemic species under climate change. Glob. Change Biol. 17, 990–996. https://doi.org/10.1111/j.1365-2486.2010.02266.x

Domine, F., Gauthier, G., Vionnet, V., Fauteux, D., Dumont, M., Barrere, M., 2018. Snow physical properties may be a significant determinant of lemming population dynamics in the high Arctic. Arct. Sci. 4, 813–826. https://doi.org/10.1139/as-2018-0008

Douhard, M., Loe, L.E., Stien, A., Bonenfant, C., Irvine, R.J., Veiberg, V., Ropstad, E., Albon, S., 2016. The influence of weather conditions during gestation on life histories in a wild Arctic ungulate. Proc. R. Soc. B Biol. Sci. 283, 20161760. https://doi.org/10.1098/rspb.2016.1760

Duquette, L.S., 1988. Snow Characteristics along Caribou Trails and within Feeding Areas during Spring Migration. ARCTIC 41, 143–144. https://doi.org/10.14430/arctic1706

Gaillard, J.-M., Festa-Bianchet, M., Yoccoz, N.G., 1998. Population dynamics of large herbivores: variable recruitment with constant adult survival. Trends Ecol. Evol. 13, 58–63. https://doi.org/10.1016/S0169-5347(97)01237-8

Geist, V., 1971. Mountain sheep; a study in behavior and evolution., Wildlife behavior and ecology. University of Chicago Press, Chicago.

Gelaro, R., McCarty, W., Suárez, M.J., Todling, R., Molod, A., Takacs, L., Randles, C.A., Darmenov, A., Bosilovich, M.G., Reichle, R., Wargan, K., Coy, L., Cullather, R., Draper, C., Akella, S., Buchard, V., Conaty, A., da Silva, A.M., Gu, W., Kim, G.-K., Koster, R., Lucchesi, R., Merkova, D., Nielsen, J.E., Partyka, G., Pawson, S., Putman, W., Rienecker, M., Schubert, S.D., Sienkiewicz, M., Zhao, B., Gelaro, R., McCarty, W., Suárez, M.J., Todling, R., Molod, A., Takacs, L., Randles, C.A., Darmenov, A., Bosilovich, M.G., Reichle, R., Wargan, K., Coy, L., Cullather, R., Draper, C., Akella, S., Buchard, V., Conaty, A., da Silva, A.M., Gu, W., Kim, G.-K., Koster, R., Lucchesi, R., Merkova, D., Nielsen, J.E., Partyka, G., Pawson, S., Putman, W., Rienecker, M., Schubert, S.D., Sienkiewicz, M., Zhao, B., 2017. The Modern-Era Retrospective Analysis for Research and Applications, Version 2 (MERRA-2). J. Clim. 30, 5419–5454. https://doi.org/10.1175/JCLI-D-16-0758.1

Gilbert, S.L., Hundertmark, K.J., Person, D.K., Lindberg, M.S., Boyce, M.S., 2017. Behavioral plasticity in a variable environment: snow depth and habitat interactions drive deer movement in winter. J. Mammal. 98, 246–259. https://doi.org/10.1093/jmammal/gyw167

Hansen, B.B., Aanes, R., Herfindal, I., Kohler, J., S\a ether, B.-E.E., Oli, M.K., 2011. Climate, icing, and wild arctic reindeer: Past relationships and future prospects. Ecology 92, 1917–1923. https://doi.org/10.1890/11-0095.1

Hansen, B.B., Aanes, R., Sæther, B.-E., 2010. Feeding-crater selection by high-arctic reindeer facing ice-blocked pastures. Can. J. Zool. 88, 170–177. https://doi.org/10.1139/Z09-130

Hinzman, L.D., Bettez, N.D., Bolton, W.R., Chapin, F.S., Dyurgerov, M.B., Fastie, C.L., Griffith, B., Hollister, R.D., Hope, A., Huntington, H.P., Jensen, A.M., Jia, G.J., Jorgenson, T., Kane, D.L., Klein, D.R., Kofinas, G., Lynch, A.H., Lloyd, A.H., McGuire, A.D., Nelson, F.E., Oechel, W.C., Osterkamp, T.E., Racine, C.H., Romanovsky, V.E., Stone, R.S., Stow, D.A., Sturm, M., Tweedie, C.E., Vourlitis, G.L., Walker, M.D., Walker, D.A., Webber, P.J., Welker, J.M., Winker, K.S., Yoshikawa, K., 2005. Evidence and Implications of Recent Climate Change in Northern Alaska and Other Arctic Regions. Clim. Change 72, 251–298. https://doi.org/10.1007/s10584-005-5352-2

Hoefs, M., 1984. Productivity and Carrying Capacity of a Subarctic Sheep Winter Range. ARCTIC 37. https://doi.org/10.14430/arctic2179

Homer, C., Dewitz, J., Yang, L., Jin, S., Danielson, P., 2015. Completion of the 2011 National Land Cover Database for the Conterminous United States – Representing a Decade of Land Cover Change Information. Photogramm. Eng. 11.

Jacobson, A.R., Provenzale, A., Hardenberg, A. von, Bassano, B., Festa-Bianchet, M., 2004. Climate Forcing and Density Dependence in a Mountain Ungulate Population. Ecology 85, 1598–1610. https://doi.org/10.1890/02-0753

Jensen, P.G., Pekins, P.J., Holter, J.B., 1999. Compensatory effect of the heat increment of feeding on thermoregulation costs of white-tailed deer fawns in winter. Can. J. Zool. 77, 1474–1485. https://doi.org/10.1139/z99-111

Johansson, C., Pohjola, V.A., Jonasson, C., Callaghan, T.V., 2011. Multi-decadal changes in snow characteristics in sub-Arctic Sweden. Ambio 40, 566–574. https://doi.org/10.1007/s13280-011-0164-2

Kawaguchi, T., Desrochers, A., 2017. Short-term changes in spatial distribution pattern of an herbivore in response to accumulating snow. Can. J. Zool. 95, 949–954. https://doi.org/10.1139/cjz-2016-0287

Kelsall, J.P., 1969. Structural Adaptations of Moose and Deer for Snow. J. Mammal. 50, 302–310. https://doi.org/10.2307/1378347

Keppel, G., Niel, K.P.V., Wardell-Johnson, G.W., Yates, C.J., Byrne, M., Mucina, L., Schut, A.G.T., Hopper, S.D., Franklin, S.E., 2012. Refugia: identifying and understanding safe havens for biodiversity under climate change. Glob. Ecol. Biogeogr. 21, 393–404. https://doi.org/10.1111/j.1466-8238.2011.00686.x

Kerk, M.V. de, Arthur, S., Bertram, M., Borg, B., Herriges, J., Lawler, J., Mangipane, B., Koizumi, C.L., Wendling, B., Prugh, L., n.d. Environmental Influences on Dall's Sheep Survival. J. Wildl. Manag. n/a. https://doi.org/10.1002/jwmg.21873

Kerk, M. van de, Verbyla, D., Nolin, A.W., Sivy, K.J., Prugh, L.R., 2018. Range-wide variation in the effect of spring snow phenology on Dall sheep population dynamics. Environ. Res. Lett. 13, 075008. https://doi.org/10.1088/1748-9326/aace64

Lambert Koizumi, C., Carey, J., Branigan, M., Callaghan, K., 2011. Status of Dall's Sheep (Ovis dalli dalli) in the Northern Richardson Mountains. Yukon Fish Wildl. Branch Rep. TRC-11-01 Yukon Can. 64.

Langlois, A., Johnson, C.-A.A., Montpetit, B., Royer, A., Blukacz-Richards, E.A.A., Neave, E., Dolant, C., Roy, A., Arhonditsis, G., Kim, D.-K.K., Kaluskar, S., Brucker, L., 2017. Detection of rain-on-snow (ROS) events and ice layer formation using passive microwave radiometry: A context for Peary caribou habitat in the Canadian Arctic. Remote Sens. Environ. 189, 84–95. https://doi.org/10.1016/j.rse.2016.11.006

LaPerriere, A.J., Lent, P.C., 1977. Caribou Feeding Sites in Relation to Snow Characteristics in Northeastern Alaska. ARCTIC 30, 101–108. https://doi.org/10.14430/arctic2690

Liston, G.E., 1995. Local Advection of Momentum, Heat, and Moisture during the Melt of Patchy Snow Covers. J. Appl. Meteorol. 34, 1705–1715. https://doi.org/10.1175/1520-0450-34.7.1705

Liston, G.E., Elder, K., 2006. A Distributed Snow-Evolution Modeling System (SnowModel). J. Hydrometeorol. 7, 1259–1276. https://doi.org/10.1175/JHM548.1

Liston, G.E., Elder, K., Liston, G.E., Elder, K., 2006. A Meteorological Distribution System for High-Resolution Terrestrial Modeling (MicroMet). J. Hydrometeorol. 7, 217–234. https://doi.org/10.1175/JHM486.1

Liston, G.E., Haehnel, R.B., Sturm, M., Hiemstra, C.A., Berezovskaya, S., Tabler, R.D., 2007. Simulating complex snow distributions in windy environments using SnowTran-3D. J. Glaciol. 53, 241–256. https://doi.org/10.3189/172756507782202865

Liston, G.E., Hall, D.K., 1995. An energy-balance model of lake-ice evolution. J. Glaciol. 41, 373–382. https://doi.org/10.3189/S0022143000016245

Liston, G.E., Hiemstra, C.A., 2011. The Changing Cryosphere: Pan-Arctic Snow Trends (1979–2009). J. Clim. 24, 5691–5712. https://doi.org/10.1175/JCLI-D-11-00081.1

Liston, G.E., Hiemstra, C.A., 2008. A Simple Data Assimilation System for Complex Snow Distributions (SnowAssim). J. Hydrometeorol. 9, 989–1004. https://doi.org/10.1175/2008JHM871.1

Liston, G.E., Mcfadden, J.P., Sturm, M., Pielke, R.A., 2002. Modelled changes in arctic tundra snow, energy and moisture fluxes due to increased shrubs. Glob. Change Biol. 8, 17–32. https://doi.org/10.1046/j.1354-1013.2001.00416.x

Liston, G.E., Perham, C.J., Shideler, R.T., Cheuvront, A.N., 2016. Modeling snowdrift habitat for polar bear dens. Ecol. Model. 320, 114–134. https://doi.org/10.1016/j.ecolmodel.2015.09.010

Lundmark, C., Ball, J.P., 2008. Living in Snowy Environments: Quantifying The Influence of Snow on Moose Behavior. Arct. Antarct. Alp. Res. 40, 111–118. https://doi.org/10.1657/1523-0430(06-103)[LUNDMARK]2.0.CO;2

Mahoney, P.J., Liston, G.E., LaPoint, S., Gurarie, E., Mangipane, B., Wells, A.G., Brinkman, T.J., Eitel, J.U.H., Hebblewhite, M., Nolin, A.W., Boelman, N., Prugh, L.R., 2018. Navigating snowscapes: scale-dependent responses of mountain sheep to snowpack properties. Ecol. Appl. 0. https://doi.org/10.1002/eap.1773

McCabe, G.J., Clark, M.P., Hay, L.E., 2007. Rain-on-snow events in the western United States. Bull. Am. Meteorol. Soc. 88, 319–328. https://doi.org/10.1175/BAMS-88-3-319

Mitchell, C.D., Chaney, R., Aho, K., Kie, J.G., Bowyer, R.T., 2015. Population density of Dall's sheep in Alaska: effects of predator harvest? Mammal Res. 60, 21–28. https://doi.org/10.1007/s13364-014-0199-4

Molotch, N.P., Bales, R.C., 2005. Scaling snow observations from the point to the grid element: Implications for observation network design. Water Resour. Res. 41. https://doi.org/10.1029/2005WR004229

Murie, A., 1944. The Wolves of Mount McKinley. University of Washington Press.

Murphy, E.C., Whitten, K.R., 1976. Dall Sheep Demography in McKinley Park and a Reevaluation of Murie's Data. J. Wildl. Manag. 40, 597–609. https://doi.org/10.2307/3800554

NASA/METI/AIST/Japan Spacesystems, 2009. ASTER Global Digital Elevation Model. https://doi.org/10.5067/ASTER/ASTGTM.002

NPS - Land Resources Division, 2020. Administrative Boundaries of National Park System Units 6/30/2020 [WWW Document]. Natl. Geospatial Data Asset NGDA NPS Natl. Parks Dataset NPS - Land Resour. Div. URL https://irma.nps.gov/DataStore/Reference/Profile/2224545?lnv=True (accessed 8.15.20).

Orlanski, I., 1975. A Rational Subdivision of Scales for Atmospheric Processes. Bull. Am. Meteorol. Soc. 56, 527–530.

Ouellet, F., Langlois, A., Blukacz-Richards, E.A., Johnson, C.A., Royer, A., Neave, E., Larter, N.C., 2017. Spatialization of the SNOWPACK snow model for the Canadian Arctic to assess Peary caribou winter grazing conditions. Phys. Geogr. 38, 143–158. https://doi.org/10.1080/02723646.2016.1274200

Pan, C.G., Kirchner, P.B., Kimball, J.S., Kim, Y., Du, J., 2018. Rain-on-snow events in Alaska, their frequency and distribution from satellite observations. Environ. Res. Lett. 13, 075004. https://doi.org/10.1088/1748-9326/aac9d3

Parker, K.L., Robbins, C.T., Hanley, T.A., 1984. Energy Expenditures for Locomotion by Mule Deer and Elk. J. Wildl. Manag. 48, 474–488. https://doi.org/10.2307/3801180

Pinheiro, J., Bates, D., DebRoy, S., Sarkar, D., 2019. nlme: Linear and Nonlinear Mixed Effects Models.

Portier, C., Festa-Bianchet, M., Gaillard, J.-M., Jorgenson, J.T., Yoccoz, N.G., 1998. Effects of density and weather on survival of bighorn sheep lambs (Ovis canadensis). J. Zool. 245, 271–278. https://doi.org/10.1111/j.1469-7998.1998.tb00101.x

Pruitt, Jr., W.O., 1959. Snow as a Factor in the Winter Ecology of the Barren Ground Caribou (*Rangifer arcticus*). ARCTIC 12. https://doi.org/10.14430/arctic3723

Pulliainen, J., Hallikainen, M., 2001. Retrieval of Regional Snow Water Equivalent from Space-Borne Passive Microwave Observations. Remote Sens. Environ. 75, 76–85. https://doi.org/10.1016/S0034-4257(00)00157-7

R Core Team, 2019. R: A Language and Environment for Statistical Computing. R Foundation for Statistical Computing, Vienna, Austria.

Rachlow, J.L., Bowyer, R.T., 1994. Variability in Maternal Behavior by Dall's Sheep: Environmental Tracking or Adaptive Strategy? J. Mammal. 75, 328–337. https://doi.org/10.2307/1382551

Rattenbury, K.L., Schmidt, J.H., Swanson, D.K., Borg, B.L., Mangipane, B.A., Sousanes, P.J., 2018. Delayed spring onset drives declines in abundance and recruitment in a mountain ungulate. Ecosphere 9, e02513. https://doi.org/10.1002/ecs2.2513

Reconyx, 2017. Hyperfire(TM) High Performance Cameras Instruction Manual.

Reid, D.G., Bilodeau, F., Krebs, C.J., Gauthier, G., Kenney, A.J., Gilbert, B.S., Leung, M.C.-Y., Duchesne, D., Hofer, E., 2012. Lemming winter habitat choice: a snow-fencing experiment. Oecologia 168, 935–946. https://doi.org/10.1007/s00442-011-2167-x

RIP 1 Cutter (1000 cc) [WWW Document], n.d. . Snowmetrics. URL https://snowmetrics.com/shop/rip-1-cutter-1000-cc/ (accessed 7.9.19).

Robinson, B.G., Merrill, E.H., 2012. The influence of snow on the functional response of grazing ungulates. Oikos 121, 28–34. https://doi.org/10.1111/j.1600-0706.2011.19408.x

Roffler, G.H., Adams, L.G., Hebblewhite, M., 2017. Summer habitat selection by Dall's sheep in Wrangell-St. Elias National Park and Preserve, Alaska. J. Mammal. 98, 94–105. https://doi.org/10.1093/jmammal/gyw135

Schaefer, J.A., Messier, F., 1995. Winter Foraging by Muskoxen: A Hierarchical Approach to Patch Residence Time and Cratering Behaviour. Oecologia 104, 39–44.

Schmidt, J.H., Rattenbury, K.L., Lawler, J.P., Maccluskie, M.C., 2012. Using distance sampling and hierarchical models to improve estimates of Dall's sheep abundance. J. Wildl. Manag. 76, 317–327. https://doi.org/10.1002/jwmg.216

Schults, B.S., 2004. Abundance survey of Dall's sheep in the western Baird Mountains, Alaska, July 2004. Natural Resource Technical Report No. NPS/AR/ NRTR-2004-46.

Serrano, E., Granados, J.E., Sarasa, M., González, F.J., Fandos, P., Soriguer, R.C., Pérez, J.M., 2011. The effects of winter severity and population density on body stores in the Iberian wild goat (Capra pyrenaica) in a highly seasonal mountain environment. Eur. J. Wildl. Res. Heidelb. 57, 45–55. http://dx.doi.org.ezproxy.proxy.library.oregonstate.edu/10.1007/s10344-010-0398-5

Serreze, M.C., Barry, R.G., 2011. Processes and impacts of Arctic amplification: A research synthesis. Glob. Planet. Change 77, 85–96. https://doi.org/10.1016/j.gloplacha.2011.03.004

Sexstone, G.A., Clow, D.W., Fassnacht, S.R., Liston, G.E., Hiemstra, C.A., Knowles, J.F., Penn, C.A., 2018. Snow Sublimation in Mountain Environments and Its Sensitivity to Forest Disturbance and Climate Warming. Water Resour. Res. 54, 1191–1211. https://doi.org/10.1002/2017WR021172

Sivy, K.J., Nolin, A.W., Cosgrove, C., Prugh, L., 2018. Critical snow density threshold for Dall sheep (Ovis dalli dalli). Can. J. Zool. https://doi.org/10.1139/cjz-2017-0259

Sturm, M., Holmgren, J., 2018. An Automatic Snow Depth Probe for Field Validation Campaigns. Water Resour. Res. 54, 9695–9701. https://doi.org/10.1029/2018WR023559

Sturm, M., Holmgren, J., Liston, G.E., Holmgren, J., Liston, G.E., 1995. A Seasonal Snow Cover Classification System for Local to Global Applications. J. Clim. 8, 1261–1283. https://doi.org/10.1175/1520-0442(1995)008<1261:ASSCCS>2.0.CO;2

Telfer, E.S., Kelsall, J.P., 1984. Adaptation of Some Large North American Mammals for Survival In Snow. Ecology 65, 1828–1834. https://doi.org/10.2307/1937779

Tyler N. J. C., 2010. Climate, snow, ice, crashes, and declines in populations of reindeer and caribou (Rangifer tarandus L.). Ecol. Monogr. 80, 197–219. https://doi.org/10.1890/09-1070.1

U.S. Geological Survey, 2017. 1 Arc-second Digital Elevation Models (DEMs) - USGS National Map 3DEP Downloadable Data Collection: U.S. Geological Survey [WWW Document]. URL https://www.sciencebase.gov/catalog/item/4f70aa71e4b058caae3f8de1 (accessed 8.15.20).

U.S. Geological Survey, 2015. NLCD 2011 Land Cover Alaska 2001 to 2011 From To Change Index - National Geospatial Data Asset (NGDA) Land Use Land Cover [WWW Document]. URL https://www.mrlc.gov/data/nlcd-2001-2011-land-cover-change-alaska-0

Verbyla, D., Hegel, T., Nolin, A.W., van de Kerk, M., Kurkowski, T.A., Prugh, L.R., 2017. Remote Sensing of 2000–2016 Alpine Spring Snowline Elevation in Dall Sheep Mountain Ranges of Alaska and Western Canada. Remote Sens. 9, 1157. https://doi.org/10.3390/rs9111157

Vikhamar-Schuler, D., Hanssen-Bauer, I., Schuler, T.V., Mathiesen, S.D., Lehning, M., 2013. Use of a multilayer snow model to assess grazing conditions for reindeer. Ann. Glaciol. 54, 214–226. https://doi.org/10.3189/2013AoG62A306

Vors, L.S., Boyce, M.S., 2009. Global declines of caribou and reindeer. Glob. Change Biol. 15, 2626–2633. https://doi.org/10.1111/j.1365-2486.2009.01974.x

Wells, J.J., 2018. Dall sheep management report and plan, Game Management Unit 12, Mentasta, Nutzotin, and northern Wrangell Mountains: Report period 1 July 2011–30 June 2016, and plan period 1 July 2016–30 June 2021. Alsk. Dep. Fish Game Species Manag. Rep. Plan ADFGDWCSMRP-2018-46 Juneau 26.

White, K.S., White, K.S., Pendleton, G.W., Crowley, D., Griese, H.J., Hundertmark, K.J., McDonough, T., Nichols, L., Nichols, L., Robus, M., Smith, C.A., Schoen, J.W., 2011. Mountain Goat Survival in Coastal Alaska: Effects of Age, Sex, and Climate. J. Wildl. Manag. 75, 1731–1744. https://doi.org/10.1002/jwmg.238

WRST Sheep and Goat Count Units - data.doi.gov [WWW Document], n.d. URL https://data.doi.gov/dataset/wrst-sheep-and-goat-count-units (accessed 5.24.20).

Zuur, A., Ieno, E.N., Walker, N., Saveliev, A.A., Smith, G.M., 2009. Mixed Effects Models and Extensions in Ecology with R, Statistics for Biology and Health. Springer-Verlag, New York.

2.9 Appendix

2.9.1 Figures and tables

Appendix 2.1. Northern Wrangell-St. Elias National Park and Preserve (WRST) sheep surveys 1981 to 2017 conducted by the Alaska Department of Fish and Games (ADF&G) and the National Park Service (NPS); 41 surveys across 19 years in 9 survey units had a mean lamb-to-ewe ratio of 0.30 (SD ±0.10).

Year	Survey unit	Survey unit name	Survey agency	Date(s) of Survey	Ewes	Lambs	Lamb:Ewe	Sum
1981	4W	Nikonda Creek	ADF&G Tok	26 June, 28 June, 7 July, and 13 July	547	220	0.40	767
	4E	Cross Creek	ADF&G Tok	26 June, 28 June, 7 July, and 13 July	147	46	0.31	193
	5W	Stone Creek	ADF&G Tok	21-22 June	474	153	0.32	627
	5E	Mt Allen	ADF&G Tok	21-22 June	224	81	0.36	305
	7W	Chisana	ADF&G Tok	26-27 June	470	208	0.44	678
	10	Mount Drum	ADF&G Glennallen	Unknown	107	59	0.55	166
1984	5W	Stone Creek	ADF&G Tok	16-17 July	278	74	0.27	352
	5E	Mt Allen	ADF&G Tok	16-17 July	231	63	0.27	294
	7W	Chisana	ADF&G Tok	16-17 July	392	173	0.44	565
1987	1	Mentasta	ADF&G Tok	17 and 31 July, and 1 August	771	287	0.37	1058
1993	3	Jacksina	NPS	23 July	1628	144	0.09	1772
1997	1	Mentasta	ADF&G Tok	15, 17, 27 July	692	196	0.28	888
1998	7W	Chisana	NPS	4 August	373	118	0.32	491
1999	7W	Chisana	NPS	8 July	336	127	0.38	463
2001	10	Mount Drum	ADF&G Glennallen	12 July	65	13	0.20	78
	5E	Mt Allen	ADF&G Tok	22 July	215	27	0.13	242
	5W	Stone Creek	ADF&G Tok	22 July	301	63	0.21	364
2002	1	Mentasta	NPS	2 August	575	123	0.21	698
	2	Mount Sanford	NPS	2 August	105	38	0.36	143
	10	Mount Drum	ADF&G Glennallen	31 July	53	13	0.25	66
	7W	Chisana	ADF&G Tok	21 July	270	76	0.28	346
2005	7W	Chisana	NPS	27 July	260	63	0.24	323
2006	4E	Cross Creek	ADF&G Tok	2 August	65	25	0.38	90
	4W	Nikonda Creek	ADF&G Tok	2-3 August	315	136	0.43	451
2007	5W	Stone Creek	ADF&G Tok	28 June and 15 July	209	66	0.32	275
2011	4E	Cross Creek	ADF&G Tok	25 June	72	29	0.40	101
	5E	Mt Allen	ADF&G Tok	9 July	142	35	0.25	177
	7W	Chisana	ADF&G Tok	24-25 June	235	59	0.25	294
2012	1	Mentasta	NPS	30-31 July	664	167	0.25	831
	3	Jacksina	NPS	20, 28, and 30 July	1064	202	0.19	1266
2013	2	Mount Sanford	NPS	2 August	79	12	0.15	91
	4W	Nikonda Creek	NPS	31 July	308	67	0.22	375
2014	1	Mentasta	ADF&G Tok	22 July	360	81	0.23	441
	2	Mount Sanford	NPS	21 July	102	19	0.19	121
	5W	Stone Creek	NPS	17 July	162	41	0.25	203
	7W	Chisana	ADF&G Tok	10 July	252	95	0.38	347
2015	4E	Cross Creek	ADF&G Tok	3 August	55	22	0.40	77
	4W	Nikonda Creek	ADF&G Tok	3 August	359	120	0.33	479
2016	1	Mentasta	ADF&G Tok	15 and 27 July	555	123	0.22	678
	5E	Mt Allen	NPS	29 July	183	54	0.30	237
2017	3	Jacksina	ADF&G Tok and Glennallen	22-23 July	1386	490	0.35	1876

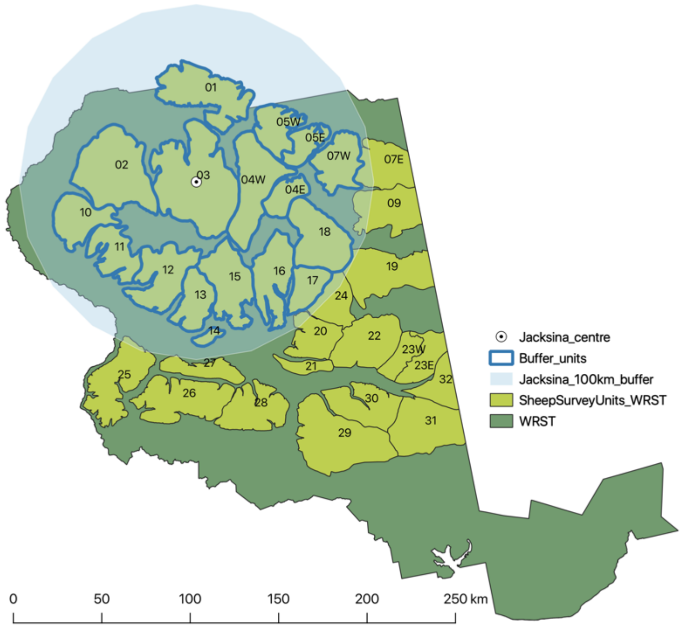

Appendix 2.2. Map of Wrangell-St. Elias National Park and Preserve (WRST; dark green), including; all WRST Survey Units (SheepSurveyUnits_WRST; light green, numbered); 100 km radius buffer (Jacksina_100km_buffer; transparent light blue) from the centre of the Jacksina Survey Unit (Survey Unit 03; Jacksina_centre); Survey Units with centres within the 100 km radius buffer (Buffer_units, dark blue outline). GIS data for sheep survey units and WRST park boundary were sourced from ("WRST Sheep and Goat Count Units - data.doi.gov," n.d.; "National Park Boundaries - Data.gov," n.d.) respectively. For context please see Figure 2.1.

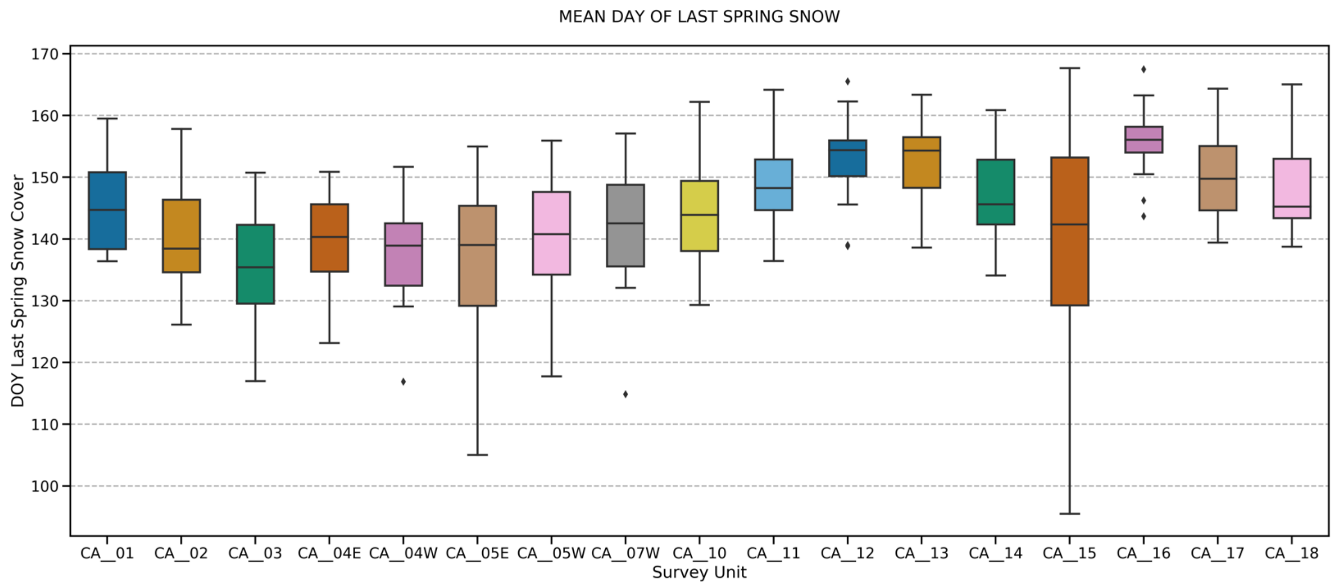

Appendix 2.3. Box plot of the mean day of last spring snow cover in Dall's sheep habitat by Survey Unit from 2000 to 2016. Date reported as Day of Year (DOY).

To calculate the mean last day of spring snow (SDD) for a given year by Survey Unit we used Verbyla's (2017) MODIS derived product for the years 2000 to 2016, please see the data reference for further details. To constrain the SDD to areas of Dall's sheep habitat we resampled the National Land Cover Database 2011 (NLCD) product (Homer et al., 2015) to the same projection and resolution as the SDD product, calculating the majority land cover in each of the 500 m SDD pixels from the higher resolution 30 m NLCD product. We then clipped the yearly raster maps of SDD and the resampled NLCD product by each individual Survey Unit included in the 100 km buffer from the centre of the Jacksina Survey Unit (see Appendix 2.2). Finally, we found the yearly mean SDD for each Survey Unit by finding all pixels that were either Shrub/Scrub or Barren Land in the clipped NLCD raster of each Survey Unit. These two land cover types are known to be preferentially selected by Dall's sheep (Mahoney et al., 2018). The corresponding pixels to these land covers were then used to find the mean SDD of each year for each Survey Unit

Appendix 2.4. NLCD 2001 to NLCD 2011 Land Cover Change across Survey Units 1, 2, 3, 4E, 4W, 5E, 5W, 7W and 10 in the Northern Wrangell St Elias National Park and Preserve (WRST)

Code	Area km-2	Area %	Changed?	Classification
23	6.00	0.069	No	Open Water to Open Water
29	0.32	0.004	Yes	Open Water to Barren Land
44	0.02	0.000	Yes	Perennial Ice/Snow to Open Water
45	1210.31	13.947	No	Perennial Ice/Snow to Perennial Ice/Snow
50	1.51	0.017	Yes	Perennial Ice/Snow to Barren Land
149	0.39	0.005	Yes	Barren Land to Open Water
150	25.18	0.290	Yes	Barren Land to Perennial Ice/Snow
155	3592.57	41.400	No	Barren Land to Barren Land
177	15.58	0.180	No	Deciduous Forest to Deciduous Forest
191	0.02	0.000	Yes	Evergreen Forest to Open Water
199	114.50	1.319	No	Evergreen Forest to Evergreen Forest
221	25.64	0.296	No	Mixed Forest to Mixed Forest
233	0.00	0.000	Yes	Dwarf Scrub to Open Water
234	0.01	0.000	Yes	Dwarf Scrub to Perennial Ice/Snow
243	1233.50	14.214	No	Dwarf Scrub to Dwarf Scrub
254	0.01	0.000	Yes	Shrub/Scrub to Open Water
255	0.01	0.000	Yes	Shrub/Scrub to Perennial Ice/Snow
262	0.02	0.000	Yes	Shrub/Scrub to Evergreen Forest
265	2400.22	27.659	No	Shrub/Scrub to Shrub/Scrub
275	0.00	0.000	Yes	Grassland/Herbaceous to Open Water
287	7.74	0.089	No	Grassland/Herbaceous to Grassland/Herbaceous
309	2.41	0.028	No	Sedge/Herbaceous to Sedge Herbaceous
401	0.01	0.000	Yes	Woody Wetlands to Open Water
419	41.70	0.481	No	Woody Wetlands to Wood Wetlands
441	0.08	0.001	No	Herbaceous Wetlands to Herbaceous Wetlands
Total Area	8677.75	100.00		
Area unchanged	8650.2582	99.68		
Area changed	27.4932	0.32		

For the selected Survey Units (see *Survey Unit Selection* in manuscript) we calculated the amount and type of land cover change using the NLCD 2011 Land Cover Alaska 2001 to 2011 From To Change Index (U.S. Geological Survey, 2015). To do this we first clipped the NLCD Land Cover Alaska 2001 to 2011 product to all the 9 selected units. Using the clipped layer we then ran the Raster Layer Unique Values Report in QGIS (QGIS Development Team, 2019) to find the area of each type of change and simply calculated the area changed or unchanged using the product's change classification scheme (Appendix 2.4).

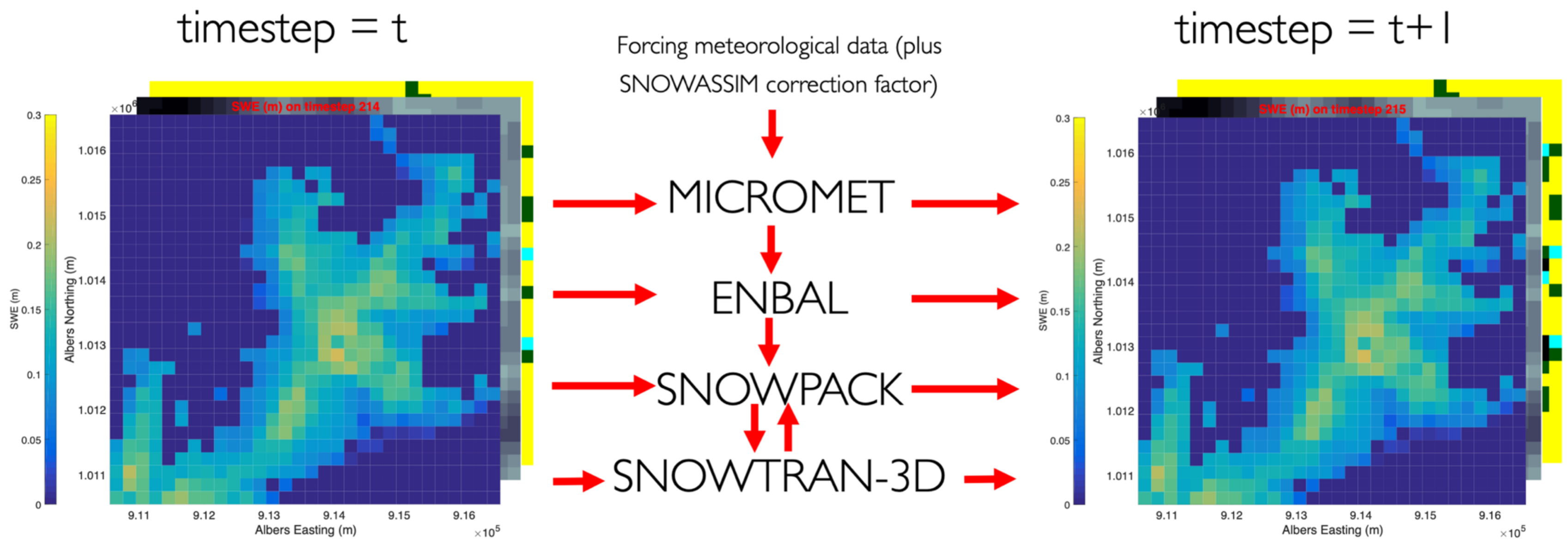

Appendix 2.5. Workflow diagram of SnowModel showing the interactions between each sub-model, meteorological forcing data (corrected by DataAssim), static layers (vegetation and elevation set furthest back and behind example spatially distributed SWE output respectively) and the previous timestep's snow condition. Full descriptions can be found for each submodel in the following references; MicroMet (Liston et al., 2006), EnBal (Liston, 1995), SnowPack (Liston and Hall, 1995), SnowTran-3D (Liston et al., 2007), and SnowAssim (Liston and Hiemstra, 2008)

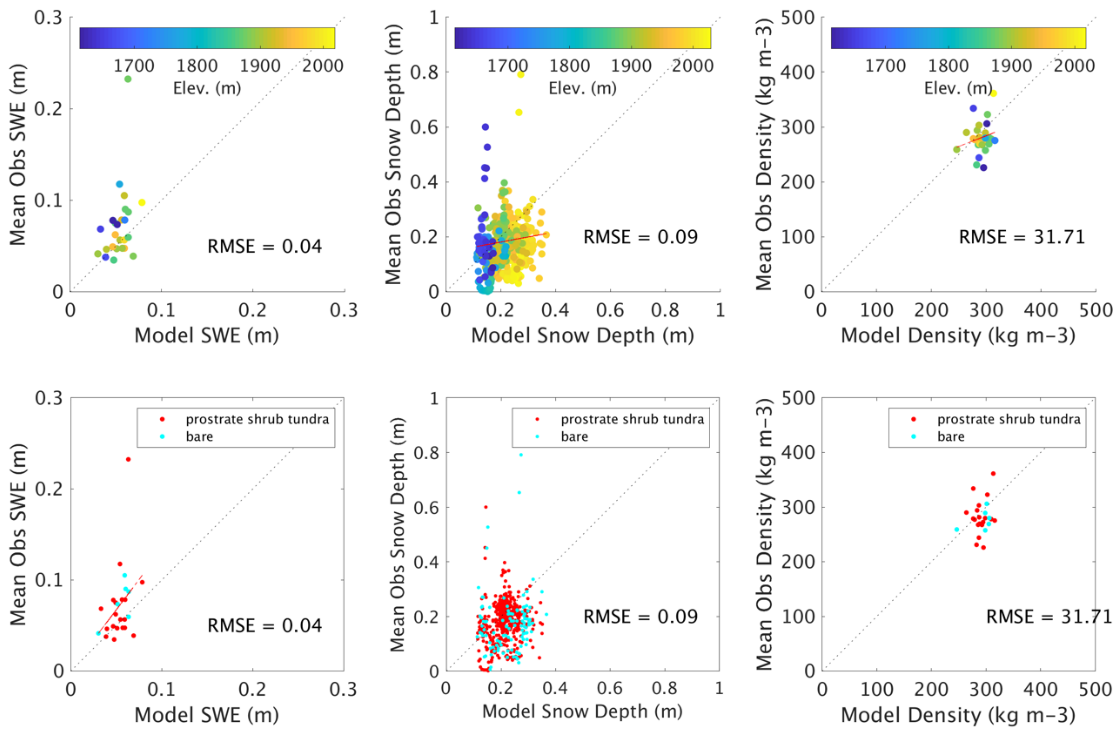

Appendix 2.6. Best calibration (ro_adj = 6.0; wspd_increase = 2.5) model vs observed SWE, Snow Depth and Snow Density by elevation and land cover class

After an initial sensitivity analysis, our calibration involved 72 SnowModel simulations from 1st September 2016 to 1st April 2017 with the density adjustment factor (*ro_adj*) ranging from 2.0 to 10.0 in increments of 1.0, and the wind speed scalar (*wspd_increase*) ranging from 1.5 to 5.0 in increments of 0.5.

Appendix 2.7. RMSE for SWE, depth and density for each calibration simulation. Ranking is determined by minimum RMSE and Mean ranking is used to select the best calibration.

Parameters	RMSE SWE (m)	RMSE Depth (m)	RMSE Density (kg m-3)	SWE rank	Depth rank	Density rank	Mean ranking
ro_adj06.0-wspd2.5	0.04	0.09	31.71	5	13	6	**8.00**
ro_adj07.0-wspd2.5	0.04	0.09	34.30	6	9	10	**8.33**
ro_adj08.0-wspd2.5	0.04	0.09	37.22	7	6	15	**9.33**
ro_adj04.0-wspd2.5	0.04	0.10	30.45	4	24	5	**11.00**
ro_adj09.0-wspd2.5	0.04	0.09	40.23	8	5	22	**11.67**
ro_adj10.0-wspd2.5	0.04	0.09	43.19	9	4	27	**13.33**
ro_adj03.0-wspd2.5	0.04	0.10	34.53	3	33	12	**16.00**
ro_adj15.0-wspd2.5	0.04	0.09	48.76	10	3	36	**16.33**
ro_adj20.0-wspd2.5	0.04	0.08	66.29	11	2	56	**23.00**
ro_adj09.0-wspd3.0	0.06	0.10	33.05	44	21	9	**24.67**
ro_adj08.0-wspd3.0	0.06	0.10	34.35	43	20	11	**24.67**
ro_adj10.0-wspd3.0	0.06	0.10	32.34	45	22	8	**25.00**
ro_adj07.0-wspd3.0	0.06	0.10	36.39	42	19	14	**25.00**
ro_adj25.0-wspd2.5	0.04	0.08	69.72	12	1	62	**25.00**
ro_adj15.0-wspd3.0	0.06	0.10	32.24	46	26	7	**26.33**
ro_adj06.0-wspd3.0	0.06	0.10	39.37	41	18	21	**26.67**
ro_adj02.0-wspd2.5	0.04	0.11	44.75	1	50	30	**27.00**
ro_adj05.0-wspd2.5	0.04	0.11	44.75	2	51	31	**28.00**
ro_adj04.0-wspd3.0	0.06	0.09	49.45	40	14	37	**30.33**
ro_adj03.0-wspd3.0	0.06	0.09	57.70	39	10	45	**31.33**
ro_adj20.0-wspd3.0	0.06	0.10	38.88	48	29	19	**32.00**
ro_adj25.0-wspd3.0	0.06	0.10	41.00	47	30	23	**33.33**
ro_adj02.0-wspd3.0	0.06	0.09	70.12	37	11	63	**37.00**
ro_adj05.0-wspd3.0	0.06	0.09	70.12	38	12	64	**38.00**
ro_adj02.0-wspd2.0	0.04	0.18	29.07	23	91	1	**38.33**
ro_adj05.0-wspd2.0	0.04	0.18	29.07	24	92	2	**39.33**
ro_adj06.0-wspd3.5	0.06	0.10	52.00	53	28	39	**40.00**
ro_adj07.0-wspd3.5	0.06	0.10	48.34	54	34	33	**40.33**
ro_adj03.0-wspd2.0	0.04	0.16	34.83	22	87	13	**40.67**
ro_adj15.0-wspd3.5	0.06	0.11	38.87	60	44	18	**40.67**
ro_adj09.0-wspd3.5	0.06	0.11	43.16	58	38	26	**40.67**
ro_adj10.0-wspd3.5	0.06	0.11	41.35	59	41	24	**41.33**
ro_adj20.0-wspd3.5	0.06	0.12	37.45	56	53	16	**41.67**
ro_adj08.0-wspd3.5	0.06	0.11	45.45	57	36	32	**41.67**
ro_adj04.0-wspd3.5	0.06	0.10	62.66	52	23	50	**41.67**
ro_adj25.0-wspd3.5	0.06	0.12	38.18	55	55	17	**42.33**
ro_adj04.0-wspd2.0	0.04	0.15	42.80	21	83	25	**43.00**
ro_adj02.0-wspd1.5	0.05	0.23	29.97	35	95	3	**44.33**
ro_adj03.0-wspd3.5	0.06	0.09	70.79	51	17	65	**44.33**
ro_adj02.0-wspd3.5	0.06	0.09	82.56	49	7	79	**45.00**
ro_adj05.0-wspd1.5	0.05	0.23	29.97	36	96	4	**45.33**
ro_adj05.0-wspd3.5	0.06	0.09	82.56	50	8	80	**46.00**
ro_adj20.0-wspd2.0	0.04	0.11	104.03	14	40	91	**48.33**
ro_adj25.0-wspd2.0	0.04	0.11	107.94	16	35	94	**48.33**
ro_adj06.0-wspd2.0	0.04	0.14	56.65	20	82	44	**48.67**
ro_adj07.0-wspd2.0	0.04	0.13	62.37	19	79	48	**48.67**
ro_adj03.0-wspd1.5	0.05	0.21	39.13	34	94	20	**49.33**

ro_adj08.0-wspd2.0	0.04	0.13	67.44	18	76	58	**50.67**
ro_adj06.0-wspd4.0	0.06	0.11	62.44	65	39	49	**51.00**
ro_adj10.0-wspd2.0	0.04	0.12	76.12	15	65	73	**51.00**
ro_adj15.0-wspd2.0	0.04	0.12	83.35	13	59	81	**51.00**
ro_adj07.0-wspd4.0	0.06	0.11	58.89	66	42	46	**51.33**
ro_adj09.0-wspd2.0	0.04	0.13	72.00	17	71	66	**51.33**
ro_adj25.0-wspd4.0	0.06	0.12	44.01	67	61	28	**52.00**
ro_adj09.0-wspd4.0	0.06	0.11	53.60	70	46	40	**52.00**
ro_adj20.0-wspd4.0	0.06	0.12	44.12	68	60	29	**52.33**
ro_adj10.0-wspd4.0	0.06	0.11	51.63	71	48	38	**52.33**
ro_adj08.0-wspd4.0	0.06	0.11	55.99	69	45	43	**52.33**
ro_adj15.0-wspd4.0	0.06	0.11	48.64	72	52	35	**53.00**
ro_adj04.0-wspd4.0	0.06	0.10	72.58	64	27	68	**53.00**
ro_adj04.0-wspd1.5	0.05	0.19	48.48	33	93	34	**53.33**
ro_adj02.0-wspd4.0	0.06	0.09	91.20	61	15	85	**53.67**
ro_adj03.0-wspd4.0	0.06	0.10	80.19	63	25	76	**54.67**
ro_adj05.0-wspd4.0	0.06	0.09	91.20	62	16	86	**54.67**
ro_adj06.0-wspd1.5	0.05	0.18	63.48	32	90	52	**58.00**
ro_adj07.0-wspd1.5	0.05	0.17	69.49	31	89	61	**60.33**
ro_adj25.0-wspd4.5	0.06	0.12	54.43	77	64	41	**60.67**
ro_adj20.0-wspd4.5	0.06	0.12	54.82	78	62	42	**60.67**
ro_adj15.0-wspd4.5	0.06	0.12	59.94	83	58	47	**62.67**
ro_adj07.0-wspd4.5	0.06	0.11	69.41	80	49	59	**62.67**
ro_adj08.0-wspd1.5	0.05	0.17	74.79	30	88	71	**63.00**
ro_adj09.0-wspd1.5	0.05	0.16	79.52	28	86	75	**63.00**

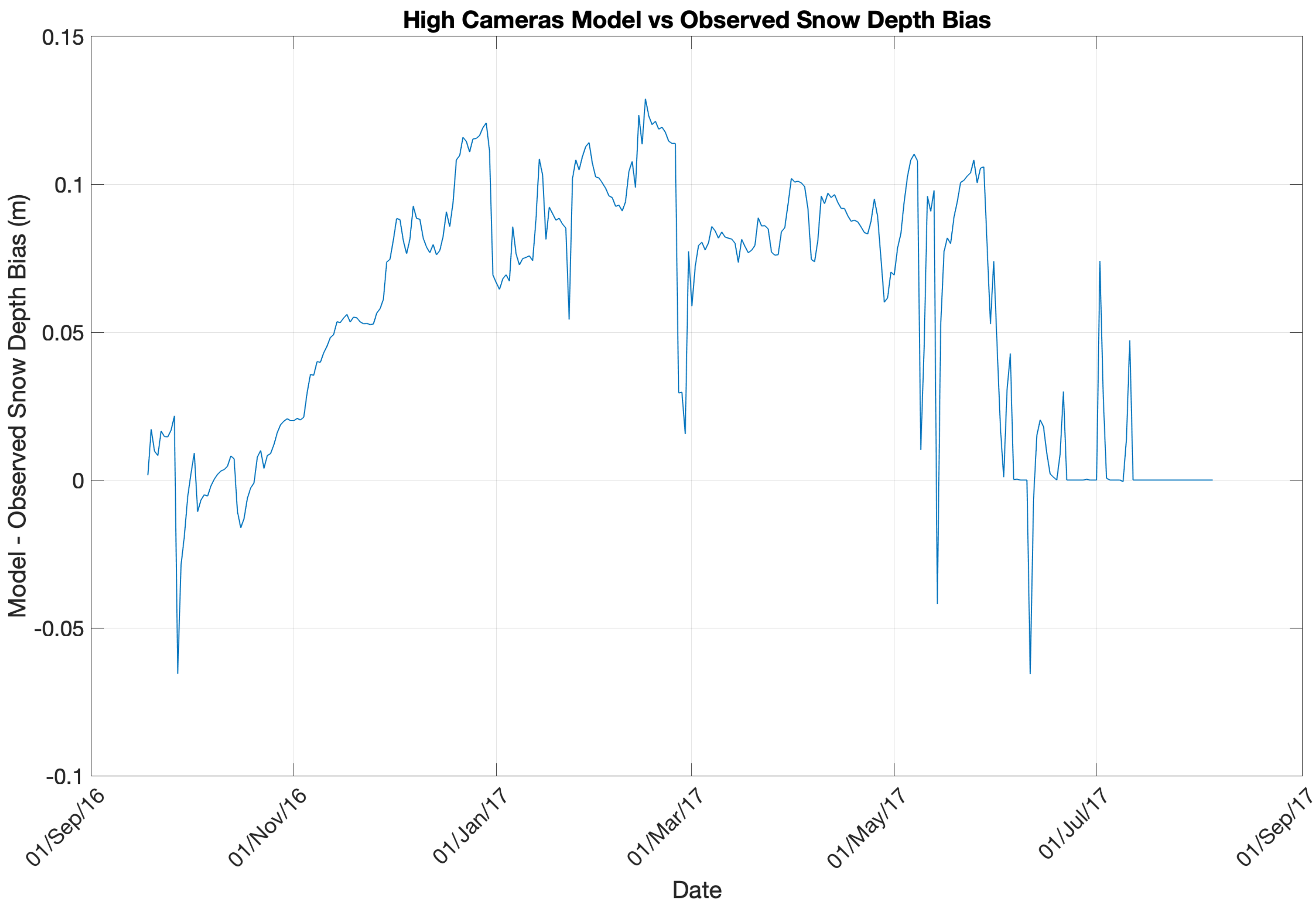

Appendix 2.8. Modelled vs Observed snow depth bias through time from the best calibration (ro_adj = 6.0; wspd_increase = 2.5) to observations of snow depth from cameras located at high elevations above shrubline. Mean bias is 0.06 cm.

Appendix 2.9. Summary statistics of model-derived snow and climate covariates by season within the Jacksina sheep survey unit within Wrangell-St. Elias National Park and Preserve, Alaska.

Variable	Season	N	Mean	SD	CV	Min	25%	75%	Max
Snow Depth (m)	Fall	37	0.25	0.06	22.21	0.15	0.21	0.28	0.40
	Winter	37	0.36	0.05	15.10	0.25	0.32	0.40	0.46
	Spring	37	0.37	0.06	15.45	0.23	0.33	0.41	0.47
Snow Density (kg m-3)	Fall	37	251.36	20.25	8.06	213.17	233.82	267.16	299.64
	Winter	37	283.35	16.92	5.97	247.39	272.26	294.15	316.21
	Spring	37	323.26	14.13	4.37	299.70	314.31	329.65	350.99
Forageable Area (%)	Fall	37	77.46	7.63	9.85	53.62	73.51	82.42	93.13
	Winter	37	61.59	9.52	15.46	40.70	54.57	66.58	80.99
	Spring	37	49.86	7.50	15.05	34.53	46.48	55.09	65.82
Snowfall (m)	Fall	37	0.16	0.03	21.47	0.08	0.13	0.18	0.22
	Winter	37	0.11	0.02	21.87	0.06	0.09	0.12	0.16
	Spring	37	0.10	0.02	17.32	0.07	0.09	0.11	0.14
Air Temperature (ºC)	Fall	37	-8.40	1.36	-16.14	-11.71	-9.26	-7.51	-5.05
	Winter	37	-15.27	1.92	-12.59	-20.42	-16.07	-14.01	-11.75
	Spring	37	-8.75	1.52	-17.36	-11.10	-10.04	-7.89	-5.16

Appendix 2.10. Table of single predictor models and null model showing; p-values (ANOVA P-value) for an ANOVA test between the model fitted with and without a random effect (Survey Unit) and using Restricted Maximum Likelihood; the second-order Akaike Information Criterion (AICc) of the single predictor model fitted without a random effect and by Ordinary Least Squares. Models are ranked by AICc and all predictors with an AICc greater than the Null model are taken forward into multiple predictor models (see Appendix 2.11 below)

Variable	ANOVA P-value	AICc
Fall Snow Depth (m)	0.64	-89.35
Spring Snow Depth (m)	0.86	-87.23
Winter Snow Depth (m)	0.77	-86.56
Fall Air Temperature (ºC)	1.00	-80.76
Spring Forageable Area (%)	0.60	-77.62
Fall Forageable Area (%)	0.22	-77.20
Fall Snowfall (m)	0.22	-76.33
Winter Snowfall (m)	0.62	-75.13
Spring Snow Density (kg m-3)	0.66	-74.99
Fall Snow Density (kg m-3)	0.26	-74.49
Spring Snowfall (m)	0.29	-74.06
Null	0.43	-73.47
Winter Forageable Area (%)	0.31	-72.01
Previous Year Air Temperature (ºC)	0.45	-71.48
Winter Snow Density (kg m-3)	0.34	-70.96
Spring Air Temperature (ºC)	0.45	-70.51
Winter Air Temperature (ºC)	0.47	-70.47
Previous Summer Snow Depth (m)	0.46	-68.98
Previous Year Snow Density (kg m-3)	0.21	-68.46
Previous Summer Snowfall (m)	0.36	-67.99
Previous Year Snow Depth (m)	0.45	-67.80
Previous Year Forageable Area (%)	0.30	-67.61
Previous Summer Forageable Area (%)	0.35	-67.57
Previous Summer Air Temperature (ºC)	0.36	-67.40
Previous Year Snowfall (m)	0.32	-67.28
Previous Summer Snow Density (kg m-3)	1.00	-17.58

Appendix 2.11. Complete table of multi-predictor models and Null model ranked by their second-order Akaike Information Criterion (AICc). Standard error (SE) shown in brackets for both the intercept and estimate of each predictor in each model. 1st Predictor indicates the 1st snow and climate covariable listed in the Model column. ** indicates significance at a Bonferroni corrected alpha level of 0.00125 (alpha / total models); * indicates significance at alpha = 0.05. P-values were computed in R by the Wald test method via use of the 'summary' core package (R Core Team, 2019).

Model	Intercept (SE)	1st Predictor Estimate (SE)	Fall Air Temperature (SE)	Fall Snowfall (SE)	K	Delta AICc	AICc weight	R-Sq.	Adjusted R-Sq.
Fall Snow Depth + Fall Air Temperature	0.690 (0.094)**	-0.738 (0.193)**	0.027 (0.012)*	–	3	0	0.188	0.439	0.41
Winter Snow Depth + Fall Air Temperature + Fall Snowfall	0.900 (0.112)**	-0.599 (0.214)*	0.032 (0.012)*	-0.818 (0.398)*	4	0.134	0.176	0.472	0.429
Spring Snow Depth + Fall Air Temperature + Fall Snowfall	0.851 (0.111)**	-0.522 (0.192)*	0.027 (0.013)*	-0.940 (0.388)*	4	0.523	0.145	0.467	0.424
Fall Snow Depth + Fall Air Temperature + Fall Snowfall	0.780 (0.114)**	-0.593 (0.219)*	0.030 (0.012)*	-0.593 (0.435)	4	0.592	0.14	0.466	0.423
Winter Snow Depth + Fall Air Temperature	0.792 (0.103)**	-0.738 (0.211)**	0.029 (0.012)*	–	3	1.963	0.071	0.412	0.381
Fall Snow Depth	0.511 (0.046)**	-0.895 (0.187)**	–	–	2	2.328	0.059	0.37	0.354
Spring Snow Depth + Fall Snowfall	0.689 (0.081)**	-0.720 (0.173)**	–	-0.848 (0.402)*	3	2.374	0.057	0.406	0.375
Spring Snow Depth + Fall Air Temperature	0.706 (0.099)**	-0.623 (0.199)*	0.023 (0.014)	–	3	3.949	0.026	0.383	0.35
Fall Snow Depth + Fall Snowfall	0.552 (0.068)**	-0.818 (0.211)**	–	-0.367 (0.452)	3	4.084	0.024	0.381	0.348
Spring Snow Depth	0.577 (0.064)**	-0.788 (0.177)**	–	–	2	4.45	0.02	0.336	0.319
Winter Snow Depth + Fall Snowfall	0.689 (0.086)**	-0.807 (0.215)**	–	-0.687 (0.426)	3	4.87	0.017	0.369	0.335
Winter Snow Depth	0.614 (0.074)**	-0.909 (0.210)**	–	–	2	5.121	0.015	0.326	0.308
Fall Air Temperature + Fall Snowfall	0.847 (0.120)**	0.045 (0.012)**	–	-1.170 (0.410)*	3	5.411	0.013	0.36	0.327
Fall Forageable Area + Fall Air Temperature	0.314 (0.165)	0.004 (0.002)*	0.041 (0.012)*		3	6.592	0.007	0.342	0.307
Spring Snowfall + Fall Air Temperature + Fall Snowfall	0.878 (0.123)**	-0.696 (0.622)	0.040 (0.013)*	-1.181 (0.409)*	4	6.649	0.007	0.381	0.331
Fall Forageable Area + Fall Air Temperature + Fall Snowfall	0.609 (0.257)*	0.002 (0.002)	0.043 (0.012)*	-0.802 (0.540)	4	6.817	0.006	0.379	0.328
Winter Snowfall + Fall Air Temperature + Fall Snowfall	0.881 (0.124)**	-0.712 (0.690)	0.042 (0.013)*	-1.060 (0.423)*	4	6.851	0.006	0.378	0.328
Spring Forageable Area + Fall Air Temperature + Fall Snowfall	0.699 (0.208)*	0.002 (0.002)	0.041 (0.013)*	-0.983 (0.463)*	4	7.169	0.005	0.373	0.323
Fall Snow Density + Fall Air Temperature + Fall Snowfall	0.951 (0.180)**	-0.001 (0.001)	0.044 (0.012)**	-0.959 (0.494)	4	7.353	0.005	0.371	0.32
Spring Snow Density + Fall Air Temperature + Fall Snowfall	1.013 (0.314)*	-0.001 (0.001)	0.043 (0.013)*	-1.072 (0.448)*	4	7.653	0.004	0.366	0.315
Fall Snow Density + Fall Air Temperature	0.986 (0.186)**	-0.001 (0.001)*	0.043 (0.013)*	–	3	8.732	0.002	0.306	0.27
Spring Forageable Area + Fall Air Temperature	0.407 (0.163)*	0.004 (0.002)	0.036 (0.013)*	–	3	9.274	0.002	0.297	0.26
Winter Snowfall + Fall Air Temperature	0.740 (0.118)**	-1.150 (0.712)	0.039 (0.013)*	–	3	10.658	0.001	0.273	0.235
Fall Air Temperature	0.657 (0.108)**	0.044 (0.013)*	–	–	2	10.917	0.001	0.223	0.203
Spring Snow Density + Fall Air Temperature	1.130 (0.328)*	-0.002 (0.001)	0.039 (0.014)*	–	3	10.944	0.001	0.268	0.229
Spring Snowfall + Fall Air Temperature	0.684 (0.112)**	-0.656 (0.680)	0.040 (0.014)*	–	3	12.386	0	0.242	0.202
Spring Snowfall + Fall Snowfall	0.622 (0.099)**	-1.357 (0.645)*	–	-1.181 (0.451)*	3	13.289	0	0.225	0.184
Spring Forageable Area	0.037 (0.096)	0.005 (0.002)*	–		2	14.054	0	0.161	0.14
Spring Forageable Area + Fall Snowfall	0.224 (0.158)	0.004 (0.002)	–	-0.746 (0.508)	3	14.247	0	0.206	0.165
Fall Forageable Area	-0.059 (0.135)	0.005 (0.002)*	–	–	2	14.48	0	0.153	0.131
Winter Snowfall + Fall Snowfall	0.591 (0.098)**	-1.277 (0.750)	–	-0.961 (0.474)*	3	14.795	0	0.196	0.153
Fall Snowfall	0.483 (0.077)**	-1.158 (0.471)*	–	–	2	15.346	0	0.134	0.112
Spring Snow Density + Fall Snowfall	0.959 (0.352)*	-0.002 (0.001)	–	-0.902 (0.501)	3	15.79	0	0.176	0.133
Fall Forageable Area + Fall Snowfall	0.156 (0.252)	0.003 (0.002)	–	-0.619 (0.611)	3	15.848	0	0.175	0.131
Winter Snowfall	0.477 (0.084)**	-1.649 (0.756)*	–	–	2	16.546	0	0.109	0.086
Spring Snow Density	1.063 (0.357)*	-0.002 (0.001)*	–	–	2	16.687	0	0.106	0.083
Fall Snow Density + Fall Snowfall	0.619 (0.177)**	-0.001 (0.001)	–	-0.894 (0.566)	3	17.038	0	0.151	0.106
Fall Snow Density	0.657 (0.179)**	-0.001 (0.001)	–	–	2	17.186	0	0.095	0.072
Spring Snowfall	0.428 (0.070)**	-1.316 (0.691)	–	–	2	17.619	0	0.085	0.062
Null	0.290 (0.015)**	–	–	–	1	18.207	0	–	–

Appendix 2.12. Coefficients and fit statistics of the linear models testing for trends in each variable by season from 1980 to 2017

Variable	Season	Estimate	R-squared	P-value
Snow Depth (m)	Fall	-0.001	0.023	0.37
	Winter	0.000	0.009	0.58
	Spring	-0.001	0.019	0.41
Snow Density (kg m-3)	Fall	-0.322	0.030	0.31
	Winter	-0.211	0.018	0.43
	Spring	-0.208	0.025	0.35
Forageable Area (%)	Fall	0.100	0.020	0.40
	Winter	0.120	0.018	0.42
	Spring	0.150	0.047	0.20
Snowfall (m)	Fall	0.000	0.004	0.71
	Winter	0.000	0.009	0.57
	Spring	0.000	0.040	0.23
Air Temperature (°C)	Fall	0.033	0.068	0.12
	Winter	0.038	0.046	0.20
	Spring	0.002	0.000	0.93

Appendix 2.13. Coefficients and fit statistics of the linear models testing for trends in the rolling 10-year coefficient of variation of each variable by season from 1980 to 2017

Variable	Season	Estimate	R-squared	P-value
Snow Depth (m)	Fall	-0.019	0.002	0.81
	Winter	0.041	0.018	0.46
	Spring	-0.038	0.011	0.57
Snow Density (kg m-3)	Fall	0.027	0.068	0.14
	Winter	0.057	0.292	0.00
	Spring	-0.002	0.000	0.93
Forageable Area (%)	Fall	0.051	0.028	0.35
	Winter	-0.080	0.065	0.15
	Spring	-0.019	0.011	0.55
Snowfall (m)	Fall	0.050	0.012	0.54
	Winter	-0.165	0.254	0.00
	Spring	0.087	0.064	0.16
Air Temperature (°C)	Fall	0.076	0.123	0.05
	Winter	0.005	0.000	0.92
	Spring	0.002	0.000	0.96

2.9.2 Appendix References

Homer, C., Dewitz, J., Yang, L., Jin, S., Danielson, P., 2015. Completion of the 2011 National Land Cover Database for the Conterminous United States – Representing a Decade of Land Cover Change Information. PHOTOGRAMMETRIC ENGINEERING 11.

Liston, G.E., 1995. Local Advection of Momentum, Heat, and Moisture during the Melt of Patchy Snow Covers. J. Appl. Meteor. 34, 1705–1715. https://doi.org/10.1175/1520-0450-34.7.1705

Liston, G.E., Elder, K., Liston, G.E., Elder, K., 2006. A Meteorological Distribution System for High-Resolution Terrestrial Modeling (MicroMet). Journal of Hydrometeorology 7, 217–234. https://doi.org/10.1175/JHM486.1

Liston, G.E., Haehnel, R.B., Sturm, M., Hiemstra, C.A., Berezovskaya, S., Tabler, R.D., 2007. Simulating complex snow distributions in windy environments using SnowTran-3D. Journal of Glaciology 53, 241–256. https://doi.org/10.3189/172756507782202865

Liston, G.E., Hall, D.K., 1995. An energy-balance model of lake-ice evolution. Journal of Glaciology 41, 373–382. https://doi.org/10.3189/S0022143000016245

Liston, G.E., Hiemstra, C.A., 2008. A Simple Data Assimilation System for Complex Snow Distributions (SnowAssim). J. Hydrometeor. 9, 989–1004. https://doi.org/10.1175/2008JHM871.1

Mahoney, P.J., Liston, G.E., LaPoint, S., Gurarie, E., Mangipane, B., Wells, A.G., Brinkman, T.J., Eitel, J.U.H., Hebblewhite, M., Nolin, A.W., Boelman, N., Prugh, L.R., 2018. Navigating snowscapes: scale-dependent responses of mountain sheep to snowpack properties. Ecological Applications 0. https://doi.org/10.1002/eap.1773

National Park Boundaries - Data.gov [WWW Document], n.d. URL https://catalog.data.gov/dataset/national-park-boundariesf0a4c (accessed 5.24.20).

QGIS Development Team, 2019. QGIS Geographic Information System. Open Source Geospatial Foundation Project.

R Core Team, 2019. R: A Language and Environment for Statistical Computing. R Foundation for Statistical Computing, Vienna, Austria.

U.S. Geological Survey, 2015. NLCD 2011 Land Cover Alaska 2001 to 2011 From To Change Index - National Geospatial Data Asset (NGDA) Land Use Land Cover [WWW Document]. URL https://www.mrlc.gov/data/nlcd-2001-2011-land-cover-change-alaska-0

Verbyla, D., 2017. ABoVE: Last Day of Spring Snow, Alaska, USA, and Yukon Territory, Canada, 2000-2016. ORNL DAAC. https://doi.org/10.3334/ORNLDAAC/1528

WRST Sheep and Goat Count Units - data.doi.gov [WWW Document], n.d. URL https://data.doi.gov/dataset/wrst-sheep-and-goat-count-units (accessed 5.24.20).

Chapter 3 Assessment of a passive microwave algorithm to map layers of high-density snow and ice across Alaska; influences of topographic complexity, land cover, and meteorological conditions on detections

Chris L. Cosgrove and Anne W. Nolin

3.1 Abstract

Layers of high-density snow and ice affect Arctic-boreal wildlife's locomotion, foraging, den and nesting strategies, vulnerability to, and efficacy of, predation. Field observations of these layer's increased occurrence in high-latitude snowpacks, and their catastrophic consequence for grazing ungulates, has driven research into their detection using remote sensing. Passive microwave (PM) radiometry has shown promise in several studies, but it has so far been limited to narrow spatio-temporal extents where known animal mass-mortality events have occurred and by its relatively coarse resolution ~25 km. To address this, we used a passive microwave algorithm to map detections of layers of high-density snow and ice across a study domain encompassing the Alaskan peninsula. Via use of the Calibrated Enhanced-Resolution Passive Microwave Daily EASE-Grid 2.0 Brightness Temperature product daily maps of detections from 1988 to 2019 were produced with data derived from the Special Sensor Microwave/Imager (SSM/I) upon three different satellites. Two different frequencies were contrasted for their sensitivity to changes in the snow stratigraphy, 19 and 37 GHz, which have an enhanced resolution of 6.25 km and 3.125 km respectively. We assessed the regional and interannual variability, and influences of topographic complexity and vegetation of detections, upon detections. Additionally presented is a preliminary assessment of the algorithm's promise via comparison of the preceding meteorological conditions, as measured by two climatological station networks, of algorithm-detected high-density layer occurrence, persistence, and disappearance. With a limited dataset of snowpit-measured snow density we also looked for relationships between ground-observations of stratigraphy and the PM record. The algorithm appeared to perform best in coastal regions of low topographic complexity and tundra-like vegetation, as evidenced by a greater frequency of detections, and the 19 GHz channel was generally more sensitive than the 37 GHz, possibly due to its greater footprint and lower density threshold for

detection. We found significant differences between the preceding meteorology of days where an occurrence, persistence, and disappearance event was observed, and the meteorological conditions that corresponded to known controls on the formation, maintenance, and destruction of layers of high-density snow and ice. In contrast to this promising result, no relationships between snowpit measured density and the PM record. We anticipate that this research will be of great interest to wildlife ecologists examining different scales of animal's responses to snow properties but counsel that further work needs to be completed to ensure its accuracy.

3.2 Introduction

Seasonal snow cover is an integral and vital element in high-latitude areas' ecosystem function, its properties lending both opportunity and hindrance to culturally important wildlife dynamically in space and time (Berteaux et al., 2016; Bokhorst et al., 2016). In the Arctic Boreal region, increasing air temperatures and observations of mid-winter melt events have led to widespread concern for populations of grazing wildlife, e.g., caribou (*Rangifer tarandus*) and Dall's sheep (*Ovis dalli dalli*), due to layers of high-density snow and ice impeding access to forage (Tyler N. J. C., 2010; Mallory and Boyce, 2017; Rattenbury et al., 2018). Yet, the region's remoteness and inaccessibility, as well as the wide geographic range of these species, mean that there are scant measurements of snow coincident to the presence, or indeed absence, of ungulate populations (Boelman et al., 2018). The so-called 'golden age' of animal-born sensors, where advances in technology now offer researchers the possibility of high-accuracy and high-frequency location data for individual animals, has driven insights into northern species previously challenging to study (Wilmers et al., 2015; Davidson et al., 2020). However, despite the utilization of this technology, there remain limits to our understanding of animal behaviour and possible population responses to climate change, as we have little knowledge of the spatiotemporal scale of the occurrence and persistence of important snow properties, such as depth, density and the presence of ice layers (Boelman et al., 2018). To address this, we here assess the applicability of a high-density snow layer detection algorithm utilizing space-borne passive microwave (PM) observations across Arctic boreal Alaska.

Microwave remote sensing from orbiting satellite platforms began in the 1960s (Ulaby et al., 1981) and, in contrast to observations utilizing the visible light and near-infrared spectrums, offers unique information on the properties of snow cover, as well as data collection uninhibited by night or cloud conditions (Foster et al., 1984; Saberi et al., 2019). The development of algorithms to estimate snow's various properties is ongoing but has primarily concentrated on producing information important to hydrological processes, most notably snow water equivalent (SWE) and snow-covered area (SCA; Saberi, 2019). Inherent to the method of using PM is their characteristic interaction with snow grains and liquid water – a feature that has been exploited to infer further important properties and dynamics of snow cover, such as freeze-thaw events (e.g. Kim et al., 2018), snow-off date (e.g. Pan et al., 2020), instances of rain-on-snow (e.g. Grenfell T. C. and Putkonen J., 2008; Pan et al., 2018), and stratigraphic features like depth hoar (e.g. Hall et al., 1986) or the presence of ice lenses or high-density layers (e.g. Montpetit et al., 2013). The traditionally large footprint of space-born PM measurements, typically ~25 km^2 in the 19 GHz and 37 GHz bands most commonly used in snow applications, consequently limits the accuracy of their derived data products in areas of complex topography or landcover (Mätzler and Standley, 2000; Tong et al., 2010). However, the 2016 release of the Calibrated Enhanced-Resolution Passive Microwave Daily EASE-Grid 2.0 Brightness Temperature (CETB; Brodzik, M.J. and Long, D.G., 2016) Earth System Data Record (ESDR) offers an opportunity to test whether mapping snow properties at resolutions more appropriate to important spatial scales of wildlife habitat selection is possible (Holland et al., 2004).

Northern wildlife is affected by snow properties in contrasting ways. Both rodents, e.g., lemmings (*Lemmus lemmus*), and species of bears, e.g., brown bears (*Ursus arctos*), rely on thermo-insulative properties of snow cover to protect them from the harsh winter environment when nesting and denning respectively (Reid et al., 2012; Vroom et al., 1980). Years with minimal snow cover hence comes at an increased fitness cost, and in the case of lemmings, increased exposure to predation (Bilodeau et al., 2013). For species that instead have a *supraniveal* winter habitat, snow cover instead influences their access to nutrition (e.g. Collins and Smith, 1991), locomotive energy expenditure (e.g. Fancy and White, 2011), and therefore their efficacy of, or vulnerability to, predation (e.g. Nelson and Mech, 1986). For grazing ungulates, the depth, density, and hardness of snow cover have been linked to recruitment success rates (e.g. Kerk et al., 2018) and corresponding shifts in population dynamics (Tyler N. J. C., 2010). In separate locations, Svalbard and Banks Island, Canada, a mid-winter formation of a high density or ice-layer, has had catastrophic consequences for caribou populations unable to access forage (Grenfell T. C. and Putkonen J., 2008; Descamps et al., 2017). Such mass-mortality events have ecological impacts, such as increasing populations of scavenging species (Sokolov et al., 2016), economic impacts in the instance of reduced harvest and sport-hunting opportunities (Alaska Department of Fish and Game, 2014), and threatens the continued culture and traditional knowledge of indigenous people in the circumpolar North (Eira et al., 2018). Wildlife studies incorporating PM data have primarily been locally-focused on known mass-mortality events (e.g. Grenfell T. C. and Putkonen J., 2008; Langlois et al., 2017; Dolant et al., 2018). Alternatively, they have used datasets that do not explicitly indicate challenging snow conditions but instead have mapped events, such as surface thawing, which *could* lead to reduced forage access (Kerk et al., 2020). In this study, we instead aim to broaden the spatial scope of enquiry and look for the potentially persistent *consequence* of meteorological events, by examining the degree to which we can map high-density snow or ice layers across Alaska, an Arctic boreal region of diverse landscapes and home to large populations of caribou and other ungulates.

Seasonal snow cover can be thought of as aeolian sediment that develops a dynamic stratigraphy as it accumulates, metamorphizes, and ablates in a variety of different processes (Fierz et al., 2009). High-density layers are formed in both dry and wet snow conditions (Colbeck, 1982). In dry snow conditions, where the temperature gradient across a snow layer is low, equi-temperature metamorphism rounds snowflakes due to water vapour gradients between convex and concave surfaces. The process of rounding decreases the snow's surface area relative to its mass, increasing its density. Snow deposited during periods of higher wind speeds, either as new snow or that redistributed by the wind, are higher density than that deposited in relatively still conditions (Sommer, 2018). While the mechanisms for this remain unclear (Sommer et al., 2018), there is substantial evidence for its occurrence - leading to the commonly used stratigraphic descriptions of 'wind-crust' and 'wind-slab' (Fierz et al., 2009). Wet snow conditions, where liquid water is introduced to the snowpack due to surface melting or liquid precipitation, increases density by eliminating smaller snow crystals and growing larger crystals while conserving the total mass (Colbeck, 1982). Depending on the amount of liquid water and the existing stratigraphic properties of the snow, ice lenses and layers can form at the snowpack's surface or interface with the soil. With temperatures in the Arctic increasing at a rate greater than elsewhere, rain-on-snow and melt events are expected to occur with greater frequency (Semmens et al., 2013; Jeong and Sushama, 2018). Already there is multi-dataset evidence of increases in both these events (e.g. Liston and Hiemstra, 2011) and their effect upon snow stratigraphy and conditions (Johansson et al., 2011b; Eira et al., 2018; Rasmus et al., 2018), causing concern for the continued sustainability of traditional reindeer husbandry (Eira et al., 2018).

The use of an enhanced resolution passive microwave product with a multi-decadal record has promise for wildlife studies requiring long-term data to compare to records of population dynamics, but also those requiring finer-scale data to understand habitat selection behaviour. To assess the algorithm, we compare instances where it 'detects' a high-density snow layer to in-situ meteorological and snow stratigraphy data. Additionally, we consider the spatio-temporal pattern of detections in relation to the diverse climate, vegetation, and topography of Alaska. The following questions lead our research; 1) where and when do we detect high-density and ice-layers in Alaskan snowpacks? 2) Can we establish the meteorological cause of detected high-density and ice-layers? We additionally test whether we can validate our results by comparing the PM observations to snow density data obtained via snowpit excavation within our study domain.

3.3 Materials and methods

3.3.1 Study domain

Alaska extends from ~51º N to ~71º N and from ~130 W to ~172º E, encompassing a great diversity of landscapes and climates. Bordered to the east by the Yukon Territory, Canada, the south by the Gulf of Alaska, the southwest by the Bering Sea, the northeast by the Chukchi Sea, and the north by the Beaufort Sea, there exist multiple influences on its climate due to gradients of latitude, proximity to coastal waters, elevation, and topography. Snow covers much of the region for 6 to 9 months of the year and is hence a primary component in the area's energy, hydrological, and carbon cycles, as well as ecosystem function. Alaskan snowpacks reflect the state's distinct climate zones; deep, warm maritime snow is found in high elevations of southeast Alaska, whereas low-density taiga type snow is typical in the interior's extensive boreal forest (Sturm et al., 1995). Elsewhere, tundra type snow, with its classic stratigraphy of depth hoar and wind-slabs, extends across sub-Arctic and Arctic areas (Sturm and Benson, 2004). To examine regional patterns in the frequency of high-density snow detections, we here use Bieniek et al.'s (2012) climate divisions. However, due to masking areas close to major water-bodies, such as the entirety of the Alaskan Panhandle, we present data only from Bristol Bay, Central Interior, Cook Inlet, North Slope, Northeast Gulf, Northeast Interior, Northwest Gulf, Southeast Interior, and West Coast climate divisions (Appendix 3.1).

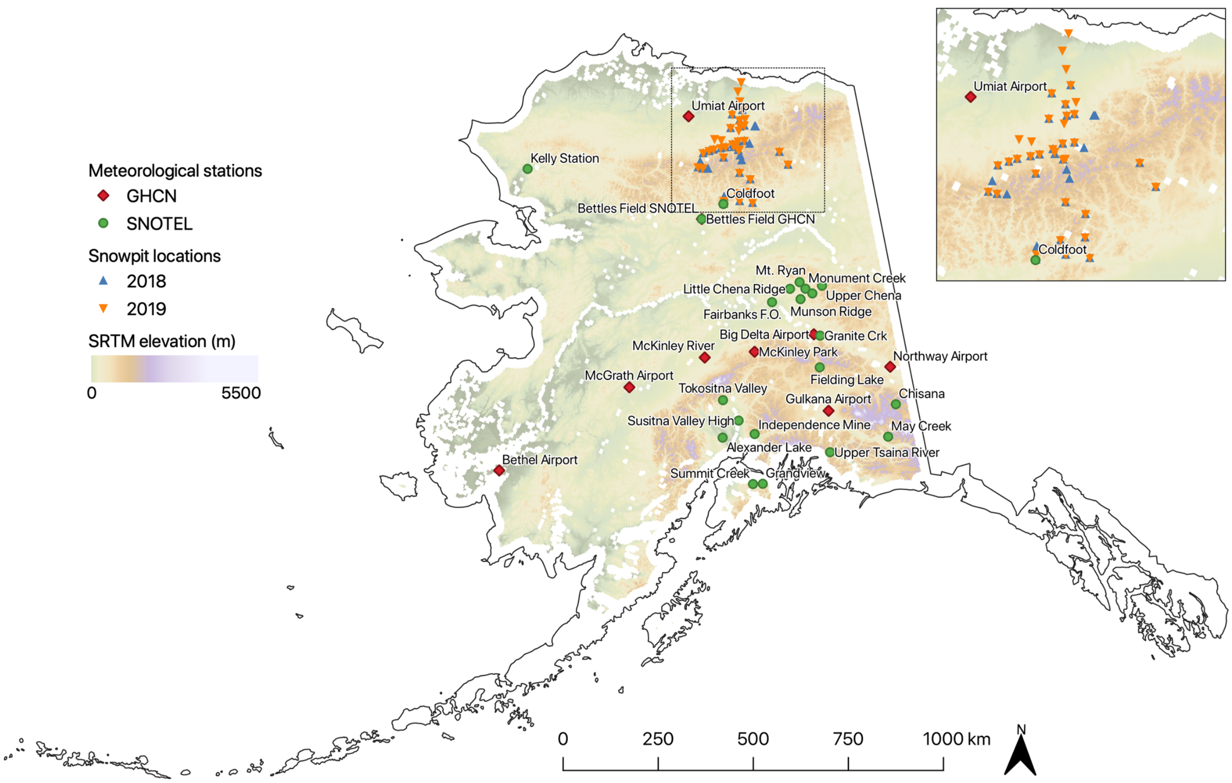

Figure 3.1. map of study area. The digital elevation model derived from the Shuttle Radar Topography Mission (SRTM) is shown with a 25 km water body buffer applied. Inset shows snowpit locations at greater detail.

3.3.2 Passive microwave data

The CETB ESDR was publicly released in 2017 as part of the National Aeronautics and Space Administration's Making Earth System Data Records for Use in Research Environments (NASA MEaSUREs) program (Brodzik, M.J. and Long, D.G., 2016). It assembles Level-2 satellite PM observations from 4 different sensors - the Scanning Multichannel Microwave Radiometer (SMMR), the Special Sensor Microwave/Imager (SSM/I), the Special Sensor Microwave Imager/Sounder (SSMIS), and the Advanced Microwave Scanning Radiometer – Earth Observing System (AMSR-E), and re-grids them to the Equal-Area Scalable Earth Grid 2.0 (EASE-2) format at both a standard resolution (25 km) and a nested, enhanced resolution dependent on channel frequency. Standard resolutions, which we do not use here, are generated using a 'drop-in-the-bucket' averaging technique, whereas enhanced resolutions are derived using a radiometer version of the Scatterometer Image Reconstruction (rSIR) algorithm (Brodzik and Long, 2018). While the complete CETB dataset has twice-daily, global data from 12 different satellite platforms, and has temporal coverage from 1978 through 2019, we present enhanced resolution data for the 19 and 37 GHz channels derived from SSM/I sensors onboard the Defence Meteorological Satellite Program's (DMSP) F08, F11 and F15 satellite platforms. Measurements by the SSMI/S sensor are highly correlated across platforms, so use of data from F08, F11 and F15 DMSP satellites allows for a continuous and consistent record from the 7th of September 1988 to the 31st of December 2019. Both 19 and 37 GHz channels are sensitive to changes in snow stratigraphy (Grenfell T. C. and Putkonen J., 2008), and the CETB dataset grids each at 6.25 km and 3.125 km resolution respectively. We further selected a subset of data corresponding to the descending pass of the satellites as descending orbits have a local overpass in the early morning (~0600), which is more likely to be unaffected by high PM emissions from wet snowpacks in contrast to ascending afternoon passes (Derksen et al., 2000).

3.3.3 High-density and ice-layer detection algorithm

The high-density and ice-layer detection algorithm we use here is based upon the methodology first used in a wildlife context by Grenfell and Putkonen (2008), and elaborated by the work of Montpetit et al. (2013), Langlois et al. (2017), and Dolant et al. (2018). The algorithm calculates the ratio between the brightness temperatures observed in the vertical and horizontal polarizations of a single channel (Langlois et al., 2017). A positive increase in the ratio suggests the establishment of layers in the snowpack as the horizontal polarization is more sensitive to layering than that of the vertical polarization. For a given frequency f, the polarization ratio PR_f is calculated as

$$\mathrm{PR}_f = \frac{T_{\mathrm{B}_f}^{\mathrm{V-pol}} - T_{\mathrm{B}_f}^{\mathrm{H-pol}}}{T_{\mathrm{B}_f}^{\mathrm{V-pol}} + T_{\mathrm{B}_f}^{\mathrm{H-pol}}}$$

Where T_{B_f} is the brightness temperature in Kelvin (K) for a given frequency, and V-pol and H-pol refer to the vertical and horizontal polarizations respectively. A thresholding approach for detecting high-density or ice-layers was established by Montpetit (2015) and developed by Dolant et al. (2018). Both studies used a radiative transfer model to simulate the expected PM emissions of an ensemble of snowpacks with and without high-density or ice-layers. Dolant et al. (2018) report that a difference of greater than 0.0127 (19 GHz) and 0.0124 (37 GHz) in the daily PR_f, when compared to the mean winter PR ($\overline{\mathrm{PR}_f}$), indicated the presence of a layer greater than 425 kg m^{-3} (19 GHz) and 520 kg m^{-3} (37 GHz). We hence calculated $\Delta\mathrm{PR}_f$ for each pixel in our study domain using the following equation

$$\Delta\mathrm{PR}_f = \mathrm{PR}_f - \overline{\mathrm{PR}_f}$$

Where $\overline{\mathrm{PR}_f}$ is calculated from daily data between the 1st of November and the 31st of April of each water year (WY), following Dolant et al. (2018) and a timeframe where seasonal snow is highly likely to be present. When the threshold is reached in the daily record, we hereafter refer to this as a 'detection' while acknowledging that this does not necessarily mean that a high-density layer is actually present. Several studies have linked persistent snow layers greater than >350 kg m^{-3} in density with population declines in caribou (Vikhamar-Schuler et al., 2013; Ouellet et al., 2017), and other research has described a doubling in energy expenditure for caribou foraging in snow densities between 280 and 500 kg m^{-3} versus 'fluffy' snow of ~180 kg m^{-3} (Fancy and White, 1985). For Dall's sheep, a critical density of 327 kg m^{-3} has been identified as the threshold above which the animals do not break the snow surface while walking (Sivy et al., 2018). Hence, the densities corresponding to the detection thresholds for $\Delta\mathrm{PR}_f$ are within and above density ranges known to have effects on grazing animals.

3.3.4 Processing approach

The CETB product was released with a high degree of interoperability and usability in mind, utilizing the highly flexible netCDF file format and machine-readable metadata (Brodzik et al., 2018). As such, our processing workflow could employ the xarray Python package (Hoyer and Hamman, 2017) to efficiently apply the high-density snow detection algorithm at a hemispheric scale, and to nimbly construct, manage, and analyze spatial and temporal subsets of the resulting multidimensional dataset. While we focus on Alaska in this research, we have processed polarization data for the entire Northern hemisphere for the frequencies and platforms described above. We anticipate that this will aid similar research in other spatial domains. A schematic of the processing approach is shown in Appendix 3.2.

Table 3.1. List of meteorological stations used. RMSD refers to the Root Mean Standard Deviation of sub-pixel topography for the 3.125 km EASE-2 pixel where the station is located. Likewise, TRI is the mean Topographic Ruggedness Index, and NLCD is the majority land cover class found for the same pixel (see landcover and topographic complexity section for details). Climate division is determined using the divisions proposed by Bieniek et al. (2012).

Station Name	Network	Latitude	Longitude	Elevation	RMSD	TRI	Climate division	NLCD
Bethel Airport	GHCN	60.79	-161.83	31.10	7.89	4.90	West Coast	Dwarf Scrub
Bettles Field	GHCN	66.92	-151.52	193.20	18.42	15.88	Central Interior	Shrub/Scrub
Big Delta Airport	GHCN	63.99	-145.72	389.20	27.55	5.01	Southeast Interior	Evergreen
Gulkana Airport	GHCN	62.16	-145.46	476.10	37.44	13.06	Southeast Interior	Evergreen
McGrath Airport	GHCN	62.96	-155.61	101.50	55.37	4.27	Central Interior	Deciduous
McKinley Park	GHCN	63.72	-148.97	630.90	145.91	90.34	Southeast Interior	Shrub/Scrub
McKinley River	GHCN	63.65	-151.64	256.00	11.16	2.75	Central Interior	Evergreen
Northway Airport	GHCN	62.96	-141.99	522.10	2.86	1.60	Southeast Interior	Woody Wetlands
Umiat Airport	GHCN	69.37	-152.14	81.10	21.94	14.01	North Slope	Dwarf Scrub
Alexander Lake	SNOTEL	61.75	-150.89	48.77	33.37	2.08	Cook Inlet	Emergent Herb. Wetlands
Bettles Field	SNOTEL	66.92	-151.53	195.07	18.42	15.88	Central Interior	Shrub/Scrub
Chisana	SNOTEL	62.07	-142.05	1011.94	82.87	26.69	Southeast Interior	Evergreen
Coldfoot	SNOTEL	67.25	-150.18	316.99	98.46	58.36	Central Interior	Shrub/Scrub
Fairbanks F.O.	SNOTEL	64.85	-147.80	137.16	0.80	3.34	Southeast Interior	Developed, Low Intensity
Fielding Lake	SNOTEL	63.20	-145.63	914.40	74.02	38.23	Southeast Interior	Shrub/Scrub
Grandview	SNOTEL	60.61	-149.06	335.28	143.98	170.20	Cook Inlet	Shrub/Scrub
Granite Creek	SNOTEL	63.94	-145.40	377.95	14.48	3.43	Southeast Interior	Cultivated Crops
Independence Mine	SNOTEL	61.79	-149.28	1082.04	146.86	134.19	Cook Inlet	Dwarf Scrub
Kelly Station	SNOTEL	67.93	-162.28	94.49	15.74	5.97	West Coast	Shrub/Scrub
Little Chena Ridge	SNOTEL	65.12	-146.73	609.60	109.94	77.37	Southeast Interior	Shrub/Scrub
May Creek	SNOTEL	61.35	-142.71	490.73	46.14	45.94	Southeast Interior	Evergreen
Monument Creek	SNOTEL	65.08	-145.87	563.88	123.73	106.98	Southeast Interior	Shrub/Scrub
Mt. Ryan	SNOTEL	65.25	-146.15	853.44	112.54	64.98	Southeast Interior	Evergreen
Munson Ridge	SNOTEL	64.85	-146.21	944.88	114.01	84.77	Southeast Interior	Shrub/Scrub
Summit Creek	SNOTEL	60.62	-149.53	426.72	145.93	159.45	Cook Inlet	Shrub/Scrub
Susitna Valley High	SNOTEL	62.13	-150.04	114.30	21.32	11.52	Cook Inlet	Deciduous
Teuchet Creek	SNOTEL	64.95	-145.52	499.87	136.02	80.26	Southeast Interior	Evergreen
Tokositna Valley	SNOTEL	62.63	-150.78	259.08	110.48	79.98	Cook Inlet	Shrub/Scrub
Upper Chena	SNOTEL	65.10	-144.93	868.68	143.33	98.59	Southeast Interior	Shrub/Scrub
Upper Tsaina River	SNOTEL	61.19	-145.65	533.40	155.06	122.62	Northeast Gulf	Shrub/Scrub

3.3.5 Meteorological data

To examine the meteorological conditions of the occurrence, persistence and disappearance of a high-density layer we utilized climate observations from two weather station networks established in Alaska; the Global Historical Climatology Network (GHCN), downloaded from the National Oceanic and Atmospheric Administration's Nation Centers for Environmental Information (NOAA, 2020), and the Snow Telemetry (SNOTEL) network run by the Natural Resources Conservation Service (NCRS). The SNOTEL data used is the Bias Correction and Quality Control data distributed by the Pacific Northwest National Laboratory (Yan et al., 2018; Sun et al., 2019). In total, 30 climate stations across the two networks were available in EASE-2 pixels that were not masked by their proximity to major water-bodies (see below). For each station, we retrieved available surface observations of daily mean/maximum/minimum air temperature, average/peak wind speed, total precipitation, snowfall, rainfall, snow depth, and SWE for a subset of our study period (see Figure 3.1 and Table 3.1).

3.3.6 Land cover and topographic data

To consider the effects of different land covers on high-density layer detections we calculated the majority land cover class within each 3.125 km (37 GHz) and 6.25 km (19 GHz) EASE-2 pixel by use of the 30 meter National Land Cover Database 2011 Alaska data product (NLCD; Homer et al., 2015). For both resolutions, we also derived two metrics of topographic complexity by calculating the sub-pixel Root Mean Standard Deviation (RMSD) of elevation and the mean sub-pixel Topographic Ruggedness Index (TRI; Riley et al., 1999) via the use of the United States Geological Services' Global 30 Arc-Second Elevation dataset (GTOPO30; Earth Resources Observation And Science (EROS) Center, 2017). Measures of rugosity have been used extensively in wildlife studies (e.g. Nellemann and Fry, 1995; Danks and Klein, 2002; Sappington et al., 2007) and have also been used to describe sub-pixel topographic complexity in research utilizing space-borne PM observations (e.g. Pan et al., 2020). The QGIS program (QGIS Development Team, 2020) was used to produce the raster grids for both landcover and topographic complexity and to additionally mask all pixels within 25 km of, and including, pixels classified as 'Open Water' in both the 3.125 km and 6.25 km land cover raster products (see Figure 3.1). This latter step is to reduce contamination of PM retrievals by major water-bodies in the native footprint of the SSMI/S sensor.

3.3.7 Snowpit data

Snow density data for 84 snow pits excavated in 2018 and 2019 (see Figure 3.1) in the Brooks Range, North Slope and Coastal Plain of Alaska was obtained from the Arctic Data Centre (Pedersen et al., 2019). For each snowpit, we averaged the density observations for each stratigraphic layer and then derived the maximum, standard deviation, and range in density across the pit's layers.

3.3.8 Spatiotemporal assessment of potential high-density layer detections

To assess the spatial variability of possible detections of high-density snow layers, we first mapped the mean count of detections per WY for each pixel across the study domain. To gauge the temporal variability, we found and mapped the mean count of possible detections for each of the six months included in our analysis window (November through April). Further, we mapped the total count of possible detections for each pixel on a WY-by-WY basis. Lastly, we found the percentage of the total possible detections within each of Bieniek et al.'s (2012) climate divisions and compared this to the percentage area of the total study domain each climate division represents.

3.3.9 Assessment of the influence of topographic complexity and landcover on the frequency of high-density layer detection

As with the assessment of total possible detections by climate division, we found the percentage of total possible detections within each NLCD landcover class and compared it to the percentage area each landcover class represents in the study domain. For the metrics of topographic complexity, we categorized each metric into ten equally incremented bins. Across the study domain, sub-pixel RMSD of elevation ranged from 0 to 180 m and was hence binned at 18 m increments, mean sub-pixel TRI likewise ranged from 0 to 450 m and was therefore binned in 45 m increments. For both metrics, we then compared the percentage of total detections within each bin to the percentage area of the study domain represented by each bin.

3.3.10 Analysis of meteorological conditions coincident to occurring, persisting, and disappearing high-density snow layers

For each of the 30 climate stations, according to their pixel location in both the 19 and 37 GHz datasets we extracted a time series of ΔPR_f and matched it to the corresponding time-series of meteorological data available from the station. As an initial step, for each station we plotted the ΔPR_f data next to the meteorological data for each WY where meteorological data was available, see figure 2 below. Study of these time-series revealed patches of missing meteorological and PM data, so to ensure fair comparison we further selected for WYs with >95% data completeness. To fill the remaining gaps, we used linear interpolation. According to the thresholds described above, we then classified the daily ΔPR data into four categories of detection. If ΔPR was below the threshold for the present day and the previous day, the present day was classed *no detection*. If the threshold was met in the present day but not the previous, we classed the day as an *occurrence*. When both the present and previous day exceeded the ΔPR threshold, the *persistence* class was used. Finally, if the previous day was above the threshold, but the present day was below, we counted the day as a *disappearance*. To our knowledge, this is the first time that the meteorological conditions of a potentially persisting and latterly disappearing high-density snow layer have been assessed. To examine differences in the meteorological conditions for each category of ΔPR observation, we aggregated data for all of the stations and tested the distributions of meteorological data between each detection category on a variable-by-variable basis. As the PM observations occurred in the morning, we compiled the previous day's and the previous two days' meteorological data for each of the detection categories across all 30 stations. We additionally compare to the previous two days because meteorological conditions that form high-density layers, such as a warm snow-storm, can occur over a period longer than a single day. The meteorological data distributions were tested for normalcy, and pairwise t-tests were conducted between the categories when normal distributions were found. Otherwise, pairwise Wilcoxon tests were used. All analyses were conducted in the R program (R Core Team, 2019) and the Bonferroni Correction was utilized for tests of significance.

3.3.11 Comparison between in-situ observations of snow density and satellite-observed polarization ratios

As with the climate stations, for the snowpit observations of layer density we extracted by location the time-series of PR observations in the WY prior to the date of each snowpit's excavation. From these time-series we found the maximum observed PR and compared the aggregated paired maximum PR and density metrics via linear regression.

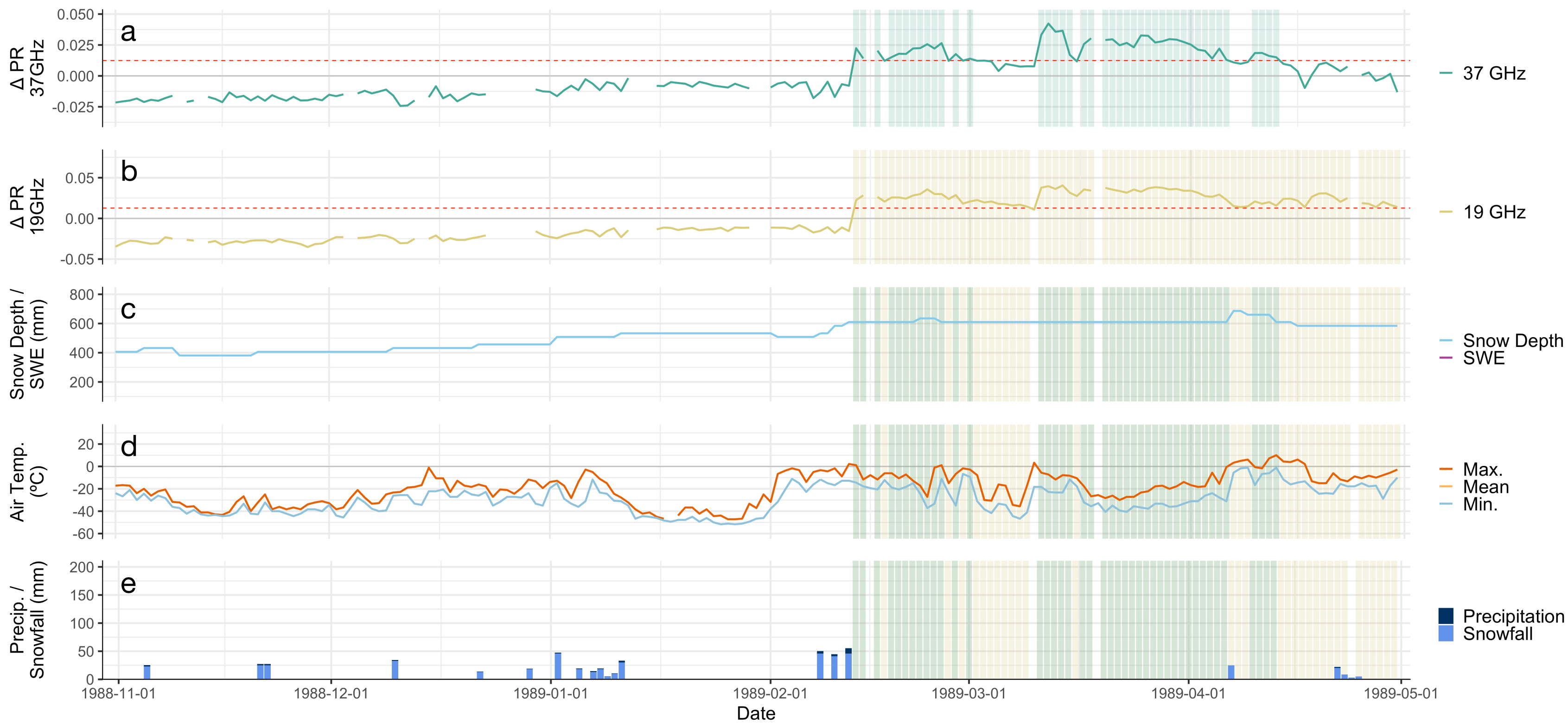

Figure 3.2. time series of ΔPR and meteorological observations for the 1989 water year at Umiat Airport GHCN climate station. Panel a shows the evolution of ΔPR in the 37 GHz channel, with the dashed horizontal line representing the threshold for a high-density layer detection. Green vertical lines extend down through the other panels for all days where this threshold is met. Panel b shows the same for the 19 GHz channel, with yellow lines indicating days where a detection occurs. Panel c shows observations of snow depth, panel d maximum and minimum daily temperatures, and panel e daily snowfall and precipitation.

3.4 Results

3.4.1 Where and when high-density snow layer detections occur

There are distinct spatial and temporal patterns in detections of high-density layers across Alaska, as well as variation in the pattern of detections between the two PM frequencies utilized. In the 19 GHz observations, the West Coast, Bristol Bay, and the Central Interior climate divisions each have a greater percentage of detections versus the percentage area they represent, whereas the Southeast Interior and Northeast Interior have very few detections given their relatively large size (see Figure 3.3 andFigure 3.4, and Table 3.2). In contrast, in the 37 GHz data, the North Slope also has a greater percentage of the total detections compared to the percentage area it represents in the study domain, but the Central Interior instead has much less (see Figure 3.3 andFigure 3.4, and Table 3.2). In each frequency, the West Coast leads the average number of detections per WY, followed by Bristol Bay (see Figure 3.3 andFigure 3.4, and Table 3.2). The timing of when detections most frequently occur appears to be consistent between frequencies; the highest mean detections are observed in February or March for all climate divisions except for the North Slope, where April shows the highest mean number of detections (see Table 3.2 and Figure 3.5). On a WY-by-WY basis, there are WYs with a far greater frequency of detections, e.g. 1984, 1994, 2008, and 2019, however, there exists regionality to this pattern. For example, there are many detections across the North Slope and northern West Coast in WY 2019, yet little for the southern West Coast or Bristol Bay (Figure 3.6). Notably, a greater frequency and area of detections are observed in the data from the 19 GHz frequency (see Figure 3.3 toFigure 3.6, and Table 3.2).

Table 3.2. Climate division percentage of total high-density snow layer detections by frequency compared to the percentage of the study area, and the mean number of days with a detection per water year (WY) and month (November through April).

			%		Mean Detections						
Frequency	**Climate Division**	**Detections**	**Area**	**Difference**	**WY**	**Nov**	**Dec**	**Jan**	**Feb**	**Mar**	**Apr**
19 GHz	Bristol Bay	16.48	6.95	9.53	24.74	0.65	2.19	4.97	7.30	8.08	1.56
	Central Interior	29.08	26.65	2.43	11.39	0.06	0.51	1.88	3.11	4.45	1.38
	Cook Inlet	2.93	4.08	-1.14	7.51	0.06	0.53	1.60	2.91	2.22	0.20
	North Slope	11.79	17.06	-5.27	7.21	1.11	0.61	0.87	1.03	1.42	2.17
	Northeast Gulf	0.39	1.27	-0.88	3.20	0.29	0.34	0.70	1.14	0.60	0.11
	Northeast Interior	1.55	11.79	-10.24	1.37	0.05	0.15	0.14	0.27	0.44	0.32
	Northwest Gulf	0.17	0.20	-0.03	8.78	0.10	0.78	1.72	2.69	3.02	0.47
	Southeast Interior	2.74	16.92	-14.19	1.69	0.02	0.08	0.20	0.53	0.70	0.15
	West Coast	34.86	15.07	19.79	24.13	0.38	1.45	4.58	6.48	7.91	3.32
37 GHz	Bristol Bay	17.04	7.39	9.65	11.99	0.83	1.69	2.32	3.40	3.34	0.40
	Central Interior	15.97	26.34	-10.37	3.15	0.03	0.17	0.54	0.86	1.37	0.19
	Cook Inlet	1.87	4.10	-2.22	2.38	0.04	0.26	0.57	0.84	0.64	0.02
	North Slope	18.15	16.94	1.20	5.57	0.64	0.36	0.70	0.84	1.37	1.66
	Northeast Gulf	0.52	1.26	-0.74	2.15	0.12	0.29	0.46	0.57	0.48	0.24
	Northeast Interior	0.67	11.63	-10.96	0.30	0.02	0.02	0.04	0.03	0.10	0.07
	Northwest Gulf	0.09	0.18	-0.09	2.53	0.02	0.27	0.51	0.81	0.86	0.07
	Southeast Interior	2.20	16.47	-14.27	0.70	0.01	0.04	0.08	0.18	0.31	0.07
	West Coast	43.49	15.69	27.81	14.42	0.31	1.17	3.15	4.03	4.55	1.20

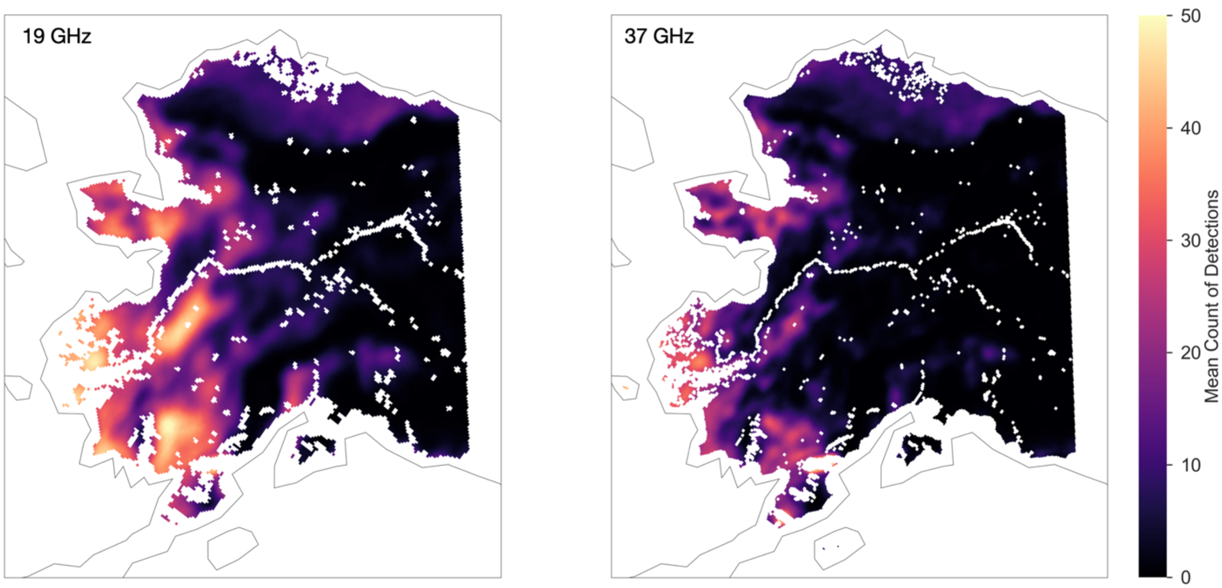

Figure 3.3. Mean count of possible high-density layer detections per WY across Alaska as derived by SSMI/S PM observations from water years 1988 to 2019.

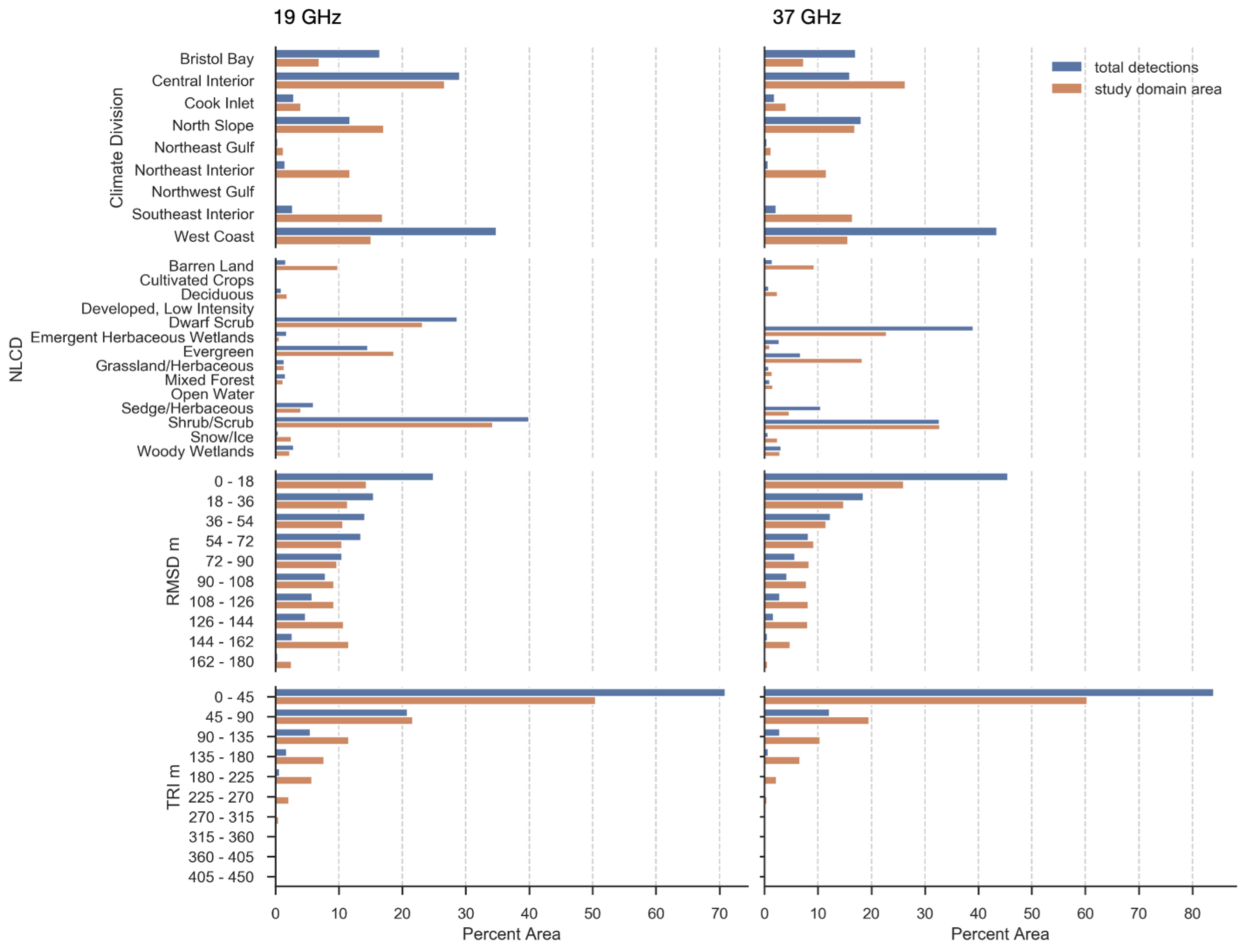

Figure 3.4. Percentage high-density layer detections (orange bars) versus percentage study domain area (blue bars) for climate divisions (top), NLCD classes (2nd from top), RMSD bins (3rd from top), and TRI bins (bottom). Note that the x-axes are different for the 19 GHz (left column) and 37 GHz (right column) results.

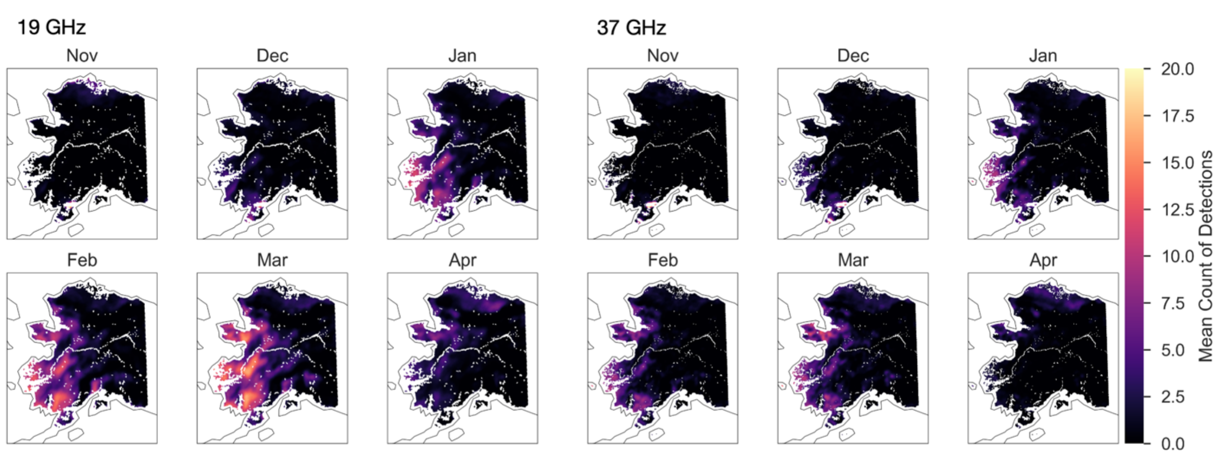

Figure 3.5. Mean count of possible high-density snow layer detections per WY grouped by month, as derived from SSMI/S PM observations from 1988 to 2019.

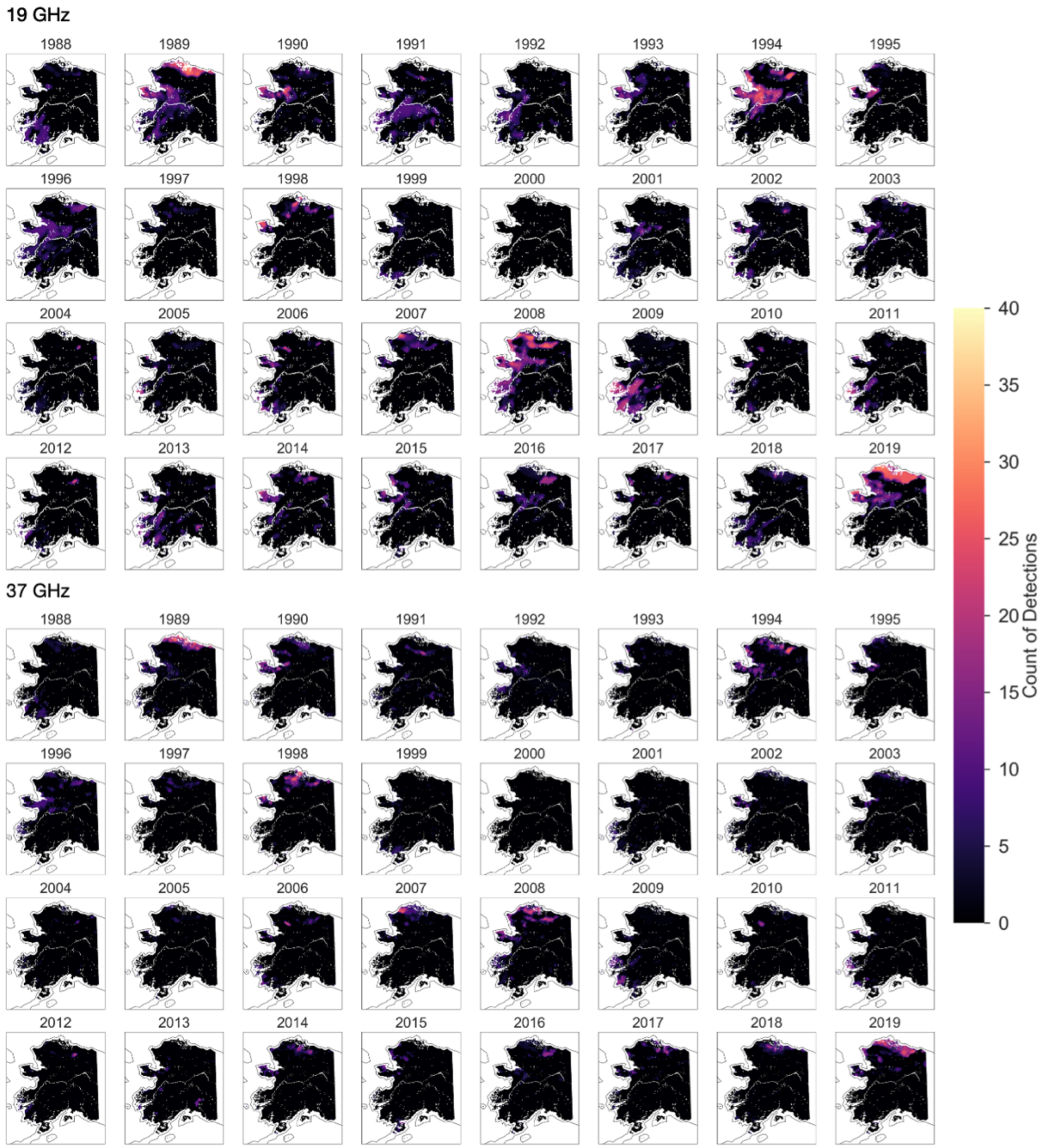

Figure 3.6. Total high-density snow layer detections in both frequencies by WY, 1988 to 2019

Table 3.3. NLCD derived land cover class percentage of total high-density snow layer detections by frequency compared to the percentage of the study area.

Frequency	NLCD Land Cover Class	Detections	% Area	Difference
19 GHz	Barren Land	1.63	9.86	-8.23
	Cultivated Crops	0.00	0.02	-0.02
	Deciduous	0.98	1.88	-0.90
	Developed, Low Intensity	0.00	0.00	0.00
	Dwarf Scrub	28.66	23.22	5.44
	Emergent Herbaceous Wetlands	1.83	0.62	1.21
	Evergreen	14.54	18.67	-4.13
	Grassland/Herbaceous	1.38	1.37	0.01
	Mixed Forest	1.62	1.25	0.37
	Open Water	0.01	0.00	0.00
	Sedge/Herbaceous	6.04	4.04	2.00
	Shrub/Scrub	39.94	34.27	5.67
	Snow/Ice	0.48	2.51	-2.03
	Woody Wetlands	2.90	2.29	0.61
37 GHz	Barren Land	1.49	9.34	-7.85
	Cultivated Crops	0.00	0.02	-0.02
	Deciduous	0.83	2.48	-1.65
	Developed, Low Intensity	0.00	0.00	0.00
	Developed, Open Space	0.00	0.00	0.00
	Dwarf Scrub	39.07	22.85	16.22
	Emergent Herbaceous Wetlands	2.87	1.02	1.85
	Evergreen	6.84	18.32	-11.49
	Grassland/Herbaceous	0.83	1.47	-0.63
	Mixed Forest	0.99	1.55	-0.55
	Moss	0.00	0.00	0.00
	Sedge/Herbaceous	10.52	4.66	5.86
	Shrub/Scrub	32.73	32.82	-0.09
	Snow/Ice	0.70	2.53	-1.82
	Woody Wetlands	3.13	2.93	0.20

3.4.2 Meteorological conditions of occurring, persisting, disappearing high-density snow layers

Compared to days where there was *no detection* of a high-density snow layer, the previous day's maximum temperature and mean temperature were higher on average when there was an *occurrence* of a high-density snow layer (Figure 3.7). For the 37 GHz channel, this difference was significant, and while there was no significance found for the previous day's data in the 19 GHz channel, the mean temperature and mean maximum temperature across the previous two days was significantly higher for an occurrence versus no detection (see Appendix 3.3). The same pattern is observed in the mean wind speed data; significantly higher wind speeds in the previous day for occurrences versus no detections when observed in the 37 GHz channel, and likewise for the 19 GHz channel but only when considering the average wind speed over the previous two days (Appendix 3.3). Occurrences had a significantly higher rainfall in the previous day than days where there was no detection for both channels (Figure 3.7). Snowfall was significantly higher in the previous day to an occurrence than that of a non-detection in the 19 GHz data, and in the 37 GHz channel if the previous two days snowfall was considered (Figure 3.7 and Appendix 3.4).

The previous day's maximum temperature, mean temperature, rainfall, and snowfall were all significantly lower when a *persistence* versus an *occurrence* of a high-density snow layer was detected in both frequencies (Figure 3.7). Mean wind speeds, however, showed no significant difference between an occurrence or a persistence in either the previous or previous two days (Appendix 3.3 and Appendix 3.4). Maximum temperature in the previous day was significantly higher when a *disappearance* versus a *persistence* was detected in both frequencies. Likewise, the previous day's mean temperature in the 19 GHz channel was higher in the case of a disappearance versus a persistence (Figure 3.7). However, neither the previous day's nor previous two day's mean temperature was significantly different in this comparison when using observations from the 37 GHz frequency (see Appendix 3.4). Other significant differences between a persistence and a disappearance were shown for the previous day's rainfall in the 37 GHz channel (higher in a disappearance), and the previous day's mean wind speed in the 19 GHz channel (lower in a disappearance; Figure 3.7).

3.4.3 Comparisons between maximum snow density and observed polarization ratio

No significant relationships were found when comparing the snowpit observations of maximum density, density range, and density standard deviation to the maximum PR derived from prior PM observations (see Table 3.4 and Figure 3.8). However, in the observations for maximum density, it was notable that the pits with lower maximum PR were in locations of greater topographic complexity (Figure 3.8).

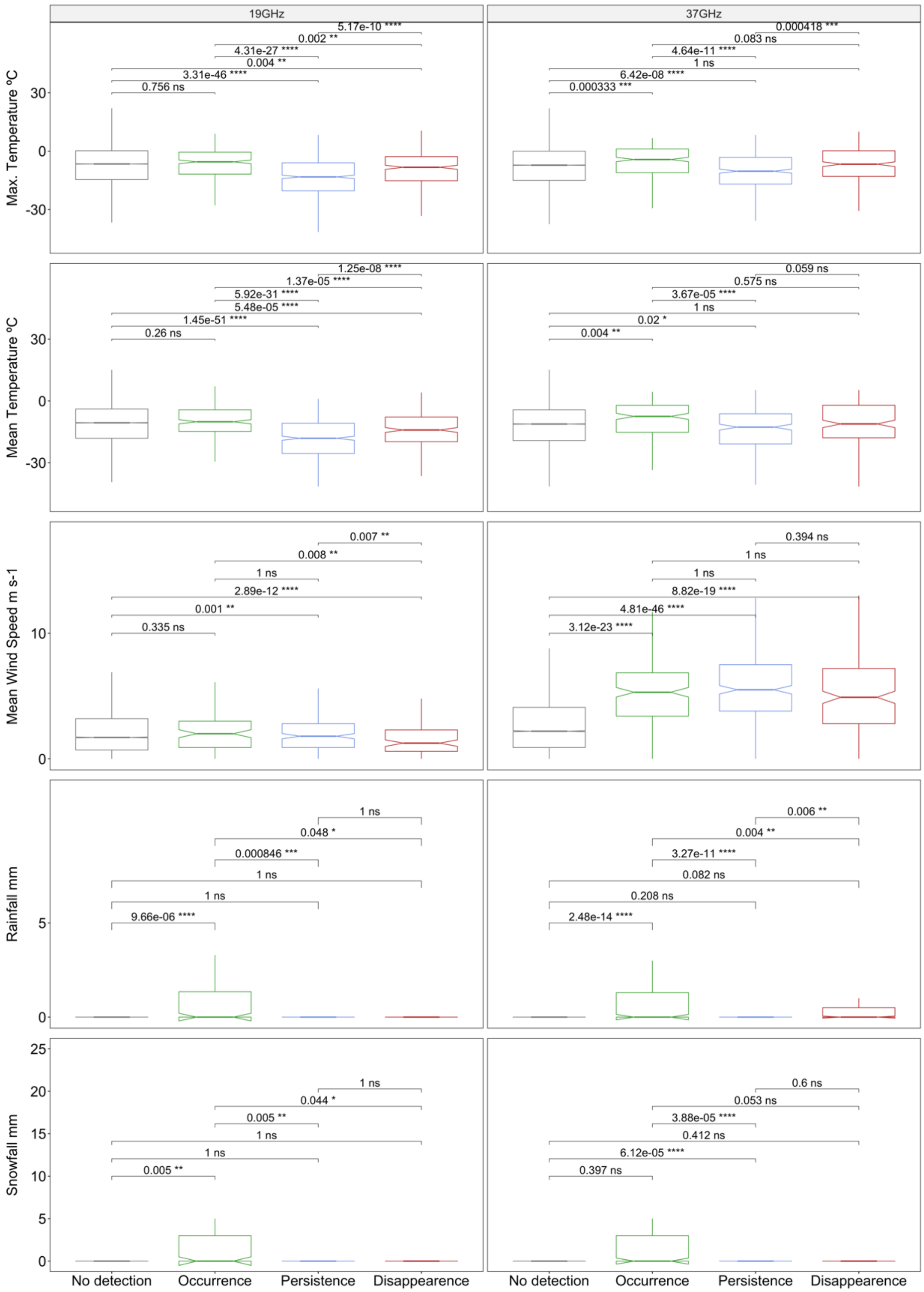

Figure 3.7. Boxplots of the previous days' meteorological variables for the four different categories of high-density snow layer observations; no detection, occurrence, persistence, and disappearance. Results from the 19 GHz observations are in the left column, 37 GHz in the right column. Bonferroni corrected P-values from pairwise t-tests (parametric) and pairwise Wilcoxon tests (non-parametric) are shown between the 6 possible pairings; ns indicates no significance, * indicates p ≤0.05, ** ≤0.01, *** ≤0.001, **** ≤0.0001. Outliers are removed. Further statistics are shown in Appendix 3.4 and Appendix 3.4.

Table 3.4. statistical results of the linear regression between snowpit measured density metrics (maximum, range, and standard deviation) and maximum observed PR.

	Dependent variable:					
	Maximum PR 19 GHz			Maximum PR 37 GHz		
Max. Density kg m^{-3}	0.00002			0.00002		
	(0.00001)			(0.00002)		
Density Range kg m^{-3}		0.00001			0.00001	
		(0.00001)			(0.00001)	
Density Std. kg m^{-3}			-0.00001			-0.00002
			(0.00003)			(0.00003)
Constant	0.035^{***}	0.041^{***}	0.043^{***}	0.029^{***}	0.036^{***}	0.039^{***}
	(0.005)	(0.003)	(0.003)	(0.006)	(0.003)	(0.003)
Observations	81	81	81	81	81	81
R^2	0.025	0.003	0.001	0.027	0.003	0.004
Adjusted R^2	0.013	-0.010	-0.012	0.014	-0.010	-0.009
Residual Std. Error (df = 79)	0.009	0.009	0.009	0.010	0.010	0.010
F Statistic (df = 1; 79)	2.040	0.212	0.064	2.158	0.210	0.290

Note :*p**p***p<0.01

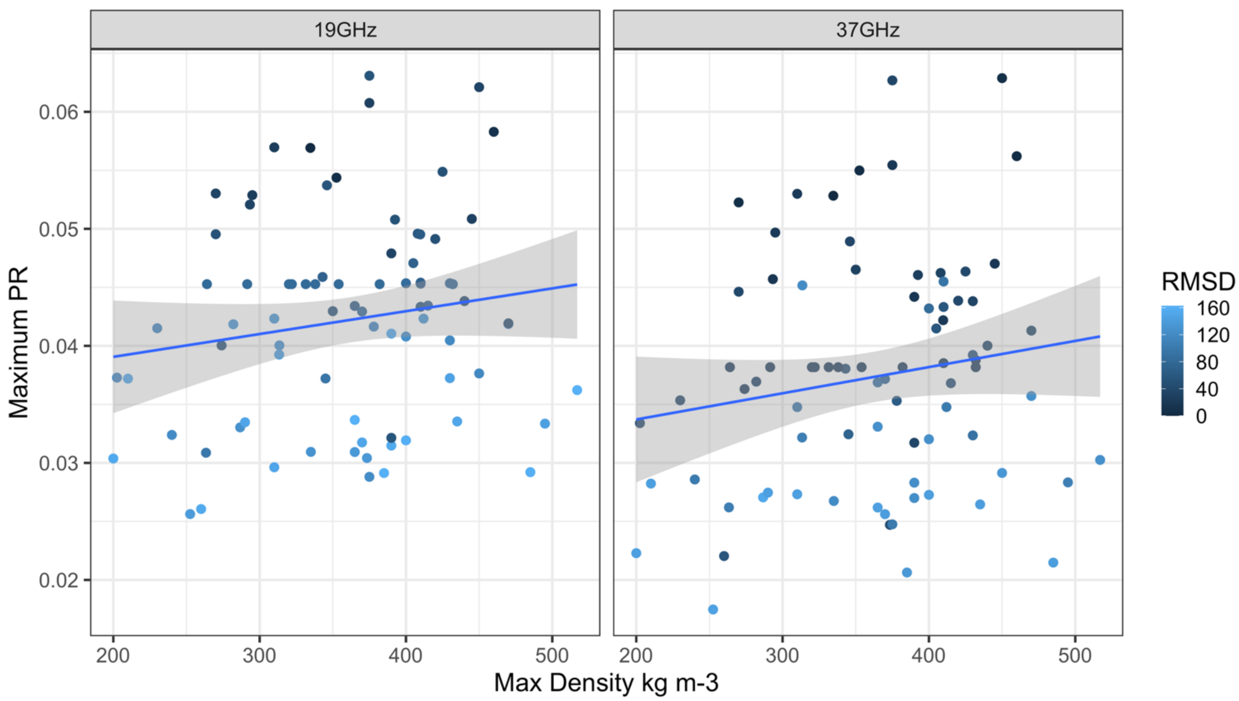

Figure 3.8. Comparison of maximum density observed in each snowpit to the maximum PR observed in both the 19 GHz (left) and 37 GHz (right) PM data. Each point corresponds to a snow pit, blue line with grey shaded area indicates the linear regression between the variables and its standard error. Point colours correspond to the snowpit's pixel RMSD with lighter blues indicating greater topographic complexity.

3.5 Discussion

In this study, we applied a high-density snow and ice layer detection algorithm to enhanced resolution PM data collected from 1988 to 2019 across Alaska. We found that the majority of detections occur in regions close to Alaska's coast and that fewer detections were observed in the continental interior. For all climate zones, most detections occurred in either February or March, except for the North Slope where April had the most detections on average. This temporal pattern is perhaps indicative of the months where sufficiently warm meteorological conditions are most likely to occur in each respective region. We further mapped detections on a WY-by-WY basis, revealing WYs where a high-degree of regionality in detections existed – a finding that has potential application in studies looking at the population dynamics and migration patterns of grazing wildlife, such as caribou. Increased sub-pixel topographic complexity corresponded to a lower frequency of detection, an expected finding as PM retrievals of snow properties in heterogenous terrain have previously been shown to be subject to errors (e.g. Mätzler and Standley, 2000; Li et al., 2014). Studies of wildlife that inhabit alpine areas, such Dall's sheep, potentially have less to gain from our results despite our use of an enhanced resolution dataset. However, if relatively flat areas of topography can be identified within their habitat, some inference of the presence of high-density layers may be possible. We also recognize that our choice of DEM to calculate the metrics of sub-pixel topographic complexity was relatively coarse in resolution compared to other available data, such as the Arctic DEM (Morin et al., 2016), which may have a bearing on our results.

Landcovers that are typical of low-land tundra, such as the NLCD classes Dwarf Scrub, Shrub/Scrub, and Sedge/Herbaceous (Homer et al., 2015), had a greater percentage of the total detections relative to their percentage area within the study domain. This result was also anticipated as dense vegetation is thought to attenuate PM emissions above snow cover, making inference of snow properties challenging (Derksen et al., 2003). The high frequency of detections in the Evergreen landcover class in the 19 GHz frequency data was therefore unexpected. We suggest two factors might be at play, albeit in opposition to each other. Across all regions the 19 GHz channel was shown to be more sensitive than that of the 37 GHz channel, described by a greater number of detections per unit time. This increased sensitivity is likely due to both the coarser resolution of the 19 GHz data, 6.25 km versus 3.125 km, and the lower density that the detection threshold corresponds to, 425 kg m^{-3} versus 520 kg m^{-3}. In a forested pixel, where the meteorological causes of high-density layers are potentially moderated, e.g. via reduced surface wind speeds and canopy interception of snowfall, higher density layers are less likely to be observed (Sturm et al., 1995). Hence, the ΔPR needed to indicate a detection in the 37 GHz channel is possibly less frequently reached. However, it is also possible that the coarser resolution of the 19 GHz pixel also means that a higher proportion of the pixel could be of a lower vegetation landcover, which might contribute enough signal to counteract that emitted in the forested area. To address this uncertainty, a more detailed analysis that considers the sub-pixel heterogeneity of land-cover, rather than utilizing the majority land cover within a pixel, is needed. Of note though, is Pan et al.'s (2020) finding that PM observations of snow-off dates within a similar study area were robust to increased percentages of sub-pixel forest fraction.

Meteorological conditions correspondent to warm snow-storms – high mean and maximum surface air temperatures, and increased wind speeds, rainfall and snowfall – preceded the detected occurrence of a high-density layer in our results. This finding compares to those from studies using similar methodologies (Grenfell T. C. and Putkonen J., 2008; Langlois et al., 2017; Dolant et al., 2018) and reflects known processes of high-density or ice-layer formation (Colbeck, 1982; Fierz et al., 2009; Sommer et al., 2018). In what we believe to be a novel analysis, we also examined the meteorological conditions for the persistence of a high-density snow layer detection. A decrease in temperature and precipitation was found when comparing days with a persistent snow-layer versus days where a snow layer occurred. This relationship is indicative of a scenario where a high-density snow layer is formed after a warm meteorological event before being 'frozen' into the snow stratigraphy by decreasing temperatures. From study of the time-series of meteorological data alongside ΔPR observations at each metrological station (e.g. Figure 3.2), this appears to be the case for the majority of persisting layers. Similarly explained by known physical processes is the finding that higher temperatures precede a disappearance of a detected high-density layer when compared to temperatures observed during a persistence. In this instance, a 'ripening' snowpack, as induced by warmer temperatures, might become isothermal and hence lose stratigraphic definition (Colbeck, 1982). However, we do not conduct a more detailed analysis here, so we can only infer the processes governing the observations in the PM record. Future work with further and more complete in-situ meteorological observations, alongside gridded climate data such as the Modern-Era Retrospective Analysis for Research and Applications (Gelaro et al., 2017), could potentially reveal a more nuanced and regional picture. In such a study, the intensity and combination of meteorological variables should be additionally considered, as well as the temporal energy balance of the existing snowpack.

In contrast to expectations, no relationship was found between the snowpit measurements of density parameters and the satellite-observed PR data. We had anticipated that higher maximum, range, and standard deviation of measured density would predict a higher maximum observed PR in the period preceding snowpit excavation. As such, what we here describe as a 'detection' has to be treated with due caution; we do not propose that any in-situ snow observations have validated our results. Rather, we suggest that this study is a step towards useful maps of the stratigraphic properties of snow as we have shown that their detections correspond to meteorological conditions *likely* to lead their occurrence, persistence, and disappearance. However, we do note that our snowpit dataset is limited in space and time within our study domain and period. Aside from being restricted to the 2018 and 2019 WYs, all snowpits were excavated before the 3rd of April and were mostly located in the North Slope climate division - where most detections occurred in April. It is also important to consider that a single snowpit of ~1 m measurement support (Sturm, 2015) represents a very small percentage of a single pixel's area. Therefore caution needs to be exercised when assuming its stratigraphic profile extends over a wider area, though there is some evidence that snow cover is consistent in its properties over large areas in Arctic tundra (Sturm and Benson, 2004). Not pursued in this study, but of worthwhile future enquiry, is an analysis of how the topographic complexity and landcover of the snowpit locations affect the observed PR data, or likewise how the stratigraphic sequence recorded corresponds to the temporal variation in ΔPR.

Further consideration needs to be paid to the accuracy of the CETB product due to its re-gridding technique. The raw footprints of the SSMI/S observations remain coarse, and hence the posted enhanced-resolution is subject to uncertainties from combining multiple footprints to derive the PM value in a higher resolution pixel (Brodzik and Long, 2018). While these uncertainties do influence our results we suggest they are of less importance when attempting to establish a binary condition of the snowpack, i.e. is there or isn't there a high-density layer, compared to seeking the absolute value of a continuous property, such as SWE. We acknowledge additional uncertainty in consideration that the ΔPR thresholds for detection are derived from simulations of high-density layers at the surface of typical Arctic tundra snowpacks, which were also observed in a domain outside of our study region (Montpetit et al., 2013; Dolant et al., 2018). However, previous work has established the similarities of snow cover throughout the North American sub-Arctic and Arctic (Sturm et al., 1995; Sturm and Benson, 2004), and our results that show a higher frequency of detections in landcovers typical of tundra suggest that the thresholds have some validity across a wider domain than originally intended. Further modelling of the expected PM signal in instances of ice-layers being present at the snow-soil interface is needed for the approach to accurately detect all configurations of stratigraphy hazardous to grazing wildlife.

Research beyond the scope of this current study could also better constrain the timeframe from which ΔPR is calculated via the use of reliable SCA products remotely-sensed in the visible light and NIR wavelengths. The snow season likely extends before the 1st of November and after the 30th of April, but it is also possible that snow-free periods occur in the study domain within this period – a factor that would critically affect PM observations. The CETB dataset has data from further satellites that could both extend the study period back to 1979 and be used to corroborate observations across sensors and platforms. Other future directions should include the use of GPS collar locations of 'snow-sensitive' wildlife species to act as living validation data, an approach that has already shown some promise (e.g. Mahoney et al., 2018). The recent release of the Arctic Animal Movement Archive (Davidson et al., 2020) greatly improves the possibility of such interdisciplinary research; we therefore hope that the findings of this research begin to address important data-gaps identified by wildlife ecologists (Boelman et al., 2018).

3.6 Acknowledgements

Valuable insights into the observation of snowpacks by passive microwave remote sensing were passed onto the lead author via correspondence with Ed Kim and from attendance of the 2018 Snow Microwave Radiative Transfer model workshop at Col du Lautaret, France. Matthew Sturm kindly shared some of his vast knowledge of Alaskan snow processes, which aided the lead author's decisions for the meteorological analysis of the detections.

3.7 References

Alaska Department of Fish and Game, 2014. Trends in Alaska Sheep Populations, Hunting, and Harvests. Division of Wildlife Conservation, Wildlife Management Report ADF&G/DWC/WMR-2014-3, Juneau.

Berteaux, D., Gauthier, G., Domine, F., Ims, R.A., Lamoureux, S.F., Lévesque, E., Yoccoz, N., 2016. Effects of changing permafrost and snow conditions on tundra wildlife: critical places and times. Arctic Science 3, 65–90. https://doi.org/10.1139/as-2016-0023

Bieniek, P.A., Bhatt, U.S., Thoman, R.L., Angeloff, H., Partain, J., Papineau, J., Fritsch, F., Holloway, E., Walsh, J.E., Daly, C., Shulski, M., Hufford, G., Hill, D.F., Calos, S., Gens, R., 2012. Climate Divisions for Alaska Based on Objective Methods. J. Appl. Meteor. Climatol. 51, 1276–1289. https://doi.org/10.1175/JAMC-D-11-0168.1

Bilodeau, F., Gauthier, G., Berteaux, D., 2013. The effect of snow cover on lemming population cycles in the Canadian High Arctic. Oecologia 172, 1007–1016.

Boelman, N., Liston, G.E., Gurarie, E., Meddens, A.J.H., Mahoney, P.J., Kirchner, P.B., Bohrer, G., Brinkman, T.J., Cosgrove, C.L., Eitel, J., Hebblewhite, M., Kimball, J.S., LaPoint, S.D., Nolin, A.W., Pedersen, S.H., Prugh, L.R., Reinking, A.K., Vierling, L., 2018. Integrating snow science and wildlife ecology in Arctic-boreal North America. Environ. Res. Lett. https://doi.org/10.1088/1748-9326/aaeec1

Bokhorst, S., Pedersen, S.H., Brucker, L., Anisimov, O., Bjerke, J.W., Brown, R.D., Ehrich, D., Essery, R.L.H., Heilig, A., Ingvander, S., Johansson, C., Johansson, M., Jónsdóttir, I.S., Inga, N., Luojus, K., Macelloni, G., Mariash, H., McLennan, D., Rosqvist, G.N., Sato, A., Savela, H., Schneebeli, M., Sokolov, A., Sokratov, S.A., Terzago, S., Vikhamar-Schuler, D., Williamson, S., Qiu, Y., Callaghan, T.V., 2016. Changing Arctic snow cover: A review of recent developments and assessment of future needs for observations, modelling, and impacts. Ambio 45, 516–537. https://doi.org/10.1007/s13280-016-0770-0

Brodzik, M.J., Long, D.G., 2016. MEaSUREs Calibrated Enhanced-Resolution Passive Microwave Daily EASE-Grid 2.0 Brightness Temperature ESDR, Version 1. https://doi.org/10.5067/MEASURES/CRYOSPHERE/NSIDC-0630.001

Brodzik, M.J., Long, D., G., 2018. Calibrated Passive Microwave Daily EASE-Grid 2.0 Brightness Temperature ESDR (CETB) Alogorithm Theoretical Basis Document 103.

Brodzik, M.J., Long, D.G., Hardman, M.A., 2018. Best Practices in Crafting the Calibrated, Enhanced-Resolution Passive-Microwave EASE-Grid 2.0 Brightness Temperature Earth System Data Record. Remote Sensing 10, 1793. https://doi.org/10.3390/rs10111793

Colbeck, S.C., 1982. An overview of seasonal snow metamorphism. https://doi.org/10.1029/RG020i001p00045

Collins, W.B., Smith, T.S., 1991. Effects of Wind-Hardened Snow on Foraging by Reindeer (Rangifer tarandus). Arctic 44, 217–222.

Danks, F.S., Klein, D.R., 2002. Using GIS to predict potential wildlife habitat: A case study of muskoxen in northern Alaska. International Journal of Remote Sensing 23, 4611–4632. https://doi.org/10.1080/01431160110113890

Davidson, S., Bohrer, G., Gurarie, E., LaPoint, S., Mahoney, P., Boelman, N., Eitel, J., Prugh, L., Vierling, L., Jennewein, J., Grier, E., Couriot, O., Kelly, A., Meddens, A., Oliver, R., Kays, R., Wikelski, M., Aarvak, T., Ackerman, J., 2020. Ecological insights from three decades of animal movement tracking across a changing Arctic. Science 370, 712–715. https://doi.org/10.1126/science.abb7080

Derksen, C., LeDrew, E., Walker, A., Goodison, B., 2000. Influence of Sensor Overpass Time on Passive Microwave-Derived Snow Cover Parameters. Remote Sensing of Environment 71, 297–308. https://doi.org/10.1016/S0034-4257(99)00084-X

Derksen, C., Walker, A., Goodison, B., 2003. A comparison of 18 winter seasons of in situ and passive microwave-derived snow water equivalent estimates in Western Canada. Remote Sensing of Environment 88, 271–282. https://doi.org/10.1016/j.rse.2003.07.003

Descamps, S., Aars, J., Fuglei, E., Kovacs, K.M., Lydersen, C., Pavlova, O., Pedersen, \AAshild, Ravolainen, V., Strøm, H., 2017. Climate change impacts on wildlife in a High Arctic archipelago – Svalbard, Norway. Global Change Biology 23, 490–502. https://doi.org/10.1111/gcb.13381

Dolant, C., Montpetit, B., Langlois, A., Brucker, L., Zolina, O., Johnson, C.A., Royer, A., Smith, P., 2018. Assessment of the Barren Ground Caribou Die-off During Winter 2015–2016 Using Passive Microwave Observations. Geophysical Research Letters 45, 4908–4916. https://doi.org/10.1029/2017GL076752

Earth Resources Observation And Science (EROS) Center, 2017. Global 30 Arc-Second Elevation (GTOPO30). https://doi.org/10.5066/F7DF6PQS

Eira, I.M.G., Oskal, A., Hanssen-Bauer, I., Mathiesen, S.D., 2018. Snow cover and the loss of traditional indigenous knowledge. Nature Clim Change 8, 928–931. https://doi.org/10.1038/s41558-018-0319-2

Fancy, S.G., White, R.G., 2011. Energy expenditures for locomotion by barren-ground caribou. Canadian Journal of Zoology. https://doi.org/10.1139/z87-018

Fancy, S.G., White, R.G., 1985. Energy Expenditures by Caribou while Cratering in Snow. The Journal of Wildlife Management 49, 987–993. https://doi.org/10.2307/3801384

Fierz, C., Armstrong, R.L., Durand, Y., Etchevers, P., Greene, E., McClung, D.M., Nishimura, K., Satyawali, P.K., Sokratov, S. a., 2009. The international classification for seasonal snow on the ground. IHP-VII Technical Documents in Hydrology 83, 90. http://www.cosis.net/abstracts/EGU05/09775/EGU05-J-09775.pdf

Foster, J.L., Hall, D.K., Chang, A.T.C., Rango, A., 1984. An overview of passive microwave snow research and results. https://doi.org/10.1029/RG022i002p00195

Gelaro, R., McCarty, W., Suárez, M.J., Todling, R., Molod, A., Takacs, L., Randles, C.A., Darmenov, A., Bosilovich, M.G., Reichle, R., Wargan, K., Coy, L., Cullather, R., Draper, C., Akella, S., Buchard, V., Conaty, A., da Silva, A.M., Gu, W., Kim, G.-K., Koster, R., Lucchesi, R., Merkova, D., Nielsen, J.E., Partyka, G., Pawson, S., Putman, W., Rienecker, M., Schubert, S.D., Sienkiewicz, M., Zhao, B., Gelaro, R., McCarty, W., Suárez, M.J., Todling, R., Molod, A., Takacs, L., Randles, C.A., Darmenov, A., Bosilovich, M.G., Reichle, R., Wargan, K., Coy, L., Cullather, R., Draper, C., Akella, S., Buchard, V., Conaty, A., da Silva, A.M., Gu, W., Kim, G.-K., Koster, R., Lucchesi, R., Merkova, D., Nielsen, J.E., Partyka, G., Pawson, S., Putman, W., Rienecker, M., Schubert, S.D., Sienkiewicz, M., Zhao, B., 2017. The Modern-Era Retrospective Analysis for Research and Applications, Version 2 (MERRA-2). Journal of Climate 30, 5419–5454. https://doi.org/10.1175/JCLI-D-16-0758.1

Grenfell T. C., Putkonen J., 2008. A method for the detection of the severe rain-on-snow event on Banks Island, October 2003, using passive microwave remote sensing. Water Resources Research 44. https://doi.org/10.1029/2007WR005929

Hall, D.K., Chang, A.T.C., Foster, J.L., 1986. Detection of the Depth-Hoar Layer in the Snow-Pack of the Arctic Coastal Plain of Alaska, U.S.A., Using Satellite Data. Journal of Glaciology 32, 87–94. https://doi.org/10.3189/S0022143000006912

Holland, J.D., Bert, D.G., Fahrig, L., 2004. Determining the Spatial Scale of Species' Response to Habitat. BioScience 54, 227–233. https://doi.org/10.1641/0006-3568(2004)054[0227:dtssos]2.0.co;2

Homer, C., Dewitz, J., Yang, L., Jin, S., Danielson, P., 2015. Completion of the 2011 National Land Cover Database for the Conterminous United States – Representing a Decade of Land Cover Change Information. PHOTOGRAMMETRIC ENGINEERING 11.

Hoyer, S., Hamman, J.J., 2017. xarray: N-D labeled Arrays and Datasets in Python. Journal of Open Research Software 5, 10. https://doi.org/10.5334/jors.148

Jeong, D.I., Sushama, L., 2018. Rain-on-snow events over North America based on two Canadian regional climate models. Climate Dynamics 50, 303–316.

Johansson, C., Pohjola, V.A., Jonasson, C., Callaghan, T.V., 2011. Multi-Decadal Changes in Snow Characteristics in Sub-Arctic Sweden. AMBIO 40, 566. https://doi.org/10.1007/s13280-011-0164-2

Kerk, M.V. de, Arthur, S., Bertram, M., Borg, B., Herriges, J., Lawler, J., Mangipane, B., Koizumi, C.L., Wendling, B., Prugh, L., 2020. Environmental Influences on Dall's Sheep Survival. The Journal of Wildlife Management. https://doi.org/10.1002/jwmg.21873

Kerk, M. van de, Verbyla, D., Nolin, A.W., Sivy, K.J., Prugh, L.R., 2018. Range-wide variation in the effect of spring snow phenology on Dall sheep population dynamics. Environ. Res. Lett. 13, 075008. https://doi.org/10.1088/1748-9326/aace64

Kim, Y., Kimball, J.S., Du, J., Schaaf, C.L.B., Kirchner, P.B., 2018. Quantifying the effects of freeze-thaw transitions and snowpack melt on land surface albedo and energy exchange over Alaska and Western Canada. Environ. Res. Lett. 13, 075009. https://doi.org/10.1088/1748-9326/aacf72

Langlois, A., Johnson, C.-A.A., Montpetit, B., Royer, A., Blukacz-Richards, E.A.A., Neave, E., Dolant, C., Roy, A., Arhonditsis, G., Kim, D.-K.K., Kaluskar, S., Brucker, L., 2017. Detection of rain-on-snow (ROS) events and ice layer formation using passive microwave radiometry: A context for Peary caribou habitat in the Canadian Arctic. Remote Sensing of Environment 189, 84–95. https://doi.org/10.1016/j.rse.2016.11.006

Li, X., Zhang, L., Weihermüller, L., Jiang, L., Vereecken, H., 2014. Measurement and Simulation of Topographic Effects on Passive Microwave Remote Sensing Over Mountain Areas: A Case Study From the Tibetan Plateau. IEEE Transactions on Geoscience and Remote Sensing 52, 1489–1501. https://doi.org/10.1109/TGRS.2013.2251887

Liston, G.E., Hiemstra, C.A., 2011. The Changing Cryosphere: Pan-Arctic Snow Trends (1979–2009). J. Climate 24, 5691–5712. https://doi.org/10.1175/JCLI-D-11-00081.1

Mahoney, P.J., Liston, G.E., LaPoint, S., Gurarie, E., Mangipane, B., Wells, A.G., Brinkman, T.J., Eitel, J.U.H., Hebblewhite, M., Nolin, A.W., Boelman, N., Prugh, L.R., 2018. Navigating snowscapes: scale-dependent responses of mountain sheep to snowpack properties. Ecological Applications 0. https://doi.org/10.1002/eap.1773

Mallory, C.D., Boyce, M.S., 2017. Observed and predicted effects of climate change on Arctic caribou and reindeer. Environ. Rev. 26, 13–25. https://doi.org/10.1139/er-2017-0032

Mätzler, C., Standley, A., 2000. Technical note: Relief effects for passive microwave remote sensing. International Journal of Remote Sensing 21, 2403–2412. https://doi.org/10.1080/01431160050030538

Montpetit, B., 2015. Analyse de la modélisation de l'émission multi-fréquences micro-onde des sols et de la neige, incluant les croutes de glace à l'aide du modèle Microwave Emission Model of Layered Snowpacks (MEMLS). Université de Sherbrooke.

Montpetit, B., Royer, A., Roy, A., Langlois, A., Derksen, C., 2013. Snow microwave emission modeling of ice lenses within a snowpack using the microwave emission model for layered snowpacks. IEEE Transactions on Geoscience and Remote Sensing 51, 4705–4717. https://doi.org/10.1109/TGRS.2013.2250509

Morin, P., Porter, C., Cloutier, M., Howat, I., Noh, M.-J., Willis, M., Bates, B., Willamson, C., Peterman, K., 2016. ArcticDEM; A Publically Available, High Resolution Elevation Model of the Arctic 18, EPSC2016-8396.

Nellemann, C., Fry, G., 1995. Quantitative analysis of terrain ruggedness in reindeer winter grounds. Arctic 172–176.

Nelson, M.E., Mech, L.D., 1986. Relationship between Snow Depth and Gray Wolf Predation on White-Tailed Deer. The Journal of Wildlife Management 50, 471–474. https://doi.org/10.2307/3801108

NOAA, 2020. Global Historical Climatology Network (GHCN) | National Centers for Environmental Information (NCEI) formerly known as National Climatic Data Center (NCDC) [WWW Document]. URL https://www.ncdc.noaa.gov/data-access/land-based-station-data/land-based-datasets/global-historical-climatology-network-ghcn (accessed 11.18.20).

Ouellet, F., Langlois, A., Blukacz-Richards, E.A., Johnson, C.A., Royer, A., Neave, E., Larter, N.C., 2017. Spatialization of the SNOWPACK snow model for the Canadian Arctic to assess Peary caribou winter grazing conditions. Physical Geography 38, 143–158. https://doi.org/10.1080/02723646.2016.1274200

Pan, C.G., Kirchner, P.B., Kimball, J.S., Du, J., 2020. A Long-Term Passive Microwave Snowoff Record for the Alaska Region 1988–2016. Remote Sensing 12, 153. https://doi.org/10.3390/rs12010153

Pan, C.G., Kirchner, P.B., Kimball, J.S., Kim, Y., Du, J., 2018. Rain-on-snow events in Alaska, their frequency and distribution from satellite observations. Environ. Res. Lett. 13, 075004. https://doi.org/10.1088/1748-9326/aac9d3

Pedersen, S.H., Liston, G.E., Welker, J.M., 2019. Snow depth and snow density measured in Arctic Alaska for caribou winter applications in 2018 and 2019.

QGIS Development Team, 2020. QGIS Geographic Information System. QGIS Association.

R Core Team, 2019. R: A Language and Environment for Statistical Computing. R Foundation for Statistical Computing, Vienna, Austria.

Rasmus, S., Kivinen, S., Irannezhad, M., 2018. Basal ice formation in snow cover in Northern Finland between 1948 and 2016. Environ. Res. Lett. 13, 114009. https://doi.org/10.1088/1748-9326/aae541

Rattenbury, K.L., Schmidt, J.H., Swanson, D.K., Borg, B.L., Mangipane, B.A., Sousanes, P.J., 2018. Delayed spring onset drives declines in abundance and recruitment in a mountain ungulate. Ecosphere 9, e02513. https://doi.org/10.1002/ecs2.2513

Reid, D.G., Bilodeau, F., Krebs, C.J., Gauthier, G., Kenney, A.J., Gilbert, B.S., Leung, M.C.-Y., Duchesne, D., Hofer, E., 2012. Lemming winter habitat choice: a snow-fencing experiment. Oecologia 168, 935–946. https://doi.org/10.1007/s00442-011-2167-x

Riley, S.J., DeGloria, S.D., Elliot, R., 1999. Index that quantifies topographic heterogeneity. intermountain Journal of sciences 5, 23–27.

Saberi, N., 2019. Snow Properties Retrieval Using Passive Microwave Observations.

Saberi, N., Kelly, R., Flemming, M., Li, Q., 2019. Review of snow water equivalent retrieval methods using spaceborne passive microwave radiometry. International Journal of Remote Sensing 0, 1–23. https://doi.org/10.1080/01431161.2019.1654144

Sappington, J.M., Longshore, K.M., Thompson, D.B., 2007. Quantifying landscape ruggedness for animal habitat analysis: a case study using bighorn sheep in the Mojave Desert. The Journal of wildlife management 71, 1419–1426.

Semmens, K.A., Ramage, J., Bartsch, A., Liston, G.E., 2013. Early snowmelt events: detection, distribution, and significance in a major sub-arctic watershed. Environ. Res. Lett. 8, 014020. https://doi.org/10.1088/1748-9326/8/1/014020

Sivy, K.J., Nolin, A.W., Cosgrove, C., Prugh, L., 2018. Critical snow density threshold for Dall sheep (Ovis dalli dalli). Can. J. Zool. https://doi.org/10.1139/cjz-2017-0259

Sokolov, A.A., Sokolova, N.A., Ims, R.A., Brucker, L., Ehrich, D., 2016. Emergent Rainy Winter Warm Spells May Promote Boreal Predator Expansion into the Arctic. Arctic 69, 121–129.

Sommer, C.G., 2018. Wind-packing of snow: How do wind crusts form? [WWW Document]. Infoscience. https://doi.org/10.5075/epfl-thesis-8628

Sommer, C.G., Lehning, M., Fierz, C., 2018. Wind tunnel experiments: influence of erosion and deposition on wind-packing of new snow. Frontiers in Earth Science 6, 4.

Sturm, M., 2015. White water: Fifty years of snow research in WRR and the outlook for the future. Water Resources Research 51, 4948–4965. https://doi.org/10.1002/2015WR017242

Sturm, M., Benson, C., 2004. Scales of spatial heterogeneity for perennial and seasonal snow layers. Annals of Glaciology 38, 253–260. https://doi.org/10.3189/172756404781815112

Sturm, M., Holmgren, J., Liston, G.E., Holmgren, J., Liston, G.E., 1995. A Seasonal Snow Cover Classification System for Local to Global Applications. Journal of Climate 8, 1261–1283. https://doi.org/10.1175/1520-0442(1995)008<1261:ASSCCS>2.0.CO;2

Sun, N., Yan, H., Wigmosta, M.S., Leung, L.R., Skaggs, R., Hou, Z., 2019. Regional Snow Parameters Estimation for Large-Domain Hydrological Applications in the Western United States. Journal of Geophysical Research: Atmospheres 124, 5296–5313. https://doi.org/10.1029/2018JD030140

Tong, J., Déry, S.J., Jackson, P.L., Derksen, C., 2010. Testing snow water equivalent retrieval algorithms for passive microwave remote sensing in an alpine watershed of western Canada. Canadian Journal of Remote Sensing 36, S74–S86. https://doi.org/10.5589/m10-009

Tyler N. J. C., 2010. Climate, snow, ice, crashes, and declines in populations of reindeer and caribou (Rangifer tarandus L.). Ecological Monographs 80, 197–219. https://doi.org/10.1890/09-1070.1

Ulaby, F.T., Moore, R.K., Fung, A.K., 1981. Microwave remote sensing: Active and passive. volume 1-microwave remote sensing fundamentals and radiometry.

Vikhamar-Schuler, D., Hanssen-Bauer, I., Schuler, T.V., Mathiesen, S.D., Lehning, M., 2013. Use of a multilayer snow model to assess grazing conditions for reindeer. Annals of Glaciology 54, 214–226. https://doi.org/10.3189/2013AoG62A306

Vroom, G.W., Herrero, S., Ogilvie, R.T., 1980. The ecology of winter den sites of grizzly bears in Banff National Park, Alberta. Bears: their biology and management 321–330.

Wilmers, C.C., Nickel, B., Bryce, C.M., Smith, J.A., Wheat, R.E., Yovovich, V., 2015. The golden age of bio-logging: how animal-borne sensors are advancing the frontiers of ecology. Ecology 96, 1741–1753. https://doi.org/10.1890/14-1401.1

Yan, H., Sun, N., Wigmosta, M., Skaggs, R., Hou, Z., Leung, R., 2018. Next-Generation Intensity-Duration-Frequency Curves for Hydrologic Design in Snow-Dominated Environments. Water Resources Research 54, 1093–1108. https://doi.org/10.1002/2017WR021290

3.8 Appendix

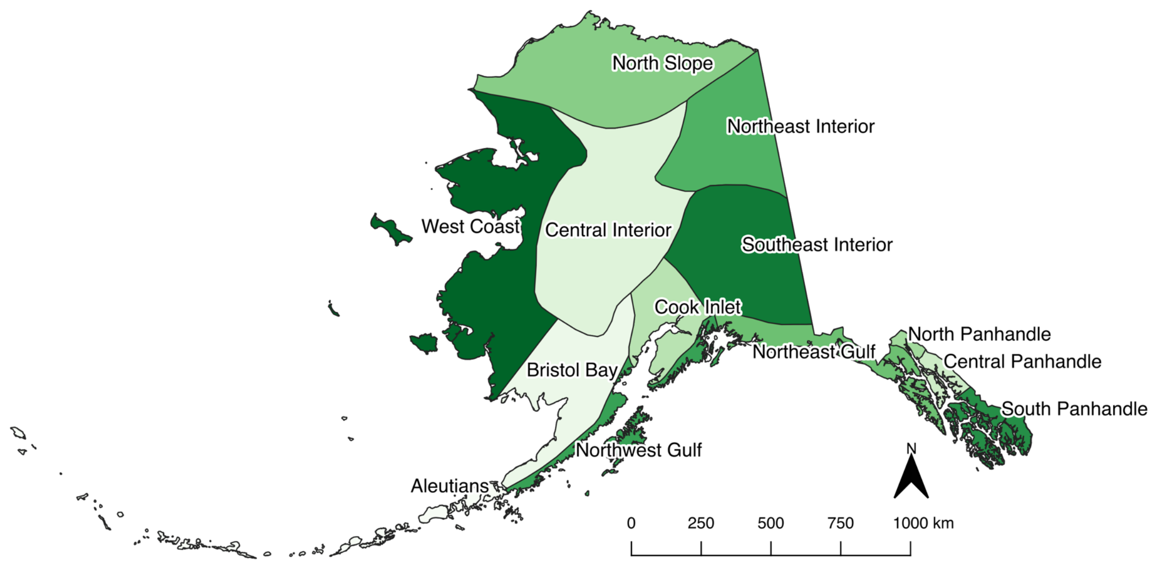

Appendix 3.1. Map of Alaska's climate divisions after Bieniek et al. (2012).

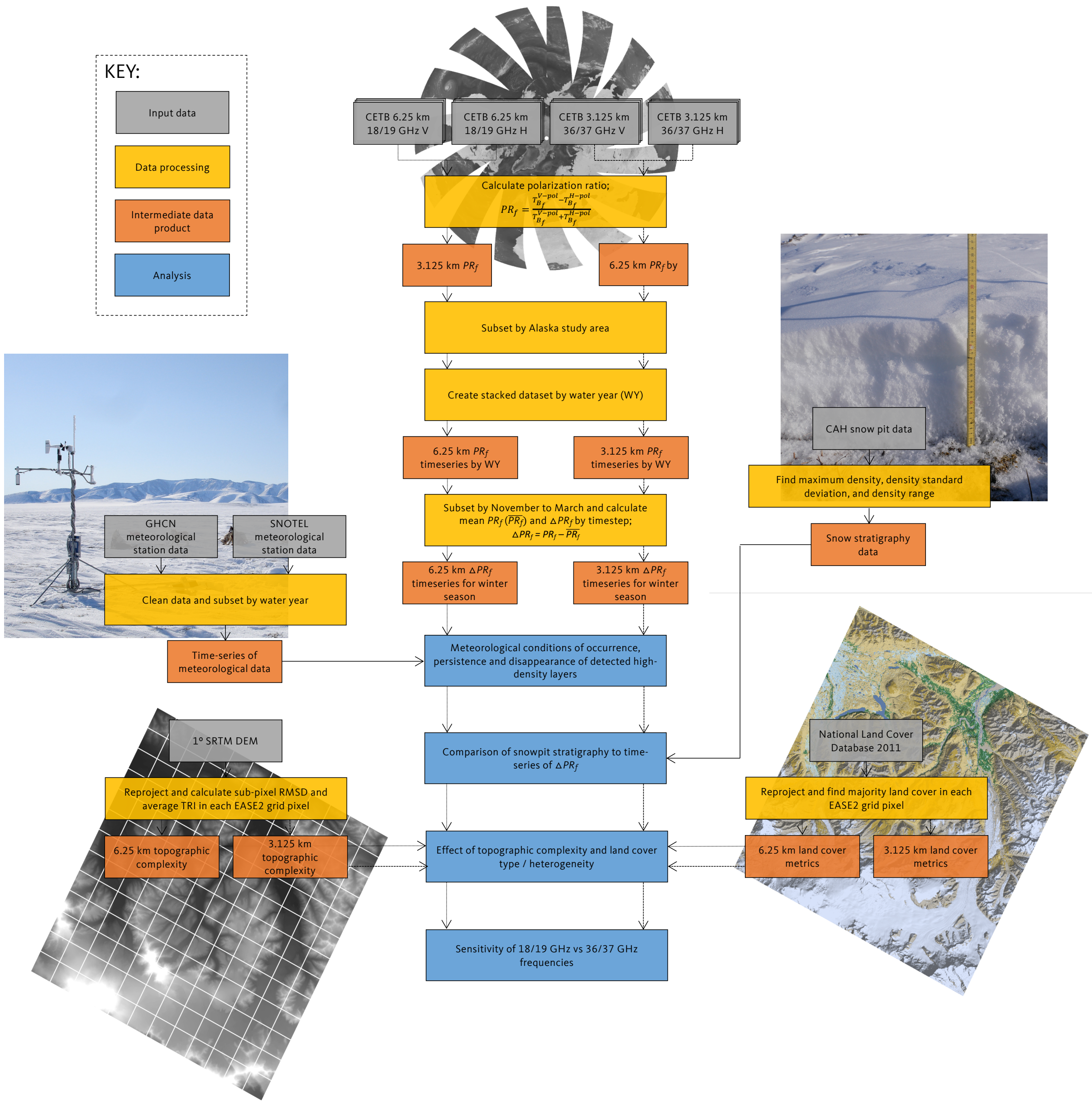

Appendix 3.2. Schematic of input data streams, processing steps, intermediate data products, and analysis.

Appendix 3.3. Table of statistics for the comparison of the previous days' (-1 day) and previous two days' (-2 day) meteorological variables between the different classes of high-density snow layer detection observed from the 19 GHz PM data

Frequency	Variable	Group 1	Group 2	n1	n2	p	p-adjusted	significance
19 GHz	Max. Temp. -1 day	No detection	Occurrence	51498	349	0.126	0.756	ns
		No detection	Persistence	51498	687	5.51E-47	3.31E-46	****
		No detection	Disappearence	51498	344	0.000725	0.004	**
		Occurrence	Persistence	349	687	7.19E-28	4.31E-27	****
		Occurrence	Disappearence	349	344	0.000344	0.002	**
		Persistence	Disappearence	687	344	8.62E-11	5.17E-10	****
	Mean. Temp. -1 day	No detection	Occurrence	37503	265	0.043	0.26	ns
		No detection	Persistence	37503	565	2.42E-52	1.45E-51	****
		No detection	Disappearence	37503	263	9.13E-06	5.48E-05	****
		Occurrence	Persistence	265	565	9.87E-32	5.92E-31	****
		Occurrence	Disappearence	265	263	2.29E-06	1.37E-05	****
		Persistence	Disappearence	565	263	2.09E-09	1.25E-08	****
	Mean Wind Speed -1 day	No detection	Occurrence	12715	109	0.056	0.335	ns
		No detection	Persistence	12715	204	1.99E-04	1.00E-03	**
		No detection	Disappearence	12715	106	4.81E-13	2.89E-12	****
		Occurrence	Persistence	109	204	5.48E-01	1.00E+00	ns
		Occurrence	Disappearence	109	106	0.001	0.008	**
		Persistence	Disappearence	204	106	1.00E-03	7.00E-03	**
	Rainfall -1 day	No detection	Occurrence	18832	118	1.61E-06	9.66E-06	****
		No detection	Persistence	18832	225	7.11E-01	1.00E+00	ns
		No detection	Disappearence	18832	113	6.45E-01	1.00E+00	ns
		Occurrence	Persistence	118	225	1.41E-04	8.46E-04	***
		Occurrence	Disappearence	118	113	8.00E-03	4.80E-02	*
		Persistence	Disappearence	225	113	5.64E-01	1.00E+00	ns
	Snowfall -1 day	No detection	Occurrence	12221	110	0.000889	0.005	**
		No detection	Persistence	12221	212	1.91E-01	1.00E+00	ns
		No detection	Disappearence	12221	105	0.433	1	ns
		Occurrence	Persistence	110	212	8.84E-04	5.00E-03	**
		Occurrence	Disappearence	110	105	0.007	0.044	*
		Persistence	Disappearence	212	105	9.15E-01	1.00E+00	ns
	Temp. Max. -2 days	No detection	Occurrence	51498	349	0.028	0.168	ns
		No detection	Persistence	51498	687	1.62E-39	9.72E-39	****
		No detection	Disappearence	51498	344	2.18E-04	1.00E-03	**
		Occurrence	Persistence	349	687	8.75E-26	5.25E-25	****
		Occurrence	Disappearence	349	344	1.99E-05	1.19E-04	***
		Persistence	Disappearence	687	344	1.98E-07	1.19E-06	****
	Temp. Mean -2 days	No detection	Occurrence	37503	265	0.005	0.028	*
		No detection	Persistence	37503	565	8.67E-44	5.20E-43	****
		No detection	Disappearence	37503	263	3.77E-05	0.000226	***
		Occurrence	Persistence	265	565	4.66E-30	2.80E-29	****
		Occurrence	Disappearence	265	263	5.8E-07	3.48E-06	****
		Persistence	Disappearence	565	263	6.48E-08	3.89E-07	****
	Mean Wind Speed -2 days	No detection	Occurrence	12715	109	1.02E-05	0.0000612	****
		No detection	Persistence	12715	204	2.70E-04	2.00E-03	**
		No detection	Disappearence	12715	106	1.04E-09	6.24E-09	****
		Occurrence	Persistence	109	204	1.92E-01	1.00E+00	ns
		Occurrence	Disappearence	109	106	1.56E-01	9.36E-01	ns
		Persistence	Disappearence	204	106	4.00E-03	2.50E-02	*
	Rainfall -2 days	No detection	Occurrence	18832	118	1.67E-08	0.0000001	****
		No detection	Persistence	18832	225	5.00E-01	1.00E+00	ns
		No detection	Disappearence	18832	113	0.464	1	ns
		Occurrence	Persistence	118	225	1.16E-04	6.96E-04	***
		Occurrence	Disappearence	118	113	0.002	0.012	*
		Persistence	Disappearence	225	113	8.50E-01	1.00E+00	ns
	Snowfall -2 days	No detection	Occurrence	12221	110	0.001	0.008	**
		No detection	Persistence	12221	212	7.73E-01	1.00E+00	ns
		No detection	Disappearence	12221	105	7.83E-01	1.00E+00	ns
		Occurrence	Persistence	110	212	1.00E-02	5.90E-02	ns
		Occurrence	Disappearence	110	105	1.80E-02	1.07E-01	ns
		Persistence	Disappearence	212	105	9.65E-01	1.00E+00	ns

Appendix 3.4. Table of statistics for the comparison of the previous days' (-1 day) and previous two days' (-2 day) meteorological variables between the different classes of high-density snow layer detection observed from the 37 GHz PM data

Frequency	Variable	Group 1	Group 2	n1	n2	p	p-adjusted	significance
37 GHz	Max. Temp. -1 day	No detection	Occurrence	57840	298	0.0000555	0.000333	***
		No detection	Persistence	57840	435	1.07E-08	6.42E-08	****
		No detection	Disappearence	57840	297	0.694	1	ns
		Occurrence	Persistence	298	435	7.73E-12	4.64E-11	****
		Occurrence	Disappearence	298	297	0.014	0.083	ns
		Persistence	Disappearence	435	297	6.97E-05	4.18E-04	***
	Mean. Temp. -1 day	No detection	Occurrence	41757	194	0.000629	0.004	**
		No detection	Persistence	41757	265	3.00E-03	2.00E-02	*
		No detection	Disappearence	41757	194	3.61E-01	1.00E+00	ns
		Occurrence	Persistence	194	265	6.11E-06	3.67E-05	****
		Occurrence	Disappearence	194	194	9.60E-02	5.75E-01	ns
		Persistence	Disappearence	265	194	1.00E-02	5.90E-02	ns
	Mean Wind Speed -1 day	No detection	Occurrence	16788	203	5.2E-24	3.12E-23	****
		No detection	Persistence	16788	298	8.02E-47	4.81E-46	****
		No detection	Disappearence	16788	203	1.47E-19	8.82E-19	****
		Occurrence	Persistence	203	298	2.63E-01	1.00E+00	ns
		Occurrence	Disappearence	203	203	0.499	1	ns
		Persistence	Disappearence	298	203	6.60E-02	3.94E-01	ns
	Rainfall -1 day	No detection	Occurrence	23097	210	4.13E-15	2.48E-14	****
		No detection	Persistence	23097	313	3.50E-02	2.08E-01	ns
		No detection	Disappearence	23097	209	1.40E-02	8.20E-02	ns
		Occurrence	Persistence	210	313	5.45E-12	3.27E-11	****
		Occurrence	Disappearence	210	209	6.43E-04	4.00E-03	**
		Persistence	Disappearence	313	209	1.00E-03	6.00E-03	**
	Snowfall -1 day	No detection	Occurrence	15771	198	0.066	0.397	ns
		No detection	Persistence	15771	293	1.02E-05	6.12E-05	****
		No detection	Disappearence	15771	197	0.069	0.412	ns
		Occurrence	Persistence	198	293	6.46E-06	3.88E-05	****
		Occurrence	Disappearence	198	197	0.009	0.053	ns
		Persistence	Disappearence	293	197	1.00E-01	6.00E-01	ns
	Temp. Max. -2 days	No detection	Occurrence	57840	298	0.000015	0.00009	****
		No detection	Persistence	57840	435	2.51E-06	1.51E-05	****
		No detection	Disappearence	57840	297	4.73E-01	1.00E+00	ns
		Occurrence	Persistence	298	435	1.63E-10	9.78E-10	****
		Occurrence	Disappearence	298	297	2.00E-02	1.18E-01	ns
		Persistence	Disappearence	435	297	4.70E-04	3.00E-03	**
	Temp. Mean -2 days	No detection	Occurrence	41757	194	0.0000783	0.00047	***
		No detection	Persistence	41757	265	3.30E-02	2.00E-01	ns
		No detection	Disappearence	41757	194	0.169	1	ns
		Occurrence	Persistence	194	265	1.14E-05	6.84E-05	****
		Occurrence	Disappearence	194	194	0.104	0.624	ns
		Persistence	Disappearence	265	194	1.60E-02	9.70E-02	ns
	Mean Wind Speed -2 days	No detection	Occurrence	16788	203	6.07E-27	3.64E-26	****
		No detection	Persistence	16788	298	2.17E-56	1.30E-55	****
		No detection	Disappearence	16788	203	8.25E-25	4.95E-24	****
		Occurrence	Persistence	203	298	2.70E-02	1.61E-01	ns
		Occurrence	Disappearence	203	203	7.21E-01	1.00E+00	ns
		Persistence	Disappearence	298	203	9.20E-02	5.53E-01	ns
	Rainfall -2 days	No detection	Occurrence	23097	210	3.8E-17	2.28E-16	****
		No detection	Persistence	23097	313	8.06E-01	1.00E+00	ns
		No detection	Disappearence	23097	209	0.000192	0.001	**
		Occurrence	Persistence	210	313	2.17E-10	1.30E-09	****
		Occurrence	Disappearence	210	209	0.003	0.016	*
		Persistence	Disappearence	313	209	3.00E-03	1.60E-02	*
	Snowfall -2 days	No detection	Occurrence	15771	198	0.003	0.016	*
		No detection	Persistence	15771	293	1.00E-03	6.00E-03	**
		No detection	Disappearence	15771	197	1.70E-02	1.00E-01	ns
		Occurrence	Persistence	198	293	4.93E-06	2.96E-05	****
		Occurrence	Disappearence	198	197	7.65E-05	4.59E-04	***
		Persistence	Disappearence	293	197	7.99E-01	1.00E+00	ns

Chapter 4 An open-source, micro weather station network with Iridium communication for remote deployment.

Chris L. Cosgrove and Anne W. Nolin

4.1 Abstract

Meteorological data scarcity in high-latitude and high-altitude areas is a significant challenge in understanding the impacts of a warming climate on seasonal snowcover; a critical component of regional hydrology and ecosystem functions. The development of low-cost, open-source wireless sensor networks (WSN) however offers an opportunity to address data gaps in these regions and widen the availability of environmental monitoring to non-traditional audiences. Here we present a WSN for snow-related applications built on the Arduino platform and utilizing Long Range Radio (LoRa) for two-way, local inter-node communication, and the Iridium constellation of satellites for data transmission from any global location with a clear view of the sky. The electronic hardware in each LoRa-enabled sensor node in our WSN costs approximately $270, the addition of an Iridium modem in a 'base-station' configuration costs an additional $250 and allows easy integration with Google Sheets, or other services, for near real-time data dissemination. Promising results are shown for low-cost sensors measuring snow depth, temperature, and relative humidity, in comparison to traditional research-grade components. Highlighting the WSN's relative strengths and weaknesses we propose three alternative deployment scenarios where it would enhance current snow-related research; the calibration and validation of physically-based models forced by gridded reanalysis data in remote regions, animal behavior and habitat selection in snowscapes, and rain-on-snow flood forecasting and monitoring. As the project is financially accessible, freely available to replicate, and has data streams that can be easily made publicly accessible, we envision its deployment in developing countries and/or in public-facing applications.

4.2 Introduction

High-latitude and high-altitude regions are being increasingly recognized as a frontline of climate change (Serreze and Barry, 2011; Pepin et al., 2015; Bormann et al., 2018; Box et al., 2019). Accelerated warming is causing dramatic changes to the hydrological cycle and unique ecosystems native to these areas, with cascading effects on the many services that each provides (AMAP, 2017). However, these regions are noted for their comparative data-scarcity and inaccessibility (Boelman et al., 2018, Figure 1; Klein et al., 2019), which is a major obstacle to research efforts and monitoring programs. A conspicuous and vital characteristic of these landscapes is the seasonal-to-perennial presence of snow. Snow cover has importance across many scales and processes, e.g.; as a feedback in land surface-atmosphere energy exchange due to its high reflectivity (Groisman et al., 1994), as terrestrial water storage depended upon by nearly 20% of the world's population (Barnett et al., 2005), and as a key component to ecosystem function in a wide range of habitats (Boelman et al., 2018). There is multi-dataset agreement that snow cover in high-latitude and high-altitude regions is decreasing (AMAP, 2017; Brown and Mote, 2009; Notarnicola, 2020) with often detrimental consequences for both natural and human systems (e.g. Brown et al., 2017). Yet there remain significant challenges in retrieving *in situ* data of snow properties from remote regions, limiting our ability to calibrate and validate physically-based models and remote-sensing datasets (Sturm, 2015).

Manual surveys of snow properties are a long-established measurement method of snow properties, most frequently snow depth (SD) and snow water equivalent (SWE), yet are expensive to conduct, which limits their coverage in space and time, even in accessible areas (Kinar and Pomeroy, 2015). The development of automatic weather stations (AWS) and instruments measuring SD using ultrasound, and SWE through a variety of methods, has allowed long-term monitoring of both snow properties and meteorological variables important to the energy balance of the snowpack (Kinar and Pomeroy, 2015). Networks of these stations, such as SNOTEL (NCRS, 2020) in the western United States, have greatly enhanced the ability to characterize different snow regimes and their interaction with climate variability. Yet, as point-scale measurement sites with high-costs of deployment and maintenance, they have poor spatial distribution and are often located in non-representative areas in terms of topography and vegetation, limiting their utility (Molotch and Bales, 2005).

More recently there has been an increased interest in developing and testing distributed sensor networks for snow-research. This research has been largely driven by the need to address critical knowledge gaps concerning the spatiotemporal scales of snow processes that a single AWS or remote sensing datasets cannot resolve (Sturm, 2015), but has been made possible by the increased availability of affordable sensors and supporting hardware (Mao et al., 2019). Early forms of these networks had no inter-station connectivity built-in, instead taking the form of standalone, cost-efficient nodes, each with data-logging capacity (e.g. Varhola et al., 2010; Pohl et al., 2014). Latterly, they have developed rapidly past wired connectivity (e.g. Rice and Bales, 2010) to wireless sensor networks (WSN) of >100 sensor nodes relaying data in near real-time to base stations connected to the internet (e.g. Kerkez et al., 2012; Malek et al., 2017). However, these advanced systems rely on either a cellular network or an ethernet connection for transmission of data to the internet for later downstream use. In remote areas, without such communication infrastructure, this reduces their usefulness for near real-time event monitoring and doesn't alert in the case of instrument failure - potentially leading to avoidable data loss. Additionally, their replicability and adaptability for development and deployment by other users is stymied due to the use of components and software that either demand a high degree of technical expertise or are proprietary (Mao et al., 2019).

Here we present a working prototype of a WSN for measuring SD and meteorological variables in remote high-latitude and high-altitude regions without traditional communication infrastructure. To examine its appropriateness in a research context in these environments, we demonstrate and compare its deployment alongside proprietary 'research-standard' equipment at a remote alpine site. The WSN uses the Iridium constellation of satellites for near real-time data transmission and monitoring, enabling its deployment at any global location with a clear view of the sky. Due to the use of open-source hardware and software that is accessible in terms of technical expertise and budget, we suggest it as an option suitable for non-traditional users and applications. Further, and in response to the recommendations proposed in Mao et al.'s (2019) review of low-cost sensor networks, we address the linking of data collection and downstream use (i.e. sharing and visualization) by demonstrating integration with Google Sheets.

4.3 Methods

4.3.1 WSN design and specifications

The WSN we present here is built entirely from off-the-shelf or open-source components, and by choosing to base hardware on the Arduino (2020) open-source electronics platform, we aim to create a low-entry point for a variety of users from non-traditional backgrounds with minimal electronic engineering experience. Arduino has an active global community of users that contribute to an impressive collective knowledge base, accessible in online tutorials and forums, and is a platform widely used for environmental sensing in peer-reviewed scientific literature (Mao et al., 2019). Following the spirit of the open-source movement, we hope that by distributing hardware and software details freely on Github interested readers can easily replicate and adapt the WSN according to their specific needs.

4.3.2 Hardware

Our system has two types of deployments, a sensor node, and a base station node. Each share a common set of components with a minimum operating temperature range of -40 ºC to 80 ºC (see Figure 4.1).

- *Adafruit Industries Feather M0 with RFM95 LoRa Radio*

  https://www.adafruit.com/product/3178. The Adafruit Feather line of development boards is available from distributors on six continents[7]. They are well-built, compact (51 mm by 23 mm), and can be neatly stacked upon one another for ease and flexibility of assembly. The Feather M0 with RFM95 LoRa Radio board comes equipped with an ATSAMD21G18 ARM Cortex M0 processor to run each nodes' software and has a Long Range (LoRa) packet radio transceiver built-in for node-to-node communication. We chose this board as the microcontroller due to its variety of digital and analog pins, processor specification, and flexible telemetry capable of operating at the non-licensed frequencies of 868 MHz or 915 MHz in Europe and North America respectively. LoRa radios have documented ranges of up to 2 km line-of-sight with simple omnidirectional aerials making them an excellent choice for remote applications looking to maximize spatial coverage.

[7] https://www.adafruit.com/distributors

- *Adafruit Industries DS3231 Precision RTC FeatherWing* https://www.adafruit.com/product/3028. The FeatherWing series of breakout boards from Adafruit easily configure with the Feather line of microprocessor boards. For time-stamping sensor measurements and to wake the microprocessor from a low-power, deep-sleep mode between measurements, we use a FeatherWing with a DS3231 Real Time Clock (RTC) run off a separate coin cell battery.
- *Adafruit Industries Adalogger Featherwing* https://www.adafruit.com/product/2922. Each sensor node is equipped with its own local data storage via the use of the Adalogger Featherwing, which has a microSD[8] memory card socket.
- *Adafruit Industries Terminal Block Breakout Featherwing* https://www.adafruit.com/product/2926. Completing the microprocessor assembly is a Terminal Block Breakout that allows flexible prototyping and deployment of different sensors by negating the need for permanently soldering them to the development boards.
- *SONBEST SHT-10 Mesh-protected Weatherproof Temperature and Humidity Sensor* https://www.adafruit.com/product/1298. Air temperature and relative humidity are fundamental meteorological variables and are required as minimum forcing data for a variety of physically-based snow evolution models (e.g. SNOWPACK, Bartelt and Lehning, 2002; SnowModel, Liston and Elder, 2006). We use a weatherproofed Sensirion SHT-10 sensor with 4.5 % and 0.5 % precision for humidity and temperature respectively, though a wide range of temperature and relative humidity sensors interface with the microprocessor. For our initial deployment, from which the data presented in this paper is derived, we 'shielded' SHT-10 sensor in a horizontal PVC pipe with holes drilled in it to allow for airflow and

---

[8] https://www.sdcard.org/index.html

drainage. Future deployments could make use of a 3D printed radiation shield such as those designed by the 3D-Printed Automatic Weather Station initiative (3D-PAWS, 2020).

- *MaxBotix® MB7374 HRXL-MaxSonar-WRST7 Ultrasonic Precision Range Finder* https://www.maxbotix.com/Ultrasonic_Sensors/MB7374.htm. To measure SD we use a MaxBotix® MB7374 (hereafter referred to as MaxBotix) ultrasonic range finder that calculates the distance to the snow-surface, or ground, from the return time of an ultrasonic pulse. It has a resolution of 1 mm, internal temperature compensation, a range of 50 to 500 cm, and is specifically calibrated for snow level measurement.

The base station node additionally has a;

- *Rock Seven RockBlock Mk II Iridium Satellite Modem* http://www.rock7.com/products-rockblock. The RockBlock Mk II's Iridium 9602 satellite modem (hereafter referred to as RockBlock) enables the transmission and reception of short messages from any global location that has a clear view of the sky. In comparison to previous systems, this allows our WSN to transfer data in near real-time from remote areas beyond the reach of traditional terrestrial communication networks. The RockBlock has a successful deployment history in research settings (e.g. Martinez et al., 2017) and line-rental and credits are easily managed via an online application[9]

4.3.3 Power Management

For successful deployment in remote and inaccessible areas effective power management is an important consideration within a WSN. The hardware above was selected for power efficiency and the ability to programmatically enable a deep-sleep mode using minimal current draw.

[9] https://rockblock.rock7.com/Operations

Complimenting this is a relatively low measurement frequency, which limits the time each node spends in power-intensive measurement or communication processes, greatly extending the deployment period without needing to replace batteries. For our test deployment, we used rechargeable 2500 mAh and 4400 mAh lithium-ion batteries in the sensor and base station nodes respectively, with the larger battery in the base station accounting for the additional power needs of the satellite modem. Further, we included a 6V solar panel[10] and battery charger[11] in the base station node set-up to 'scavenge' extra power in daylight hours. This represents a relatively light weight set-up where keeping the physical size and mass of each node to a minimum is a key criterion and where hourly measurements are adequate for the project's requirements. However, there exists great flexibility in terms of battery size/type and/or sampling interval, which is easy to implement using readily available batteries, e.g. single D-cells, AA type batteries, or other, as well as programmatically.

Figure 4.1. Photo of a SnowBot node installed at Sagehen Creek Field Station. Note the MaxBotix acoustic depth sensor mounted on the end of the boom. Radiation shield containing temperature and humidity sensors not pictured. For scale, the antenna to the right of the unit is 17 cm long.

[10] https://www.adafruit.com/product/200
[11] https://www.adafruit.com/product/390

4.3.4 Network design

For the demonstration of this prototype, we implemented a star-type network topology where only the base station node receives sample data packets from the WSN nodes. This is in contrast to other possible topologies, e.g. *mesh*, where multiple neighboring nodes communicate with one another and create multiple paths back to a base station, which can allow for deployment over a greater area depending on the communication technology employed (Kerkez et al., 2012). Here we opt for a star topology due to the simplicity of our test deployment environment (see Figure 4.2), long-range of the LoRa radios, and reduced software overhead and technical expertise it requires. To do so we make use of the Airspayce RadioHead Packet Radio[12] library for embedded microprocessors and note that mesh network topologies are possible using the above hardware/software combination.

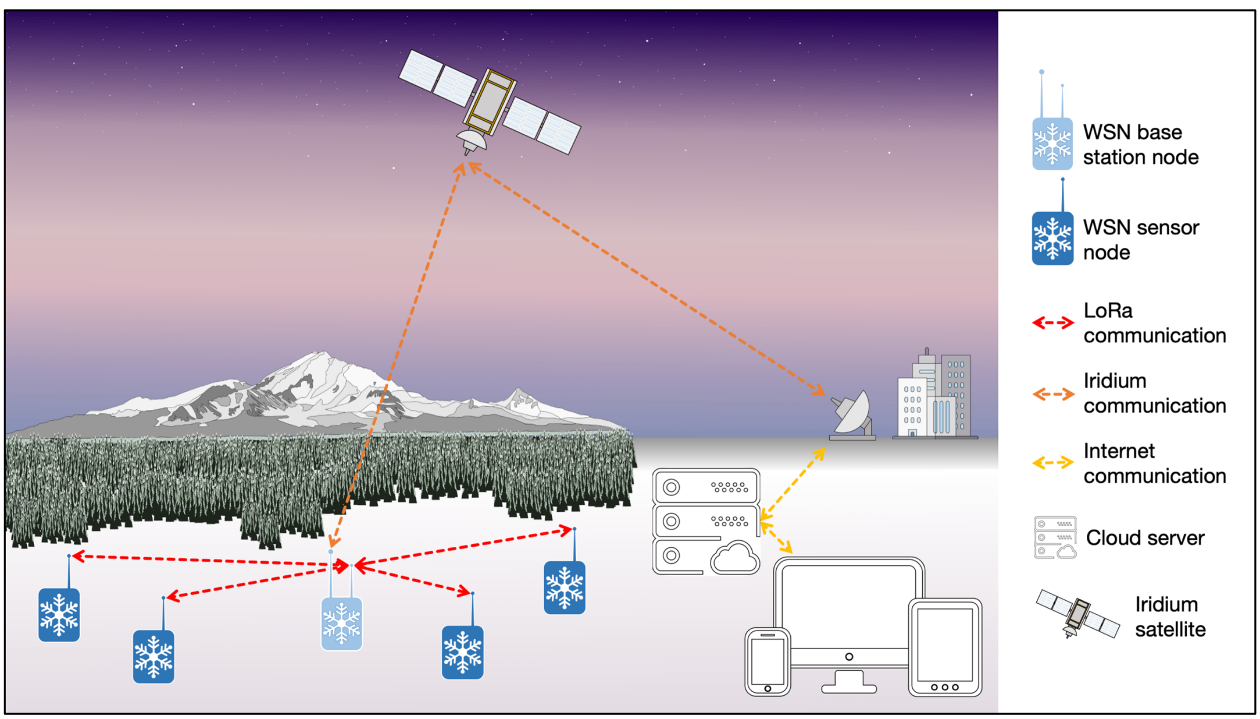

Figure 4.2. Schematic of star-topology network design between WSN sensor nodes and base station, possible two-way communication via Iridium, and data management and visualization in the cloud and on personal computers/devices.

---

[12] https://www.airspayce.com/mikem/arduino/RadioHead/

4.3.5 Software design – data collection and transmission

Adafruit Feathers are programmed using C/C++ (International Organization for Standardization, 2020) and there exists a wealth of open-source libraries for incorporating specific sensors and communication technologies. Examples of the code used for the current project can be found freely online on Github. Each sensor node is programmed to 'wake' at a user-specified interval and take readings from each sensor and of the battery's voltage. It then writes these readings with a timestamp to the local microSD card before sending them in a compressed binary format via LoRa to the base station node. Finally, it re-enters a low-power, deep 'sleep' mode before its next measurement and communication cycle. The base station fulfills these same steps but instead of sending its data via LoRa, it collects each sensor nodes' incoming data, writing this 'global' data to a specific file on its local data storage. To improve the success of data transmission, and to allow the base station to also enter into a deep-sleep state between readings and communication, both the nodes and base station are programmed to transmit and 'listen' for data for a user-specified interval and to shift to sleep mode at all other times. Additionally, a reliable datagram protocol is implemented for data-packet transmission where transmissions are addressed to the base station and sensor nodes are sent acknowledgment that their packets have been received. Lastly, the base station packages the most recent data from all nodes and transmits it via the Iridium network to a remote server at a user-defined interval. In contrast to other satellite data-transmission options, e.g. the National Aeronautics Space Agency's Geostationary Operational Environmental Satellite Program (GOES), the Iridium network has the advantage of functioning globally, making it appropriate for high-latitude deployments, and projects utilizing its technology do not require special authorization to send data over the network.

4.3.6 Software design – data storage and dissemination

A major advantage of the implementation of the RockBlock is the possibility of near-real time data monitoring and sharing. Rock Seven's remote server stores all incoming transmissions but also enables delivery of them either via email or HTTP POST. This opens up the opportunity for users to be alerted to new data locally via email client software and for publicly available databases to be updated. For this project, a relatively simple Python (Van Rossum and Drake, 2009) program was written to continuously monitor for new incoming RockBlock messages, decode those messages from their binary format, and further push the data to a Google Sheet viewable to anyone who has a copy of its link[13]. More advanced applications could deepen the data-user experience by similarly pushing near real-time data to interactive, web-based cartography and visualization platforms.

4.3.7 Field testing and sensor comparisons

To test our WSN we installed four sensor nodes and one base-station upon five research-grade meteorological towers at Sagehen Creek Field Station (SCFS), CA, USA (see Figure 4.3) from January to April 2020. Located in the northern Sierra Nevada, SCFS is maintained by the University of California, Berkeley, and encompasses 3,642 hectares of mixed forests, mountain meadows, and fens, across an elevational range of 1700 m to 2650 m. Average March SD is 1.04 m and average minimum January temperatures are -9.4 ºC (Western Regional Climate Centre, 2020).

Sensor data from the meteorological towers that we use to compare with SnowBot sensor data include temperature and humidity from Vaisala HMP155 Thermohygrometers[14] (hereafter to referred to as HMP155) housed in passive radiation shields on towers 1 to 3, incoming short-wave radiation from Campbell Scientific® CNR4 radiometers[15] (hereafter referred to as CNR4) on towers 1 to 3, and Campbell Scientific® SR50 (hereafter referred to as SR50) acoustic distance sensors[16] on all 5 towers. The WSN and meteorological tower sensors were mounted within 0.5 m height and 2 m horizontal distance of each other and at approximately 2 m above ground. We compare the performance of the co-located WSN sensors through calculating the Root Mean Standard Error (RMSE), bias, and linear regression between the WSN sensor data and the tower sensor data, both for the complete aggregated data and at each tower location. In the case of the acoustic distance sensors, we compare the distance to the snow surface as opposed to SD as the WSN was deployed after the establishment of the snowpack. Further, and to allow for comparison between locations with sensors mounted at different heights above the snowpack, we report the anomaly of each sample to its particular sensor's mean. For air temperature, humidity, and acoustic distance sensors a quality assessment was conducted on the samples prior to analysis. Anomalies and data outside of

[13] https://docs.google.com/spreadsheets/d/1bXNfe84xI_Z1eRQMcSj2ED9A3_uALM4kU8zc68iRorU/
[14] https://www.campbellsci.com/hmp155a
[15] https://www.campbellsci.com/cnr4
[16] https://www.campbellsci.com/sr50a

the range of the sensors were removed and in the SR50's case, the instrument's in-built quality flag was used to identify unreliable data.

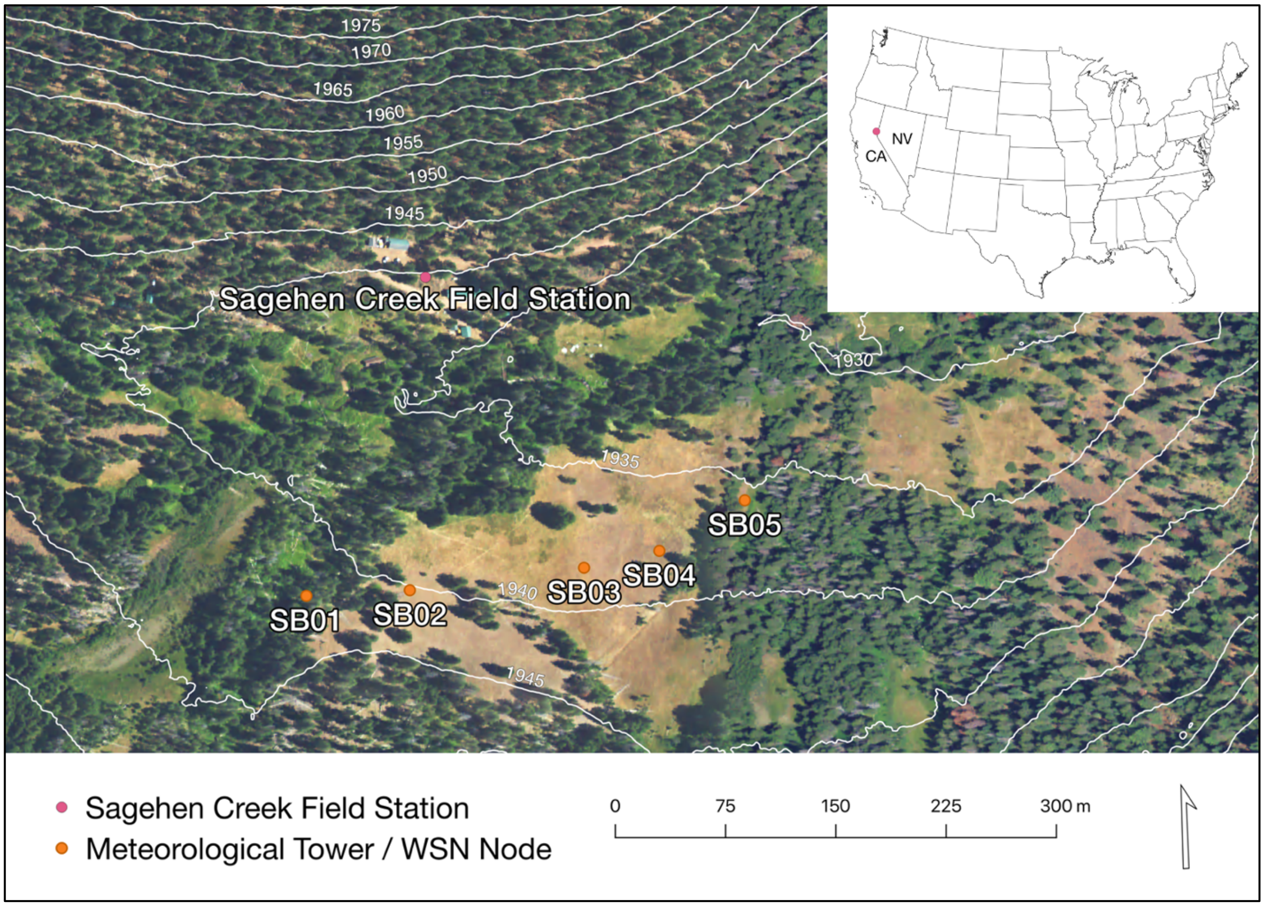

Figure 4.3. map of Sagehen Creek Field Station, CA, and its location in the conterminous USA (inset). SB01-05 are the locations of co-deployed meteorological towers and SnowBot WSN nodes in an ~250m west-east transect across an open meadow. Contour lines are at 5m intervals.

4.4 Results

4.4.1 Acoustic distance sensor comparison

A total of 925 distance samples were available after quality assessment and an RMSE of 0.028 m was found when comparing all the WSN's MaxBotix data to the meteorological tower's SR50 data (Table 4.1). An adjusted R-squared of 0.89 and β of 0.959 (SE ±0.011, p <0.001; Table 4.1) indicates that the MaxBotix data measures a comparatively greater distance than the SR50, albeit only slightly. When compared on a location-by-location basis only relatively minor local differences are observed; locations 4 and 5 showing that the MaxBotix measures a relatively shorter distance to the ground surface (Table 4.1 and Figure 4.4) instead of a greater distance. Adjusted R-squared at locations 2 and 5 are lower, <0.7, than the other locations. There is remarkably very little bias towards either of the sensors (Table 4.1 and Figure 4.4), both in the aggregated data and for each location. Likewise, RMSEs of <0.025 m demonstrate close agreement between the sensors, with the exception of location 5 (RMSE = 0.055 m).

Table 4.1. statistical comparison between the MaxBotix (x) and SR50 (y) acoustic distance sensors. Location refers to meteorological tower number (see Figure 3); n the number of sample compared; RMSE the root mean standard error in meters; Bias is in meters; Estimate is the slope coefficient of the fitted linear regression line; Std. Error is the standard error in meters; Adj. R-sq is the adjusted R-squared metric; df is the degrees of freedom.

Location	**n**	**RMSE**	**Bias**	**Estimate**	**Std. Error**	**Adj. R-sq**	**P-value**	**df**
All	925	0.028	0.0000	0.959	0.011	0.892	0.000	2
1	277	0.018	0.0000	0.850	0.025	0.807	0.000	2
2	110	0.021	0.0000	0.782	0.052	0.669	0.000	2
3	433	0.025	0.0000	0.957	0.011	0.948	0.000	2
4	3	0.003	0.0000	1.088	0.018	0.999	0.010	2
5	96	0.055	0.0000	1.143	0.081	0.671	0.000	2

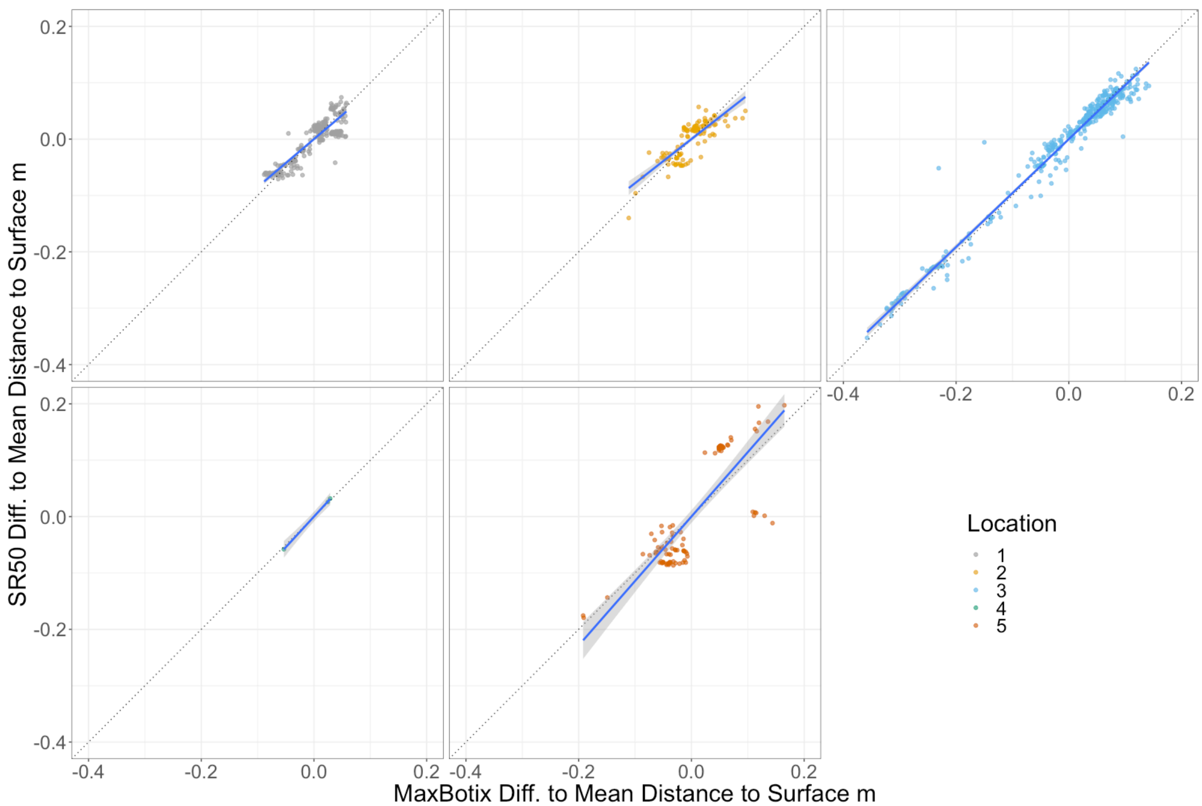

Figure 4.4. Comparison of the acoustic depth sensor performance by location. Each data point is the anomaly to the mean distance to the surface as measured by the WSN-mounted MaxBotix (x-axis) and meteorological tower-mounted SR50 (y-axis). Linear trend line shown in blue with shaded grey 95% confidence interval. Only data where both MaxBotix and SR50 measurements are available are shown.

An apparent influence of the diurnal cycle on acoustic distance sensor performance is seen in Figure 4.5 panel A. Daily spikes up to 5 cm in increased difference to the mean distance to the surface occur in both the MaxBotix and SR50 data during daylight hours (x-axis major tick marks occur at 00:00 local time, minor tick marks at 6-hr intervals) and match the daily peaks shown in the temperature measurements (Figure 4.5 panel B). The spikes are observed across a range of daytime temperature, both above and below 0 °C, suggesting an alternative cause than the effect of temperature on the speed of the ultrasonic pulse through air. A simple method for cleaning these daily spikes from the acoustic distance sensor data is to discard the data during the offending hours and instead interpolate from the distance measured prior to and after them. An example of this interpolation is shown by the solid lines in Figure 4.5 panel A.

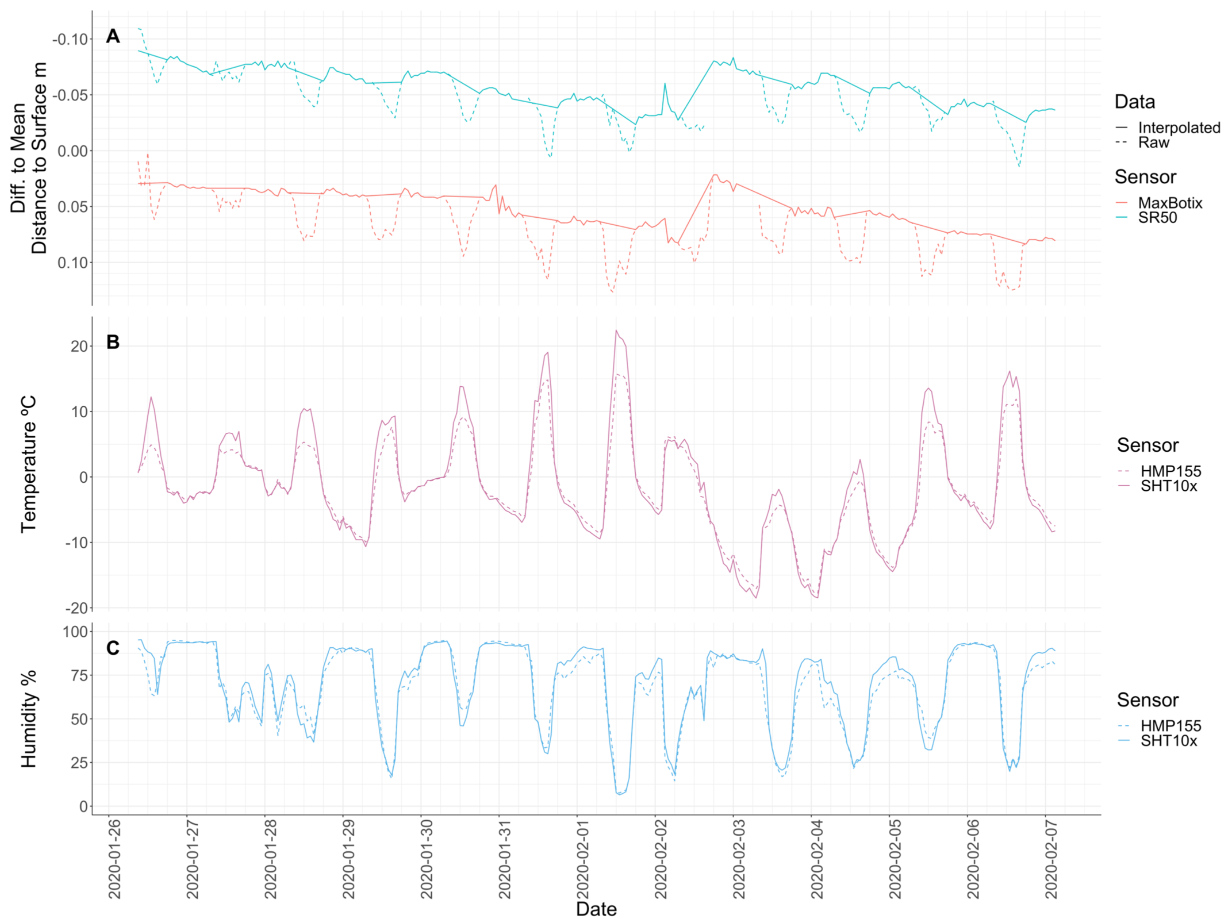

Figure 4.5. Two-week time series plot of distance to surface anomalies (panel A), air temperature (panel B), and relative humidity (panel C), as measured by the WSN-mounted MaxBotix and SHT10 sensors and meteorological tower-mounted SR50 and HMP155 sensors at location 3. Panel A shows the raw data measured by both the MaxBotix and SR50 acoustic distance sensors (dashed lines) and interpolated data to remove daily spikes in increased distance measured during daylight hours (08:00 and 17:00 Pacific Standard Time; solid lines). The y-axis in panel A is reversed to show more intuitively the changes in snow depth, i.e. greater distance measured corresponds to decreased snow depth. Panels B and C show the air temperature and relative humidity respectively, with dashed lines indicating measurements by the WSN mounted SHT10 and solid lines corresponding to measurements by the meteorological tower mounted HMP155.

4.4.2 Temperature sensor comparison

Comparison of the WSN-mounted SHT10 temperature sensors to the meteorological tower-mounted HMP155 sensors showed a general overestimation of air temperature by the SHT10 sensors when all available data points were compared (bias = -1.05 %, RMSE = 2.13 ºC, β = 0.821, SE ±0.006, p <0.001; Table 4.2). Comparing data at each individual location however reveals local differences. Locations 2 and 3, which are situated on the edge of and in an open meadow, respectively show greater biases towards lower temperature measured by the HMP155 (location 2 =

-2.12 °C, location 3 = -1.1 °C; Table 4.2 and Figure 4.6), whereas location 1, located in a dense forest stand, displays close agreement between the sensors (bias = -0.65). The role of incoming shortwave radiation in this pattern is shown in Figure 4.6 where location 1 has receives relatively little shortwave radiation in comparison to locations 2 and 3 (size of data points). It is noticeable that relatively warmer temperatures are measured by the SHT10 sensor at locations 2 and 3 when greater shortwave radiation is received; a finding that corresponds to the data shown in Figure 4.5 panel B where greater temperatures are measured by the SHT10 sensor at location 3 during daylight hours.

Table 4.2. statistical comparison between the SHT10 (x) and HMP155 (y) temperature sensors. Location refers to meteorological tower number (see Figure 4.3); n the number of sample compared; RMSE the root mean standard error in °C; Bias is in °C; Estimate is the slope of the fitted linear regression line; Std. Error is the standard error in °C; Adj. R-sq is the adjusted R-squared metric; df is the degrees of freedom.

Location	n	RMSE	Bias	Estimate	Std. Error	Adj. R-sq	P-value	df
All	1352	2.113	-1.05	0.821	0.006	0.94	0.000	2
1	503	0.950	-0.65	0.946	0.006	0.98	0.000	2
2	157	3.125	-2.12	0.754	0.024	0.86	0.000	2
3	688	2.419	-1.10	0.789	0.007	0.95	0.000	2

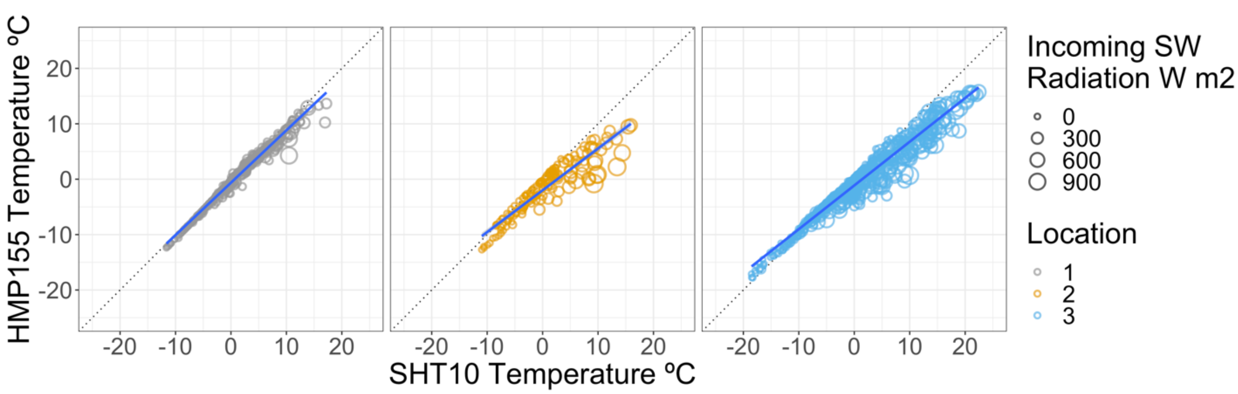

Figure 4.6. Comparison of the temperature sensor performance by location with the WSN-mounted SHT-10 on the x-axis and the meteorological tower-mounted HMP155 on the y-axis. Linear trend line shown in blue with shaded grey 95% confidence interval. Size of data-point indicates incoming shortwave radiation as measured by the CNR4.

4.4.3 Relative humidity sensor comparison

As with air temperature, and across all available data, the WSN-mounted SHT10 sensor generally recorded greater relative humidity when compared to the HMP155 sensor on the meteorological towers (RMSE = 7.08 %, bias = -1.93 %, β = 0.885; SE ±0.008, $p < 0.001$; Table 4.3). In contrast, however, local differences did not follow the same pattern with location 2 showing instead that the SHT10 measured generally lower relative humidity than the HMP155 (bias = 4.58 %; Table 4.3) and locations 1 and 3 showing bias in the opposite direction (bias = -3.70 % and -2.14 % respectively; Table 4.3). There is little noticeable influence on incoming solar radiation on the measurement of relative humidity by either sensor in any location (Figure 4.7). However, there is a noticeable cluster of datapoints below the 1:1 line with high relative humidity measured by the SHT10 (>75 %) when lower values are recorded (<75 %) by the HMP155 at location 1 (Figure 4.7). Further exploration of the data in time series (not presented) indicates that these measurements took place over the course of 2 days, suggesting that a temporal cause such as the presence of liquid water in the sensor housing might be at fault.

Table 4.3. statistical comparison between the SHT10 (x) and HMP155 (y) relative humidity measurements Location refers to meteorological tower number (see Figure 4.3); n the number of samples compared; RMSE the root mean standard error in ºC; Bias is in ºC; Estimate is the slope of the fitted linear regression line; Std. Error is the standard error in ºC; Adj. R-sq is the adjusted R-squared metric; df is the degrees of freedom.

Location	n	RMSE	Bias	Estimate	Std. Error	Adj. R-sq	P-value	df
All	1352	7.08	-1.93	0.885	0.008	0.90	0.000	2
1	503	8.15	-3.70	0.901	0.016	0.86	0.000	2
2	157	7.13	4.58	0.794	0.017	0.93	0.000	2
3	688	6.16	-2.14	0.898	0.008	0.94	0.000	2

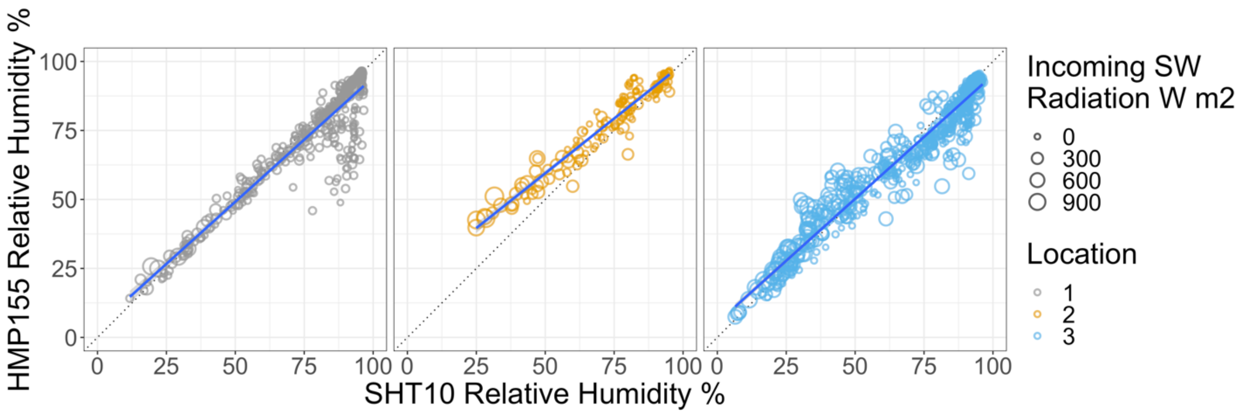

Figure 4.7. Comparison of the relative humidity sensor performance by location with the WSN-mounted SHT-10 on the x-axis and the meteorological tower-mounted HMP155 on the y-axis. Linear trend line shown in blue with shaded grey 95% confidence interval. Size of data-point indicates incoming shortwave radiation as measured by the CNR4.

4.5 Discussion

The WSN we present here was conceived as a low-cost solution to data-scarcity in high-latitude or high-altitude environments with limited accessibility. Field testing revealed its design to have some promise in comparison to traditional and proprietary 'research-grade' equipment but also presented challenges unique to working with open-source hardware and software. Here we discuss the performance of the sensors we tested, weigh the benefits and limitations of our WSN and open-source hardware and software generally, and present three deployment scenarios where our WSN would enhance snow-related research.

4.5.1 Sensor comparisons

Comparisons of the WSN-mounted MaxBotix and meteorological-tower-mounted SR50 acoustic depth sensors showed remarkably close agreement with RMSEs of <0.03 m recorded for the aggregated data and at four of the five locations. Given that the MaxBotix has a manufacture tested accuracy of less than <1 %[17] and the SR50 has a manufacture tested accuracy of ±1 cm or 0.4%[18], and that the typical distance during field testing was between 1 and 2.5 m, this error is not

---

[17] https://www.maxbotix.com/documents/HRXL-MaxSonar-WRS_Datasheet.pdf
[18] https://s.campbellsci.com/documents/us/product-brochures/b_sr50a-l.pdf

far beyond what could be reasonably expected given both the sensors' known accuracy. At location 5, an RMSE of 0.055 m was recorded yet bias remained negligible, suggesting that there were temporal differences in the evolution of SD between the surface detected by the MaxBotix and the surface detected by the SR50. Such spatial variability in SD at a meter scale is well-known in snow hydrology and is thought to be primarily caused by wind-redistribution processes working on the microtopography of the snow surface (Clark et al., 2011).

Seen in the measurements for both the MaxBotix and SR50 is a spike in the distance measured during daylight hours (Figure 4.5 panel A). These daily spikes are seen across a range of air temperatures indicating that it isn't solely due to the actual air temperature affecting the speed of the emitted and reflected ultrasonic pulse (Ryan et al., 2008). Likewise, both the MaxBotix and SR50 sensors have facility to correct their recorded distances for the effect of temperature; in this study the MaxBotix did this by default via its internal thermometer whereas the SR50 was corrected by the temperature measured by the co-deployed HMP155. Interestingly, one would hence assume that there would be a difference between the two sensors given that the SR50's temperature correction came from data measured within a passive radiation shield rather than an enclosed sensor, but that does not appear to be the case. Given the range of air temperatures where this phenomenon occurs, it is instead likely that the temperature used to correct the distance is overestimated due to shortwave radiation warming the temperature sensor - irrespective of whether it is situated internally or in a radiation shield. Further testing where the distance-correcting temperature sensor is housed in an aspirated radiation shield would help determine whether this is the case.

Comparison of air temperature values recorded by the WSN-mounted SHT10 versus the meteorological tower-mounted HMP155 further illustrates the likely effect of shortwave radiation, especially in the case of the inadequately housed SHT10 (Table 4.2, Figure 4.6). At location 1, where little shortwave radiation penetrates the thick forest canopy the two sensors are well matched. Whereas at the open sites of locations 2 and 3 it is easy to see that SHT10 records higher temperatures during increased solar loading than the HMP155. An improvement to the housing of the SHT10 is the simplest solution to this bias; the open-source 3D printed radiation shield developed by the 3D PAWS (2020) project would be an appropriate choice. Malek (2019) found that an increase of 1000 lux in light intensity led to an increase of 0.1 to 0.18 ºC in measured air temperature by sensors in passive radiation shields versus aspirated radiation shields, although this bias was reduced with increasing wind speeds. Further work by Rupp et al. (2020), produced a correction factor between paired non-aspirated and aspirated radiation shields based on light intensity – an approach that could be followed using the hardware we present here with the relatively simple addition of a low-cost light sensor. Aspirated radiation shields have both a greater financial and power cost, making them unsuitable for remote deployments of WSNs with multiple nodes. Hence, incorporating a low-cost light sensor into the WSN node design and performing calibration experiments in comparison to aspirated radiation shields would be worthwhile further research. Additionally accounting for the mitigating effect of increased wind speed on the temperature recorded in passive radiation shields would require either an anemometer as part of the WSN node design or post-processing of the data using wind-fields derived from climate re-analysis products, such as the Modern Era Retrospective analysis for Research and Applications, Version 2 (MERRA-2, Bosilovich et al., 2016).

The relative humidity measurements recorded by the SHT10 and HMP155 showed generally good agreement at locations 1 and 3 (bias less than ±4 %, β ~0.9) but a bias towards lower relative humidity recorded by the SHT10 at location 2, albeit with fewer data available, indicated inconsistency in the sensors (Figure 4.7, Table 4.3). It is likely that the SHT10 sensor is largely responsible for this inconsistency, as well as the high RMSE recorded across all locations, as its accuracy is relatively low (manufacture reported ±4.5 %) compared to the HMP155 (±1.0 + 0.008 * reading % at -20 to 40 ºC[19]). Alternative low-cost relative humidity sensors with greater accuracy are widely available and it is likely that an improved radiation shield, where the risk of the sensor being in close proximity or contact with liquid water is reduced, would improve results.

4.5.2 Benefits of open-source hardware / software

The greatest advantage of open-source hardware and software is their significantly lower financial costs compared to traditional systems. For example, the sensors and all the other electrical components for one of the sensor nodes in the WSN we present here costs approximately $270. To add the RockBlock module is another 250 USD. In comparison, the unit price of one HMP155 is nearly $800, an SR50 is nearly $1600, and a typical Campbell Scientific datalogger used alongside these instruments costs around $1800. Even without adding the additional costs of

[19] https://www.campbellsci.com/hmp155a

telemetry modules equivalent to LoRa and Iridium, 14 WSN sensor nodes and 1 base station node could be purchased for the same price as these three components. As a result, a far greater spatial area can be monitored, reducing issues with measurement representativeness and capturing important environmental gradients, for the same economic outlay.

Supporting the cost effectiveness for multiple measurement locations is the order of magnitude lower weight and size of the WSN components relative to traditional products. A major challenge in setting-up remote monitoring stations is the costs and logistics involved in the transportation of heavy equipment to them. As a consequence of their small size and weight the WSN components require less substantial fittings and support structures. As such, multiple nodes can be easily born by a single person with a ~60L volume hiking backpack.

4.5.3 Challenges with open-source hardware / software

Whilst highly accessible in terms of financial cost, working with open-source hardware and software, via the Arduino platform or otherwise, requires the user to go on a learning curve that combines basic electrical engineering, software programming and environmental monitoring. This is also the case for many proprietary systems but there exists a difference in the level of 'plug-and-play' functionality of open-source sensors and other hardware compared to off-the-shelf solutions. Likewise, the degree of technical support available is limited compared to traditional products. Additionally, there exists few ready-made enclosures and mounting solutions for open-source designs, necessitating creativity in adapting suitable products already on the market, e.g. weatherproof junction boxes, or the exploration of custom 3D printed options. In total, greater time is required by novice and even experienced users in the development and assembly of open-source solutions relative to traditional systems. However, increasingly there are fully tested and instructed open-source systems published, such as the WSN described here, which we hope will reduce the learning curve required to implement them.

Especially important to projects looking to deploy in environments similar to that described in this study, is the physical robustness of low-cost hardware for long-term environmental monitoring. The quality of materials is often sacrificed when reducing cost, for example the MaxBotix's plastic casing versus the SR50's stainless steel, and in contrast to proprietary and traditional hardware the emphasis is on the user rather than the supplier to field-test products as they are more-likely to be designed for general applications. The additional time needed for field testing open-source components is hence a further consideration if users are looking to develop solutions from scratch. Yet, wider dissemination of successful projects gives greater confidence that certain components are capable of performing in extreme environments over extended periods. For example, Cryologger, an Arduino based project using the same microcontrollers as the WSN described here, has, at the time of this writing, been uninterruptedly tracking ice-berg movement in the Canadian Arctic for over one and a half years[20].

Data quantity and quality are important to any scientific endeavour. The performance of open-source hardware in respect to the former is constrained in both similar and contrasting ways to traditional systems. Power requirements and availability are the biggest determinants of how often and for how long measurements can be taken. The power needs of open-source systems are typically less as their microcontrollers are simpler and require a lower voltage for operation (3 to 5 V versus 10 to 18 V), their sensors similarly. However, power demands for any sampling rate and duration in both open-source and traditional systems can be overcome using batteries, solar, or other sources. Instead, a limiting factor in measurement frequency for open-source systems using the Arduino platform or similar is the relatively limited clock-speed of its microprocessor and whether it can take samples from multiple sensors simultaneously. Small-scale, low-cost microcontrollers often can only run one program at one time as they lack operating system software. Low-cost, open-source systems are hence less suitable for settings requiring high frequency, e.g. greater than 1 Hz, and exactly timed coincidental data.

Similar to this study, data quality of open-source systems has been compared to traditional applications in a variety of settings, e.g. Varhola et al., (2010), Pohl et al., (2014), Castell et al., (2017), and Strigaro et al., (2019). The excitement driving the widespread development and adoption of environmental monitoring WSNs, deployed as part of the Internet of Things (IoT) or otherwise, is that their reduced burden of cost stands to democratize data (Mao et al., 2019). Yet data quality needs to be tested in these systems for them to truly help the environmental problems they seek to answer. It is critical to test and calibrate open-source systems, in and out of the field and against established hardware, and especially if the intent is to publish them for wider adoption.

[20] https://cryologger.org

A further consideration when using open-source equipment is the relatively limited availability of particular instruments. While this is changing as the technology is adopted and creative solutions are disseminated, in the context of snow research instruments found on many traditional meteorological stations do not yet have low-cost equivalents. The measurement of SWE via a snow pillow is an example (Kinar and Pomeroy, 2015). In respect of data transmission there too exists comparative limitations in satellite services available for open-source systems; hardware utilising the Iridium constellation, as used here, is accessible but two other similar platforms, the Geostationary Operational Environmental Satellite[21] (GOES) and the Argos system[22], do not yet have readily available modules for Arduino-like projects. It is worth noting though that GOES does not offer coverage in high latitudes and the maximum message length for Argos is 32 bytes versus Iridium's 340 bytes[23].

4.5.4 Potential deployments

The WSN we present here lends itself to research and/or monitoring projects where high frequency data isn't needed and there is no communications infrastructure in place. Much of the Arctic Boreal region has few *in situ* measurements of snow and meteorological variables available, yet snow cover in this vast area has a vitally important role in regional ecosystems, local economies and global climate (Bokhorst et al., 2016). To overcome the lack of *in situ* measurements an approach often taken is to downscale broad-scale, climate reanalysis products, e.g. MERRA-2 (Bosilovich et al., 2016), to force spatially-distributed, physically-based snow evolution models with, e.g. SnowModel (Liston and Elder, 2006). However, without *in situ* data to calibrate and validate to there exists uncertainty in the accuracy of the modelled variables. To improve modelled data, field campaigns to manually take snow measurements are necessary but due to the difficulty and expense of accessing remote areas they are often restricted in time and space, or the study area is selectively chosen to ensure access, which then leads to the clusters of data near easily-accessed sites that may not be representative. If a traditional AWS exists already in the field site, e.g. a SNOTEL station, or is established for the research project, it may not be representative of the study area's heterogeneity

[21] https://www.goes.noaa.gov
[22] https://www.argos-system.org
[23] https://library.wmo.int/pmb_ged/dbcp-td_44_en/doc/satellite-systems-buyers.pdf

in landcover, elevation and aspect (Molotch and Bales, 2005; Gleason et al., 2017). Further, many AWSs do not have functionality to transmit data from remote locations, inhibiting the progress of model calibration and other research until data is manually collected, which in the case of some very inaccessible sites might only be on an annual basis. The WSN we present here hence solves issues of spatial and temporal representation and the timely availability of data for research that requires *in situ* measurements to improve snow modelling.

The timing, duration, and qualities, e.g. depth and density, of seasonal snow cover has significant impacts on wildlife (Pomeroy and Brun, 2001) whether it be through restricting their movement or access to forage (Johnson et al., 2002), providing a protective winter den (Domine et al., 2018), or providing camouflage to seasonal changes in pelt or plumage colour (Zimova et al., 2014). Recently there has been great advancement of animal-borne tracking devices and sensors, allowing researchers to study how wildlife responds to its environment in ever greater detail (Wilmers et al., 2015). However, there is a recognised lack of snow data that matches the resolution and range needed to adequately study animal behaviour at the scales offered by these sensors (Boelman et al., 2018). For populations of animals whose habitat extent could reasonably be covered, the WSN we present here could provide wildlife ecologists snow and climate data in near-real time just as animal-borne GPS collars reporting location and movement metrics do. This has advantages over using remotely sensed datasets of snow properties that might be lacking in useful information, e.g. SD, or gridded data such as Snow Data Assimilation System (SNODAS; National Operational Hydrologic Remote Sensing Center, 2004) that is limited in spatial coverage and has been shown to be inaccurate in heterogeneous terrain (Sirén et al., 2018).

A third application for the WSN could be as a warning system for rain-on-snow flooding. Severe and expensive damage can occur when warm storm systems cause heavy rain to fall on snow cover as the additional water from snowmelt can produce a substantial pulse in runoff (Musselman et al., 2018). This pulse can be challenging to predict and mitigate as it requires knowledge of how much precipitation is likely to fall, the SWE of the snowpack over a large area, and the elevation of the rain-to-snow transition or freezing level (McCabe et al., 2007). Taking the Western United States as an example it is known that the spatial distribution of monitoring sites is both limited and non-representative (Molotch and Bales, 2005). A WSN of the type we describe here could therefore 'fill in the gaps' of established monitoring networks and be located in representative locations of different landcovers and across elevation gradients (Gleason et al., 2017). While SWE is not measured by the WSN it can be inferred with reasonable accuracy using known empirical equations for density evolution based on SD, the day of the year (DOY), and climatological normal values for precipitation and temperature at the location (Hill et al., 2019). An additional feature of the data transmission technology of the WSN that isn't covered in detail here is that it allows two-way communication. Hence, adaptive monitoring is possible where the network could be instructed to sample and transmit data at a higher-frequency ahead of and during potentially hazardous storms but otherwise remain in a low-power, low-frequency state (Blaen et al., 2016).

4.6 Conclusions

We present here a working prototype for a low-cost, open-source WSN suitable for high-latitude and high-altitude environments and demonstrate that its sensors have good agreement with traditional research-grade equivalents. As described in the discussion, it could have varied deployment in snow-related research and certain applications would greatly benefit from the improved spatial distribution it offers, as well as its data transmission possibilities. In other contexts, where high frequency and high accuracy data are required, different equipment is needed. Among the advantages of the technology we describe here is that it allows near-real time data dissemination to anyone who has a link to a Google Sheet. An extension of this could include data visualisation and download via web-maps or updates via social media platforms, further increasing the ease of stakeholder involvement (Mao et al., 2019). We also contemplate that it might have impact in developing nations, such as those of high-mountain Asia, where communications infrastructure and data-coverage is relatively limited, and budgets for environmental monitoring are smaller (J. A. Klein et al., 2019; Mao et al., 2019). For such applications to be fully realised, further work is needed on; the sustainability of the WSN components for multi-year deployments, assessing the appropriateness of alternative and additional sensors (e.g. anemometers, pyranometers, barometric pressure gauges), and the performance of the LoRa radio in different topographies and vegetation, as well as in a mesh topology.

4.7 Acknowledgements

An American Alpine Club Research Grant provided funding for the purchase of much of the hardware for this project. Dr. Bo Zhao was the original catalyst for the idea and offered valuable insight in its early stages. The OPEnS Lab at Oregon State University, and Dr. Chet Udell in particular, provided great support in understanding Arduino hardware. Dr. Steve Drake kindly shared data from his meteorological towers and helped installation at Sagehen Creek Research Station. Adam Garbo greatly assisted in improving the function and readability of the Arduino code. Alex Greenwald also assisted with field deployment. Countless unknown posters and their respondees on Arduino's and other technical forums made development a far less painful and quicker exercise.

4.8 References

3D-PAWS: 3D-Printed Automatic Weather Station, [online] Available from: https://sites.google.com/ucar.edu/3dpaws/ (Accessed 17 March 2020), 2020.

AMAP: Snow, Water, Ice and Permafrost in the Arctic (SWIPA) 2017 | AMAP, Arctic Monitoring and Assessment Programme (AMAP), Oslo, Norway. [online] Available from: https://www.amap.no/documents/doc/snow-water-ice-and-permafrost-in-the-arctic-swipa-2017/1610 (Accessed 15 March 2020), 2017.

Arduino: Arduino - Home, [online] Available from: https://www.arduino.cc/ (Accessed 16 March 2020), 2020.

Barnett, T. P., Adam, J. C. and Lettenmaier, D. P.: Potential impacts of a warming climate on water availability in snow-dominated regions, Nature, 438(7066), 303–309, doi:10.1038/nature04141, 2005.

Bartelt, P. and Lehning, M.: A physical SNOWPACK model for the Swiss avalanche warning Part I: numerical model, Cold Regions Science and Technology, 23, 2002.

Blaen, P. J., Khamis, K., Lloyd, C. E. M., Bradley, C., Hannah, D. and Krause, S.: Real-time monitoring of nutrients and dissolved organic matter in rivers: Capturing event dynamics, technological opportunities and future directions, Science of The Total Environment, 569–570, 647–660, doi:10.1016/j.scitotenv.2016.06.116, 2016.

Boelman, N., Liston, G. E., Gurarie, E., Meddens, A. J. H., Mahoney, P. J., Kirchner, P. B., Bohrer, G., Brinkman, T. J., Cosgrove, C. L., Eitel, J., Hebblewhite, M., Kimball, J. S., LaPoint, S. D., Nolin, A. W., Pedersen, S. H., Prugh, L. R., Reinking, A. K. and Vierling, L.: Integrating snow science and wildlife ecology in Arctic-boreal North America, Environ. Res. Lett., doi:10.1088/1748-9326/aaeec1, 2018.

Bokhorst, S., Pedersen, S. H., Brucker, L., Anisimov, O., Bjerke, J. W., Brown, R. D., Ehrich, D., Essery, R. L. H., Heilig, A., Ingvander, S., Johansson, C., Johansson, M., Jónsdóttir, I. S., Inga, N., Luojus, K., Macelloni, G., Mariash, H., McLennan, D., Rosqvist, G. N., Sato, A., Savela, H., Schneebeli, M., Sokolov, A., Sokratov, S. A., Terzago, S., Vikhamar-Schuler, D., Williamson, S., Qiu, Y. and Callaghan, T. V.: Changing Arctic snow cover: A review of recent developments and assessment of future needs for observations, modelling, and impacts, Ambio, 45(5), 516–537, doi:10.1007/s13280-016-0770-0, 2016.

Bormann, K. J., Brown, R. D., Derksen, C. and Painter, T. H.: Estimating snow-cover trends from space, Nature Clim Change, 8(11), 924–928, doi:10.1038/s41558-018-0318-3, 2018.

Bosilovich, M. G., Robertson, F. R., Takacs, L., Molod, A. and Mocko, D.: Atmospheric Water Balance and Variability in the MERRA-2 Reanalysis, J. Climate, 30(4), 1177–1196, doi:10.1175/JCLI-D-16-0338.1, 2016.

Box, J. E., Colgan, W. T., Christensen, T. R., Schmidt, N. M., Lund, M., Parmentier, F.-J. W., Brown, R., Bhatt, U. S., Euskirchen, E. S., Romanovsky, V. E., Walsh, J. E., Overland, J. E., Wang, M., Corell, R. W., Meier, W. N., Wouters, B., Mernild, S., M\aard, J., Pawlak, J. and Olsen, M. S.: Key indicators of Arctic climate change: 1971–2017, Environ. Res. Lett., 14(4), 045010, doi:10.1088/1748-9326/aafc1b, 2019.

Brown, R., Vikhamar Schuler, D., Bulygina, O. N., Derksen, C., Luojus, K., Mudryk, L. R., Wang, L. and Yang, D.: Arctic Terrestrial Snow Cover, in Snow, Water, Ice and Permafrost in the Arctic (SWIPA) 2017, Arctic Monitoring and Assessment Programme (AMAP), Oslo, Norway. (www.amap.no)., 2017.

Brown, R. D. and Mote, P. W.: The Response of Northern Hemisphere Snow Cover to a Changing Climate, J. Climate, 22(8), 2124–2145, doi:10.1175/2008JCLI2665.1, 2009.

Castell, N., Dauge, F. R., Schneider, P., Vogt, M., Lerner, U., Fishbain, B., Broday, D. and Bartonova, A.: Can commercial low-cost sensor platforms contribute to air quality monitoring and exposure estimates?, Environment International, 99, 293–302, doi:10.1016/j.envint.2016.12.007, 2017.

Clark, M. P., Hendrikx, J., Slater, A. G., Kavetski, D., Anderson, B., Cullen, N. J., Kerr, T., Örn Hreinsson, E. and Woods, R. A.: Representing spatial variability of snow water equivalent in hydrologic and land-surface models: A review, Water Resources Research, 47(7), doi:10.1029/2011WR010745, 2011.

Domine, F., Gauthier, G., Vionnet, V., Fauteux, D., Dumont, M. and Barrere, M.: Snow physical properties may be a significant determinant of lemming population dynamics in the high Arctic, Arctic Science, 4(4), 813–826, doi:10.1139/as-2018-0008, 2018.

Gleason, K. E., Nolin, A. W. and Roth, T. R.: Developing a representative snow-monitoring network in a forested mountain watershed, Hydrology and Earth System Sciences, 21(2), 1137–1147, doi:10.5194/hess-21-1137-2017, 2017.

Groisman, P. Y., Karl, T. R., Knight, R. W. and Stenchikov, G. L.: Changes of Snow Cover, Temperature, and Radiative Heat Balance over the Northern Hemisphere, J. Climate, 7(11), 1633–1656, doi:10.1175/1520-0442(1994)007<1633:COSCTA>2.0.CO;2, 1994.

Hill, D. F., Burakowski, E. A., Crumley, R. L., Keon, J., Hu, J. M., Arendt, A. A., Wikstrom Jones, K. and Wolken, G. J.: Converting snow depth to snow water equivalent using climatological variables, The Cryosphere, 13, 1767–1784, doi:10.5194/tc-13-1767-2019, 2019.

International Organization for Standardization: C++, [online] Available from: https://isocpp.org/std/the-standard (Accessed 18 March 2020), 2020.

Johnson, C. J., Parker, K. L., Heard, D. C. and Gillingham, M. P.: Movement parameters of ungulates and scale-specific responses to the environment, Journal of Animal Ecology, 71(2), 225–235, doi:10.1046/j.1365-2656.2002.00595.x, 2002.

Kerkez, B., Glaser, S. D., Bales, R. C. and Meadows, M. W.: Design and performance of a wireless sensor network for catchment-scale snow and soil moisture measurements, Water Resources Research, 48(9), 1–18, doi:10.1029/2011WR011214, 2012.

Kinar, N. J. and Pomeroy, J. W.: Measurement of the physical properties of the snowpack, Reviews of Geophysics, 53(2), 481–544, doi:10.1002/2015RG000481, 2015.

Klein, J. A., Tucker, C. M., Steger, C. E., Nolin, A., Reid, R., Hopping, K. A., Yeh, E. T., Pradhan, M. S., Taber, A., Molden, D., Ghate, R., Choudhury, D., Alcántara-Ayala, I., Lavorel, S., Müller, B., Grêt-Regamey, A., Boone, R. B., Bourgeron, P., Castellanos, E., Chen, X., Dong, S., Keiler, M., Seidl, R., Thorn, J. and Yager, K.: An integrated community and ecosystem-based approach to disaster risk reduction in mountain systems, Environmental Science & Policy, 94, 143–152, doi:10.1016/j.envsci.2018.12.034, 2019a.

Klein, J. A., Tucker, C. M., Nolin, A. W., Hopping, K. A., Reid, R. S., Steger, C., Grêt-Regamey, A., Lavorel, S., Müller, B., Yeh, E. T., Boone, R. B., Bourgeron, P., Butsic, V., Castellanos, E., Chen, X., Dong, S. K., Greenwood, G., Keiler, M., Marchant, R., Seidl, R., Spies, T., Thorn, J. and Yager, K.: Catalyzing Transformations to Sustainability in the World's Mountains, Earth's Future, 7(5), 547–557, doi:10.1029/2018EF001024, 2019b.

Liston, G. E. and Elder, K.: A Distributed Snow-Evolution Modeling System (SnowModel), J. Hydrometeor., 7(6), 1259–1276, doi:10.1175/JHM548.1, 2006.

Malek, A.: Empirical Analysis of Processes Affecting Drainage Flows and Inversions in a Forested Mountain Landscape, Oregon State University, 31 May. [online] Available from: https://andrewsforest.oregonstate.edu/publications/5093 (Accessed 31 July 2020), 2019.

Malek, S., Avanzi, F., Brun-Laguna, K., Maurer, T., Oroza, C., Hartsough, P., Watteyne, T., Glaser, S., Malek, S. A., Avanzi, F., Brun-Laguna, K., Maurer, T., Oroza, C. A., Hartsough, P. C., Watteyne, T. and Glaser, S. D.: Real-Time Alpine Measurement System Using Wireless Sensor Networks, Sensors, 17(11), 2583, doi:10.3390/s17112583, 2017.

Mao, F., Khamis, K., Krause, S., Clark, J. and Hannah, D. M.: Low-Cost Environmental Sensor Networks: Recent Advances and Future Directions, Front. Earth Sci., 7, doi:10.3389/feart.2019.00221, 2019.

Martinez, K., Hart, J. K., Bragg, G. M. and Curry, J. S.: Cryospheric monitoring with new low power RTK dGPS systems, AGU Fall Meeting Abstracts, 41 [online] Available from: http://adsabs.harvard.edu/abs/2017AGUFMIN41A0019M (Accessed 4 August 2020), 2017.

McCabe, G. J., Clark, M. P. and Hay, L. E.: Rain-on-snow events in the western United States, Bulletin of the American Meteorological Society, 88(3), 319–328, doi:10.1175/BAMS-88-3-319, 2007.

Molotch, N. P. and Bales, R. C.: Scaling snow observations from the point to the grid element: Implications for observation network design, Water Resources Research, 41(11), doi:10.1029/2005WR004229, 2005.

Musselman, K. N., Lehner, F., Ikeda, K., Clark, M. P., Prein, A. F., Liu, C., Barlage, M. and Rasmussen, R.: Projected increases and shifts in rain-on-snow flood risk over western North America, Nature Climate Change, 8(9), 808–812, doi:10.1038/s41558-018-0236-4, 2018.

National Operational Hydrologic Remote Sensing Center: Snow Data Assimilation System (SNODAS) Data Products at NSIDC, , doi:10.7265/N5TB14TC, 2004.

NCRS: NRCS National Water and Climate Center | SNOTEL Data & Products, [online] Available from: https://www.wcc.nrcs.usda.gov/snow/ (Accessed 15 March 2020), 2020.

Notarnicola, C.: Hotspots of snow cover changes in global mountain regions over 2000–2018, Remote Sensing of Environment, 243, 111781, doi:10.1016/j.rse.2020.111781, 2020.

Pepin, N., Bradley, R. S., Diaz, H. F., Baraer, M., Caceres, E. B., Forsythe, N., Fowler, H., Greenwood, G., Hashmi, M. Z., Liu, X. D., Miller, J. R., Ning, L., Ohmura, A., Palazzi, E., Rangwala, I., Schöner, W., Severskiy, I., Shahgedanova, M., Wang, M. B., Williamson, S. N. and Yang, D. Q.: Elevation-dependent warming in mountain regions of the world, NatCC, 5(5), 424–430, doi:10.1038/nclimate2563, 2015.

Pohl, S., Garvelmann, J., Wawerla, J. and Weiler, M.: Potential of a low-cost sensor network to understand the spatial and temporal dynamics of a mountain snow cover, Water Resources Research, 50(3), 2533–2550, doi:10.1002/2013WR014594, 2014.

Pomeroy, J. W. and Brun, E.: Physical Properties of Snow Introduction: Snow Physics and Ecology, in Snow Ecology., 2001.

Rice, R. and Bales, R. C.: Embedded-sensor network design for snow cover measurements around snow pillow and snow course sites in the Sierra Nevada of California, Water Resources Research, 46(3), doi:10.1029/2008WR007318, 2010.

Ryan, W. A., Doesken, N. J. and Fassnacht, S. R.: Evaluation of Ultrasonic Snow Depth Sensors for U.S. Snow Measurements, J. Atmos. Oceanic Technol., 25(5), 667–684, doi:10.1175/2007JTECHA947.1, 2008.

Serreze, M. C. and Barry, R. G.: Processes and impacts of Arctic amplification: A research synthesis, Global and Planetary Change, 77(1), 85–96, doi:10.1016/j.gloplacha.2011.03.004, 2011.

Sirén, A. P. K., Somos-Valenzuela, M., Callahan, C., Kilborn, J. R., Duclos, T., Tragert, C. and Morelli, T. L.: Looking beyond wildlife: using remote cameras to evaluate accuracy of gridded snow data, Remote Sensing in Ecology and Conservation, 4(4), 375–386, doi:10.1002/rse2.85, 2018.

Strigaro, D., Cannata, M. and Antonovic, M.: Boosting a Weather Monitoring System in Low Income Economies Using Open and Non-Conventional Systems: Data Quality Analysis, Sensors, 19(5), 1185, doi:10.3390/s19051185, 2019.

Sturm, M.: White water: Fifty years of snow research in WRR and the outlook for the future, Water Resources Research, 51(7), 4948–4965, doi:10.1002/2015WR017242, 2015.

Van Rossum, G. and Drake, F. L.: Python 3 Reference Manual, CreateSpace, Scotts Valley, CA., 2009.

Varhola, A., Wawerla, J., Weiler, M., Coops, N. C., Bewley, D., Alila, Y., Varhola, A., Wawerla, J., Weiler, M., Coops, N. C., Bewley, D. and Alila, Y.: A New Low-Cost, Stand-Alone Sensor System for Snow Monitoring, Journal of Atmospheric and Oceanic Technology, 27(12), 1973–1978, doi:10.1175/2010JTECHA1508.1, 2010.

Western Regional Climate Centre: SAGEHEN CREEK, CALIFORNIA - Climate Summary, [online] Available from: https://wrcc.dri.edu/cgi-bin/cliMAIN.pl?ca7641 (Accessed 4 August 2020), 2020.

Wilmers, C. C., Nickel, B., Bryce, C. M., Smith, J. A., Wheat, R. E. and Yovovich, V.: The golden age of bio-logging: how animal-borne sensors are advancing the frontiers of ecology, Ecology, 96(7), 1741–1753, doi:10.1890/14-1401.1, 2015.

Zimova, M., Mills, L. S., Lukacs, P. M. and Mitchell, M. S.: Snowshoe hares display limited phenotypic plasticity to mismatch in seasonal camouflage, Proceedings of the Royal Society B: Biological Sciences, 281(1782), 20140029, doi:10.1098/rspb.2014.0029, 2014.

Chapter 5 Summary of findings, perceived impacts and opportunities for further work

5.1 Chapter summaries

5.1.1 A personal reflection on the motivation of this dissertation

Wildlife endemic to the high-latitude, and indeed high-altitude, regions of the Earth, are on the frontlines of climate change as their habitats shift to new states due to the effects of anthropogenically-driven global heating. From the plucky rodents, such as the collared pika (*Ochotona collari*), to the big iconic beasts of population imagination, like the polar bear (*Ursus maritimus*), all are threatened by the avarice of people many miles away. Beyond their cultural importance to indigenous peoples of the circumpolar north, Arctic-boreal wildlife today are among the canaries in our global coalmine – if they continue to exist and function as they have done for centuries, we will have done good, if they are lost or are further maligned, we will have altered the Nature of our entire planet irrevocably. In perhaps just the latest example of human swindle, many northern species are now yoked with the latest in animal-borne sensors and laboured with carrying the messages of their own struggle to survive (Davidson et al., 2020). Nonetheless, these sacrificial lambs bear data that can provide ever more detailed insights into the ecological state of their habitats and advance the cause for their protection. There is much we do not know about their ecology and its responses to climate change, particularly so in the winter months when their landscapes are bedecked by snow and are at their most inaccessible.

These 'snowscapes' are as vulnerable to climate change as the wildlife that have long adapted to the challenges and assistances they offer. The sedimentary matrix of ice crystals that we term snow is highly sensitive to warming temperatures. If you heat it up enough, it turns to water. Today, it is clear from a wide range of data that snow cover in Arctic-boreal regions is changing rapidly in response to an amplified warming effect at high-latitudes. This change has profound consequences for the ecology of the region, and observations of its acute effects on wildlife are increasing. Mass-mortality of grazing ungulates due to ice-layers caused by mid-winter rain events have been witnessed in both North America and Eurasia, with cascading effects on the trophic systems where they occurred (Mallory and Boyce, 2017; Sokolov et al., 2016). Other species have found themselves wearing a white coat when the snow has already gone for the winter, leaving them a conspicuous choice for predation (Zimova et al., 2014). However, given the Arctic-boreal region's vastness and inaccessibility, we only have limited useful snow data to compare to both long-term observations of wildlife demographics and modern GPS-collar datasets detailing their movements.

The research presented here attempts to address this and is ultimately motivated by a sense of wonder to the region it concerns. I grew up in Dorset on the southern coast of the United Kingdom, a region firmly within the 'ephemeral' snow classification zone. Through great luck my academic and personal journey took me to the higher latitudes in winter and I quickly fell in love with their beauty and spirit. This dissertation in hence my humble offering to their continued conservation in the face of great imperilment. It takes the welfare of animals as its focus - a life-long concern of mine.

5.1.2 Chapter 2 summary, key findings, and anticipated impacts

Chapter 2 combines field measurements obtained by traditional sampling methods, such as excavating snowpits and walking snow-depth transects, and less-traditional methods, like the use of time-lapse hunting cameras, with a spatially-distributed snow evolution model to better simulate snow properties over a 37-year period for a mountainous area in the Wrangell St Elias National Park, Alaska. The use of *in situ* measurements to constrain model outputs is critical in regions where the absence of local meteorological data requires the use of climate reanalysis products to force the model. As the reanalysis products are themselves reconstructed from scarce data, biases occur, for snow-modelling this is especially important in the case of the volume of precipitation. Local snow water equivalent measurements, like we obtained via bulk density measurements of snow pits, can be assimilated into a model to correct the precipitation fields, which is the primary cause of inaccuracies in model output. Spatially distributed datasets of SWE, but also snow depth, which can be measured at greater frequency per unit time and converted to SWE using density observations, can then be operationalized to better parameterize the model to replicate the observed pattern of snow redistribution by wind. In the methods we present, the model can be further examined and tweaked for accuracy by comparison to a distributed set of snow depth measurements, as obtained by remote cameras deployed across gradients of aspect, elevation, vegetation, and slope. Utilizing this approach, we were able to produce detailed, accurate daily maps of snow properties in highly heterogenous topography from 1980 to 2017. These maps are publicly available for use in other research, be it within wildlife ecology or other sciences, and we additionally used them to reveal an important response of Dall's sheep to the seasonality of snow cover in the study area.

Previous research utilizing remotely-sensed snow-covered area data had proposed that Dall's sheep productivity, as indicated by the number of lambs per ewe observed during summer surveys, was reduced by the extended presence of spring snow cover (Kerk et al., 2018; Rattenbury et al., 2018). Dall's sheep give birth between April and May, and it was hence thought that spring snow inhibited the ewe's ability to find sufficient nutrition to adequately nurse their young, as well as their facility to protect them from predation. Our dataset, which elucidated the evolution of the vertical properties of the snowpack from its inception in early fall, told a different story. Instead, we revealed that the establishment of a deep snow cover in fall, alongside colder fall temperatures, had greater ability to predict Dall's sheep productivity than spring snow depth. This finding points towards an accumulative effect of persistent forage-and-movement inhibiting snow conditions on pregnant ewes, leaving them in poor physical condition come the spring and hence decreasing the survival rate of their lambs.

The snow-covered area remote sensing product used in the earlier research of the same sheep population cannot accurately determine interannual variability in snow depth. Instead, it only can infer snow depth from snow duration, which is subject to uncertainty as thin layers of snow can persist if temperatures are low enough. Discovering a greater sensitivity of Dall's sheep to enduring snow conditions than previously thought will inform research into other large Arctic-boreal ungulates. It also gives managers a chance to preserve populations by limiting harvest opportunities when there are sequences of challenging snow years. Our results highlight the power of a snow modelling approach in wildlife-ecology when used in combination with ground-observations and long-term observation datasets of wildlife demography.

5.1.3 Chapter 3 summary, key findings, and anticipated impacts

Chapter 3 assesses a passive microwave (PM) algorithm to detect layers of high-density snow and ice. Extending previous work that developed the approach and showed promise in identifying potentially lethal snow conditions to grazing ungulates, we applied the algorithm across a diverse Arctic-boreal region and examined the frequency of detections between areas of variable topographic complexity and land cover. In a further development of previous studies, we used an enhanced resolution dataset, extending from 1988 to 2019, and compared the sensitivity between two microwave frequencies, 19 GHz and 37 GHz, available in grids of 6.25 km and 3.125 km respectively. We also compared the meteorological conditions of when a high-density layer occurred, persisted, and disappeared in the record by using *in situ* observations recorded by two climate station networks. Finally, we compared snow pit derived metrics of layer density to the PM data across 84 locations to establish the algorithm's sensitivity to known properties of the snowpack.

Our findings showed that the algorithm has potential application in areas of low topography and vegetation – a result consistent with known issues when using PM data to derive snow properties. The 19 GHz channel showed greater sensitivity, evidenced by its higher frequency of detections, which we believe to be a product of its lower density threshold in the algorithm. As the 19 GHz channel is of a coarser resolution than the 37 GHz, this could mean that the application in studies of wildlife movements is limited. However, it is nonetheless an improvement on the 25 km resolution demonstrated in earlier work. Data derived from both channels has potential to inform each other when used together. The meteorological conditions observed prior to the occurrence, persistence, and disappearance of a detected high-density snow layer corresponded to well-known processes governing the stratigraphy of the snowpack, which, while falling short of a rigorous validation, gives us optimism that the algorithm detects what it was designed to. Balancing this optimism is the inconclusive results from the snowpit data, where no relationship was found between the metrics of snow density and the PM data.

As a novel study across a diverse and large spatial domain, further research is required to validate the PM algorithms detections in the different environments it was applied. While advocating restraint in lieu of the study's limitations we outline in chapter 3's discussion, we believe that we have already produced an exciting and useful dataset. Taken alone, the annual maps of detected layers of high-density snow or ice describe great inter-annual variability in the properties of Alaska's snow cover. As increased snow density leads to an increased thermal conductivity of snow, years and regions where we detect wide and persistent expanses of high-density layers will not only impact *supra-* and *sub-niveal* fauna but also permafrost dynamics and soil biogeochemical cycles. When combined with observations of wildlife, like movement data recently collated in the Arctic Animal Movement Archive (AAMA; Davidson et al., 2020), we believe the maps have power to reveal the causes of range-shifts, demographic variation, and trophic cascades, such is the importance of snow density and icing to some Arctic species.

5.1.4 Chapter 4 summary, key findings, and anticipated impacts

Chapter 4 details the development of an open-source, low-cost wireless sensor network for snow-based research and its strong performance in relation to traditional sensors. Of all the chapters it perhaps the greatest range of application outside snow-wildlife studies. For instance, within the realms of scientific research it could be ably employed to inform avalanche hazard forecasting (e.g. Brun et al., 1992) and water resource modelling (Liston and Elder, 2006), but it also has value outside of the academy should it be used to provide easily accessible, near real-time climate data to help recreators and land-managers make informed decisions about back-country access. We are particularly pleased by its low-cost and weight, and anticipate that both of these criteria will accelerate its adoption by remote communities in high-latitude and high-altitude regions.

5.2 Future work using data-model fusion

During and after any major project, hindsight gives us the ability, and tendency in my case, to go over all the things that we would have done differently if we had the chance to start again. While mistakes and dead ends of enquiry are always part of the fun and learning, one naively hopes that setting out again with hard-earned wisdom prevents their reoccurrence. So, what would I do differently if I embarked upon this dissertation today?

Due to my love for being out in Arctic-boreal landscapes, I would first wholeheartedly grasp any opportunity to return to magnificent Wrangell St-Elias National Park where the fieldwork for chapter 2 took place on six occasions in the first 2 years of my PhD. I'd do anything I could to stay longer up there too! But more seriously speaking, given the same opportunity I would seek to develop and more effectively combine the approaches I describe in preceding chapters to better answer the essential motivation of the work outlined in chapter 1 – to improve the mapping of wildlife-relevant snow properties and to characterise how they are being impacted by a warming climate. This 'data-model fusion', as prospected by Boelman et al. (2018) for snow-ecology studies, but used widely in other snow-related fields, combines ground-observations, remote-sensing, and snow modelling to overcome the limitations of each. To hopefully guide my own and other's future endeavours, I therefore briefly propose the following application and extension of this dissertation's work in the same field site.

The open-source weather stations in chapter 4 are incomplete in respect to the range of sensors, relevant to the measurement of snow properties, available to them. Without much effort, up and down facing pyranometers, such as the Apogee SP 212[24], and a soil-moisture probe, such as the METER group's TEROS 10[25] could be integrated into them. The pyranometers would offer insight into the albedo of snow and soil surface near each station, a parameter that is infrequently or poorly parameterized in snow-evolution models, and also indicate when snow cover occurs and disappears in conjunction to the existing acoustic depth sensor, which would struggle to capture the precise timing of phenomena otherwise. The soil-moisture probe, in periods without snow cover, would indicate rainfall events, which could then lead assessment of the accuracy of the precipitation fields in reanalysis products, such as we used to force the snow model employed in chapter 2. In periods with snow cover, it could potentially both detect the severity of rain-on-snow and melt events as well as the onset of spring melt – further providing data to better constrain a snow model, but also enabling near real-time reporting of potentially hazardous conditions for wildlife.

Given that the weather stations can be used in a spatially extensive wireless sensor network (WSN) they could be deployed in much the same pattern as the remote cameras described in chapter 2, or even alongside the cameras. Such an addition would aid the simulation of accurate meteorological-forcing data in a snow model as *in situ* measurements across elevation, vegetation, and topographic gradients of important variables, e.g. air temperature and relative humidity, are of greater accuracy than downscaled reanalysis data. As the stations do not yet include anemometers to measure wind-speed and direction, sensors that are anyway subject to riming events in the deep-cold of high-altitude Alaska, wind-fields from gridded climate data would still need to be used. However, in contrast to retrospectively retrieving model-constraining snow depth data from the cameras nearly a year later, the WSN's near real-time data transmission capabilities advance the pace of model calibration by providing data immediately after deployment. Instead, the bottleneck in terms of progress would come from the availability of the reanalysis forcing data – in the case of MERRA-2, the reanalysis which we use in chapter 2, aggregated monthly data is released between the 15th and 20th of each month[26], so there would be a maximum post-deployment period of ~6 weeks before a

---

[24] https://www.apogeeinstruments.com/sp-212-ss-amplified-0-2-5-volt-pyranometer/
[25] https://www.metergroup.com/environment/products/teros-10/
[26] https://gmao.gsfc.nasa.gov/reanalysis/MERRA-2/FAQ/

model calibration effort can be started, and further calibrations can be run on a monthly basis thereafter.

The availability of *in situ* data from the WSN wouldn't mean that snow surveys are redundant. Rather, they could be better planned to focus on areas in the study domain already identified by early model calibrations as being subject to greater uncertainty. The efficiencies of this pre-planning could also be leveraged to instead dedicate more time to appropriately sample, via snowpit excavation, stratigraphic properties of the snow in pre-identified pixels of the PM product described in chapter 3. These pixels could span gradients of elevation, vegetation and topographic complexity, the snowpits within them hence can provide more representative data and at a greater vertical detail than that used in chapter 3. The latest developments in spatially distributed snow models, such as that shown by Weiss, Nolin and Liston (*in progress*), include the accurate simulation of the stratigraphy of snow properties important to the remote-sensing of PM, such as grain size, correlation length, and surface specific area (Foster et al., 1984). If time and funding allowed, these properties could be additionally measured in each snow pit using a variety of techniques, such as near-infrared photography or high-resolution penetrometers (Matzl and Schneebeli, 2006; Schneebeli et al., 1999).

The detailed pit data can then be used to further calibrate the spatially distributed snow model so that it produces accurate simulations of snow stratigraphy across the study domain's varying topography and vegetation. In turn, this model-derived snow stratigraphy data can be ingested into a snow microwave radiative transfer model, such as the Snow Microwave Radiative Transfer model (SMRT; Picard et al., 2018), which can then simulate the expected PM signal from each pixel at different frequencies and polarizations. This simulated PM data can then be used to identify more precise polarization ratio thresholds that correspond to the presence of high-density and ice layers in pixels of differing vegetation and topographic complexity. Hence, via use of the PM data product described in chapter 3, a confident longitudinal study of the occurrence of layers of high-density snow and ice can be made for the study domain, but also other similar Arctic-boreal regions. In the latter case without needing to undertake the ground-observation and modelling steps.

The sketch of the study above lacks detail but is eminently achievable. It need not be conducted in the WRST, but given the inaccuracies of PM remote-sensing of snow water equivalent in mountain regions, and these region's importance as water-towers for much of the world's population, selecting a field site that does have gradients of elevation, topographic complexity, and vegetation would broaden its impact. Its design, I believe, leverages the advantages and reduces the disadvantages of each of three types of observation; *in situ* measurements are highly accurate but limited in time and space; snow models provide a wealth of detail but without accurate forcing and calibration data are subject to uncertainty, and their use over wide spatial extents at high-resolution is limited by computational demands; PM remote-sensing observations have a long-term record at a hemispherical scale, but haven't yet been adequately exploited to provide accurate maps of wildlife-relevant snow properties.

5.3 References

Boelman, N., Liston, G.E., Gurarie, E., Meddens, A.J.H., Mahoney, P.J., Kirchner, P.B., Bohrer, G., Brinkman, T.J., Cosgrove, C.L., Eitel, J., Hebblewhite, M., Kimball, J.S., LaPoint, S.D., Nolin, A.W., Pedersen, S.H., Prugh, L.R., Reinking, A.K., Vierling, L., 2018. Integrating snow science and wildlife ecology in Arctic-boreal North America. Environ. Res. Lett. https://doi.org/10.1088/1748-9326/aaeec1

Brun, E., David, P., Sudul, M., Brunot, G., 1992. A numerical model to simulate snow-cover stratigraphy for operational avalanche forecasting. Journal of Glaciology 38, 13–22. https://doi.org/10.3189/S0022143000009552

Davidson, S., Bohrer, G., Gurarie, E., LaPoint, S., Mahoney, P., Boelman, N., Eitel, J., Prugh, L., Vierling, L., Jennewein, J., Grier, E., Couriot, O., Kelly, A., Meddens, A., Oliver, R., Kays, R., Wikelski, M., Aarvak, T., Ackerman, J., 2020. Ecological insights from three decades of animal movement tracking across a changing Arctic. Science 370, 712–715. https://doi.org/10.1126/science.abb7080

Foster, J.L., Hall, D.K., Chang, A.T.C., Rango, A., 1984. An overview of passive microwave snow research and results. https://doi.org/10.1029/RG022i002p00195

Kerk, M. van de, Verbyla, D., Nolin, A.W., Sivy, K.J., Prugh, L.R., 2018. Range-wide variation in the effect of spring snow phenology on Dall sheep population dynamics. Environ. Res. Lett. 13, 075008. https://doi.org/10.1088/1748-9326/aace64

Liston, G.E., Elder, K., 2006. A Distributed Snow-Evolution Modeling System (SnowModel). J. Hydrometeor. 7, 1259–1276. https://doi.org/10.1175/JHM548.1

Mallory, C.D., Boyce, M.S., 2017. Observed and predicted effects of climate change on Arctic caribou and reindeer. Environ. Rev. 26, 13–25. https://doi.org/10.1139/er-2017-0032

Matzl, M., Schneebeli, M., 2006. Measuring specific surface area of snow by near-infrared photography. Journal of Glaciology 52, 558–564. https://doi.org/10.3189/172756506781828412

Picard, G., Sandells, M., Löwe, H., 2018. SMRT: an active–passive microwave radiative transfer model for snow with multiple microstructure and scattering formulations (v1.0). Geoscientific Model Development 11, 2763–2788. https://doi.org/10.5194/gmd-11-2763-2018

Rattenbury, K.L., Schmidt, J.H., Swanson, D.K., Borg, B.L., Mangipane, B.A., Sousanes, P.J., 2018. Delayed spring onset drives declines in abundance and recruitment in a mountain ungulate. Ecosphere 9, e02513. https://doi.org/10.1002/ecs2.2513

Schneebeli, M., Pielmeier, C., Johnson, J.B., 1999. Measuring snow microstructure and hardness using a high resolution penetrometer. Cold Regions Science and Technology 30, 101–114. https://doi.org/10.1016/S0165-232X(99)00030-0

Sokolov, A.A., Sokolova, N.A., Ims, R.A., Brucker, L., Ehrich, D., 2016. Emergent Rainy Winter Warm Spells May Promote Boreal Predator Expansion into the Arctic. Arctic 69, 121–129.

Zimova, M., Mills, L.S., Lukacs, P.M., Mitchell, M.S., 2014. Snowshoe hares display limited phenotypic plasticity to mismatch in seasonal camouflage. Proceedings of the Royal Society B: Biological Sciences 281, 20140029. https://doi.org/10.1098/rspb.2014.0029

Chapter 6 Bibliography for all chapters

3D-PAWS, 2020. 3D-Printed Automatic Weather Station [WWW Document]. URL https://sites.google.com/ucar.edu/3dpaws/ (accessed 3.17.20).

Alaska Department of Fish and Game, 2014. Trends in Alaska Sheep Populations, Hunting, and Harvests. Division of Wildlife Conservation, Wildlife Management Report ADF&G/DWC/WMR-2014-3, Juneau.

AMAP, 2017. Snow, Water, Ice and Permafrost in the Arctic (SWIPA) 2017 | AMAP. Arctic Monitoring and Assessment Programme (AMAP), Oslo, Norway.

Arduino, 2020. Arduino - Home [WWW Document]. URL https://www.arduino.cc/ (accessed 3.16.20).

Arthur, S.M., Prugh, L.R., 2010. Predator-Mediated Indirect Effects of Snowshoe Hares on Dall's Sheep in Alaska. Journal of Wildlife Management 74, 1709–1721. https://doi.org/10.2193/2009-322

Barnett, T.P., Adam, J.C., Lettenmaier, D.P., 2005. Potential impacts of a warming climate on water availability in snow-dominated regions. Nature 438, 303–309. https://doi.org/10.1038/nature04141

Bartelt, P., Lehning, M., 2002. A physical SNOWPACK model for the Swiss avalanche warning Part I: numerical model. Cold Regions Science and Technology 23.

Berteaux, D., Gauthier, G., Domine, F., Ims, R.A., Lamoureux, S.F., Lévesque, E., Yoccoz, N., 2016. Effects of changing permafrost and snow conditions on tundra wildlife: critical places and times. Arctic Science 3, 65–90. https://doi.org/10.1139/as-2016-0023

Bieniek, P.A., Bhatt, U.S., Thoman, R.L., Angeloff, H., Partain, J., Papineau, J., Fritsch, F., Holloway, E., Walsh, J.E., Daly, C., Shulski, M., Hufford, G., Hill, D.F., Calos, S., Gens, R., 2012. Climate Divisions for Alaska Based on Objective Methods. J. Appl. Meteor. Climatol. 51, 1276–1289. https://doi.org/10.1175/JAMC-D-11-0168.1

Bilodeau, F., Gauthier, G., Berteaux, D., 2013. The effect of snow cover on lemming population cycles in the Canadian High Arctic. Oecologia 172, 1007–1016.

Blaen, P.J., Khamis, K., Lloyd, C.E.M., Bradley, C., Hannah, D., Krause, S., 2016. Real-time monitoring of nutrients and dissolved organic matter in rivers: Capturing event dynamics, technological opportunities and future directions. Science of The Total Environment 569–570, 647–660. https://doi.org/10.1016/j.scitotenv.2016.06.116

Boelman, N., Liston, G.E., Gurarie, E., Meddens, A.J.H., Mahoney, P.J., Kirchner, P.B., Bohrer, G., Brinkman, T.J., Cosgrove, C.L., Eitel, J., Hebblewhite, M., Kimball, J.S., LaPoint, S.D., Nolin, A.W., Pedersen, S.H., Prugh, L.R., Reinking, A.K., Vierling, L., 2018. Integrating snow science and wildlife ecology in Arctic-boreal North America. Environ. Res. Lett. https://doi.org/10.1088/1748-9326/aaeec1

Boelman, N.T., Liston, G.E., Gurarie, E., Meddens, A.J.H., Mahoney, P.J., Kirchner, P.B., Bohrer, G., Brinkman, T.J., Cosgrove, C.L., Eitel, J.U.H., Hebblewhite, M., Kimball, J.S., LaPoint, S., Nolin, A.W., Pedersen, S.H., Prugh, L.R., Reinking, A.K., Vierling, L.A., 2019. Integrating snow science and wildlife ecology in Arctic-boreal North America. Environ. Res. Lett. 14, 010401. https://doi.org/10.1088/1748-9326/aaeec1

Boertje, R.D., Frye, G.G., Young, D.D., 2019. Lifetime, known-age moose reproduction in a nutritionally stressed population. The Journal of Wildlife Management 83, 610–626. https://doi.org/10.1002/jwmg.21613

Bokhorst, S., Pedersen, S.H., Brucker, L., Anisimov, O., Bjerke, J.W., Brown, R.D., Ehrich, D., Essery, R.L.H., Heilig, A., Ingvander, S., Johansson, C., Johansson, M., Jónsdóttir, I.S., Inga, N., Luojus, K., Macelloni, G., Mariash, H., McLennan, D., Rosqvist, G.N., Sato, A., Savela, H., Schneebeli, M., Sokolov, A., Sokratov, S.A., Terzago, S., Vikhamar-Schuler, D., Williamson, S., Qiu, Y., Callaghan, T.V., 2016. Changing Arctic snow cover: A review of recent developments and assessment of future needs for observations, modelling, and impacts. Ambio 45, 516–537. https://doi.org/10.1007/s13280-016-0770-0

Bormann, K.J., Brown, R.D., Derksen, C., Painter, T.H., 2018. Estimating snow-cover trends from space. Nature Clim Change 8, 924–928. https://doi.org/10.1038/s41558-018-0318-3

Bosilovich, M.G., Robertson, F.R., Takacs, L., Molod, A., Mocko, D., 2016. Atmospheric Water Balance and Variability in the MERRA-2 Reanalysis. J. Climate 30, 1177–1196. https://doi.org/10.1175/JCLI-D-16-0338.1

Box, J.E., Colgan, W.T., Christensen, T.R., Schmidt, N.M., Lund, M., Parmentier, F.-J.W., Brown, R., Bhatt, U.S., Euskirchen, E.S., Romanovsky, V.E., Walsh, J.E., Overland, J.E., Wang, M., Corell, R.W., Meier, W.N., Wouters, B., Mernild, S., M\aard, J., Pawlak, J., Olsen, M.S., 2019. Key indicators of Arctic climate change: 1971–2017. Environ. Res. Lett. 14, 045010. https://doi.org/10.1088/1748-9326/aafc1b

Boyce, M.S., Haridas, C.V., Lee, C.T., the NCEAS Stochastic Demography Working Group, 2006. Demography in an increasingly variable world. Trends in Ecology & Evolution 21, 141–148. https://doi.org/10.1016/j.tree.2005.11.018

Brodzik, M.J., Long, D.G., 2016. MEaSUREs Calibrated Enhanced-Resolution Passive Microwave Daily EASE-Grid 2.0 Brightness Temperature ESDR, Version 1. https://doi.org/10.5067/MEASURES/CRYOSPHERE/NSIDC-0630.001

Brodzik, M.J., Long, D., G., 2018. Calibrated Passive Microwave Daily EASE-Grid 2.0 Brightness Temperature ESDR (CETB) Alogorithm Theoretical Basis Document 103.

Brodzik, M.J., Long, D.G., Hardman, M.A., 2018. Best Practices in Crafting the Calibrated, Enhanced-Resolution Passive-Microwave EASE-Grid 2.0 Brightness Temperature Earth System Data Record. Remote Sensing 10, 1793. https://doi.org/10.3390/rs10111793

Brown, R., Vikhamar Schuler, D., Bulygina, O.N., Derksen, C., Luojus, K., Mudryk, L.R., Wang, L., Yang, D., 2017. Arctic Terrestrial Snow Cover, in: Snow, Water, Ice and Permafrost in the Arctic (SWIPA) 2017. Arctic Monitoring and Assessment Programme (AMAP), Oslo, Norway. (www.amap.no).

Brown, R.D., Mote, P.W., 2009. The Response of Northern Hemisphere Snow Cover to a Changing Climate. J. Climate 22, 2124–2145. https://doi.org/10.1175/2008JCLI2665.1

Brun, E., David, P., Sudul, M., Brunot, G., 1992. A numerical model to simulate snow-cover stratigraphy for operational avalanche forecasting. Journal of Glaciology 38, 13–22. https://doi.org/10.3189/S0022143000009552

Bunnell, F.L., 1982. The lambing period of mountain sheep: synthesis, hypotheses, and tests. Can. J. Zool. 60, 1–14. https://doi.org/10.1139/z82-001

Burles, D.W., Hoefs, M., 1984. Winter mortality of Dall sheep, Ovis dalli dalli , in Kluane National Park, Yukon. Canadian field-naturalist 98(4), 479–484.

Callaghan, T.V., Johansson, M., Brown, R.D., Groisman, P.Y., Labba, N., Radionov, V., Barry, R.G., Bulygina, O.N., Essery, R.L.H., Frolov, D.M., Golubev, V.N., Grenfell, T.C., Petrushina, M.N., Razuvaev, V.N., Robinson, D.A., Romanov, P., Shindell, D., Shmakin, A.B., Sokratov, S.A., Warren, S., Yang, D., 2011a. The changing face of arctic snow cover: A synthesis of observed and projected changes. Ambio 40, 17–31. https://doi.org/10.1007/s13280-011-0212-y

Callaghan, T.V., Johansson, M., Brown, R.D., Groisman, P.Ya., Labba, N., Radionov, V., Bradley, R.S., Blangy, S., Bulygina, O.N., Christensen, T.R., Colman, J.E., Essery, R.L.H.H., Forbes, B.C., Forchhammer, M.C., Golubev, V.N., Honrath, R.E., Juday, G.P., Meshcherskaya, A.V., Phoenix, G.K., Pomeroy, J., Rautio, A., Robinson, D.A., Schmidt, N.M., Serreze, M.C., Shevchenko, V.P., Shiklomanov, A.I., Shmakin, A.B., Sköld, P., Sturm, M., Woo, M.K., Wood, E.F., Skoĺd, P., Sturm, M., Woo, M.K., Wood, E.F., 2011b. Multiple Effects of Changes in Arctic Snow Cover. AMBIO 40, 32–45. https://doi.org/10.1007/s13280-011-0213-x

Castell, N., Dauge, F.R., Schneider, P., Vogt, M., Lerner, U., Fishbain, B., Broday, D., Bartonova, A., 2017. Can commercial low-cost sensor platforms contribute to air quality monitoring and exposure estimates? Environment International 99, 293–302. https://doi.org/10.1016/j.envint.2016.12.007

Chapin, F.S., Sturm, M., Serreze, M.C., McFadden, J.P., Key, J.R., Lloyd, A.H., McGuire, A.D., Rupp, T.S., Lynch, A.H., Schimel, J.P., Beringer, J., Chapman, W.L., Epstein, H.E., Euskirchen, E.S., Hinzman, L.D., Jia, G., Ping, C.-L., Tape, K.D., Thompson, C.D.C., Walker, D.A., Welker, J.M., 2005. Role of Land-Surface Changes in Arctic Summer Warming. Science 310, 657–660. https://doi.org/10.1126/science.1117368

Chen, W., Russell, D.E., Gunn, A., Croft, B., Chen, W.R., Fernandes, R., Zhao, H., Li, J., Zhang, Y., Koehler, K., Olthof, I., Fraser, R.H., Leblanc, S.G., Henry, G.R., White, R.G., Finstad, G.L., 2013. Monitoring habitat condition changes during winter and pre-calving migration for Bathurst Caribou in northern Canada. Biodiversity 14, 36–44. https://doi.org/10.1080/14888386.2012.705110

Cherry, J.E., Zhu, J., Kirchner, P.B., 2017. Snow Cover Monitoring with MODIS Satellite Data in Alaska's National Parks, 2000-2015. National Park Service, Fort Collins, Colorado, Natural Resource Report NPS/SWAN/NRR—2017/1566 96.

Clark, M.P., Hendrikx, J., Slater, A.G., Kavetski, D., Anderson, B., Cullen, N.J., Kerr, T., Örn Hreinsson, E., Woods, R.A., 2011. Representing spatial variability of snow water equivalent in hydrologic and land-surface models: A review. Water Resources Research 47. https://doi.org/10.1029/2011WR010745

Colbeck, S.C., 1982. An overview of seasonal snow metamorphism. https://doi.org/10.1029/RG020i001p00045

Collins, W.B., Smith, T.S., 1991. Effects of Wind-Hardened Snow on Foraging by Reindeer (Rangifer tarandus). Arctic 44, 217–222.

Cooper, E.J., 2014. Warmer Shorter Winters Disrupt Arctic Terrestrial Ecosystems. Annual Review of Ecology, Evolution, and Systematics 45, 271–295. https://doi.org/10.1146/annurev-ecolsys-120213-091620

Coulson, T., Milner–Gulland, E.J., Clutton–Brock, T., 2000. The relative roles of density and climatic variation on population dynamics and fecundity rates in three contrasting ungulate species. Proceedings of the Royal Society of London. Series B: Biological Sciences 267, 1771–1779. https://doi.org/10.1098/rspb.2000.1209

Coumou, D., Rahmstorf, S., 2012. A decade of weather extremes. Nature Climate Change 2, 491–496. https://doi.org/10.1038/nclimate1452

Couturier, S., Côté, S.D., Otto, R.D., Weladji, R.B., Huot, J., 2009. Variation in Calf Body Mass in Migratory Caribou: The Role of Habitat, Climate, and Movements. J Mammal 90, 442–452. https://doi.org/10.1644/07-MAMM-A-279.1

Danby, R.K., Slocombe, D.S., 2005. Regional Ecology, Ecosystem Geography, and Transboundary Protected Areas in the St. Elias Mountains. Ecological Applications 15, 405–422. https://doi.org/10.1890/04-0043

Danks, F.S., Klein, D.R., 2002. Using GIS to predict potential wildlife habitat: A case study of muskoxen in northern Alaska. International Journal of Remote Sensing 23, 4611–4632. https://doi.org/10.1080/01431160110113890

Davidson, S., Bohrer, G., Gurarie, E., LaPoint, S., Mahoney, P., Boelman, N., Eitel, J., Prugh, L., Vierling, L., Jennewein, J., Grier, E., Couriot, O., Kelly, A., Meddens, A., Oliver, R., Kays, R., Wikelski, M., Aarvak, T., Ackerman, J., 2020. Ecological insights from three decades of animal movement tracking across a changing Arctic. Science 370, 712–715. https://doi.org/10.1126/science.abb7080

Derksen, C., LeDrew, E., Walker, A., Goodison, B., 2000. Influence of Sensor Overpass Time on Passive Microwave-Derived Snow Cover Parameters. Remote Sensing of Environment 71, 297–308. https://doi.org/10.1016/S0034-4257(99)00084-X

Derksen, C., Walker, A., Goodison, B., 2003. A comparison of 18 winter seasons of in situ and passive microwave-derived snow water equivalent estimates in Western Canada. Remote Sensing of Environment 88, 271–282. https://doi.org/10.1016/j.rse.2003.07.003

Descamps, S., Aars, J., Fuglei, E., Kovacs, K.M., Lydersen, C., Pavlova, O., Pedersen, \AAshild, Ravolainen, V., Strøm, H., 2017. Climate change impacts on wildlife in a High Arctic archipelago – Svalbard, Norway. Global Change Biology 23, 490–502. https://doi.org/10.1111/gcb.13381

Dirnböck, T., Essl, F., Rabitsch, W., 2011. Disproportional risk for habitat loss of high-altitude endemic species under climate change. Global Change Biology 17, 990–996. https://doi.org/10.1111/j.1365-2486.2010.02266.x

Dolant, C., Langlois, A., Brucker, L., Royer, A., Roy, A., Montpetit, B., 2017. Meteorological inventory of rain-on-snow events and detection assessment in the Canadian arctic archipelago using passive microwave radiometry, in: 2017 IEEE International Geoscience and Remote Sensing Symposium (IGARSS). Presented at the 2017 IEEE International Geoscience and Remote Sensing Symposium (IGARSS), pp. 315–318. https://doi.org/10.1109/IGARSS.2017.8126959

Dolant, C., Montpetit, B., Langlois, A., Brucker, L., Zolina, O., Johnson, C.A., Royer, A., Smith, P., 2018. Assessment of the Barren Ground Caribou Die-off During Winter 2015–2016 Using Passive Microwave Observations. Geophysical Research Letters 45, 4908–4916. https://doi.org/10.1029/2017GL076752

Domine, F., Gauthier, G., Vionnet, V., Fauteux, D., Dumont, M., Barrere, M., 2018. Snow physical properties may be a significant determinant of lemming population dynamics in the high Arctic. Arctic Science 4, 813–826. https://doi.org/10.1139/as-2018-0008

Douhard, M., Loe, L.E., Stien, A., Bonenfant, C., Irvine, R.J., Veiberg, V., Ropstad, E., Albon, S., 2016. The influence of weather conditions during gestation on life histories in a wild Arctic ungulate. Proceedings of the Royal Society B: Biological Sciences 283, 20161760. https://doi.org/10.1098/rspb.2016.1760

Droghini, A., Boutin, S., 2017. Snow conditions influence grey wolf (Canis lupus) travel paths: the effect of human-created linear features. Can. J. Zool. 96, 39–47. https://doi.org/10.1139/cjz-2017-0041

Duquette, L.S., 1988. Snow Characteristics along Caribou Trails and within Feeding Areas during Spring Migration. ARCTIC 41, 143–144. https://doi.org/10.14430/arctic1706

Earth Resources Observation And Science (EROS) Center, 2017. Global 30 Arc-Second Elevation (GTOPO30). https://doi.org/10.5066/F7DF6PQS

Eira, I.M.G., Oskal, A., Hanssen-Bauer, I., Mathiesen, S.D., 2018. Snow cover and the loss of traditional indigenous knowledge. Nature Clim Change 8, 928–931. https://doi.org/10.1038/s41558-018-0319-2

Fancy, S.G., White, R.G., 2011. Energy expenditures for locomotion by barren-ground caribou. Canadian Journal of Zoology. https://doi.org/10.1139/z87-018

Fancy, S.G., White, R.G., 1985. Energy Expenditures by Caribou while Cratering in Snow. The Journal of Wildlife Management 49, 987–993. https://doi.org/10.2307/3801384

Fierz, C., Armstrong, R.L., Durand, Y., Etchevers, P., Greene, E., McClung, D.M., Nishimura, K., Satyawali, P.K., Sokratov, S. a., 2009. The international classification for seasonal snow on the ground. IHP-VII Technical Documents in Hydrology 83, 90. http://www.cosis.net/abstracts/EGU05/09775/EGU05-J-09775.pdf

Formozov, A.N., 1946. Snow cover as an integral factor of the environment and its importance in the ecology of mammals and birds. Fauna and Flora of the USSR. New Ser. Zool. 5, 1–152.

Foster, J.L., Hall, D.K., Chang, A.T.C., Rango, A., 1984. An overview of passive microwave snow research and results. https://doi.org/10.1029/RG022i002p00195

Fuller, T.K., 1991. Effect of snow depth on wolf activity and prey selection in north central Minnesota. Can. J. Zool. 69, 283–287. https://doi.org/10.1139/z91-044

Gaillard, J.-M., Festa-Bianchet, M., Yoccoz, N.G., 1998. Population dynamics of large herbivores: variable recruitment with constant adult survival. Trends in Ecology & Evolution 13, 58–63. https://doi.org/10.1016/S0169-5347(97)01237-8

Geist, V., 1971. Mountain sheep; a study in behavior and evolution., Wildlife behavior and ecology. University of Chicago Press, Chicago.

Gelaro, R., McCarty, W., Suárez, M.J., Todling, R., Molod, A., Takacs, L., Randles, C.A., Darmenov, A., Bosilovich, M.G., Reichle, R., Wargan, K., Coy, L., Cullather, R., Draper, C., Akella, S., Buchard, V., Conaty, A., da Silva, A.M., Gu, W., Kim, G.-K., Koster, R., Lucchesi, R., Merkova, D., Nielsen, J.E., Partyka, G., Pawson, S., Putman, W., Rienecker, M., Schubert, S.D., Sienkiewicz, M., Zhao, B., Gelaro, R., McCarty, W., Suárez, M.J., Todling, R., Molod, A., Takacs, L., Randles, C.A., Darmenov, A., Bosilovich, M.G., Reichle, R., Wargan, K., Coy, L., Cullather, R., Draper, C., Akella, S., Buchard, V., Conaty, A., da Silva, A.M., Gu, W., Kim, G.-K., Koster, R., Lucchesi, R., Merkova, D., Nielsen, J.E., Partyka, G., Pawson, S., Putman, W., Rienecker, M., Schubert, S.D., Sienkiewicz, M., Zhao, B., 2017. The Modern-Era Retrospective Analysis for Research and Applications, Version 2 (MERRA-2). Journal of Climate 30, 5419–5454. https://doi.org/10.1175/JCLI-D-16-0758.1

Gilbert, S.L., Hundertmark, K.J., Person, D.K., Lindberg, M.S., Boyce, M.S., 2017. Behavioral plasticity in a variable environment: snow depth and habitat interactions drive deer movement in winter. J Mammal 98, 246–259. https://doi.org/10.1093/jmammal/gyw167

Gleason, K.E., Nolin, A.W., Roth, T.R., 2017. Developing a representative snow-monitoring network in a forested mountain watershed. Hydrology and Earth System Sciences 21, 1137–1147. https://doi.org/10.5194/hess-21-1137-2017

Goetz, S., Kimball, J., Mack, M., Kasischke, E., 2011. Scoping Completed for an Experiment to Assess Vulnerability of Arctic and Boreal Ecosystems. Eos, Transactions American Geophysical Union 92, 150–151. https://doi.org/10.1029/2011EO180002

Grenfell T. C., Putkonen J., 2008. A method for the detection of the severe rain-on-snow event on Banks Island, October 2003, using passive microwave remote sensing. Water Resources Research 44. https://doi.org/10.1029/2007WR005929

Groisman, P.Y., Karl, T.R., Knight, R.W., Stenchikov, G.L., 1994. Changes of Snow Cover, Temperature, and Radiative Heat Balance over the Northern Hemisphere. J. Climate 7, 1633–1656. https://doi.org/10.1175/1520-0442(1994)007<1633:COSCTA>2.0.CO;2

Hall, D.K., Chang, A.T.C., Foster, J.L., 1986. Detection of the Depth-Hoar Layer in the Snow-Pack of the Arctic Coastal Plain of Alaska, U.S.A., Using Satellite Data. Journal of Glaciology 32, 87–94. https://doi.org/10.3189/S0022143000006912

Hall, D.K., Riggs, G.A., Salomonson, V.V., DiGirolamo, N.E., Bayr, K.J., 2002. MODIS snow-cover products. Remote Sensing of Environment 83, 181–194.

Hansen, B.B., Aanes, R., Herfindal, I., Kohler, J., S\a ether, B.-E.E., Oli, M.K., 2011. Climate, icing, and wild arctic reindeer: Past relationships and future prospects. Ecology 92, 1917–1923. https://doi.org/10.1890/11-0095.1

Hansen, B.B., Aanes, R., Sæther, B.-E., 2010. Feeding-crater selection by high-arctic reindeer facing ice-blocked pastures. Can. J. Zool. 88, 170–177. https://doi.org/10.1139/Z09-130

Hansen, B.B., Grotan, V., Aanes, R., Saether, B.-E., Stien, A., Fuglei, E., Ims, R.A., Yoccoz, N.G., Pedersen, A.O., 2013. Climate Events Synchronize the Dynamics of a Resident Vertebrate Community in the High Arctic. Science 339, 313–315. https://doi.org/10.1126/science.1226766

Hill, D.F., Burakowski, E.A., Crumley, R.L., Keon, J., Hu, J.M., Arendt, A.A., Wikstrom Jones, K., Wolken, G.J., 2019. Converting snow depth to snow water equivalent using climatological variables. The Cryosphere 13, 1767–1784. https://doi.org/10.5194/tc-13-1767-2019

Hinzman, L.D., Bettez, N.D., Bolton, W.R., Chapin, F.S., Dyurgerov, M.B., Fastie, C.L., Griffith, B., Hollister, R.D., Hope, A., Huntington, H.P., Jensen, A.M., Jia, G.J., Jorgenson, T., Kane, D.L., Klein, D.R., Kofinas, G., Lynch, A.H., Lloyd, A.H., McGuire, A.D., Nelson, F.E., Oechel, W.C., Osterkamp, T.E., Racine, C.H., Romanovsky, V.E., Stone, R.S., Stow, D.A., Sturm, M., Tweedie, C.E., Vourlitis, G.L., Walker, M.D., Walker, D.A., Webber, P.J., Welker, J.M., Winker, K.S., Yoshikawa, K., 2005. Evidence and Implications of Recent Climate Change in Northern Alaska and Other Arctic Regions. Climatic Change 72, 251–298. https://doi.org/10.1007/s10584-005-5352-2

Hoefs, M., 1984. Productivity and Carrying Capacity of a Subarctic Sheep Winter Range. ARCTIC 37. https://doi.org/10.14430/arctic2179

Hoefs, M., 1976. Ecological investigation of Dall sheep (Ovis dalli dalli, Nelson) and their habitat on Sheep Mountain, Kluane National Park, Yukon Territory, Canada (Text). The University of Bristish Columbia.

Holland, J.D., Bert, D.G., Fahrig, L., 2004. Determining the Spatial Scale of Species' Response to Habitat. BioScience 54, 227–233. https://doi.org/10.1641/0006-3568(2004)054[0227:dtssos]2.0.co;2

Homer, C., Dewitz, J., Yang, L., Jin, S., Danielson, P., 2015. Completion of the 2011 National Land Cover Database for the Conterminous United States – Representing a Decade of Land Cover Change Information. PHOTOGRAMMETRIC ENGINEERING 11.

Hoyer, S., Hamman, J.J., 2017. xarray: N-D labeled Arrays and Datasets in Python. Journal of Open Research Software 5, 10. https://doi.org/10.5334/jors.148

International Organization for Standardization, 2020. C++ [WWW Document]. URL https://isocpp.org/std/the-standard (accessed 3.18.20).

Jacobson, A.R., Provenzale, A., Hardenberg, A. von, Bassano, B., Festa-Bianchet, M., 2004. Climate Forcing and Density Dependence in a Mountain Ungulate Population. Ecology 85, 1598–1610. https://doi.org/10.1890/02-0753

Jensen, P.G., Pekins, P.J., Holter, J.B., 1999. Compensatory effect of the heat increment of feeding on thermoregulation costs of white-tailed deer fawns in winter. Can. J. Zool. 77, 1474–1485. https://doi.org/10.1139/z99-111

Jeong, D.I., Sushama, L., 2018. Rain-on-snow events over North America based on two Canadian regional climate models. Climate Dynamics 50, 303–316.

Johansson, C., Pohjola, V.A., Jonasson, C., Callaghan, T.V., 2011a. Multi-decadal changes in snow characteristics in sub-Arctic Sweden. Ambio 40, 566–574. https://doi.org/10.1007/s13280-011-0164-2

Johansson, C., Pohjola, V.A., Jonasson, C., Callaghan, T.V., 2011b. Multi-Decadal Changes in Snow Characteristics in Sub-Arctic Sweden. AMBIO 40, 566. https://doi.org/10.1007/s13280-011-0164-2

Johnson, C.J., Parker, K.L., Heard, D.C., Gillingham, M.P., 2002. Movement parameters of ungulates and scale-specific responses to the environment. Journal of Animal Ecology 71, 225–235. https://doi.org/10.1046/j.1365-2656.2002.00595.x

Kawaguchi, T., Desrochers, A., 2017. Short-term changes in spatial distribution pattern of an herbivore in response to accumulating snow. Can. J. Zool. 95, 949–954. https://doi.org/10.1139/cjz-2016-0287

Kelsall, J.P., 1969. Structural Adaptations of Moose and Deer for Snow. Journal of Mammalogy 50, 302–310. https://doi.org/10.2307/1378347

Keppel, G., Niel, K.P.V., Wardell-Johnson, G.W., Yates, C.J., Byrne, M., Mucina, L., Schut, A.G.T., Hopper, S.D., Franklin, S.E., 2012. Refugia: identifying and understanding safe havens for biodiversity under climate change. Global Ecology and Biogeography 21, 393–404. https://doi.org/10.1111/j.1466-8238.2011.00686.x

Kerk, M.V. de, Arthur, S., Bertram, M., Borg, B., Herriges, J., Lawler, J., Mangipane, B., Koizumi, C.L., Wendling, B., Prugh, L., 2020. Environmental Influences on Dall's Sheep Survival. The Journal of Wildlife Management. https://doi.org/10.1002/jwmg.21873

Kerk, M.V. de, Arthur, S., Bertram, M., Borg, B., Herriges, J., Lawler, J., Mangipane, B., Koizumi, C.L., Wendling, B., Prugh, L., n.d. Environmental Influences on Dall's Sheep Survival. The Journal of Wildlife Management n/a. https://doi.org/10.1002/jwmg.21873

Kerk, M. van de, Verbyla, D., Nolin, A.W., Sivy, K.J., Prugh, L.R., 2018. Range-wide variation in the effect of spring snow phenology on Dall sheep population dynamics. Environ. Res. Lett. 13, 075008. https://doi.org/10.1088/1748-9326/aace64

Kerkez, B., Glaser, S.D., Bales, R.C., Meadows, M.W., 2012. Design and performance of a wireless sensor network for catchment-scale snow and soil moisture measurements. Water Resources Research 48, 1–18. https://doi.org/10.1029/2011WR011214

Kim, Y., Kimball, J.S., Du, J., Schaaf, C.L.B., Kirchner, P.B., 2018. Quantifying the effects of freeze-thaw transitions and snowpack melt on land surface albedo and energy exchange over Alaska and Western Canada. Environ. Res. Lett. 13, 075009. https://doi.org/10.1088/1748-9326/aacf72

Kinar, N.J., Pomeroy, J.W., 2015. Measurement of the physical properties of the snowpack. Reviews of Geophysics 53, 481–544. https://doi.org/10.1002/2015RG000481

Klein, J. A., Tucker, C.M., Nolin, A.W., Hopping, K.A., Reid, R.S., Steger, C., Grêt-Regamey, A., Lavorel, S., Müller, B., Yeh, E.T., Boone, R.B., Bourgeron, P., Butsic, V., Castellanos, E., Chen, X., Dong, S.K., Greenwood, G., Keiler, M., Marchant, R., Seidl, R., Spies, T., Thorn, J., Yager, K., 2019. Catalyzing Transformations to Sustainability in the World's Mountains. Earth's Future 7, 547–557. https://doi.org/10.1029/2018EF001024

Klein, Julia A., Tucker, C.M., Steger, C.E., Nolin, A., Reid, R., Hopping, K.A., Yeh, E.T., Pradhan, M.S., Taber, A., Molden, D., Ghate, R., Choudhury, D., Alcántara-Ayala, I., Lavorel, S., Müller, B., Grêt-Regamey, A., Boone, R.B., Bourgeron, P., Castellanos, E., Chen, X., Dong, S., Keiler, M., Seidl, R., Thorn, J., Yager, K., 2019. An integrated community and ecosystem-based approach to disaster risk reduction in mountain systems. Environmental Science & Policy 94, 143–152. https://doi.org/10.1016/j.envsci.2018.12.034

Lambert Koizumi, C., Carey, J., Branigan, M., Callaghan, K., 2011. Status of Dall's Sheep (Ovis dalli dalli) in the Northern Richardson Mountains. Yukon Fish and Wildlife Branch Report TRC-11-01. Yukon, Canada. 64.

Langlois, A., Johnson, C.-A.A., Montpetit, B., Royer, A., Blukacz-Richards, E.A.A., Neave, E., Dolant, C., Roy, A., Arhonditsis, G., Kim, D.-K.K., Kaluskar, S., Brucker, L., 2017. Detection of rain-on-snow (ROS) events and ice layer formation using passive microwave radiometry: A context for Peary caribou habitat in the Canadian Arctic. Remote Sensing of Environment 189, 84–95. https://doi.org/10.1016/j.rse.2016.11.006

LaPerriere, A.J., Lent, P.C., 1977. Caribou Feeding Sites in Relation to Snow Characteristics in Northeastern Alaska. ARCTIC 30, 101–108. https://doi.org/10.14430/arctic2690

Le Corre, M., Dussault, C., Côté, S.D., 2017. Weather conditions and variation in timing of spring and fall migrations of migratory caribou. J Mammal 98, 260–271. https://doi.org/10.1093/jmammal/gyw177

Li, X., Zhang, L., Weihermüller, L., Jiang, L., Vereecken, H., 2014. Measurement and Simulation of Topographic Effects on Passive Microwave Remote Sensing Over Mountain Areas: A Case Study From the Tibetan Plateau. IEEE Transactions on Geoscience and Remote Sensing 52, 1489–1501. https://doi.org/10.1109/TGRS.2013.2251887

Liston, G.E., 1995. Local Advection of Momentum, Heat, and Moisture during the Melt of Patchy Snow Covers. J. Appl. Meteor. 34, 1705–1715. https://doi.org/10.1175/1520-0450-34.7.1705

Liston, G.E., Elder, K., 2006. A Distributed Snow-Evolution Modeling System (SnowModel). J. Hydrometeor. 7, 1259–1276. https://doi.org/10.1175/JHM548.1

Liston, G.E., Elder, K., Liston, G.E., Elder, K., 2006. A Meteorological Distribution System for High-Resolution Terrestrial Modeling (MicroMet). Journal of Hydrometeorology 7, 217–234. https://doi.org/10.1175/JHM486.1

Liston, G.E., Haehnel, R.B., Sturm, M., Hiemstra, C.A., Berezovskaya, S., Tabler, R.D., 2007. Simulating complex snow distributions in windy environments using SnowTran-3D. Journal of Glaciology 53, 241–256. https://doi.org/10.3189/172756507782202865

Liston, G.E., Hall, D.K., 1995. An energy-balance model of lake-ice evolution. Journal of Glaciology 41, 373–382. https://doi.org/10.3189/S0022143000016245

Liston, G.E., Hiemstra, C.A., 2011. The Changing Cryosphere: Pan-Arctic Snow Trends (1979–2009). J. Climate 24, 5691–5712. https://doi.org/10.1175/JCLI-D-11-00081.1

Liston, G.E., Hiemstra, C.A., 2008. A Simple Data Assimilation System for Complex Snow Distributions (SnowAssim). J. Hydrometeor. 9, 989–1004. https://doi.org/10.1175/2008JHM871.1

Liston, G.E., Mcfadden, J.P., Sturm, M., Pielke, R.A., 2002. Modelled changes in arctic tundra snow, energy and moisture fluxes due to increased shrubs. Global Change Biology 8, 17–32. https://doi.org/10.1046/j.1354-1013.2001.00416.x

Liston, G.E., Perham, C.J., Shideler, R.T., Cheuvront, A.N., 2016. Modeling snowdrift habitat for polar bear dens. Ecological Modelling 320, 114–134. https://doi.org/10.1016/j.ecolmodel.2015.09.010

Lundmark, C., Ball, J.P., 2008. Living in Snowy Environments: Quantifying The Influence of Snow on Moose Behavior. Arctic, Antarctic, and Alpine Research 40, 111–118. https://doi.org/10.1657/1523-0430(06-103)[LUNDMARK]2.0.CO;2

Mahoney, P.J., Liston, G.E., LaPoint, S., Gurarie, E., Mangipane, B., Wells, A.G., Brinkman, T.J., Eitel, J.U.H., Hebblewhite, M., Nolin, A.W., Boelman, N., Prugh, L.R., 2018. Navigating snowscapes: scale-dependent responses of mountain sheep to snowpack properties. Ecological Applications 0. https://doi.org/10.1002/eap.1773

Malek, A., 2019. Empirical Analysis of Processes Affecting Drainage Flows and Inversions in a Forested Mountain Landscape. Oregon State University.

Malek, S., Avanzi, F., Brun-Laguna, K., Maurer, T., Oroza, C., Hartsough, P., Watteyne, T., Glaser, S., Malek, S.A., Avanzi, F., Brun-Laguna, K., Maurer, T., Oroza, C.A., Hartsough, P.C., Watteyne, T., Glaser, S.D., 2017. Real-Time Alpine Measurement System Using Wireless Sensor Networks. Sensors 17, 2583. https://doi.org/10.3390/s17112583

Mallory, C.D., Boyce, M.S., 2017. Observed and predicted effects of climate change on Arctic caribou and reindeer. Environ. Rev. 26, 13–25. https://doi.org/10.1139/er-2017-0032

Mao, F., Khamis, K., Krause, S., Clark, J., Hannah, D.M., 2019. Low-Cost Environmental Sensor Networks: Recent Advances and Future Directions. Front. Earth Sci. 7. https://doi.org/10.3389/feart.2019.00221

Martinez, K., Hart, J.K., Bragg, G.M., Curry, J.S., 2017. Cryospheric monitoring with new low power RTK dGPS systems. AGU Fall Meeting Abstracts 41.

Matzl, M., Schneebeli, M., 2006. Measuring specific surface area of snow by near-infrared photography. Journal of Glaciology 52, 558–564. https://doi.org/10.3189/172756506781828412

Mätzler, C., Standley, A., 2000. Technical note: Relief effects for passive microwave remote sensing. International Journal of Remote Sensing 21, 2403–2412. https://doi.org/10.1080/01431160050030538

McCabe, G.J., Clark, M.P., Hay, L.E., 2007. Rain-on-snow events in the western United States. Bulletin of the American Meteorological Society 88, 319–328. https://doi.org/10.1175/BAMS-88-3-319

Meltofte, H., Høye, T.T., Schmidt, N.M., Forchhammer, M.C., 2006. Differences in food abundance cause inter-annual variation in the breeding phenology of High Arctic waders. Polar Biol 30, 601. https://doi.org/10.1007/s00300-006-0219-1

Mitchell, C.D., Chaney, R., Aho, K., Kie, J.G., Bowyer, R.T., 2015. Population density of Dall's sheep in Alaska: effects of predator harvest? Mamm Res 60, 21–28. https://doi.org/10.1007/s13364-014-0199-4

Molotch, N.P., Bales, R.C., 2005. Scaling snow observations from the point to the grid element: Implications for observation network design. Water Resources Research 41. https://doi.org/10.1029/2005WR004229

Montpetit, B., 2015. Analyse de la modélisation de l'émission multi-fréquences micro-onde des sols et de la neige, incluant les croutes de glace à l'aide du modèle Microwave Emission Model of Layered Snowpacks (MEMLS). Université de Sherbrooke.

Montpetit, B., Royer, A., Roy, A., Langlois, A., Derksen, C., 2013. Snow microwave emission modeling of ice lenses within a snowpack using the microwave emission model for layered snowpacks. IEEE Transactions on Geoscience and Remote Sensing 51, 4705–4717. https://doi.org/10.1109/TGRS.2013.2250509

Morin, P., Porter, C., Cloutier, M., Howat, I., Noh, M.-J., Willis, M., Bates, B., Willamson, C., Peterman, K., 2016. ArcticDEM; A Publically Available, High Resolution Elevation Model of the Arctic 18, EPSC2016-8396.

Murie, A., 1944. The Wolves of Mount McKinley. University of Washington Press.

Murphy, E.C., Whitten, K.R., 1976. Dall Sheep Demography in McKinley Park and a Reevaluation of Murie's Data. The Journal of Wildlife Management 40, 597–609. https://doi.org/10.2307/3800554

Musselman, K.N., Lehner, F., Ikeda, K., Clark, M.P., Prein, A.F., Liu, C., Barlage, M., Rasmussen, R., 2018. Projected increases and shifts in rain-on-snow flood risk over western North America. Nature Climate Change 8, 808–812. https://doi.org/10.1038/s41558-018-0236-4

NASA/METI/AIST/Japan Spacesystems, 2009. ASTER Global Digital Elevation Model. https://doi.org/10.5067/ASTER/ASTGTM.002

National Operational Hydrologic Remote Sensing Center, 2004. Snow Data Assimilation System (SNODAS) Data Products at NSIDC. https://doi.org/10.7265/N5TB14TC

NCRS, 2020. NRCS National Water and Climate Center | SNOTEL Data & Products [WWW Document]. URL https://www.wcc.nrcs.usda.gov/snow/ (accessed 3.15.20).

Nellemann, C., Fry, G., 1995. Quantitative analysis of terrain ruggedness in reindeer winter grounds. Arctic 172–176.

Nelson, M.E., Mech, L.D., 1986. Relationship between Snow Depth and Gray Wolf Predation on White-Tailed Deer. The Journal of Wildlife Management 50, 471–474. https://doi.org/10.2307/3801108

NOAA, 2020. Global Historical Climatology Network (GHCN) | National Centers for Environmental Information (NCEI) formerly known as National Climatic Data Center (NCDC) [WWW Document]. URL https://www.ncdc.noaa.gov/data-access/land-based-station-data/land-based-datasets/global-historical-climatology-network-ghcn (accessed 11.18.20).

Notarnicola, C., 2020. Hotspots of snow cover changes in global mountain regions over 2000–2018. Remote Sensing of Environment 243, 111781. https://doi.org/10.1016/j.rse.2020.111781

NPS - Land Resources Division, 2020. Administrative Boundaries of National Park System Units 6/30/2020 [WWW Document]. National Geospatial Data Asset (NGDA) NPS National Parks Dataset. NPS - Land Resources Division. URL https://irma.nps.gov/DataStore/Reference/Profile/2224545?lnv=True (accessed 8.15.20).

Orlanski, I., 1975. A Rational Subdivision of Scales for Atmospheric Processes. Bulletin of the American Meteorological Society 56, 527–530.

Ouellet, F., Langlois, A., Blukacz-Richards, E.A., Johnson, C.A., Royer, A., Neave, E., Larter, N.C., 2017. Spatialization of the SNOWPACK snow model for the Canadian Arctic to assess Peary caribou winter grazing conditions. Physical Geography 38, 143–158. https://doi.org/10.1080/02723646.2016.1274200

Painter, T.H., Rittger, K., McKenzie, C., Slaughter, P., Davis, R.E., Dozier, J., 2009. Retrieval of subpixel snow covered area, grain size, and albedo from MODIS. Remote Sensing of Environment 113, 868–879. https://doi.org/10.1016/j.rse.2009.01.001

Pan, C.G., Kirchner, P.B., Kimball, J.S., Du, J., 2020. A Long-Term Passive Microwave Snowoff Record for the Alaska Region 1988–2016. Remote Sensing 12, 153. https://doi.org/10.3390/rs12010153

Pan, C.G., Kirchner, P.B., Kimball, J.S., Kim, Y., Du, J., 2018. Rain-on-snow events in Alaska, their frequency and distribution from satellite observations. Environ. Res. Lett. 13, 075004. https://doi.org/10.1088/1748-9326/aac9d3

Parker, K.L., Robbins, C.T., Hanley, T.A., 1984. Energy Expenditures for Locomotion by Mule Deer and Elk. The Journal of Wildlife Management 48, 474–488. https://doi.org/10.2307/3801180

Pedersen, S.H., Liston, G.E., Welker, J.M., 2019. Snow depth and snow density measured in Arctic Alaska for caribou winter applications in 2018 and 2019.

Penczykowski, R.M., Connolly, B.M., Barton, B.T., 2017. Winter is changing: Trophic interactions under altered snow regimes. Food Webs 13, 80–91. https://doi.org/10.1016/j.fooweb.2017.02.006

Pepin, N., Bradley, R.S., Diaz, H.F., Baraer, M., Caceres, E.B., Forsythe, N., Fowler, H., Greenwood, G., Hashmi, M.Z., Liu, X.D., Miller, J.R., Ning, L., Ohmura, A., Palazzi, E., Rangwala, I., Schöner, W., Severskiy, I., Shahgedanova, M., Wang, M.B., Williamson, S.N., Yang, D.Q., 2015. Elevation-dependent warming in mountain regions of the world. NatCC 5, 424–430. https://doi.org/10.1038/nclimate2563

Picard, G., Sandells, M., Löwe, H., 2018. SMRT: an active–passive microwave radiative transfer model for snow with multiple microstructure and scattering formulations (v1.0). Geoscientific Model Development 11, 2763–2788. https://doi.org/10.5194/gmd-11-2763-2018

Pinheiro, J., Bates, D., DebRoy, S., Sarkar, D., 2019. nlme: Linear and Nonlinear Mixed Effects Models.

Pohl, S., Garvelmann, J., Wawerla, J., Weiler, M., 2014. Potential of a low-cost sensor network to understand the spatial and temporal dynamics of a mountain snow cover. Water Resources Research 50, 2533–2550. https://doi.org/10.1002/2013WR014594

Pomeroy, J.W., Brun, E., 2001. Physical Properties of Snow Introduction: Snow Physics and Ecology, in: Snow Ecology.

Portier, C., Festa-Bianchet, M., Gaillard, J.-M., Jorgenson, J.T., Yoccoz, N.G., 1998. Effects of density and weather on survival of bighorn sheep lambs (Ovis canadensis). Journal of Zoology 245, 271–278. https://doi.org/10.1111/j.1469-7998.1998.tb00101.x

Pozzanghera, C. b., Sivy, K. j., Lindberg, M. s., Prugh, L. r., 2016. Variable effects of snow conditions across boreal mesocarnivore species. Can. J. Zool. 94, 697–705. https://doi.org/10.1139/cjz-2016-0050

Pruitt, Jr., W.O., 1959. Snow as a Factor in the Winter Ecology of the Barren Ground Caribou (*Rangifer arcticus*). ARCTIC 12. https://doi.org/10.14430/arctic3723

Pulliainen, J., Hallikainen, M., 2001. Retrieval of Regional Snow Water Equivalent from Space-Borne Passive Microwave Observations. Remote Sensing of Environment 75, 76–85. https://doi.org/10.1016/S0034-4257(00)00157-7

Putkonen, J., Grenfell, T.C., Rennert, K., Bitz, C., Jacobson, P., Russell, D., 2009. Rain on Snow: Little Understood Killer in the North. Eos, Transactions American Geophysical Union 90, 221–222. https://doi.org/10.1029/2009EO260002

Putkonen, J., Roe, G., 2003. Rain-on-snow events impact soil temperatures and affect ungulate survival. Geophysical Research Letters 30. https://doi.org/10.1029/2002GL016326

QGIS Development Team, 2020. QGIS Geographic Information System. QGIS Association.

QGIS Development Team, 2019. QGIS Geographic Information System. Open Source Geospatial Foundation Project.

R Core Team, 2019. R: A Language and Environment for Statistical Computing. R Foundation for Statistical Computing, Vienna, Austria.

Rachlow, J.L., Bowyer, R.T., 1994. Variability in Maternal Behavior by Dall's Sheep: Environmental Tracking or Adaptive Strategy? Journal of Mammalogy 75, 328–337. https://doi.org/10.2307/1382551

Rasmus, S., Kivinen, S., Irannezhad, M., 2018. Basal ice formation in snow cover in Northern Finland between 1948 and 2016. Environ. Res. Lett. 13, 114009. https://doi.org/10.1088/1748-9326/aae541

Rattenbury, K.L., Schmidt, J.H., Swanson, D.K., Borg, B.L., Mangipane, B.A., Sousanes, P.J., 2018. Delayed spring onset drives declines in abundance and recruitment in a mountain ungulate. Ecosphere 9, e02513. https://doi.org/10.1002/ecs2.2513

Reconyx, 2017. Hyperfire(TM) High Performance Cameras Instruction Manual.

Reid, D.G., Bilodeau, F., Krebs, C.J., Gauthier, G., Kenney, A.J., Gilbert, B.S., Leung, M.C.-Y., Duchesne, D., Hofer, E., 2012. Lemming winter habitat choice: a snow-fencing experiment. Oecologia 168, 935–946. https://doi.org/10.1007/s00442-011-2167-x

Rice, R., Bales, R.C., 2010. Embedded-sensor network design for snow cover measurements around snow pillow and snow course sites in the Sierra Nevada of California. Water Resources Research 46. https://doi.org/10.1029/2008WR007318

Riley, S.J., DeGloria, S.D., Elliot, R., 1999. Index that quantifies topographic heterogeneity. intermountain Journal of sciences 5, 23–27.

Robinson, B.G., Merrill, E.H., 2012. The influence of snow on the functional response of grazing ungulates. Oikos 121, 28–34. https://doi.org/10.1111/j.1600-0706.2011.19408.x

Roffler, G.H., Adams, L.G., Hebblewhite, M., 2017. Summer habitat selection by Dall's sheep in Wrangell-St. Elias National Park and Preserve, Alaska. J Mammal 98, 94–105. https://doi.org/10.1093/jmammal/gyw135

Ryan, W.A., Doesken, N.J., Fassnacht, S.R., 2008. Evaluation of Ultrasonic Snow Depth Sensors for U.S. Snow Measurements. J. Atmos. Oceanic Technol. 25, 667–684. https://doi.org/10.1175/2007JTECHA947.1

Saberi, N., 2019. Snow Properties Retrieval Using Passive Microwave Observations.

Saberi, N., Kelly, R., Flemming, M., Li, Q., 2019. Review of snow water equivalent retrieval methods using spaceborne passive microwave radiometry. International Journal of Remote Sensing 0, 1–23. https://doi.org/10.1080/01431161.2019.1654144

Sappington, J.M., Longshore, K.M., Thompson, D.B., 2007. Quantifying landscape ruggedness for animal habitat analysis: a case study using bighorn sheep in the Mojave Desert. The Journal of wildlife management 71, 1419–1426.

Schaefer, J.A., Messier, F., 1995. Winter Foraging by Muskoxen: A Hierarchical Approach to Patch Residence Time and Cratering Behaviour. Oecologia 104, 39–44.

Schmidt, J.H., Rattenbury, K.L., Lawler, J.P., Maccluskie, M.C., 2012. Using distance sampling and hierarchical models to improve estimates of Dall's sheep abundance. The Journal of Wildlife Management 76, 317–327. https://doi.org/10.1002/jwmg.216

Schneebeli, M., Pielmeier, C., Johnson, J.B., 1999. Measuring snow microstructure and hardness using a high resolution penetrometer. Cold Regions Science and Technology 30, 101–114. https://doi.org/10.1016/S0165-232X(99)00030-0

Schults, B.S., 2004. Abundance survey of Dall's sheep in the western Baird Mountains, Alaska, July 2004. Natural Resource Technical Report No. NPS/AR/ NRTR-2004-46.

Semmens, K.A., Ramage, J., Bartsch, A., Liston, G.E., 2013. Early snowmelt events: detection, distribution, and significance in a major sub-arctic watershed. Environ. Res. Lett. 8, 014020. https://doi.org/10.1088/1748-9326/8/1/014020

Serrano, E., Granados, J.E., Sarasa, M., González, F.J., Fandos, P., Soriguer, R.C., Pérez, J.M., 2011. The effects of winter severity and population density on body stores in the Iberian wild goat (Capra pyrenaica) in a highly seasonal mountain environment. European Journal of Wildlife Research; Heidelberg 57, 45–55. http://dx.doi.org.ezproxy.proxy.library.oregonstate.edu/10.1007/s10344-010-0398-5

Serreze, M.C., Barry, R.G., 2011. Processes and impacts of Arctic amplification: A research synthesis. Global and Planetary Change 77, 85–96. https://doi.org/10.1016/j.gloplacha.2011.03.004

Sexstone, G.A., Clow, D.W., Fassnacht, S.R., Liston, G.E., Hiemstra, C.A., Knowles, J.F., Penn, C.A., 2018. Snow Sublimation in Mountain Environments and Its Sensitivity to Forest Disturbance and Climate Warming. Water Resources Research 54, 1191–1211. https://doi.org/10.1002/2017WR021172

Sirén, A.P.K., Somos-Valenzuela, M., Callahan, C., Kilborn, J.R., Duclos, T., Tragert, C., Morelli, T.L., 2018. Looking beyond wildlife: using remote cameras to evaluate accuracy of gridded snow data. Remote Sensing in Ecology and Conservation 4, 375–386. https://doi.org/10.1002/rse2.85

Sivy, K.J., Nolin, A.W., Cosgrove, C., Prugh, L., 2018. Critical snow density threshold for Dall sheep (Ovis dalli dalli). Can. J. Zool. https://doi.org/10.1139/cjz-2017-0259

Skalka, C., Frolik, J., 2014. Snowcloud: A Complete Data Gathering System for Snow Hydrology Research. Springer International Publishing, pp. 3–14. https://doi.org/10.1007/978-3-319-03071-5_1

Skogland, T., 1978. Characteristics of the Snow Cover and Its Relationship to Wild Mountain Reindeer (Rangifer tarandus tarandus L.) Feeding Strategies. Arctic and Alpine Research 10, 569–579. https://doi.org/10.2307/1550680

Sokolov, A.A., Sokolova, N.A., Ims, R.A., Brucker, L., Ehrich, D., 2016. Emergent Rainy Winter Warm Spells May Promote Boreal Predator Expansion into the Arctic. Arctic 69, 121–129.

Sommer, C.G., 2018. Wind-packing of snow: How do wind crusts form? [WWW Document]. Infoscience. https://doi.org/10.5075/epfl-thesis-8628

Sommer, C.G., Lehning, M., Fierz, C., 2018. Wind tunnel experiments: influence of erosion and deposition on wind-packing of new snow. Frontiers in Earth Science 6, 4.

Strigaro, D., Cannata, M., Antonovic, M., 2019. Boosting a Weather Monitoring System in Low Income Economies Using Open and Non-Conventional Systems: Data Quality Analysis. Sensors 19, 1185. https://doi.org/10.3390/s19051185

Sturm, M., 2015. White water: Fifty years of snow research in WRR and the outlook for the future. Water Resources Research 51, 4948–4965. https://doi.org/10.1002/2015WR017242

Sturm, M., Benson, C., 2004. Scales of spatial heterogeneity for perennial and seasonal snow layers. Annals of Glaciology 38, 253–260. https://doi.org/10.3189/172756404781815112

Sturm, M., Holmgren, J., 2018. An Automatic Snow Depth Probe for Field Validation Campaigns. Water Resources Research 54, 9695–9701. https://doi.org/10.1029/2018WR023559

Sturm, M., Holmgren, J., Liston, G.E., Holmgren, J., Liston, G.E., 1995. A Seasonal Snow Cover Classification System for Local to Global Applications. Journal of Climate 8, 1261–1283. https://doi.org/10.1175/1520-0442(1995)008<1261:ASSCCS>2.0.CO;2

Sun, N., Yan, H., Wigmosta, M.S., Leung, L.R., Skaggs, R., Hou, Z., 2019. Regional Snow Parameters Estimation for Large-Domain Hydrological Applications in the Western United States. Journal of Geophysical Research: Atmospheres 124, 5296–5313. https://doi.org/10.1029/2018JD030140

Telfer, E.S., Kelsall, J.P., 1984. Adaptation of Some Large North American Mammals for Survival In Snow. Ecology 65, 1828–1834. https://doi.org/10.2307/1937779

Tong, J., Déry, S.J., Jackson, P.L., Derksen, C., 2010. Testing snow water equivalent retrieval algorithms for passive microwave remote sensing in an alpine watershed of western Canada. Canadian Journal of Remote Sensing 36, S74–S86. https://doi.org/10.5589/m10-009

Tyler N. J. C., 2010. Climate, snow, ice, crashes, and declines in populations of reindeer and caribou (Rangifer tarandus L.). Ecological Monographs 80, 197–219. https://doi.org/10.1890/09-1070.1

Ulaby, F.T., Moore, R.K., Fung, A.K., 1981. Microwave remote sensing: Active and passive. volume 1-microwave remote sensing fundamentals and radiometry.

U.S. Geological Survey, 2017. 1 Arc-second Digital Elevation Models (DEMs) - USGS National Map 3DEP Downloadable Data Collection: U.S. Geological Survey [WWW Document]. URL https://www.sciencebase.gov/catalog/item/4f70aa71e4b058caae3f8de1 (accessed 8.15.20).

U.S. Geological Survey, 2015. NLCD 2011 Land Cover Alaska 2001 to 2011 From To Change Index - National Geospatial Data Asset (NGDA) Land Use Land Cover [WWW Document]. URL https://www.mrlc.gov/data/nlcd-2001-2011-land-cover-change-alaska-0

Van Rossum, G., Drake, F.L., 2009. Python 3 Reference Manual. CreateSpace, Scotts Valley, CA.

Varhola, A., Wawerla, J., Weiler, M., Coops, N.C., Bewley, D., Alila, Y., Varhola, A., Wawerla, J., Weiler, M., Coops, N.C., Bewley, D., Alila, Y., 2010. A New Low-Cost, Stand-Alone Sensor

System for Snow Monitoring. Journal of Atmospheric and Oceanic Technology 27, 1973–1978. https://doi.org/10.1175/2010JTECHA1508.1

Verbyla, D., 2017. ABoVE: Last Day of Spring Snow, Alaska, USA, and Yukon Territory, Canada, 2000-2016. ORNL DAAC. https://doi.org/10.3334/ORNLDAAC/1528

Verbyla, D., Hegel, T., Nolin, A.W., van de Kerk, M., Kurkowski, T.A., Prugh, L.R., 2017. Remote Sensing of 2000–2016 Alpine Spring Snowline Elevation in Dall Sheep Mountain Ranges of Alaska and Western Canada. Remote Sensing 9, 1157. https://doi.org/10.3390/rs9111157

Vikhamar-Schuler, D., Hanssen-Bauer, I., Schuler, T.V., Mathiesen, S.D., Lehning, M., 2013. Use of a multilayer snow model to assess grazing conditions for reindeer. Annals of Glaciology 54, 214–226. https://doi.org/10.3189/2013AoG62A306

Vors, L.S., Boyce, M.S., 2009. Global declines of caribou and reindeer. Global Change Biology 15, 2626–2633. https://doi.org/10.1111/j.1365-2486.2009.01974.x

Vroom, G.W., Herrero, S., Ogilvie, R.T., 1980. The ecology of winter den sites of grizzly bears in Banff National Park, Alberta. Bears: their biology and management 321–330.

Wells, J.J., 2018. Dall sheep management report and plan, Game Management Unit 12, Mentasta, Nutzotin, and northern Wrangell Mountains: Report period 1 July 2011–30 June 2016, and plan period 1 July 2016–30 June 2021. Alaska Department of Fish and Game, Species Management Report and Plan ADF&G/DWC/SMR&P-2018-46, Juneau. 26.

Western Regional Climate Centre, 2020. SAGEHEN CREEK, CALIFORNIA - Climate Summary [WWW Document]. URL https://wrcc.dri.edu/cgi-bin/cliMAIN.pl?ca7641 (accessed 8.4.20).

White, K.S., White, K.S., Pendleton, G.W., Crowley, D., Griese, H.J., Hundertmark, K.J., McDonough, T., Nichols, L., Nichols, L., Robus, M., Smith, C.A., Schoen, J.W., 2011. Mountain Goat Survival in Coastal Alaska: Effects of Age, Sex, and Climate. wild 75, 1731–1744. https://doi.org/10.1002/jwmg.238

Wilmers, C.C., Nickel, B., Bryce, C.M., Smith, J.A., Wheat, R.E., Yovovich, V., 2015. The golden age of bio-logging: how animal-borne sensors are advancing the frontiers of ecology. Ecology 96, 1741–1753. https://doi.org/10.1890/14-1401.1

WRST Sheep and Goat Count Units - data.doi.gov [WWW Document], n.d. URL https://data.doi.gov/dataset/wrst-sheep-and-goat-count-units (accessed 5.24.20).

Yan, H., Sun, N., Wigmosta, M., Skaggs, R., Hou, Z., Leung, R., 2018. Next-Generation Intensity-Duration-Frequency Curves for Hydrologic Design in Snow-Dominated Environments. Water Resources Research 54, 1093–1108. https://doi.org/10.1002/2017WR021290

Zimova, M., Mills, L.S., Lukacs, P.M., Mitchell, M.S., 2014. Snowshoe hares display limited phenotypic plasticity to mismatch in seasonal camouflage. Proceedings of the Royal Society B: Biological Sciences 281, 20140029. https://doi.org/10.1098/rspb.2014.0029

Zuur, A., Ieno, E.N., Walker, N., Saveliev, A.A., Smith, G.M., 2009. Mixed Effects Models and Extensions in Ecology with R, Statistics for Biology and Health. Springer-Verlag, New York.